Westinghouse Non-Proprietary Class 3

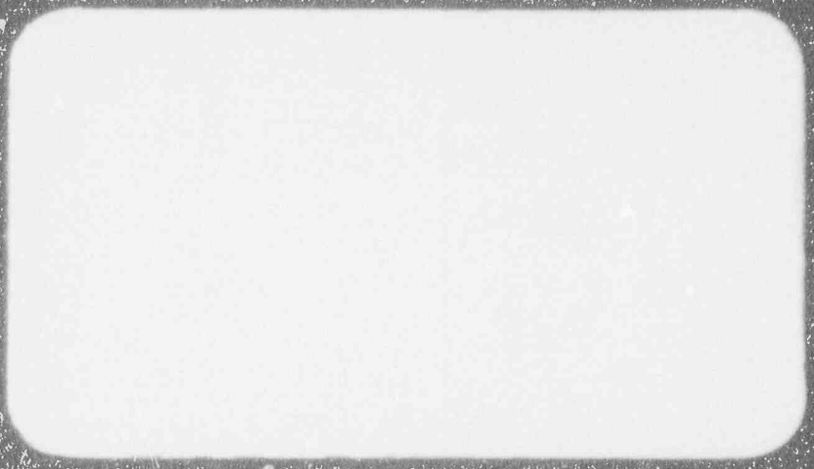

Westinghouse Energy Systems

Westinghouse Non-Proprietary Class 3

Westinghouse Energy Systems

WCAP-14172

WCOBRA/TRAC APPLICABILITY TO AP600 LARGE-BREAK LOSS-OF-COOLANT ACCIDENT

L. E. Hochreiter
S. M. Bajorek
M. Y. Young

September 1994

WESTINGHOUSE ELECTRIC CORPORATION
Nuclear Technology Division
P. O. Box 355
Pittsburgh, Pennsylvania 15230-355

AP600 DOCUMENT COVER SHEET

TDC: _____ IDS: I _____ S _____

Form 58202G(5/94) [u:\1194w-0.wpf:1b] AP600 CENTRAL FILE USE ONLY:

0058.FRM RFS#: RFS ITEM #:

AP600 DOCUMENT NO.	REVISION NO.		ASSIGNED TO
RCS-GSR-001		Page 1 of ___	

ALTERNATE DOCUMENT NUMBER: WCAP 14172 & 14171 WORK BREAKDOWN #: 3.1.1.9.1

DESIGN AGENT ORGANIZATION:

TITLE: WCOBRA/TRAC Applicability to AP600 Large-Break Loss-of-Coolant Accident

ATTACHMENTS:	DCP #/REV. INCORPORATED IN THIS DOCUMENT REVISION:
CALCULATION/ANALYSIS REFERENCE:	

ELECTRONIC FILENAME	ELECTRONIC FILE FORMAT	ELECTRONIC FILE DESCRIPTION
1410w-0.wpf	Word Perfect	

COMPLETE 1 IF WORK PERFORMED UNDER DESIGN CERTIFICATION OR COMPLETE 2 IF WORK PERFORMED UNDER FOAKE.

1 ☒ **DOE DESIGN CERTIFICATION PROGRAM** – GOVERNMENT LIMITED RIGHTS STATEMENT [See page 2]

☐ DOE CONTRACT DELIVERABLES (DELIVERED DATA)
Subject to specified exceptions, disclosure of this data is restricted until September 30, 1995 or Design Certification under DOE contract DE-AC03-90SF18495, whichever is later.

EPRI CONFIDENTIAL: NOTICE: 1 ☐ 2 ☐ 3 ☐ 4 ☐ 5 ☐ CATEGORY: A ☐ B ☐ C ☐ D ☐ E ☐ F ☐

2 ☐ **ARC FOAKE PROGRAM** – ARC LIMITED RIGHTS STATEMENT [See page 2]

☐ ARC CONTRACT DELIVERABLES (CONTRACT DATA)
Subject to specified exceptions, disclosure of this data is restricted under ARC Subcontract ARC-93-3-SC-001.

ORIGINATOR	SIGNATURE/DATE	
L. E. Hochreiter	L E Hochreiter	9/26/94
AP600 RESPONSIBLE MANAGER	SIGNATURE*	APPROVAL DATE
E. H. Novendstern	E H Novendstern	9/27/94

*Approval of the responsible manager signifies that document is complete, all required reviews are complete, electronic file is attached and document is released for use.

Form 58202G(5/94)

LIMITED RIGHTS STATEMENTS

DOE GOVERNMENT LIMITED RIGHTS STATEMENT

(A) These data are submitted with limited rights under government contract No. DE-AC03-90SF18495. These data may be reproduced and used by the government with the express limitation that they will not, without written permission of the contractor, be used for purposes of manufacturer nor disclosed outside the government; except that the government may disclose these data outside the government for the following purposes, if any, provided that the government makes such disclosure subject to prohibition against further use and disclosure:
(I) This "Proprietary Data" may be disclosed for evaluation purposes under the restrictions above.
(II) The "Proprietary Data" may be disclosed to the Electric Power Research Institute (EPRI), electric utility representatives and their direct consultants, excluding direct commercial competitors, and the DOE National Laboratories under the prohibitions and restrictions above.

(B) This notice shall be marked on any reproduction of these data, in whole or in part.

ARC LIMITED RIGHTS STATEMENT:

This proprietary data, furnished under Subcontract Number ARC-93-3-SC-001 with ARC may be duplicated and used by the government and ARC, subject to the limitations of Article H-17.F. of that subcontract, with the express limitations that the proprietary data may not be disclosed outside the government or ARC, or ARC's Class 1 & 3 members or EPRI or be used for purposes of manufacture without prior permission of the Subcontractor, except that further disclosure or use may be made solely for the following purposes:

This proprietary data may be disclosed to other than commercial competitors of Subcontractor for evaluation purposes of this subcontract under the restriction that the proprietary data be retained in confidence and not be further disclosed, and subject to the terms of a non-disclosure agreement between the Subcontractor and that organization, excluding DOE and its contractors.

DEFINITIONS

CONTRACT/DELIVERED DATA — Consists of documents (e.g. specifications, drawings, reports) which are generated under the DOE or ARC contracts which contain no background proprietary data.

EPRI CONFIDENTIALITY / OBLIGATION NOTICES

NOTICE 1: The data in this document is subject to no confidentiality obligations.

NOTICE 2: The data in this document is proprietary and confidential to Westinghouse Electric Corporation and/or its Contractors. It is forwarded to recipient under an obligation of Confidence and Trust for limited purposes only. Any use, disclosure to unauthorized persons, or copying of this document or parts thereof is prohibited except as agreed to in advance by the Electric Power Research Institute (EPRI) and Westinghouse Electric Corporation. Recipient of this data has a duty to inquire of EPRI and/or Westinghouse as to the uses of the information contained herein that are permitted.

NOTICE 3: The data in this document is proprietary and confidential to Westinghouse Electric Corporation and/or its Contractors. It is forwarded to recipient under an obligation of Confidence and Trust for use only in evaluation tasks specifically authorized by the Electric Power Research Institute (EPRI). Any use, disclosure to unauthorized persons, or copying this document or parts thereof is prohibited except as agreed to in advance by EPRI and Westinghouse Electric Corporation. Recipient of this data has a duty to inquire of EPRI and/or Westinghouse as to the uses of the information contained herein that are permitted. This document and any copies or excerpts thereof that may have been generated are to be returned to Westinghouse, directly or through EPRI, when requested to do so.

NOTICE 4: The data in this document is proprietary and confidential to Westinghouse Electric Corporation and/or its Contractors. It is being revealed in confidence and trust only to Employees of EPRI and to certain contractors of EPRI for limited evaluation tasks authorized by EPRI. Any use, disclosure to unauthorized persons, or copying of this document or parts thereof is prohibited. This Document and any copies or excerpts thereof that may have been generated are to be returned to Westinghouse, directly or through EPRI, when requested to do so.

NOTICE 5: The data in this document is proprietary and confidential to Westinghouse Electric Corporation and/or its Contractors. Access to this data is given in Confidence and Trust only at Westinghouse facilities for limited evaluation tasks assigned by EPRI. Any use, disclosure to unauthorized persons, or copying of this document or parts thereof is prohibited. Neither this document nor any excerpts therefrom are to be removed from Westinghouse facilities.

EPRI CONFIDENTIALITY / OBLIGATION CATEGORIES

CATEGORY "A" — (See Delivered Data) Consists of CONTRACTOR Foreground Data that is contained in an issued reported.

CATEGORY "B" — (See Delivered Data) Consists of CONTRACTOR Foreground Data that is not contained in an issued report, except for computer programs.

CATEGORY "C" — Consists of CONTRACTOR Background Data except for computer programs.

CATEGORY "D" — Consists of computer programs developed in the course of performing the Work.

CATEGORY "E" — Consists of computer programs developed prior to the Effective Date or after the Effective Date but outside the scope of the Work.

CATEGORY "F" — Consists of administrative plans and administrative reports.

TABLE OF CONTENTS

LIST OF TABLES

LIST OF FIGURES

LIST OF FIGURES (Cont.)

LIST OF FIGURES (Cont.)

LIST OF FIGURES (Cont.)

SUMMARY

The WCOBRA/TRAC-Mod7 code is a general systems analysis code with the capability to model and analyze thermal-hydraulic transients in pressurized water reactors. Westinghouse three- and four-loop operating plants have been analyzed with this version of the code. An earlier version of the code has been licensed and used to analyze large-break LOCA transients in two-loop pressurized water reactors equipped with upper plenum safety injection systems.

While the AP600 design has several unique features, the key thermal-hydraulic phenomena for an AP600 large-break LOCA are expected to be the same as those in a conventional operating PWR. Therefore, the modeling methods and code validation performed in support of operating plants is directly applicable to the AP600 design.

One area that is different in the AP600 design relative to current operating Westinghouse PWRs is the use of downcomer injection of the emergency core cooling water. The accumulator, core makeup tank, in-containment water refueling storage tank, and sump recirculation injection flow enter the vessel through two opposite direct vessel injection locations. WCOBRA/TRAC has been assessed using tests from two separate experimental facilities that investigated direct vessel injection to ensure that the accuracy of the code prediction for this injection mode is acceptable.

The AP600 Standard Safety Analysis Report (SSAR) calculations are shown and compared to transients for a current three-loop PWR to show that the AP600 large-break behavior is similar to that of current PWRs.

The results of this study confirm that WCOBRA/TRAC can accurately model the AP600 large-break transient without any AP600-specific code or model modification. The results predicted by WCOBRA/TRAC for the AP600 indicate that a substantial large-break LOCA margin exists for this new design with passive safety systems.

1.0 INTRODUCTION

The WCOBRA/TRAC code is a generalized thermal-hydraulic systems code that has the capability to model either boiling water or pressurized water reactors (PWRs). The COBRA portion of the code represents the reactor vessel component. The TRAC portion of the code represents the loop components, such as the steam generators, pumps, accumulators, and the associated piping. The active emergency core cooling systems (ECCSs) of the current generation PWRs are modeled as boundary conditions using pressure- and temperature-dependent tables to represent the high- and low-pressure safety injection systems. Breaks of different sizes and types, either guillotine or communicative, can also be simulated at different locations on the reactor piping. The WCOBRA/TRAC-Mod7 version of the code was developed and verified with the intent of satisfying the requirements of the revised Appendix K rule with regards to best estimate methods. This version of the code has been used to analyze large-break LOCAs in several operating PWRs with cold leg injection. An earlier version of the code, WCOBRA/TRAC-Mod4, was approved by the NRC for use with plants with upper plenum injection systems. This version has been used to analyze several two-loop PWRs.

The WCOBRA/TRAC code has been used successfully to model PWRs with different ECCS designs. WCOBRA/TRAC has been used to analyze a four-loop PWR,[1] which has no accumulators, and employs, instead, large-capacity, high-pressure pumps that inject vertically downward into the upper plenum to refill the reactor vessel for a large-break LOCA. Detailed upper plenum noding was used to model the safety injection flow path. Sensitivity studies were then used to quantify the uncertainty in the upper plenum modeling, and the resulting conservative upper plenum model was used.

Westinghouse two-loop PWRs also have the low-pressure emergency core cooling system (ECCS) injection flowing into the upper plenum. The safety injection flow enters the upper plenum as horizontal jets at the same elevation as the reactor hot and cold legs. Sensitivity studies and comparisons to scaled test data validated the capability of the WCOBRA/TRAC code to model this plant configuration.

The NRC version of the COBRA/TRAC code has also been used to model Westinghouse PWRs, which utilize upper head injection ECCSs.[2] In this design, separate high-pressure accumulators are used to inject flow into the upper head during the blowdown phase of the transient. A very detailed model of the reactor system was used to best determine the blowdown behavior to the new ECCS that was added to these plants. In addition to these unique PWR ECCS designs, WCOBRA/TRAC has also been used to model and predict the ECCS performance of conventional three- and four-loop Westinghouse PWRs.[3] All the above calculations indicate that the WCOBRA/TRAC code has the capabilities to model different classes of PWRs that utilize different ECCS designs with confidence.

The AP600 is an advanced PWR design that incorporates passive safety systems that perform the same function as the active systems on current PWRs. The principal difference is that natural forces, such as gravity, are used for the injection of the ECCS water into the reactor vessel, rather than active ac-powered systems, such as pumps and heat exchangers. It should be noted that only the injection

mode is different for the AP600. Once the emergency coolant is injected into the vessel, the flow of that coolant into the core is gravity-driven by the driving head in the downcomer the same as a current PWR. For the large-break LOCA, any excess injected flow will spill out the broken cold leg break. Figure 1-1 shows the AP600 ECCS safety design, and Table 1-1 gives the safety function of the different passive system components used in the AP600 safety system design. The two components that are of most interest for the large-break LOCA performance of the AP600 design are the accumulators and the core makeup tanks (CMTs). As indicated in Table 1-1, the CMTs perform the same function as the ECCS high-pressure active pumps in existing PWR designs. The AP600 accumulators are of a similar design to current plants, except that they have a larger capacity and will discharge at a slower rate compared to existing PWRs. This results in an accumulator injection period that is greater than 120 seconds, as compared to the 45-second injection period of existing two-loop PWRs. Both the accumulator flow and the CMT flow are injected into the vessel through separate direct vessel-injection nozzles that are located slightly below the reactor cold and hot legs. This is a different injection location than that typically used in most Westinghouse PWRs. However, Babcock and Wilcox PWRs also use direct vessel injection, as well as newer Westinghouse two-loop PWRs, such as KRSKO and ANGRA.

The key thermal-hydraulic phenomena for the large-break LOCA are given in Table 1-2, and the uniqueness of AP600 design features are assessed. The objective is to make an assessment of the design features relative to WCOBRA/TRAC's code validation and capabilities. The first column gives the key large-break LOCA phenomena that the computer code must correctly calculate. The second column indicates if there is a uniqueness in the AP600 design relative to the phenomena for which additional verification may be needed. The third column indicates whether WCOBRA/TRAC has been verified over a broad enough range to encompass the uniqueness of the AP600 design. The fourth column indicates what validation is available or indicates the need for a specific test to validate the code for this phenomena. There are specific comments in the last column that also indicate specific sources for code validation that can be used to assess WCOBRA/TRAC.

Table 1-2 indicates that there are very few items that are unique for the AP600 large-break LOCA transient relative to existing plant designs. Since WCOBRA/TRAC has already been used extensively to model the large break LOCA for existing plants, this code is applicable to assess and model the AP600 large-break LOCA transient. The unique items include direct vessel injection (or downcomer injection) and modeling the CMTs; which is a new component for the code. Therefore, the ability of WCOBRA/TRAC to model direct vessel injection of the ECCS flow will be specifically addressed in this report. The relative importance of the core makeup tank behavior for the large-break LOCA will also be discussed.

TABLE 1-1 AP600 PASSIVE SAFETY SYSTEM COMPONENTS		
Function	**Current PWRs**	**AP600**
Reactor Shutdown	- control rods - rideout (negative power coefficient, auxiliary feedwater, chemical and volume control)	- control rods - rideout (more negative power, PRHR, CMT)
RCS Overpressure	- pressurizer relief - high-pressure trip - pressurizer safety valves	- larger pressurizer - high-pressure trip - pressurizer safety valves
RCS Heat Removal	- main feedwater - auxiliary feedwater - manual feed/bleed (PZR, PORV, HHSI)	- PRHR HX - auto feed/bleed (CMT/IRWST, ADS) - manual feed/bleed (accumulators/RNS, ADS)
High-Pressure Injection	- charging pumps - high-head pumps	- CMT - accumulator/IRWST (ADS) - accumulator/residual heat removal (ADS)
Low-Pressure Injection	- accumulators - low-head pumps	- accumulators - IRWST (ADS)
Long-Term Recirculation	- low-head pumps feeding - high-head pumps	- containment sump (ADS)
Containment Heat Removal	- fan coolers - containment spray pumps/heat exchanger	- external air + water drain - external air only cooling

TABLE 1-2
ASSESSMENT OF THE AP600 LARGE-BREAK LOCA PROCESSES

LOCA Process	AP600 Uniqueness WRT W Plants	WC/T Validation Does It Exist	AP600-Specific Validation Needed	Comments
• Blowdown				
– Critical flow	None	Yes	None	
– Post-critical heat flux heat transfer • Transient critical heat flux • Rewetting • Film boiling	None	Yes	None	
– Structure heat transfer	Yes, reflector	Yes, not AP600-specific	None	Modeled by input
– Accumulator ECCS bypass	None	Yes	None	
– 2ϕ ΔP in loops	None	Yes	None	
– Steam generator heat transfer	None	Yes	None	
– High-head safety injection	Yes, CMT delivery, behavior	No	Yes	Very little CMT delivery before PCT
– Pump 2ϕ behavior	Yes, canned rotor	No	No	Obtain data

TABLE 1-2 (Cont.)
ASSESSMENT OF THE AP600 LARGE-BREAK LOCA PROCESSES

LOCA Process	AP600 Uniqueness WRT W Plants	WC/T Validation Does It Exist	AP600-Specific Validation Needed	Comments
• Refill/Reflood				
– ECCS bypass	Yes, accumulator delivery in downcomer	No	None, use existing data	UPTF, CCTF downcomer injection tests
– Non-condensible gas effect	None	Yes	None	LOFT
– Post-critical heat flux heat transfer	None	Yes	None	
– Structure heat transfer	Yes, radial reflector	Not specific	None	Not needed, code can calculate
– Safety injection/high-head safety injection, ow-head safety injection	Yes, CMT delivery in downcomer	No	Yes	No CMT delivery, during this period
– Steam generator behavior	None	Yes	None	
– 2-phase ΔP	None	Yes	None	

TABLE 1-2 (Cont.)
ASSESSMENT OF THE AP600 LARGE-BREAK LOCA PROCESSES

LOCA Process	AP600 Uniqueness WRT W Plants	WC/T Validation Does It Exist	AP600-Specific Validation Needed	Comments
• Reflood				
– SI/HHSI/LHSI injection	Yes, CMT downcomer delivery	No	None, use existing data	UPTF, CCTF downcomer injection tests
– Accumulator behavior	Long-term delivery	Yes, short-term for LOFT	No	Use LOFT data could use for verification. Other plant data available.
– Core heat transfer	None	Yes	None	
– Structure heat transfer	Yes, reflector	Not specific	Not needed	LOFT test had structures typical of a PWR
– SG effects	None	Yes	None	
– Vessel/de-entrainment	None	Yes	None	
– Pump ΔP	Yes, canned rotor	Yes, other pumps	None	Pump is a known resistance

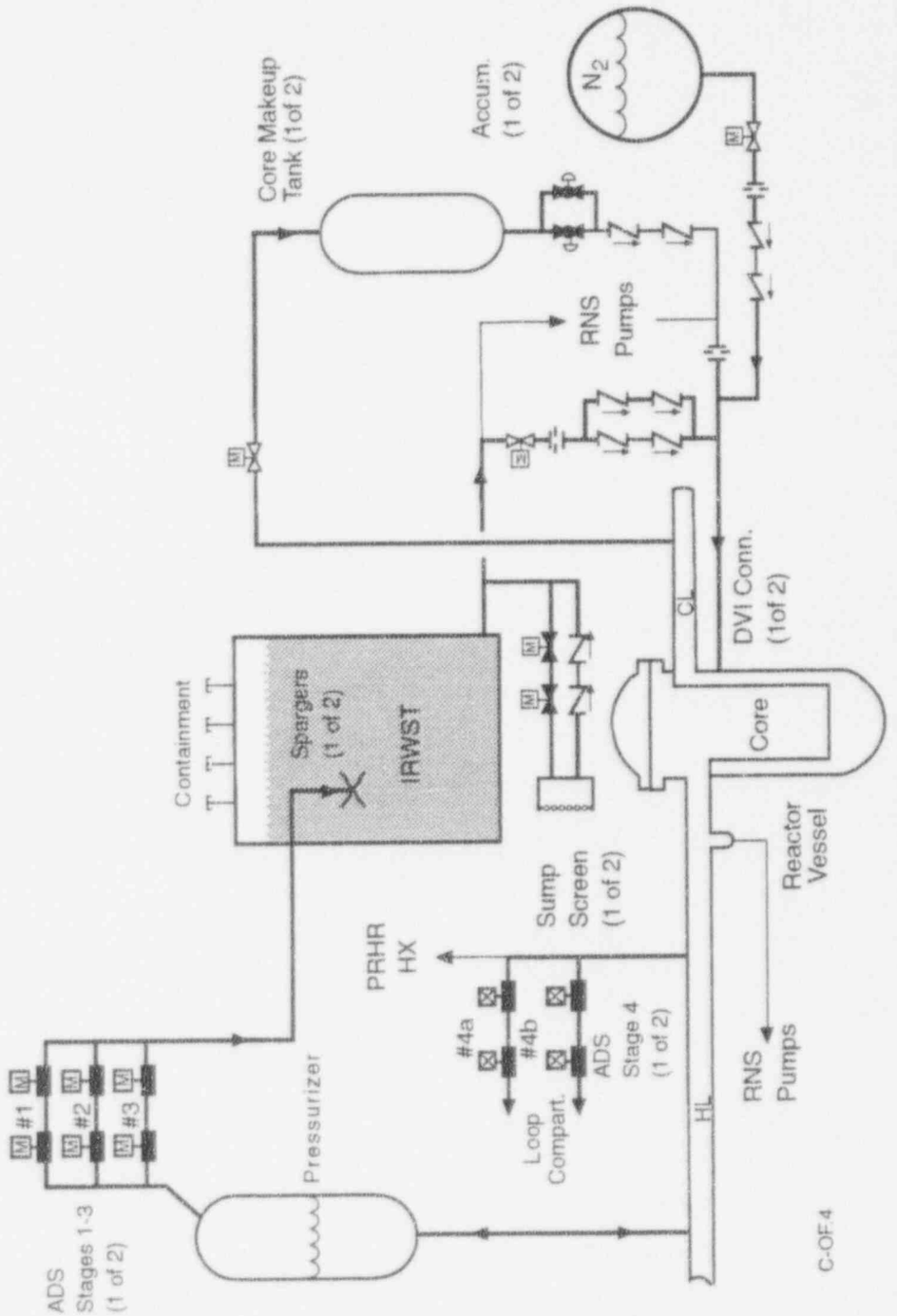

Figure 1-1 AP600 Passive Safety Injection System

2.0 DESCRIPTION OF THE AP600 LARGE-BREAK LOCA TRANSIENT

Introduction

This section will show that the existing large-break LOCA Phenomena Importance Ranking Table (PIRT) that has been developed for operating PWRs is still applicable to the AP600. Also, the most limiting large-break LOCA transient for the AP600 will be presented and compared to that for current Westinghouse three-loop plants.

2.1 Large-Break LOCA Phenomena Importance Ranking Table (PIRT)

As part of the code scaling, applicability, and uncertainty (CSAU) work that the NRC performed,[4] tables of large-break LOCA phenomena were developed, assessed, and ranked. The ranking process resulted in the development of PIRT tables that indicated which physical processes had the most important impact on the progression of the large-break LOCA transient. The PIRT tables also identified which processes were the most important for a safety analysis computer code to simulate with acceptable accuracy. Table 2.1-1 shows the PIRT tables developed by the NRC as part of peer reviews on the key large-break LOCA phenomena. Table 2.1-2 is a similar PIRT table that was developed as a summary of expert rankings for analysis of three- and four-loop operating PWRs. Comparing these tables indicates that most, if not all, parameters are identical and have been given the same relative ranking. These tables form a consensus of what is important to model in the large-break LOCA.

Table 2.1-3 is a revision of Table 2.1-1, with the addition of AP600 design features and ranking the phenomena of importance for that design, to compare to the three- and four-loop PWRs.

If the blowdown phase is examined, the key phenomena are the same between the AP600 and the operating plants with very little difference. The reactor coolant pumps in the AP600 are canned motor pumps with less inertia than the larger centrifugal pumps used in operating plants. The coast down times of the reactor coolant pumps in the AP600 are much faster than operating plants. The difference in the pump coast down is modeled by input directly in WCOBRA/TRAC and can account for different flows in the various loops.

One difference that does exist between the large-break LOCA PIRT for the existing PWRs and the AP600 is the direct vessel injection of the emergency core cooling system (ECCS) flow. For all Westinghouse three- and four-loop plants with accumulators, the injection of the ECCS flow is into the reactor cold legs. There are Babcock and Wilcox PWRs that have direct vessel injection, so this concept is not unique to the AP600 design. The AP600 has direct vessel injection in which the accumulator, core makeup, incontainment water refueling storage tank (IRWST), and the sump injection flow enters the reactor vessel. The injection of the ECCS water will result in different condensation, mixing, and entrainment and de-entrainment effects in the downcomer as compared to the cold leg injection. The primary injection during the blowdown phase is from the accumulators. As the transient progresses into reflood, the larger AP600 accumulators extend the injection past the

peak cladding temperature period until the entire core is quenched and the plant transitions into long-term cooling.

Another difference in the two PIRT tables shown in Tables 2.1-1 and 2.1-3 is the presence of the CMTs as the high-pressure injection system for the AP600. This particular passive system is primarily designed to provide injection flow for the small-break LOCA and is much less important for core cooling considerations for the large-break LOCA situations since the core cooling flow comes from the accumulators.

Therefore, the most significant difference between the large-break LOCA PIRT charts for existing PWRs and the AP600 is the direct vessel injection utilized in the AP600 design. Specific WCOBRA/TRAC code validation beyond that given in the WCOBRA/TRAC Code Qualification Document is provided in this report to address that design feature.

TABLE 2.1-1
COMPONENT AND PHENOMENA HIERARCHY DURING LBLOCA BLOWDOWN*

Components	Fuel Rods	Core	Upper Plenum	Hot Leg	PZR	Steam Gen	Pump	Cold Leg/ Accum	Downcomer	Lower Plenum	Break	Loop
Phenomena:	stored energy		entrain/ de-entrain		early quench		2ϕ performance		entrain/ de-entrain		critical flow	
	decay heat		phase separation		crit flow in surge line		ΔP, form loss		3-D		flashing	
	GAP conduct-ance		CCF (drain/ fallback)		flashing/ steam expansion				CCF, slug, nonequil flow		contain-ment pressure	
			2ϕ convection			ΔP, form loss			2ϕ convection			2ϕ ΔP
		DNB		entrain/ deentrain					saturated nucleate boiling			oscillations flow split
		post-CHF HT		flow rev & stagnation				condensation oscillations	flashing	sweep out		
		rewet		void dist. void gen				HPI mixing		hot wall		
		nucleate boiling		2ϕ convection						multi-D flow		
		3-D flow										
		void dist. void gen										
		entrain/ de-entrain										
		flow rev & stagnation										

*From NUREG-CR-5249

TABLE 2.1-1 (Cont.)
COMPONENT AND PHENOMENA HIERARCHY DURING LBLOCA REFILL

Components	Fuel Rods	Core	Upper Plenum	Hot Leg	PZR	Steam Gen	Pump	Cold Leg/ Accum	Downcomer	Lower Plenum	Break	Loop
Phenomena:	stored energy		entrain/ de-entrain		flashing/ steam expansion		2φ performance		entrain/ de-entrain		critical flow	
	oxidation		phase separation				ΔP, form loss		condensation		flashing	
	decay heat		CCF (drain/ fallback)						hot wall		contain-ment pressure	
	gap conductance		2φ convection						3-D			2φΔP
		DNB		entrain/ de-entrain		steam binding			CCF, slug, nonequil flow			oscillations
		post-CHF HT		flow rev & stagnation		ΔP, form loss			liq level osc			flow split
		rewet/ top quench		void dist. void gen					2φ convection			
		nucleate boiling		2φ convection					saturated nucleate boiling			
		1φ vapor NC						condensation oscillations		sweep out		
		3-D flow						noncondensible gases		hot wall		
		void dist. void gen						HPI mixing		multi-D flow		
		entrain/ de-entrain										
		flow rev & stagnation										

*From NUREG-CR-5249

TABLE 2.1-1 (Cont.)
COMPONENT AND PHENOMENA HIERARCHY DURING LBLOCA REFLOOD*

Components:	Fuel Rods	Core	Upper Plenum	Hot Leg	PZR	Steam Gen	Pump	Cold Leg/Accum	Downcomer	Lower Plenum	Break	Loop
Phenomena:	stored energy		entrain/ de-entrain				ΔP, form loss		entrain/ de-entrain		critical flow	
	oxidation		phase separation						condensation		flashing	
	decay heat		CCF (drain/ fallback)		flashing/steam expansion				hot wall		contain-ment pressure	
	gap conductance		2ϕ convection						3-D			2ϕ ΔP
		DNB		entrain/ de-entrain		steam binding			CCF, slug, nonequil flow			oscillations
		post-CHF HT		void dist. void gen		ΔP, form. loss			liq level OSC			flow split
		rewet		2ϕ convection					2ϕ convection			
		reflood HT plus quench							saturated nucleate boiling			
		nucleate boiling						condensation oscillations		sweep out		
		1ϕ vapor NC						noncondensible gases		hot wall		
		3-D flow						HPI mixing		multi-D flow		
		void dist. void gen										
		entrain/ de-entrain										
		flow rev & stagnation										
		radiation HT										

*From NUREG-CR-5249

TABLE 2.1-2
SUMMARY OF EXPERT RANKINGS AND AHP-CALCULATED RESULTS*

	Blowdown		Refill		Reflood	
	Expert Rank	Base Line (AHP)	Expert Rank	Base Line (AHP)	Expert Rank	Base Line (AHP)
Fuel rod						
stored energy	9**	9		2		2
oxidation		–		1	8	7
decay heat		2		1	8	8
gas conductance		3		1	8	6
Core						
DNB		6		2		2
post-CHF	7	5	8	8		4
rewet	8	8	7	6		1
reflood heat transfer		–		–	9	9
nucleate boiling		4		2		2
1-phase vapor		–		6		4
natural circulation						
3-D Flow		1		3	9	7
void generation/distribution		4		6	9	7
entrainment/de-entrainment		2		3		6
flow reversal/stagnation		3		1		1
radiation heat transfer						3
Break						
critical flow	9	9	7	7		1
		3		2		1
		2		4		2
Loop						
2-phase Δp	7	7		7		6
oscillations		–	7	7	9	9
flow split		7	7	7		2

*From NUREG-CR-5249
**10 is the highest, most important; 1 is the lowest

TABLE 2.1-3
COMPONENT AND PHENOMENA HIERARCHY DURING LBLOCA BLOWDOWN, MODIFIED FOR AP600 DESIGN

Components:	Fuel Rods	Core	Upper Plenum	Hot Leg	PZR	Steam Gen	Pump	Direct Vessel Injection	Downcomer	Lower Plenum	Break	Loop	CMT Injection
Phenomena:	stored energy		entrain/ de-entrain		early quench		2ϕ performance		entrain/ de-entrain		critical flow		
	decay heat		phase separation		crit flow in surge line		ΔP, form loss		3-D		flashing		
	gap conductance		CCF (drain/ fallback)		flashing/ steam expansion				CCF, slug, nonequil flow		contain-ment pressure		
			2ϕ convection			ΔP, form loss			2ϕ convection			2ϕ Δp	recircula-tion injection
		DNB		entrain/ de-entrain					saturated nucleate boiling			flow split	(almost no injection)
		post-CHF HT		flow rev & stagnation				condensation oscillations	flashing	sweep out			
		rewet		void dist. void gen				mixing	AP600 injection into reactor vessel	hot wall			
		nucleate boiling		2ϕ convection				injection flow of dowacomer		multi-D flow			
		3-D flow											
		void dist. void gen											
		entrain/ de-entrain											
		flow rev & stagnation											

TABLE 2.1-3 (Cont.)
COMPONENT AND PHENOMENA HIERARCHY DURING LBLOCA REFILL, MODIFIED FOR AP600 DESIGN

Components:	Fuel Rods	Core	Upper Plenum	Hot Leg	PZR	Steam Gen	Pump	Direct Vessel Injection	Downcomer	Lower Plenum	Break	Loop	CMT Injection
Phenomena:	stored energy		entrain/ de-entrain		flashing/ steam expansion		2φ performance		entrain/ de-entrain		critical flow		
	oxidation		phase separation				Δp, form loss		condensation		flashing		
	decay heat		CCF (drain/ fallback)						hot wall		containment pressure		
	gap conductance		2φ convection						3-D			2φ Δp	no injection due to accumulator
		DNB		entrain/ de-entrain		steam binding			CCF, slug, nonequil flow			oscillations	
		post-CHF HT		flow rev & stagnation		ΔP, form loss			liq level osc			flow split	
		rewet/ top quench		void dist. void gen					2φ convection				
		nucleate boiling		2φ convection					saturated nucleate boiling				
		1φ vapor NC						condensation oscillations		sweep out			
		3-D flow						noncondensible gases		hot wall			
		void dist. void gen						mixing		multi-D flow			
		entrain/ de-entrain											
		flow rev & stagnation											

TABLE 2.1-3 (Cont.)
COMPONENT AND PHENOMENA HIERARCHY DURING LBLOCA REFLOOD, MODIFIED FOR AP600 DESIGN

Components:	Fuel Rods	Core	Upper Plenum	Hot Leg	PZR	Steam Gen	Pump	Direct Vessel Injection	Downcomer	Lower Plenum	Break	Loop	CMT Injection
Phenomena:	stored energy		entrain/ de-entrain		early quench		ΔP, form loss		entrain/ de-entrain		critical flow		
	oxidation		phase separation		crit flow in surge line				condensation		flashing		
	decay heat		CCF (drain/ fallback)		flashing/ steam expansion				hot wall		containment pressure		
	gap conduct-ance		2ϕ convection						3-D			2ϕ ΔP	no injection due to accumu-lator
		DNB		entrain/ de-entrain		steam binding			CCF, slug, nonequil flow			oscilla -tions	
		post-CHF HT		void dist. void gen		ΔP, form loss			liq level OSC			flow split	
		rewet		2ϕ convection					2ϕ convection				
		reflood HT plus quench							saturated nucleate boiling				
		nucleate boiling						condensation oscillations	AP600 injection into reactor vessel	sweep out			
		1ϕ vapor NC						noncondensible gases		hot wall			
		3-D flow						mixing		multi-D flow			
		void dist. void gen						injection flow into downcomer					
		entrain/ de-entrain											
		flow rev & stagnation											
		radiation HT											

2.2 Comparisons of the Large-Break LOCA Transient for Current PWRs and AP600

The current PWR large-break LOCA transient that was selected to be compared to the AP600 transient was North Anna (VRA), which is a three-loop, 17x17 fueled plant. The basis for the choice was that the fuel design is similar to the AP600 fuel type, and the AP600 has a three-loop sized reactor vessel. The details of the North Anna transient and the sensitivity studies performed on this plant are given in the WCOBRA/TRAC Code Qualification Document, Section 22.[3]

2.2.1 VRA Transient Description

The large-break LOCA transient can be divided into time periods in which specific phenomena occur. A convenient way to divide the transient is by the various heatup and cooldown transients that the hot assembly undergoes. For each of these phases, specific phenomena and heat transfer regimes are important, as discussed below:

- **Critical Heat Flux (CHF) Phase**

  In this phase, the break discharge rate is subcooled and high, the core flow reverses, the fuel rods go through departure from nucleate boiling (DNB), and the cladding rapidly heats up while core power shuts down. The hot water in the core and upper plenum flashes during this period. This phase is terminated when the water in the lower plenum and downcomer begin to flash. The mixture swells and the pumps, still rotating in single-phase liquid, push this two-phase mixture into the core.

- **Upward Core Flow Phase**

  Heat transfer is improved as the two-phase mixture is pushed into the core. This phase may be enhanced if the pumps are not degraded, and the break discharge rate is low because the fluid is saturated at the break. This phase ends as lower plenum mass is depleted, the loops become two-phase, and the pump head degrades. If pumps are highly degraded or the break flow is large, the cooling effect due to upward flow may not be significant.

- **Downward Core Flow Phase**

  The loop flow pushed into the vessel by the pumps and the level swell caused by the flashing mixture in the vessel is more than offset by the break flow. The break flow begins to dominate and pulls flow down through the core. For some plants, this period is enhanced by flow from the upper head. As the system pressure continues to fall, the break flow and consequently, the core flow, are reduced. The core begins to heat up as the system reaches containment pressure and the vessel begins to fill with emergency core cooling system (ECCS) water.

- **Refill Phase**

  The core continues to heat up as the lower plenum fills with ECCS water. This phase ends when the ECCS water enters the core and entrainment begins, resulting in improved heat transfer.

- **Early Reflood Phase**

  The accumulators begin to empty and nitrogen enters the system. Reflood oscillations occur in the core liquid level.

- **Late Reflood Phase**

  The accumulators have emptied, and the core is filled via pumped injection. A second heatup and cooldown period may occur.

2.2.2 VRA Base Case Results

The VRA base case is chosen because of its conservative plant operating conditions, which will lead to a higher peak cladding temperature. In this regard, the base case is similar to a superbounded calculation in which the uncertainties in the plant operating condition are bounded.

The VRA reactor vessel is shown in Figure 2.2-1. The WCOBRA/TRAC model of the North Anna plant is shown in Figures 2.2-2, 2.2-3, and 2.2-4. The reactor vessel model noding detail is given in Figure 2.2-2 [

]^{a,c} The important initial and boundary conditions assumed for the base calculation are summarized in Table 2.2-4.

After a 20-second steady-state calculation, which is a transient calculation with fixed boundary conditions, the LOCA transient was initiated by applying the containment pressure to two open ends of the broken cold leg in loop 2. The system pressure is shown in Figure 2.2-5. The maximum cladding temperature (or peak cladding temperature) of the hot rod in the hot assembly is shown in Figure 2.2-6. Figure 2.2-7 shows T_{clad} at various elevations. Figure 2.2-8 shows the axial profile of the hot rod cladding temperature at several points during the transient.

- **Blowdown Period**

  At the Break The blowdown period lasts for about 30 seconds until the vessel drops to the containment pressure. The mass flowrate in the vessel side and loop side of the broken pipe quickly increases to ~55,000 lbm/sec and ~25,000 lbm/sec, respectively. The fluid velocity at the break is limited by the local sonic velocity at this point. This choked flow condition exists for approximately 20 seconds. Due to a large pressure drop through the steam generator, there is a significant difference in the pressure and the void fraction between the vessel and loop side of the broken pipe during this period.

  Core Fluid Condition The liquid flowrates in the average channel adjacent to the hot assembly and in the hot assembly at the top and bottom elevations indicate that in the base case the hot rod receives little cooling due to upward liquid flow. A significant downward liquid flow occurs, resulting in improved cooling as the flow reverses due to the break. The core flow at the top and bottom of the hot assembly is shown in Figure 2.2-9. The average channel core flow is shown in Figure 2.2-10. This is consistent with the blowdown cooling pattern for a large-break flow and/or a degraded pump, as described in the previous bulleted paragraphs: CHF phase, upward core flow phase, and downward core flow phase.

- **Refill Period**

  The refill period is characterized by a rapid increase in the lower plenum collapsed liquid level and the vessel fluid mass. In this period, the cladding temperatures at all elevations increase rapidly due to the lack of liquid and steam flow in the core region. This results in poor cooling, as seen in in Figure 2.2-7 and curves 2 and 3 in Figure 2.2-8 (t=40 to 70 seconds).

- **Reflood Period**

  The early part of this period is characterized by a rigorous vapor generation when the lower section of the core receives liquid from the lower plenum and subsequent core/downcomer oscillations with steadily improving core heat transfer. At around 120 seconds, ECCS water accumulated in the lower plenum starts to boil. The vessel fluid mass also shows a long-term oscillation, caused by periodic injection of N_2 as the vessel pressure decreases, which results in a reduction in steam condensation in the cold leg. This causes injection of colder water into the downcomer where boiling is taking place. The downcomer level is shown in Figure 2.2-11, and the core level during reflood is shown in Figure 2.2-12. In the late reflood phase, the cladding at the top of the core continues to heat up while the quench front advances from the bottom-up cooling curves 4 and 5 (as shown in Figure 2.2-8).

2.2.3 AP600 Large-Break LOCA Transient

The AP600 WCOBRA/TRAC model has been developed in a consistent fashion with other PWR models.[5] The AP600-specific features, such as the reactor vessel reflector structural design, operating conditions, and loop configuration can be treated through the code input. The AP600 reactor vessel is shown in Figure 2.2-13. The reactor vessel nodalization is shown in Figure 2.2-14 and is similar in detail to the VRA vessel shown in Figure 2.2-2.

[

]^{a,c}

Figure 2.2-15 shows the cross section of the reactor vessel at the core elevation. [

]^{a,c} This modeling approach is consistent with those used in two-, three-, and four-loop plants, as discussed in the WCOBRA/TRAC CQD, where [

]^{a,c}

The loop model for the AP600, which is similar to the VRA loop, is shown in Figure 2.2-16.

The initial plant conditions for the WCOBRA/TRAC large-break LOCA analysis are summarized in Table 2.2-2 for the AP600 superbounded analysis. The 10 CFR 50.46 stipulates that the PCT be calculated at the 95 percent probability level. Such a calculation includes consideration of the components of analysis uncertainty, including: the computer code, accident initial conditions, accident boundary conditions, and the uncertainty in plant parameters/systems.

In a superbounded analysis, bounding assumptions are made concerning a number of the initial/ boundary conditions/parameters, as detailed in Table 2.2-2. Referring to that table, item by item:

- Bounding high-power and steam generator tube plugging (SGTP) values are chosen together with minimum system flow.
- Plant design is such that no active failure of a safety-related component significantly impacts large-break LOCA performance. Minimizing the accumulator delivery bounds the uncertainty in system performance pertinent to the large-break LOCA event.
- A worst-break case is identified within appropriate break modeling uncertainties.
- Hot rod fuel pellet temperature is conservatively maximized.

- A conservative axial power shape is used, based on previous WCOBRA/TRAC studies.[6]

- A minimum containment pressure is conservative.[6]

- Bounding values for peaking factors are used to provide the highest linear power and enthalpy rise heat rates.

- The AP600 contains many guide tubes that provide drain paths for upper head fluid into the core during a LOCA event and also upper support plate holes to facilitate such draining. The hot assembly location in WCOBRA/TRAC is specifically chosen so that no such direct flow communication exists for draining upper head fluid into the hot assembly. This will penalize the hot assembly during the downflow period of blowdown.

- A best-estimate decay heat approach is applied with uncertainty (2 sigma) placed on the hot rod to bound its decay power.

- Both the accumulator initial condition and the uncertainty in the gas expansion constant are set to minimize accumulator delivery. The accumulator temperature was set to the maximum containment temperature. The accumulators provide the only ECCS injection that influences the resulting PCT. Operating bands and plant uncertainty for the accumulator are accounted for in a minimum delivery case that considers maximum initial water volume, minimum gas pressure, and maximum frictional resistance. Furthermore, the gas expansion coefficient is held at a high value throughout the AP600 large-break LOCA transient, even though the extended length of the accumulator delivery indicates that a lower value is appropriate. The net effect of these assumptions is to conservatively model the accumulator injection rate for refilling the reactor vessel and core.

A spectrum of large-break LOCAs at different break locations and discharge coefficient (C_D) values were performed for the AP600.[5] A description of the most limiting break, C_D = 0.8 DECLG, follows.

The break was modeled to occur in one of the cold legs in the loop containing the core makeup tanks (CMTs). Past sensitivity studies with WCOBRA/TRAC[6] have demonstrated that locating the cold leg break in the loop that does not contain the pressurizer renders conservative results. The steam generators are assumed to be isolated immediately upon the inception of the break in order to maximize their stored energy. Shortly after the break opens, the vessel rapidly depressurizes, as shown in Figure 2.2-17, and the core flow quickly reverses, as shown in Figure 2.2-18. During the flow reversal, the hot assembly fuel rods dry out and begin to heat up. The massive size of the break causes an immediate, rapid pressurization of the containment. One second into the transient, credit is taken for receipt of an "S" signal due to high containment pressure. Applying the pertinent signal processing delay means that the valves isolating the CMT from the cold legs and direct vessel injection line begin to open at 2.2 seconds into the transient. Automatic reactor coolant pump (RCP) trip occurs 17.2 seconds into the LOCA transient, until which time the RCPs are presumed to operate

normally. Core shutdown occurs due to voiding. No credit is taken for the control rod reactivity effect.

The system depressurizes rapidly as the initial mass inventory is depleted due to break flow. The pressurizer drains completely 7 seconds into the transient, and accumulator injection begins 12.5 seconds into the transient, as shown in Figure 2.2-19. Accumulator actuation shuts off CMT flow. [illegible] the isolation valve opened. The CMT liquid level remains well above the ADS sta[illegible]tion setpoint during the blowdown phase of the C_D = 0.8 DECLG LOCA transient.

The CMT flow is illustrated in Figure 2.2-20 and shows that the CMTs initially provide flow to the reactor vessel very early on in the transient. As the pressure drops, the accumulators begin to discharge and create a sufficient backpressure to close the check valves at the CMT discharge lines. The CMT injection f[illegible]most as quickly as it begins, and only 0.5 percent of the total CMT inventory is injecte[illegible] when this injection occurs, the core flow is downward and the downcomer is in a bypass mode so that the CMT injection flow is bypassed through the break. The CMT, therefore, does not contribute to the core cooling during the large-break LOCA.

The dynamics of the C_D = 0.8 DECLG case are shown in terms of the flow rates of liquid, vapor, and entrained liquid at the top of the core for the low-power periphery, open hole/support column average power interior, guide tube average power interior, and hot fuel assemblies. The clad temperature transients are sho[illegible] the 6-ft., 8.5-ft. and 10-ft. elevations in Figures 2.2-21 to 2.2-23. In these figures, rod 1 refe[illegible] the hot rod at the maximum allowed linear heat rate; rod 2 represents the average rod in the hot assembly that contains the hot rod; rod 3, the open hole/support column rod; rod 4, the guide tube rod; and rod 5, the low-power peripheral fuel assembly rod.

Figures 2.2-24 and 2.2-25 illustrate the impact of upper head drain through the guide tubes and upper support plate holes, respectively, on core flow. While liquid remains in the upper head above the top of the guide tubes, the guide tubes (Figure 2.2-24) are the preferred path for draining liquid into the upper plenum. Top-of-core flow is relatively stagnant for the first few seconds; once the upper head begins to flash, liquid drains directly down the guide tubes, and is able to penetrate into the core against continuous steam upflow. Liquid flow rates that exceed 600 lb/sec of continuous liquid and 100 lb/sec of entrained droplets occur between 4 and 13 seconds. At that point, the flow entering the guide tubes in the upper head is almost entirely steam; residual liquid is supplied to the guide tube fuel assemblies at an ever decreasing rate up to 20 seconds. The larger flow area between the upper head and upper plenum for the AP600 results in a larger and more substantial downflow in the core as compared to VRA.

Figure 2.2-25 presents the open hole/support column assembly top-of-core flow behavior. In contrast to the guide tubes, flow of liquid down into the core open hole/support column locations does not become significant until about 8 seconds of the C_D = 0.8 DECLG transient. Between 11 and 18 seconds, the combined flow of continuous and entrained liquid is 600 to 700 lb/sec; the entrained liquid flow continues to be significant until 23 seconds. After 10 seconds of transient, the downflow

pattern in the open hole/support column locations is established to the extent that vapor downflow is also predicted. During this time interval, vapor flows up out of the core in the guide tube locations.

Thus, there is a good flow of liquid into the top of the core at these locations from before 10 seconds to almost 20 seconds. The flow in the open hole and guide tube assemblies is sufficient to quench the fuel in the assembly (rod 3 and rod 4, respectively) at the 6-ft., 8.5-ft., and 10-ft. elevations, as shown in Figures 2.2-21 to 2.2-23.

Because the hot assembly can only receive draining liquid from the upper head indirectly, liquid downflow is delayed into this assembly. Nevertheless, by 10 seconds into the transient, liquid that has built up in the global region above the upper core plate begins to flow through the plate at the hot assembly location and then proceeds into the core (Figure 2.2-18). There is a significant flow of continuous and/or entrained droplet liquid into the hot assembly from 9 to 18 seconds. The liquid flow is enough to quench the hot rod and hot assembly rod at the 10-ft. elevation (Figure 2.2-23), but not at the 6-ft and 8-ft. locations (Figures 2.2-21 and 2.2-22), although there is effective cooling at those locations. More recent WCOBRA/TRAC versions that are consistent with the CQD may predict quenching of the heat assembly rods, whereas the 1992 version reported in the SSAR has not.

Figure 2.2-26 demonstrates that liquid downflow exists through the top of the peripheral core assemblies from the first fraction of a second through the end of blowdown in the $C_D = 0.8$ DECLG transient. The low power of the fuel in this region leads to a small clad temperature excursion for the peripheral rod, shown in Figures 2.2-21 and 2.2-23. Some of the initial upper plenum inventory passes through initially, cooling the fuel. Thereafter, liquid downflow travels from the upper head into the core through open hole/support column and/or guide tube channels and into the global region above the upper core plate, and is then delivered into the low-power peripheral channel.

By 11 seconds into the transient, the entire length of the peripheral rods are quenched and remain quenched through the end of blowdown.

As the vessel depressurizes during blowdown, liquid inventory continues to be depleted and the hot assembly void fraction increases (Figure 2.2-27). Curve 1 of Figure 2.2-27 is at the bottom of the active fuel, curve 2 is the void fraction at the core midplane, and curve 3 is at the top of the core. This results in reduced core flow and the cladding temperature excursion for the hot assembly. Later, clad temperature excursions occur at other regions of the core.

About 12.5 seconds into the transient, the accumulator begins to inject water into the upper downcomer region (Figure 2.2-19), initially, bypassing some of the water to the break. At approximately 21 seconds, accumulator water begins to flow into the lower plenum. Lower plenum and downcomer liquid levels are plotted in Figures 2.2-28 and 2.2-29, and the core hot assembly liquid level is shown in Figure 2.2-30.

At approximately 56 seconds, the lower plenum fills to the point where water begins to reflood the core from below. The void fraction at the core bottom begins to decrease (Figure 2.2-27). Eventually, core cooling increases substantially and the peak cladding temperature (PCT) begins to decrease as the core water level rises.

Figures 2.2-31 through 2.2-33 present plots of PCT at the 6-, 8.5- and 10-ft. elevations for the first 2 minutes of the blowdown and reflood phases of the entire transient and shows the hot rod PCT up until the start of the long-term cooling phase. These figures illustrate the clad heatup response (and PCT turnaround) for both the blowdown and reflood phases of the limiting C_D = 0.8 DECLG break) as being 1565°F at 102 seconds.

It should be noted that more recent AP600 C_D = 1.0 large-break calculations have shown hot rod quench during blowdown with WCOBRA/TRAC-Mod7A version of the code. There calculations were supplied in response to RAI 952.46.

The gradual heat up of the fuel rod after blowdown and during refill and reflood is due to the lower accumulator flow for the AP600. The lower accumulator flow is specifically designed to extend the injection flow for a longer period of time and to provide additional injection coverage for small- break LOCAs. The AP600 accumulators are also substantially larger than the VRA accumulators, with 1700 $ft.^3$ water volume per accumulator, as compared with VRA accumulators, which have 1050 $ft.^3$ Also, both AP600 accumulators are available due to direct vessel injection, whereas in the VRA analysis, only two of three accumulators are available because the broken loop accumulator spills to containment.

The AP600 accumulators are the dominant injection system for a large-break LOCA because of their increased size and the extended duration of water flow.

The phenomena observed in the AP600 SSAR calculation is very similar to that seen in the VRA calculation. This confirms that the PIRT charts for both AP600 and existing plants should be basically the same and that WCOBRA/TRAC can represent the AP600.

TABLE 2.2-1 NORTH ANNA (VRA) INITIAL AND BOUNDARY CONDITIONS	
Parameters	**Value**
Plant Physical Description	
Pressurizer Location	intact loop
Hot Assembly Location	under flow mixer
Hot Assembly Type	17 x 17 V5H w/o IFM
Steam Generator Tube Plugging (SGTP)	15%
Plant Initial Operating Condition	
Core Power	2898 MWt (5.955 kw/ft.)
Hot Rod Average Power	10.12 kw/ft. ($F\Delta H$=1.7)
Hot Rod Peak Power	13.54 kw/ft. (FQ=2.5/1.1)
Low Power Region Relative Power	0.8
Axial Power Distribution	7.8 ft. peak (AO=12%)
Hot Assembly Burnup	BOL (500 MWD)
Plant Initial Fluid Conditions	
T_{avg}	586.8°F
Pressurizer Pressure	2250 psia
Loop Flow	92,800 gpm/loop (minimum minus uncertainty)
T_{UH}	T_{hot}
Accumulator Temperature	100°F
Accumulator Pressure	618 psia
Accident Boundary Conditions	
Break Location	cold leg
Break Type	guillotine
Break Size	1.0 x pipe area
Offsite Power	on
Safety Injection Flow	minimum minus uncertainty
Safety Injection Temperature	nominal (45°F)
Containment Pressure	lower bound

TABLE 2.2-2 AP600 CONDITIONS FOR THE LARGE-BREAK LOCA SUPERBOUNDED CASE
1. 102% core power, 10% uniform steam generator tube plugging, and minimum flow of reactor coolant are assumed.
2. Only safety-related systems operate.
3. Beginning of life cycle 1 conditions are analyzed to maximize core stored energy. Fuel average temperature uncertainty applied to hot rod only.
4. Top skewed power shape with a positiv[illegible]5% axial offset.
5. Lower bound containment pressure.
6. Conservative maximum values of peaking factors, (F_q = 2.6, $F_{\Delta H}$ = 1.65).
7. Hot assembly is placed in an isolated location to minimize blowdown cooling.
8. 1979 ANS 5.1 decay heat with uncertainty on hot rod only.
9. Accumulator flow delivery minimized to extend bottom of core recovery time.
10. Accumulator temperature set to maximum containment temperature.
11. Single failure postulated is the failure of one of the two parallel path, intact loop CMT isolation valves to open upon receipt of signal.

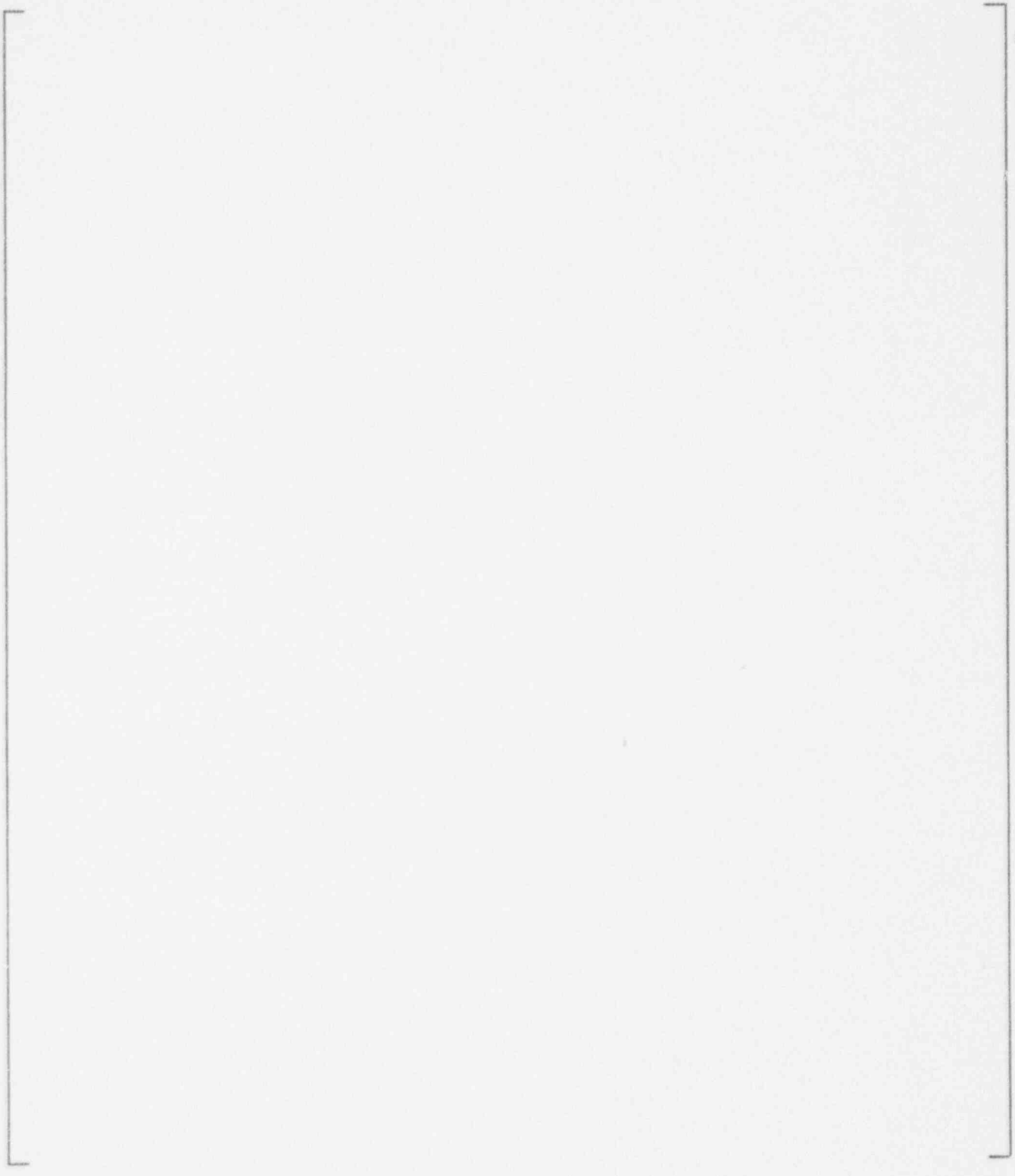

a,c

Figure 2.2-1 North Anna (VRA) Vessel Drawing

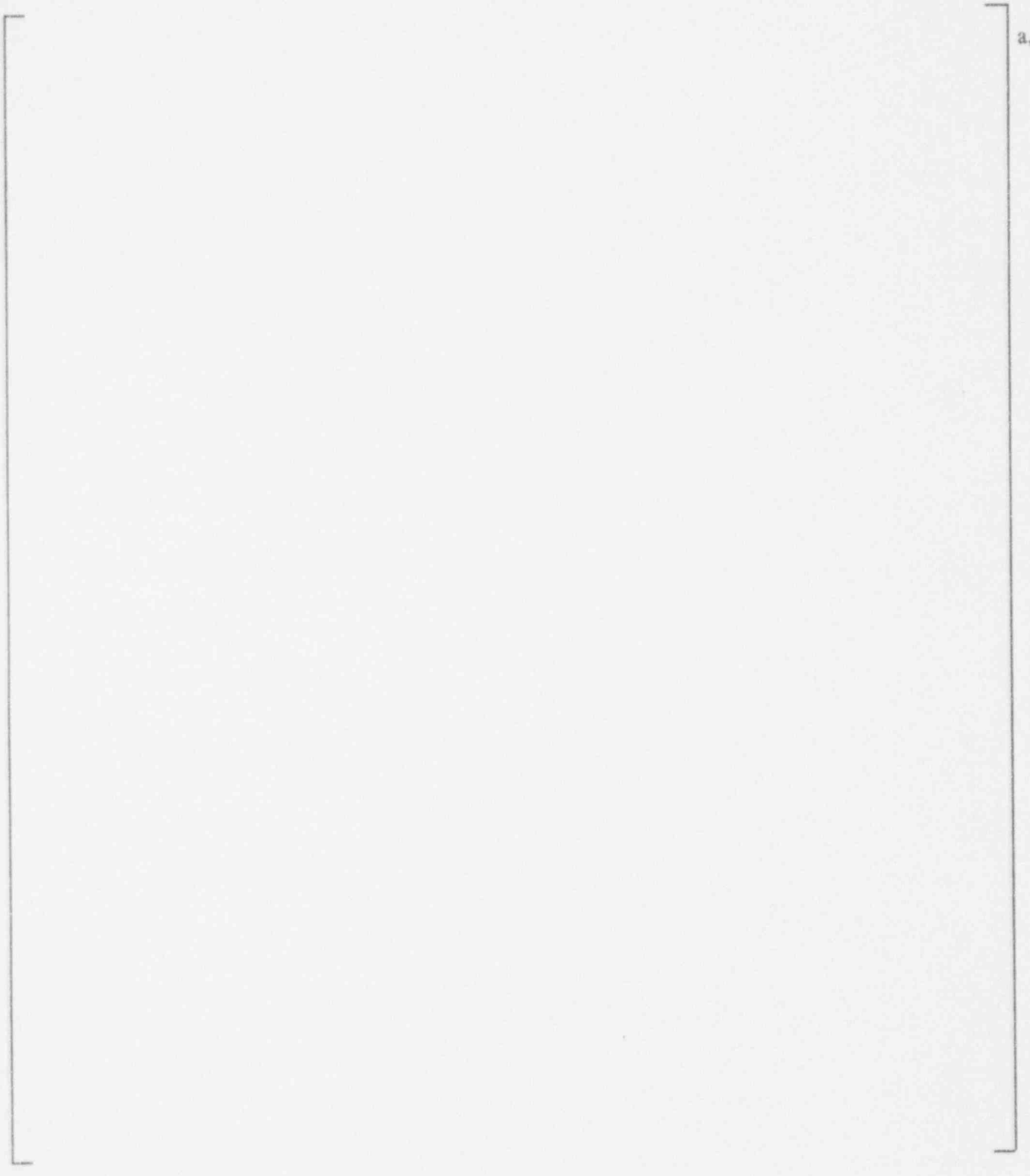

a,c

Figure 2.2-2 VRA WCOBRA/TRAC Vessel Model Noding

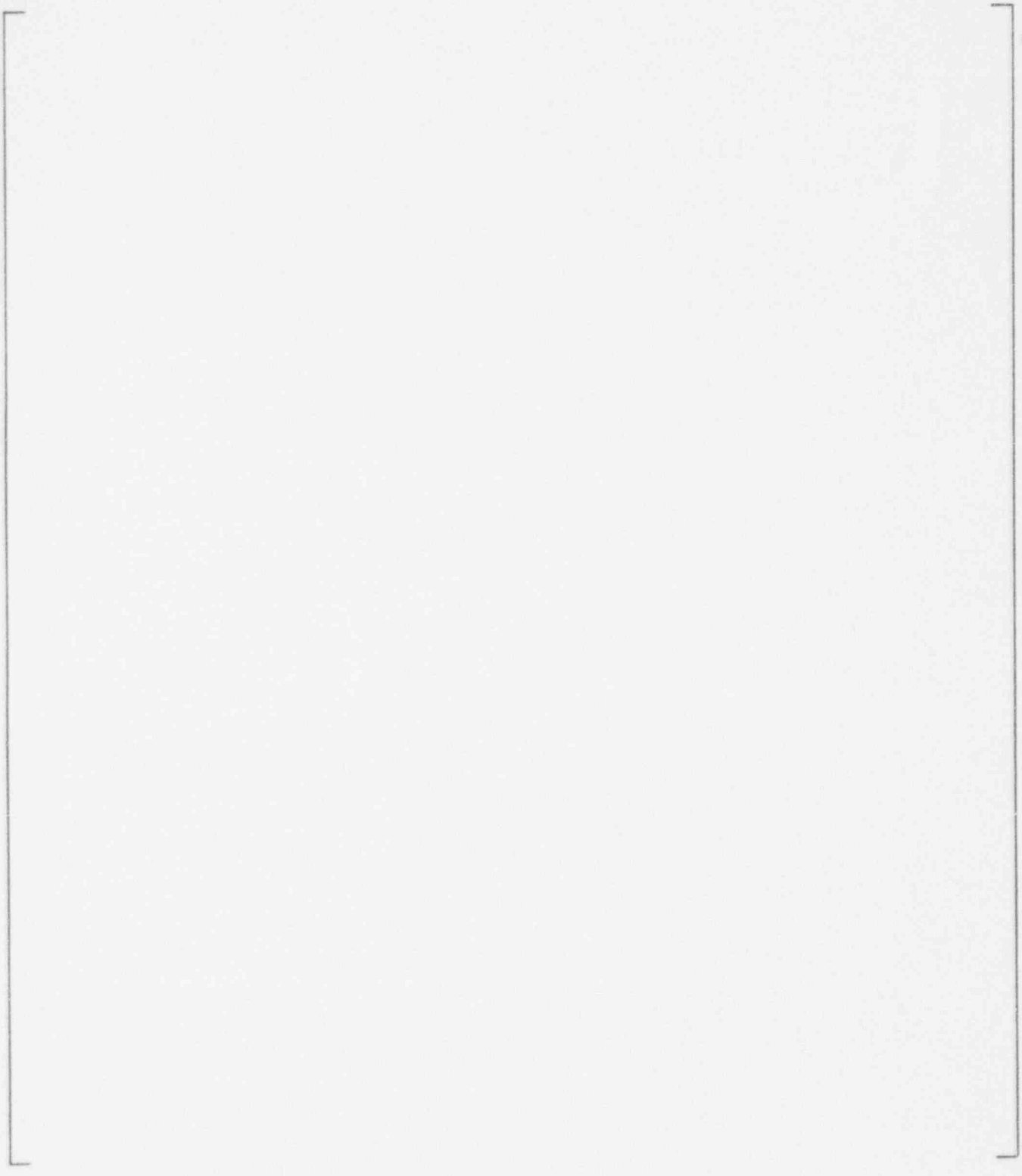

a,c

Figure 2.2-3 VRA Vessel Cross Section Noding

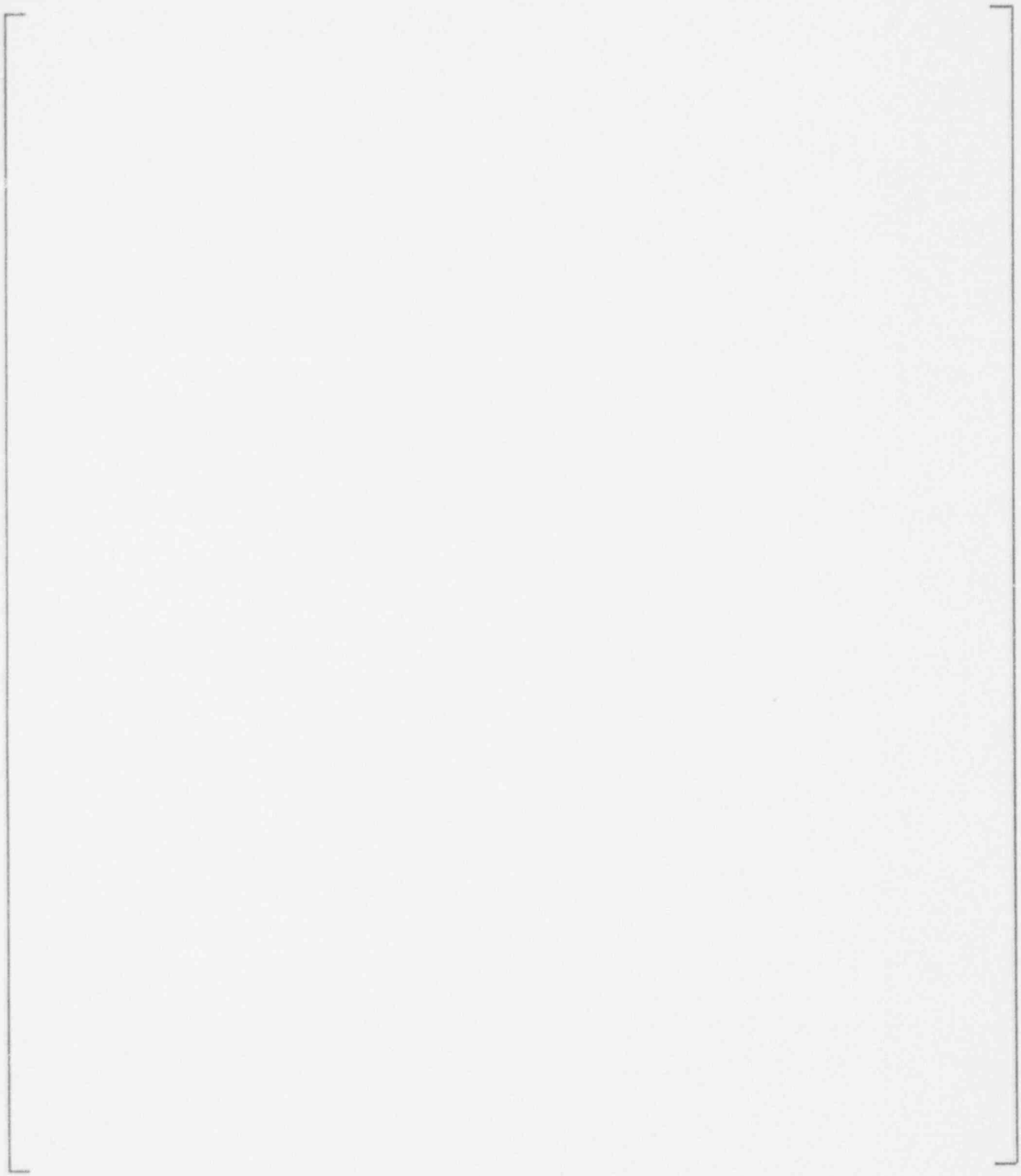

a,c

Figure 2.2-4 VRA Loop Noding

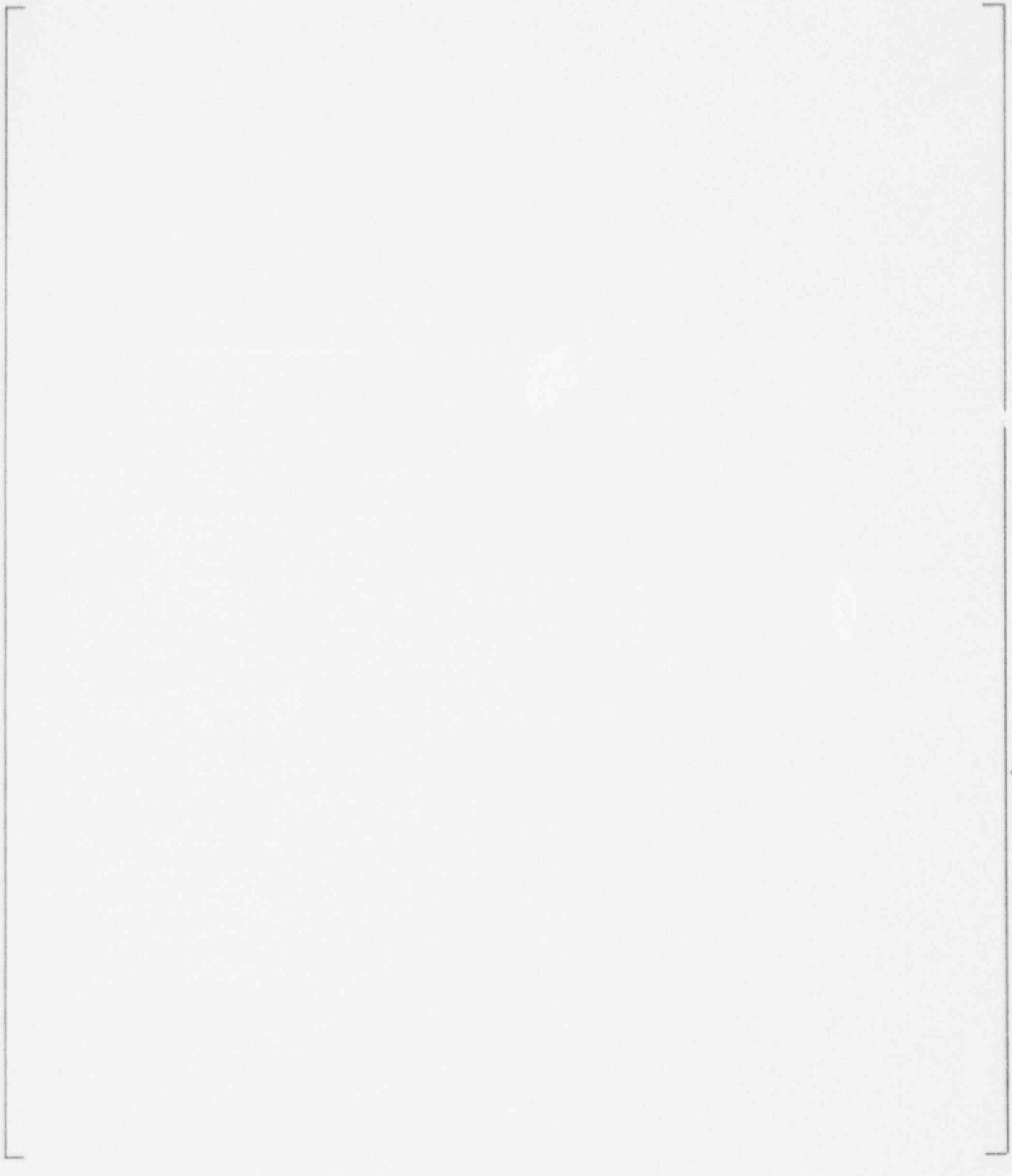

a,c

Figure 2.2-5 VRA System Pressure

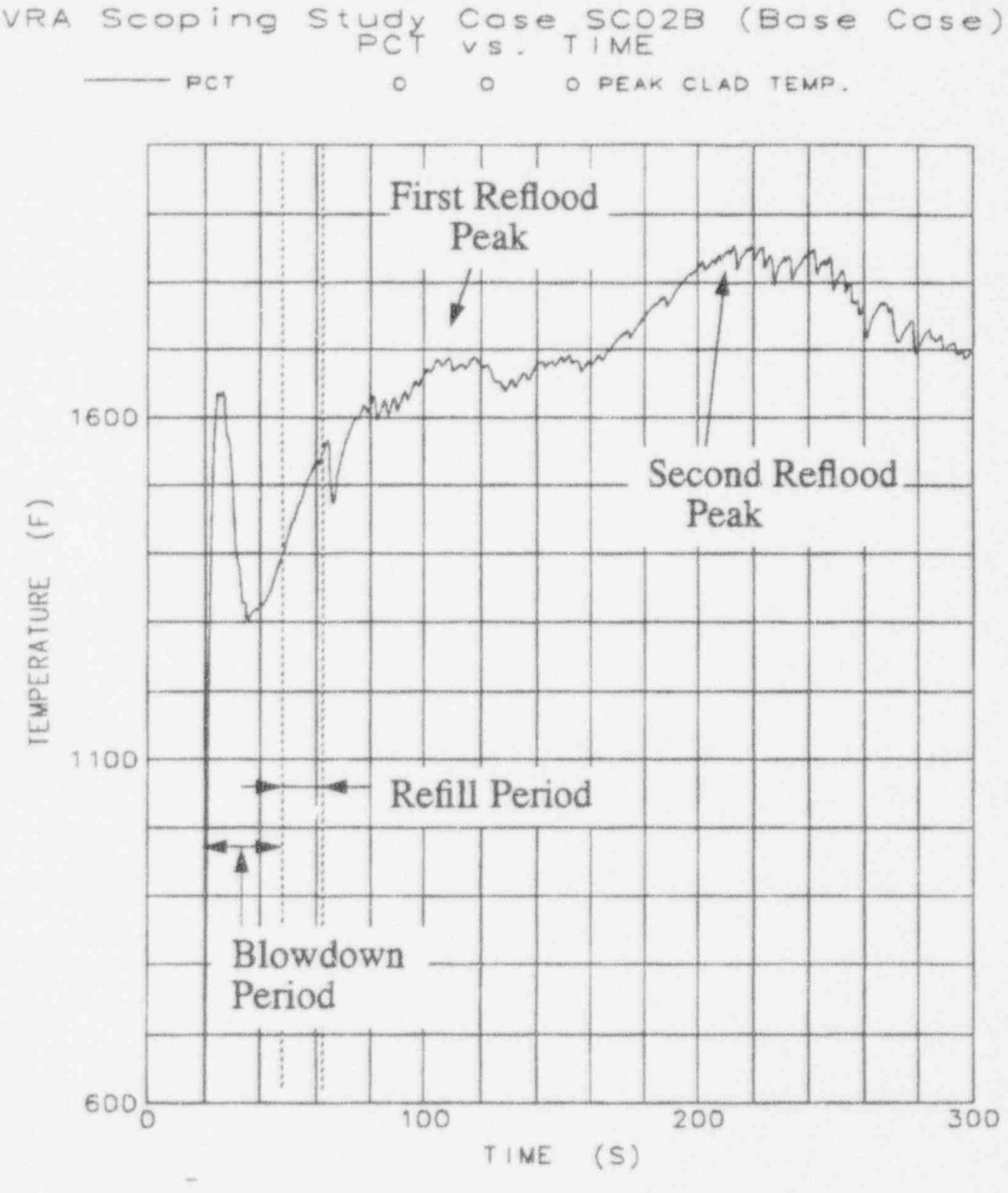

Figure 2.2-6 VRA Peak Cladding Temperature

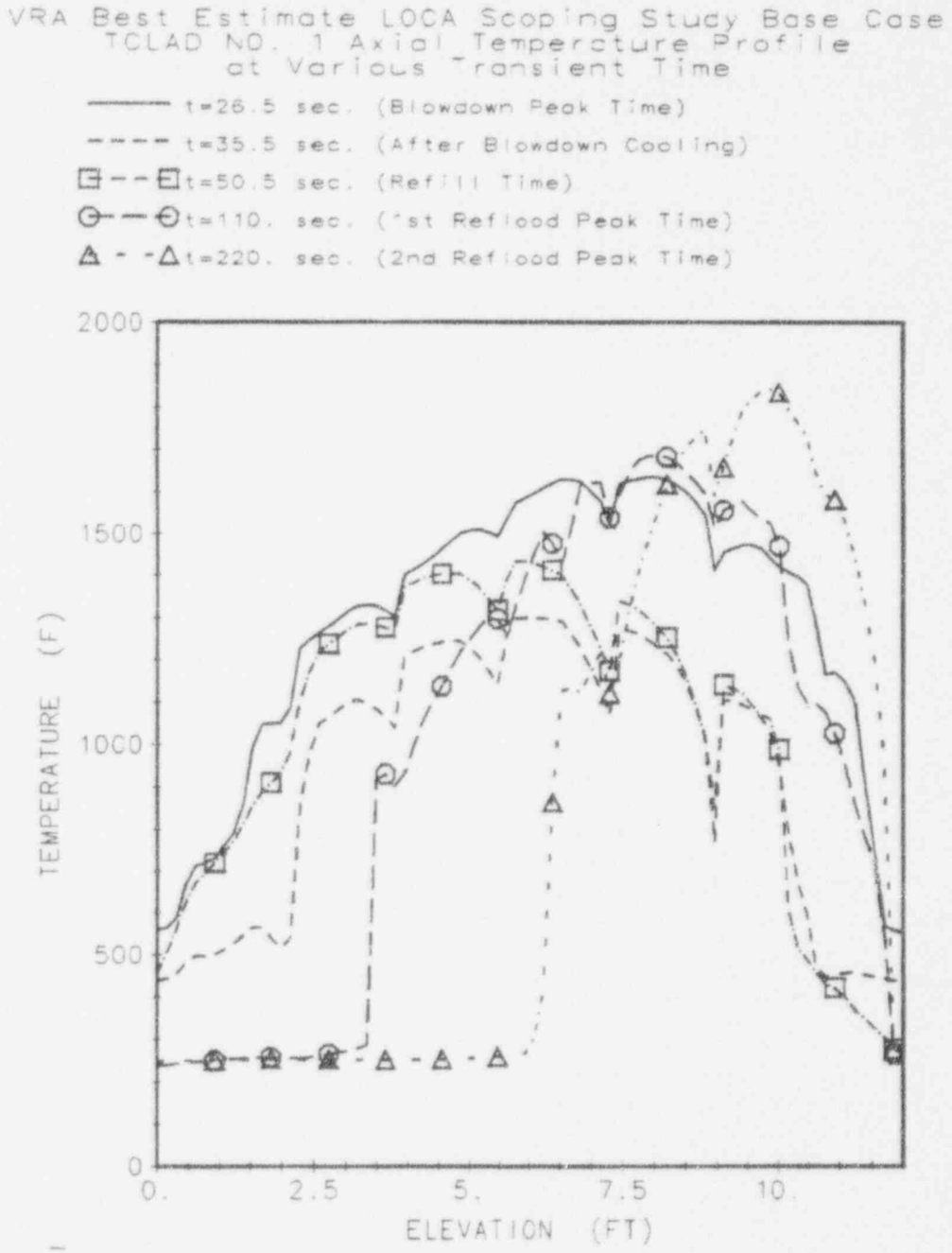

Figure 2.2-7 VRA Cladding Temperature at Different Elevations

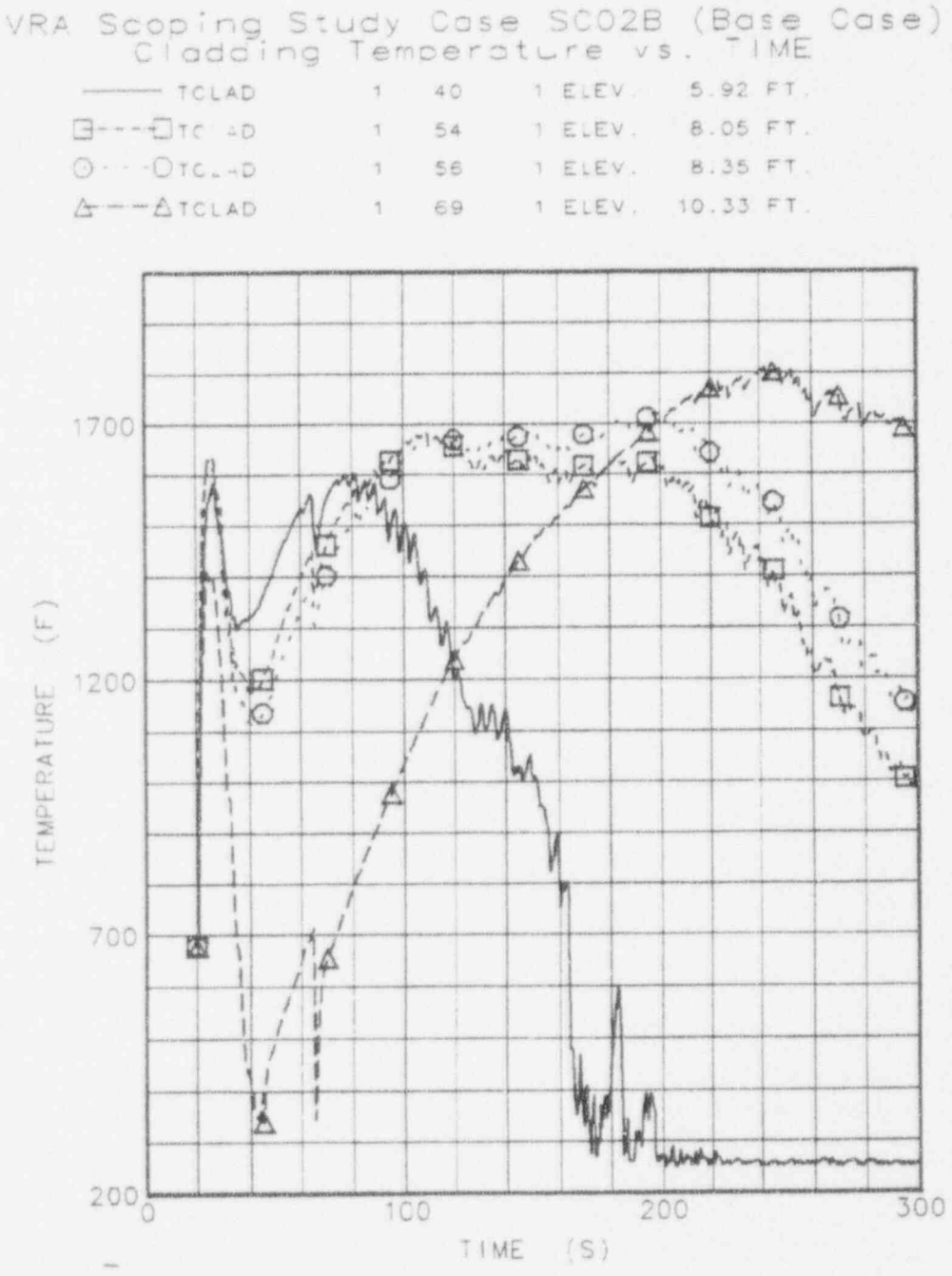

Figure 2.2-8 VRA Hot Rod Cladding Temperature at Several Points during the Transient

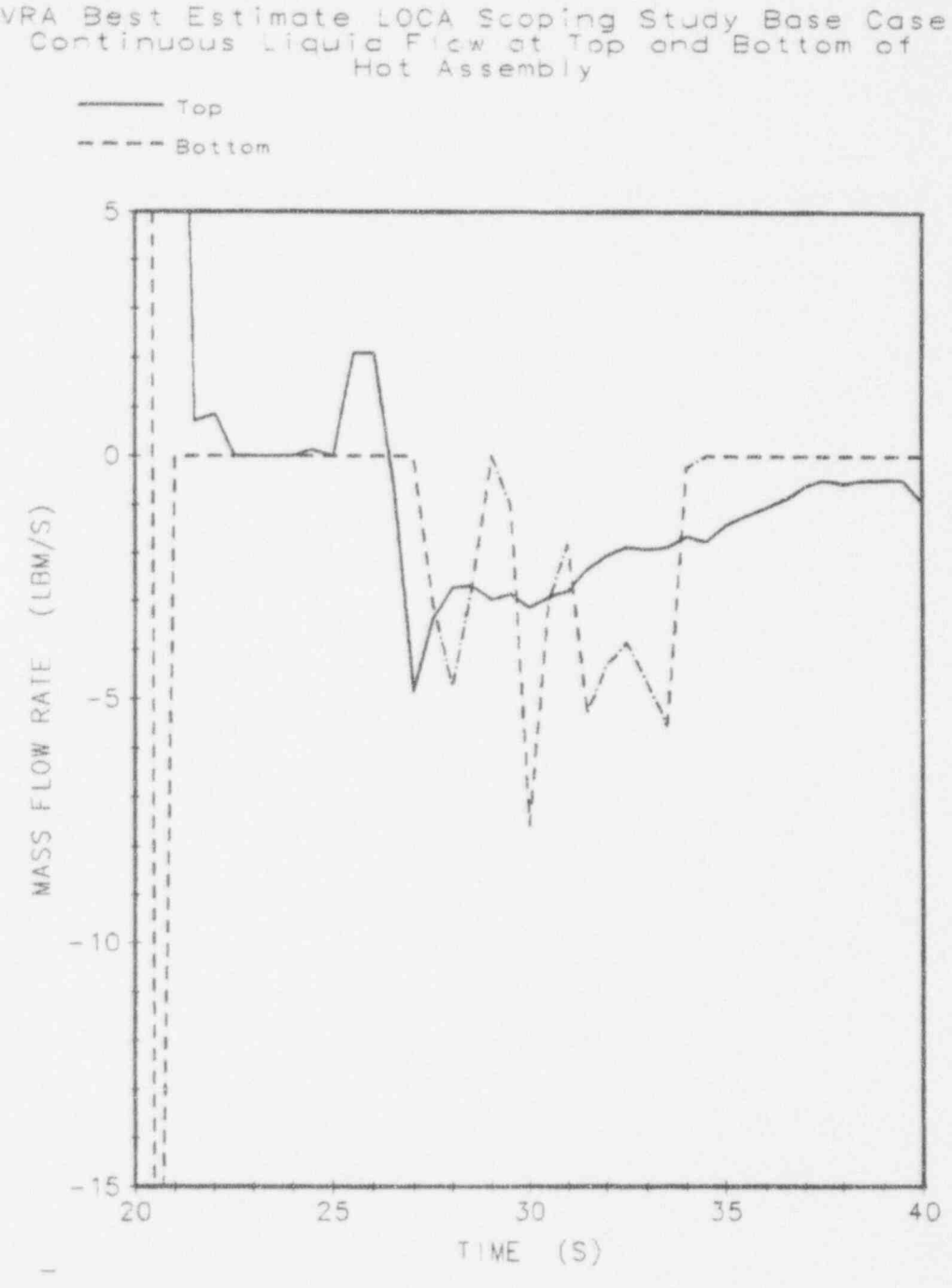

Figure 2.2-9 **Continuous Liquid Flowrate at Top and Bottom of Hot Channel during Blowdown**

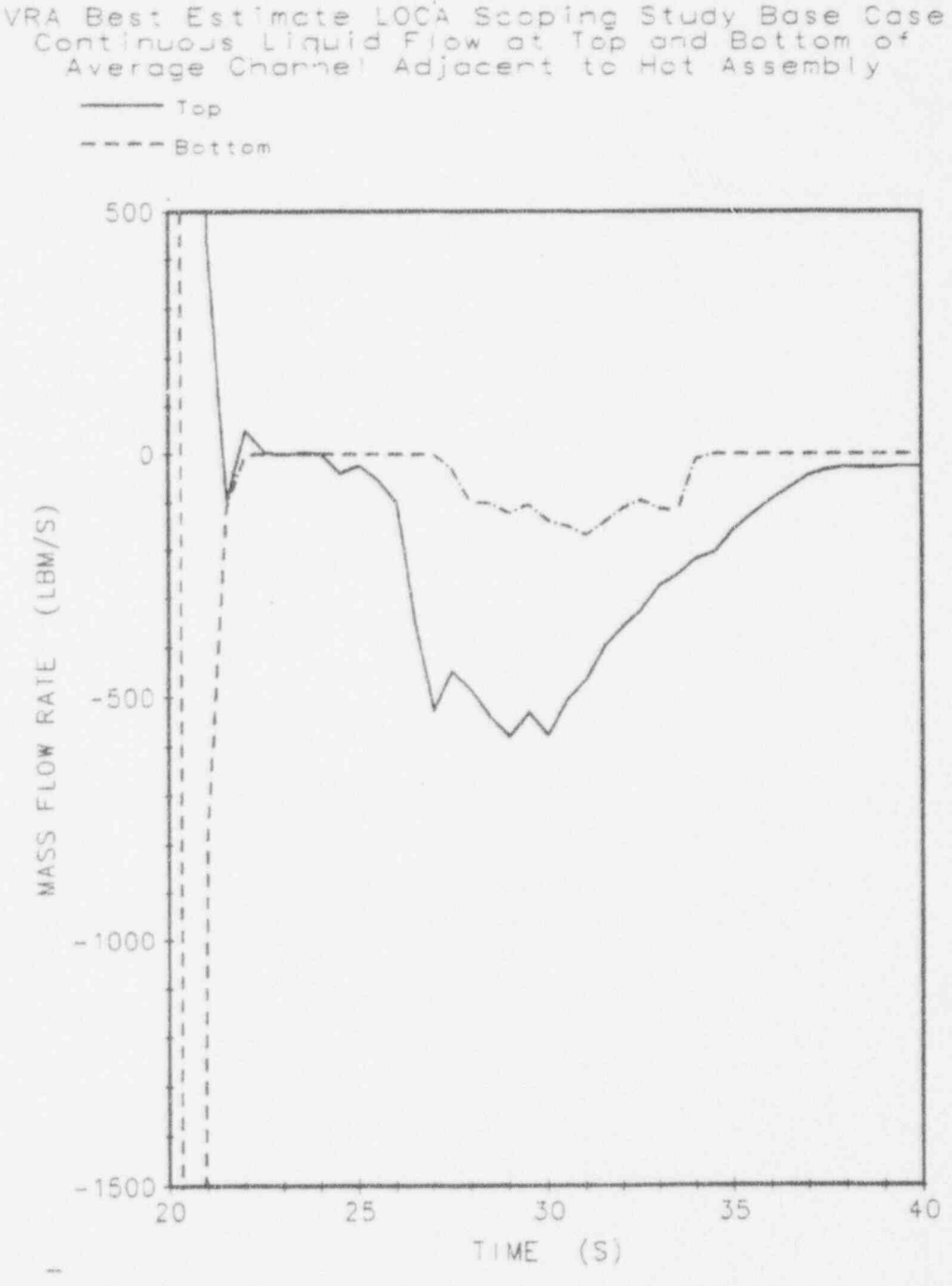

Figure 2.2-10 Continuous Liquid Flowrate at Top and Bottom of Average Channel Adjacent to Hot Channel during Blowdown

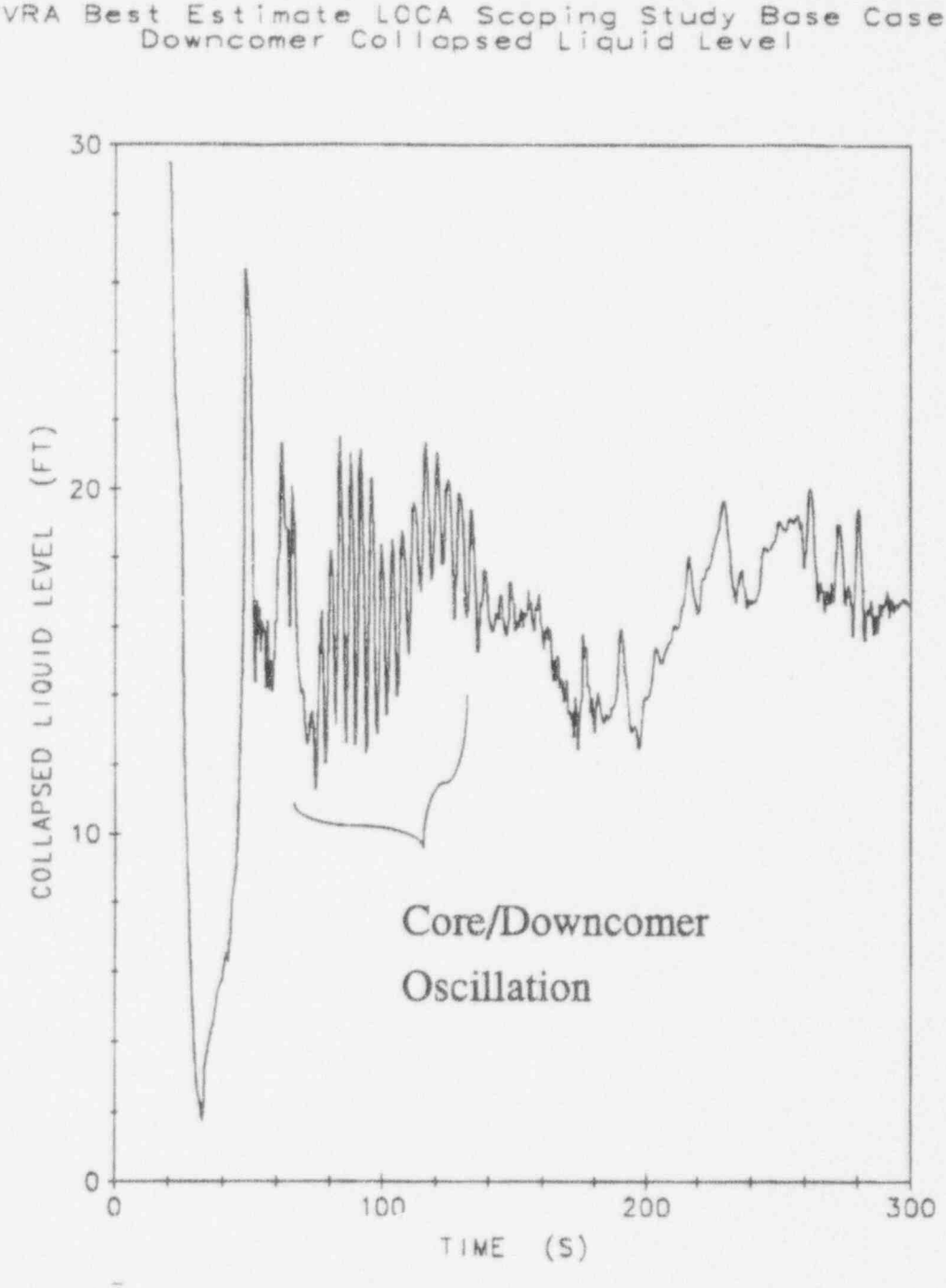

Figure 2.2-11 Collapsed Liquid Level in Downcomer

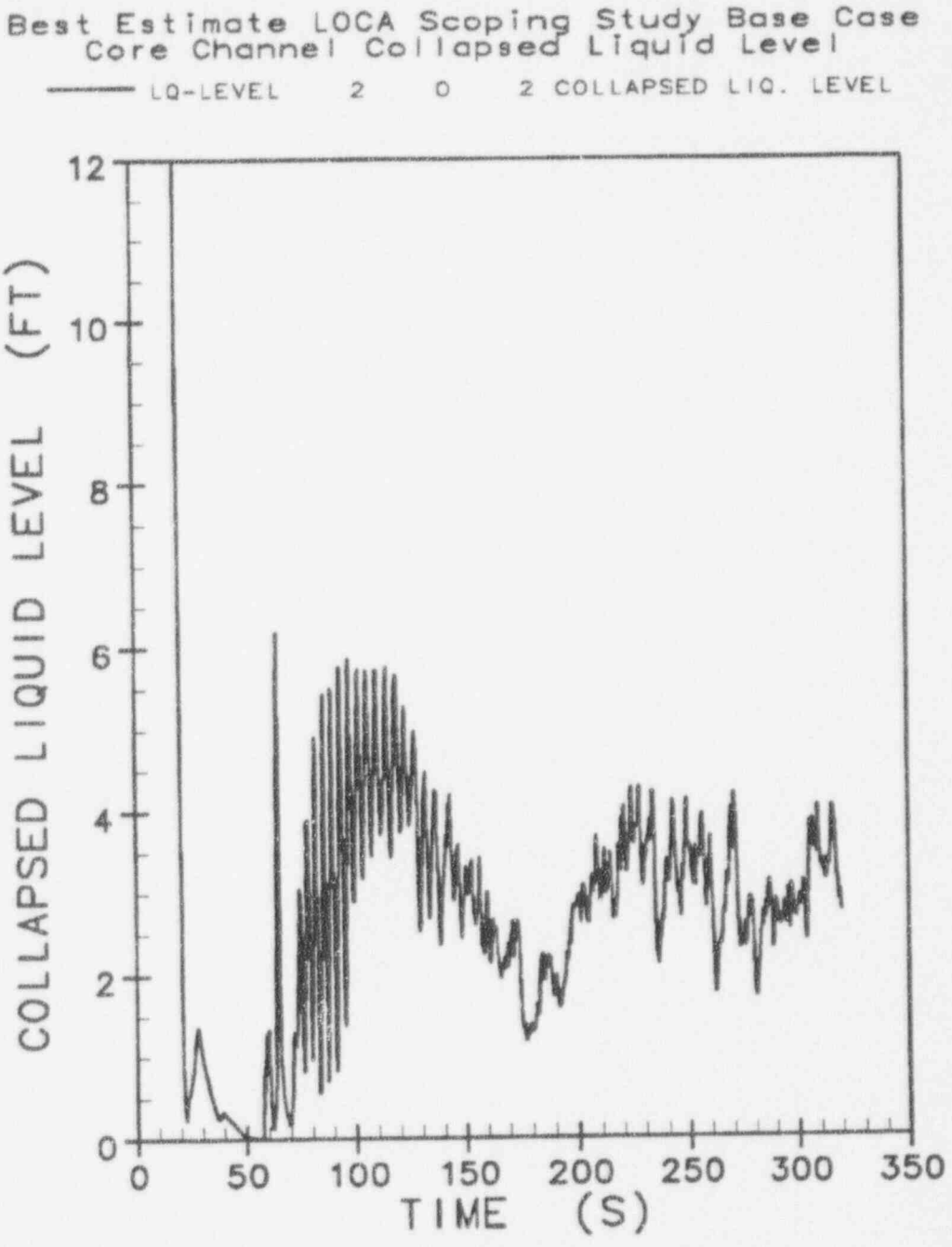

Figure 2.2-12 Collapsed Liquid Level in Core

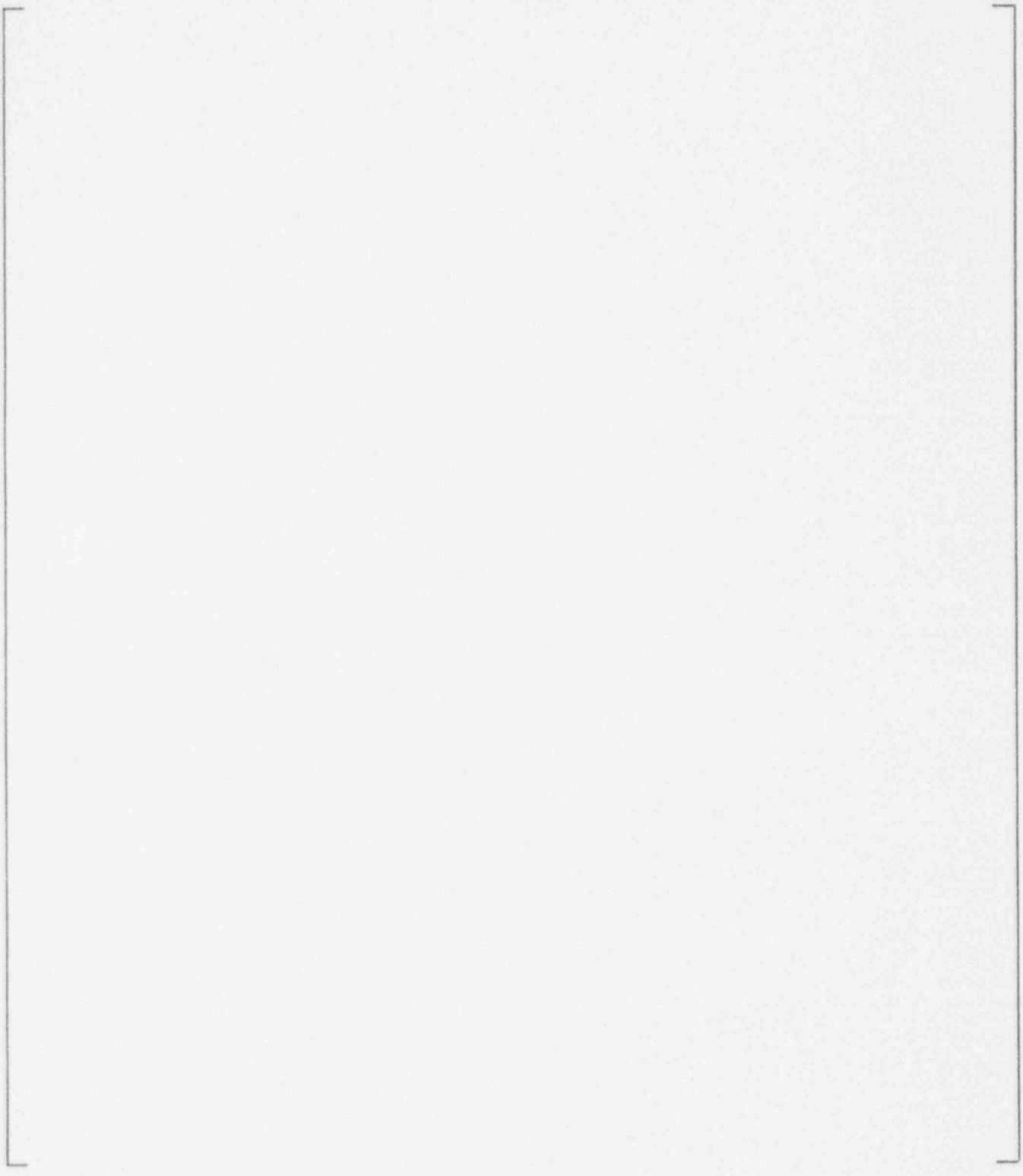

a,c

Figure 2.2-13 AP600 Vessel Schematic

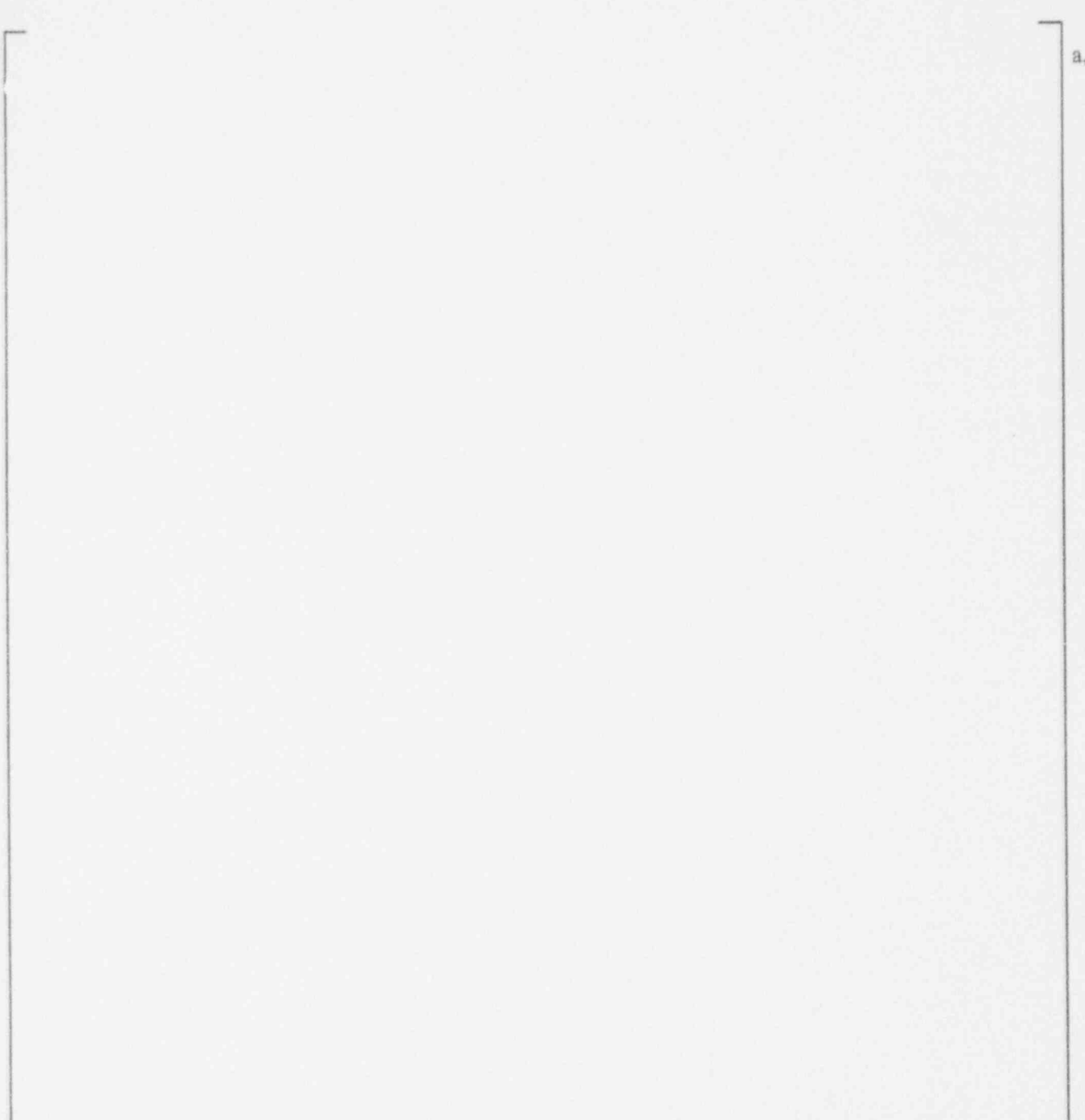

a,c

Figure 2.2-14 AP600 WCOBRA/TRAC Vessel Noding

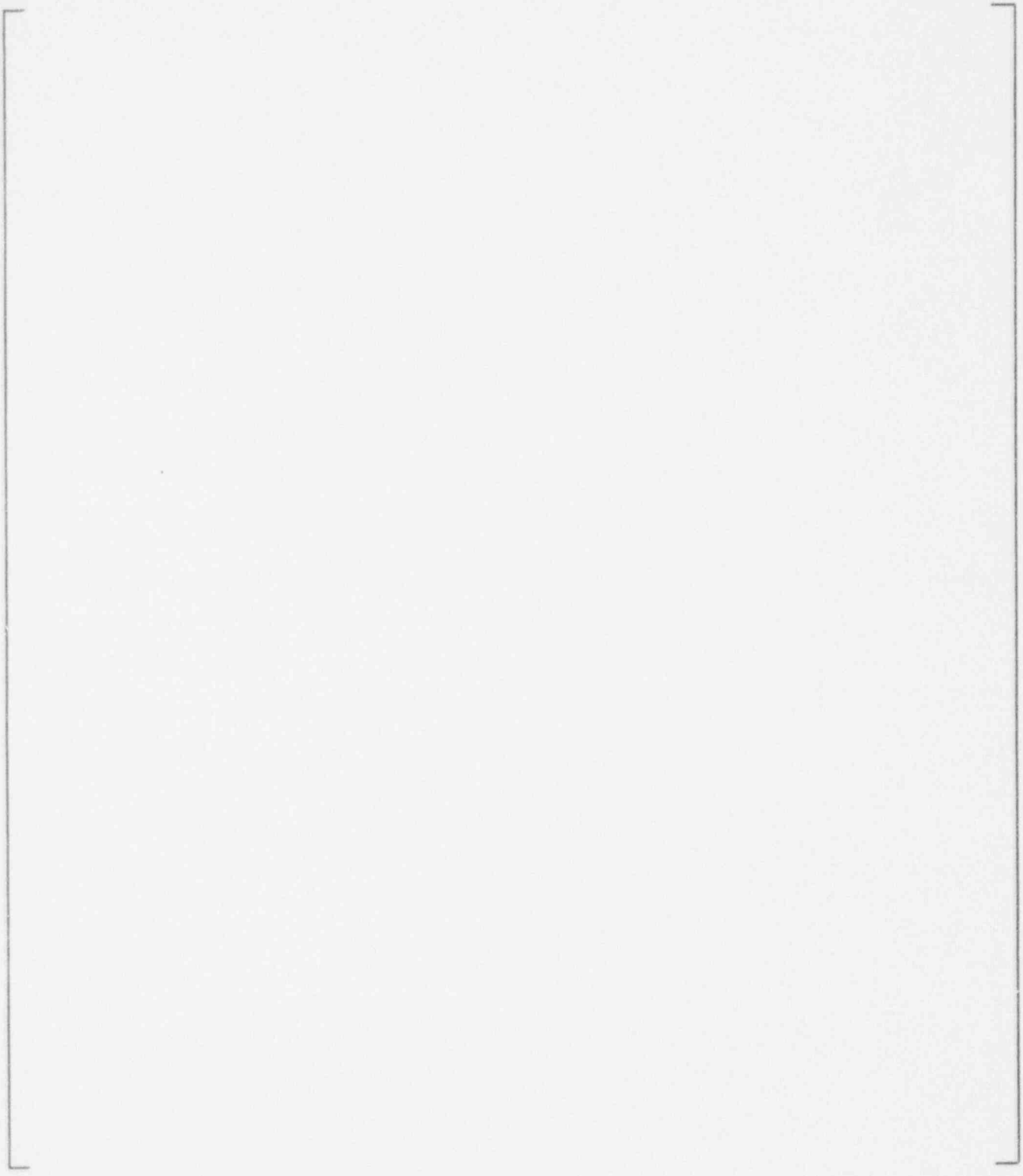

a,c

Figure 2.2-15 AP600 Section 4 Noding

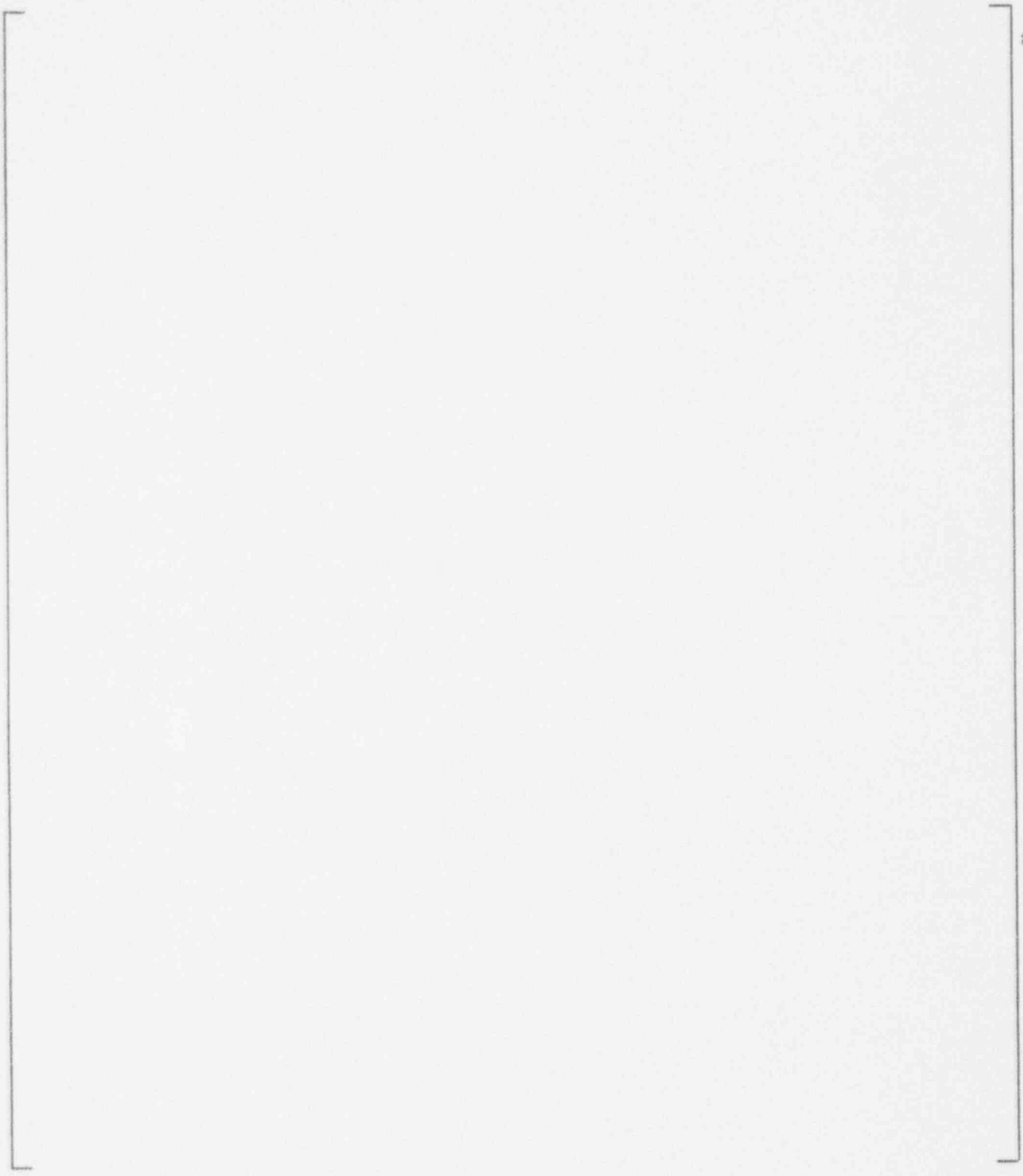

a,c

Figure 2.2-16 AP600 Loop Noding

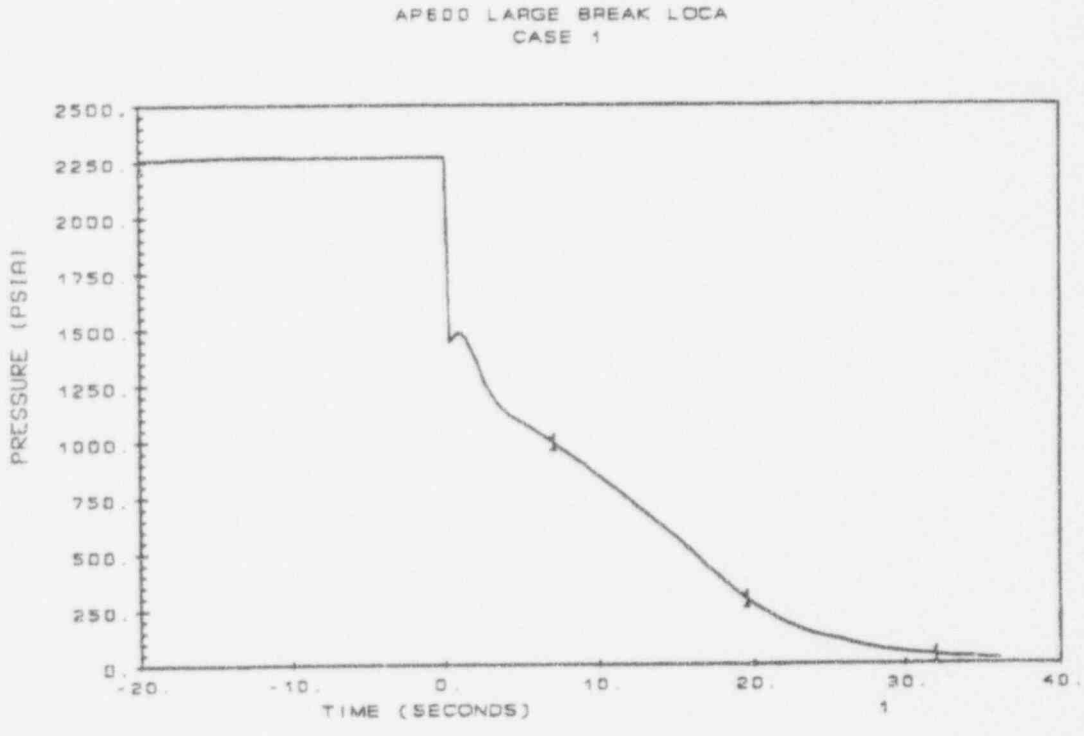

Figure 2.2-17 WCOBRA/TRAC AP600 Primary Pressure for the C_D=0.8 DECLG Break

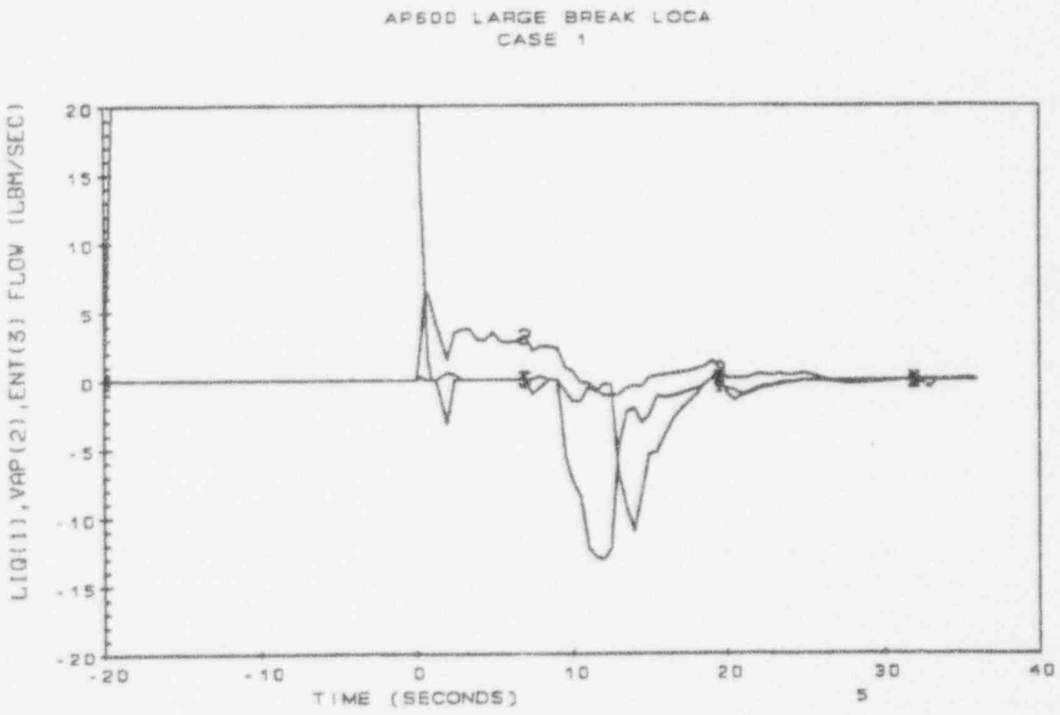

Figure 2.2-18 C_D=0.8 DECLG Blowdown, Top of Core Flow, Hot Assembly Channel

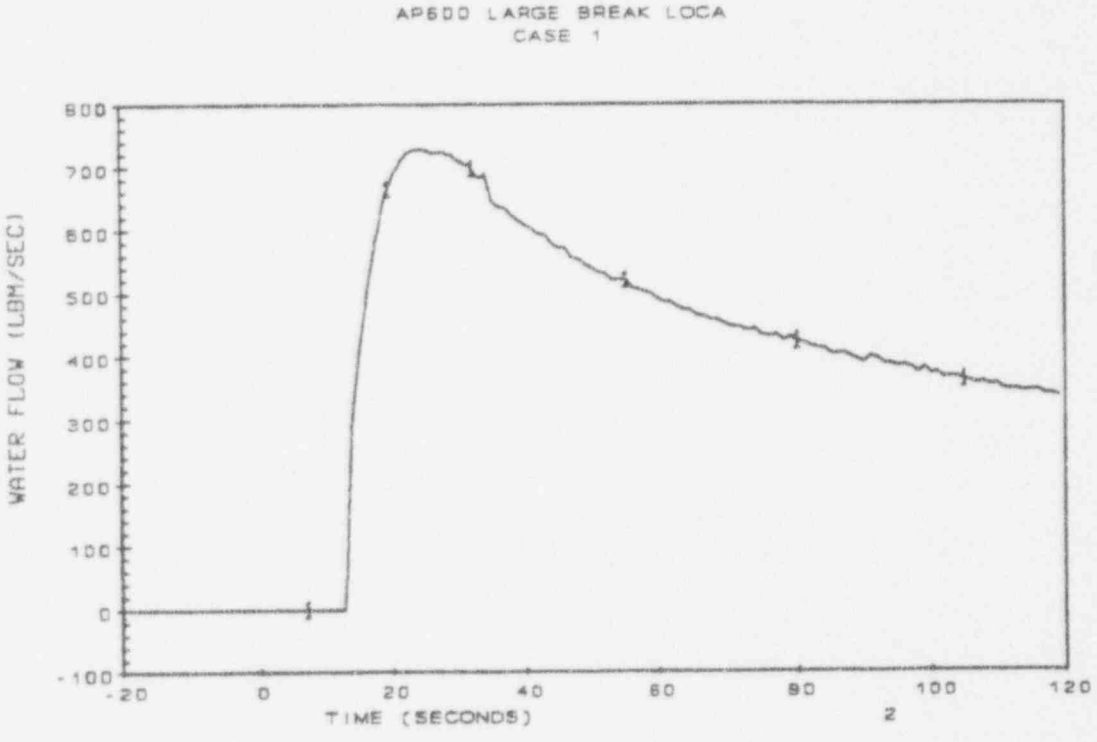

Figure 2.2-19 C_D=0.8 DECLG Transient, Accumulator Flow Rate From One Tank

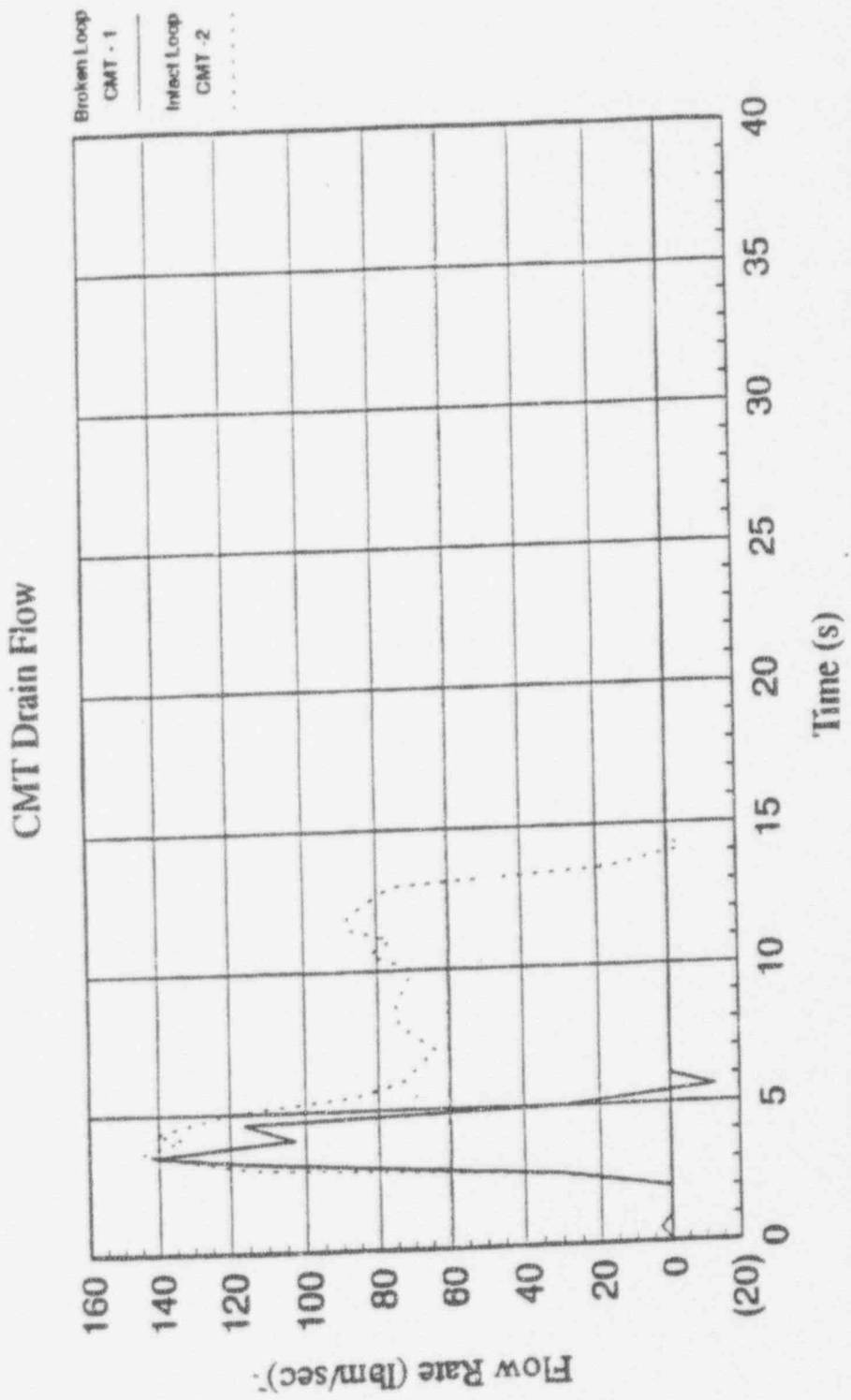

Figure 2.2-20 Core Makeup Tank Flow for C_D=0.8 DECLG Break

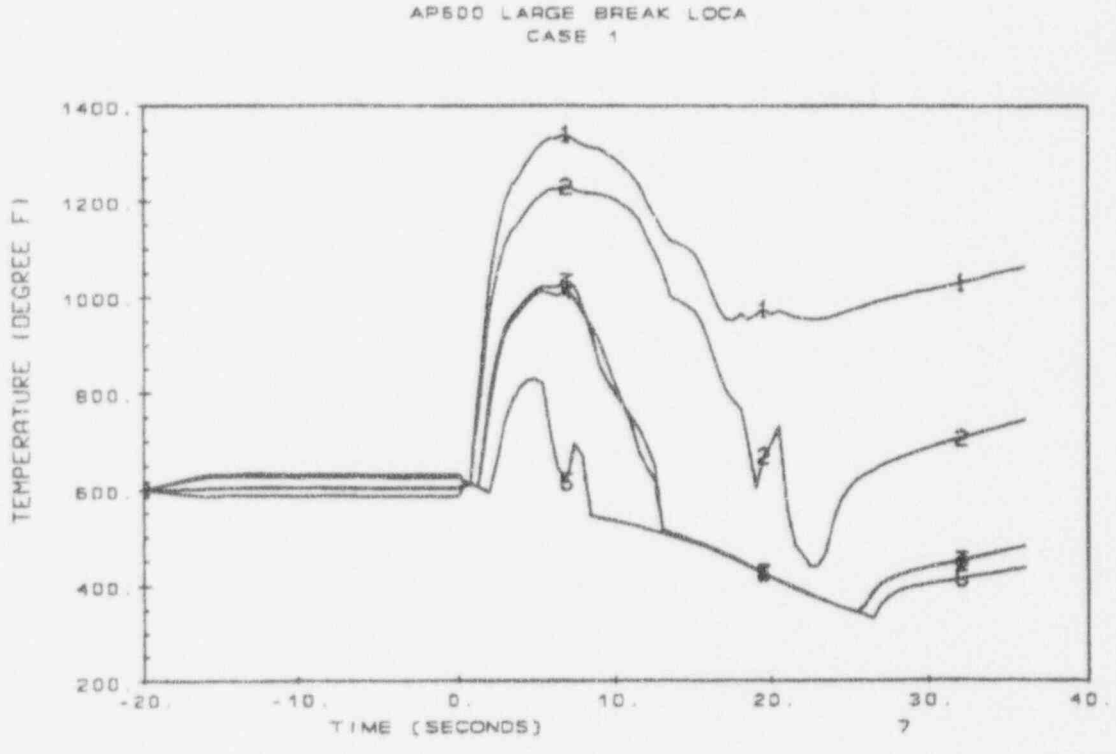

Figure 2.2-21 C_D=0.8 DECLG Blowdown, PCT at 6.0 Ft. Elevation, Rods 1 thru 5

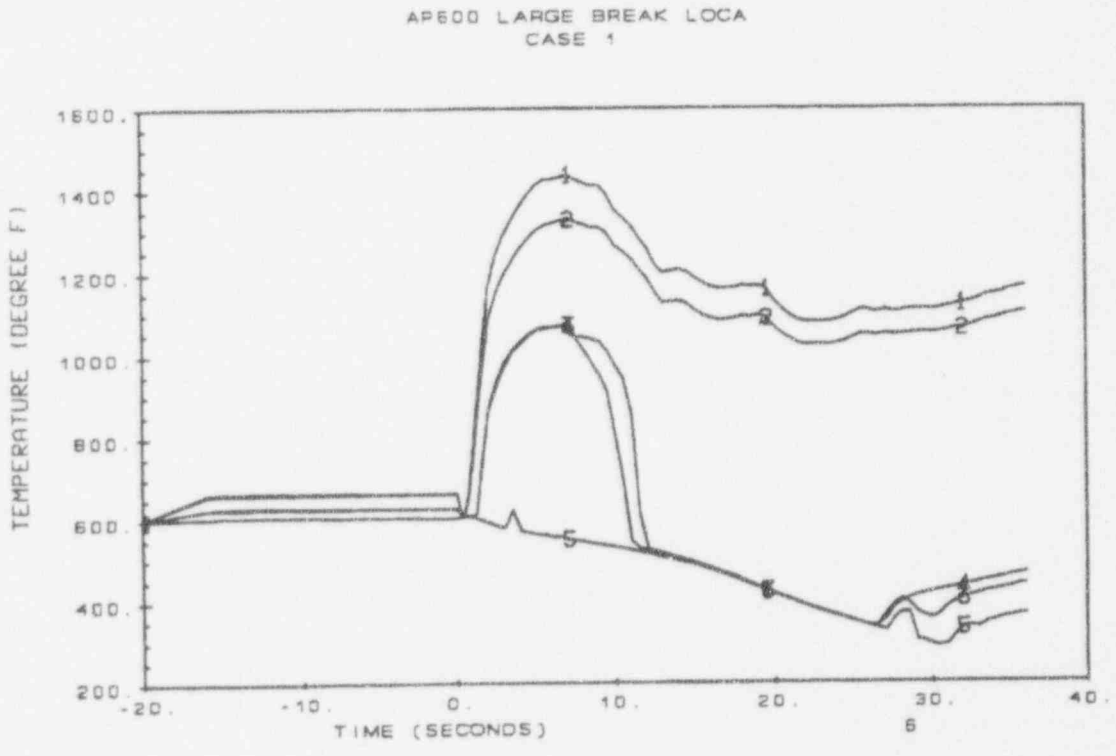

Figure 2.2-22 C_D=0.8 DECLG Blowdown, PCT at 8.5 Ft. Elevation, Rods 1 thru 5

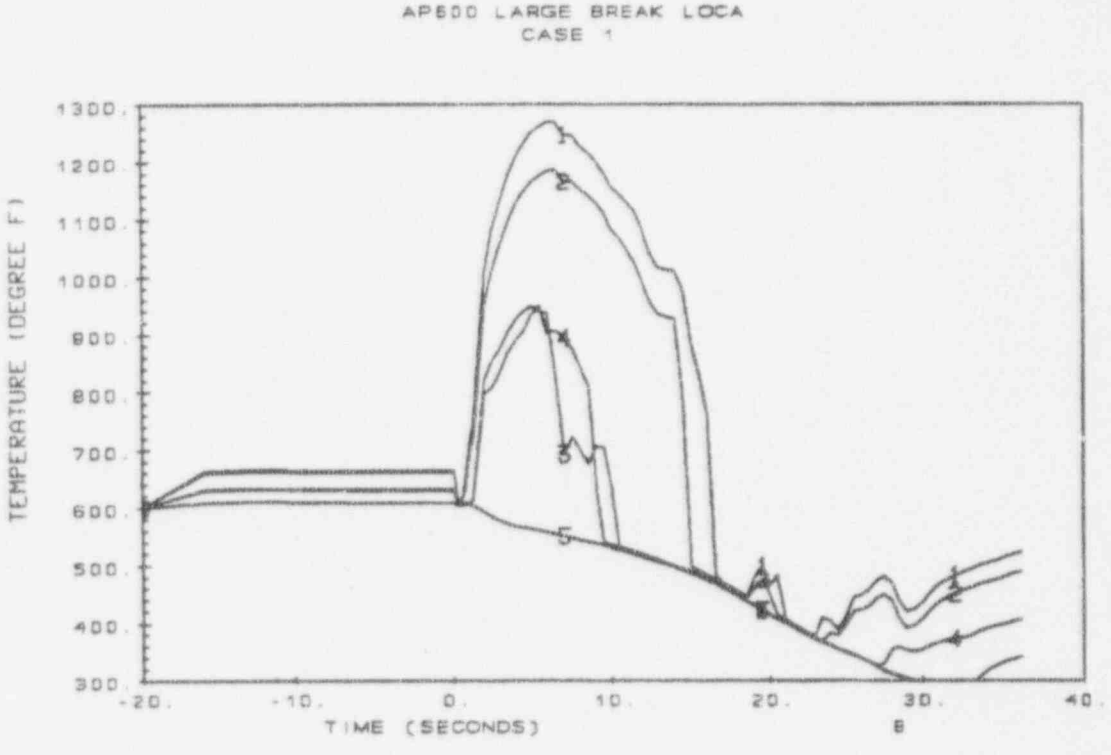

Figure 2.2-23 C_D=0.8 DECLG Blowdown, PCT at 10.0 Ft. Elevation, Rods 1 thru 5

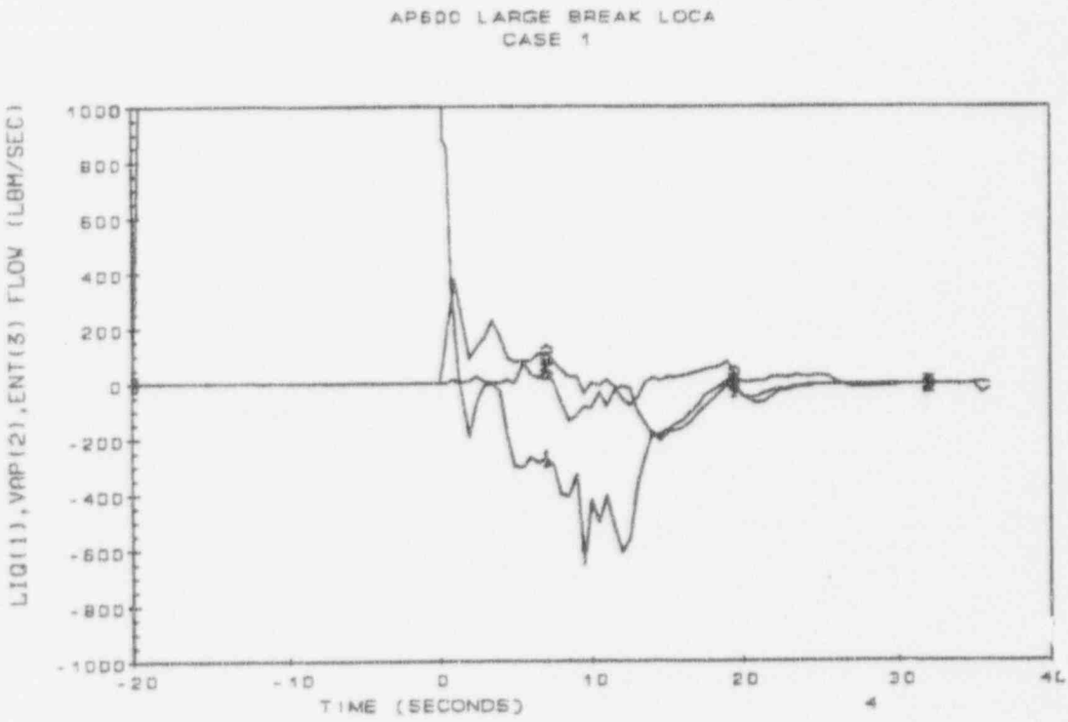

Figure 2.2-24 C_D=0.8 DECLG Blowdown, Top of Core Flow, Guide Tube Channel

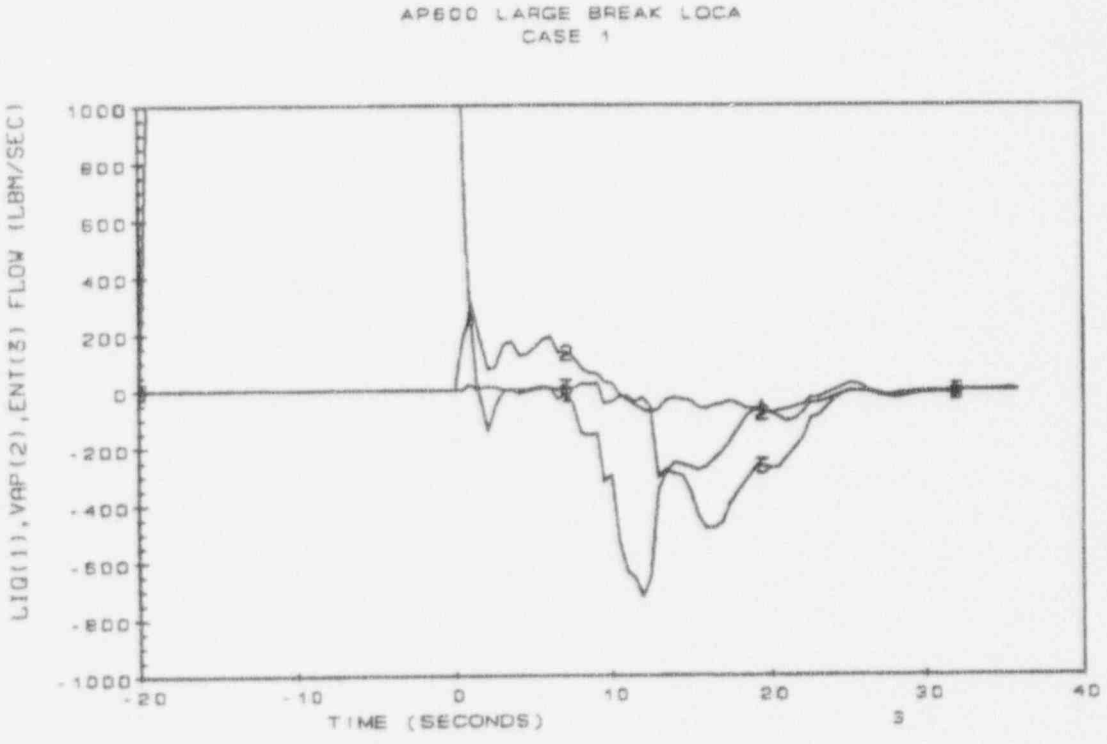

Figure 2.2-25 C_D=0.8 DECLG Blowdown, Top of Core Flow, Open Hole/Support Column Channel

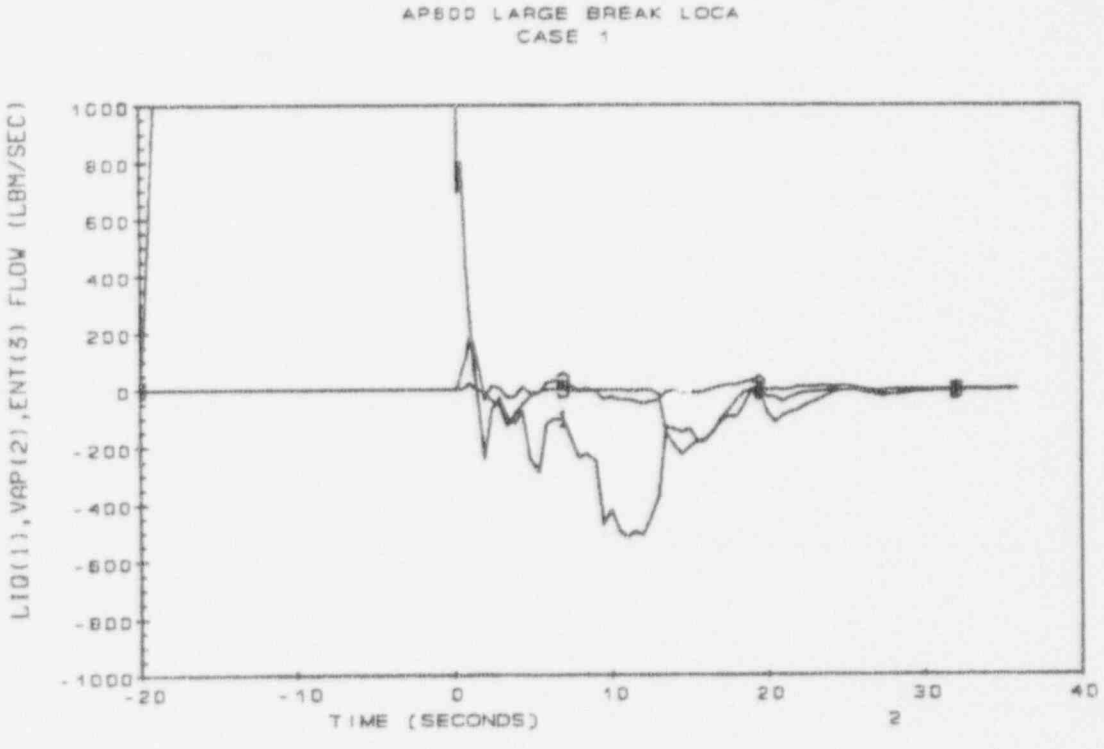

Figure 2.2-26 C_D=0.8 DECLG Blowdown, Top of Core Flow, Peripheral Channel

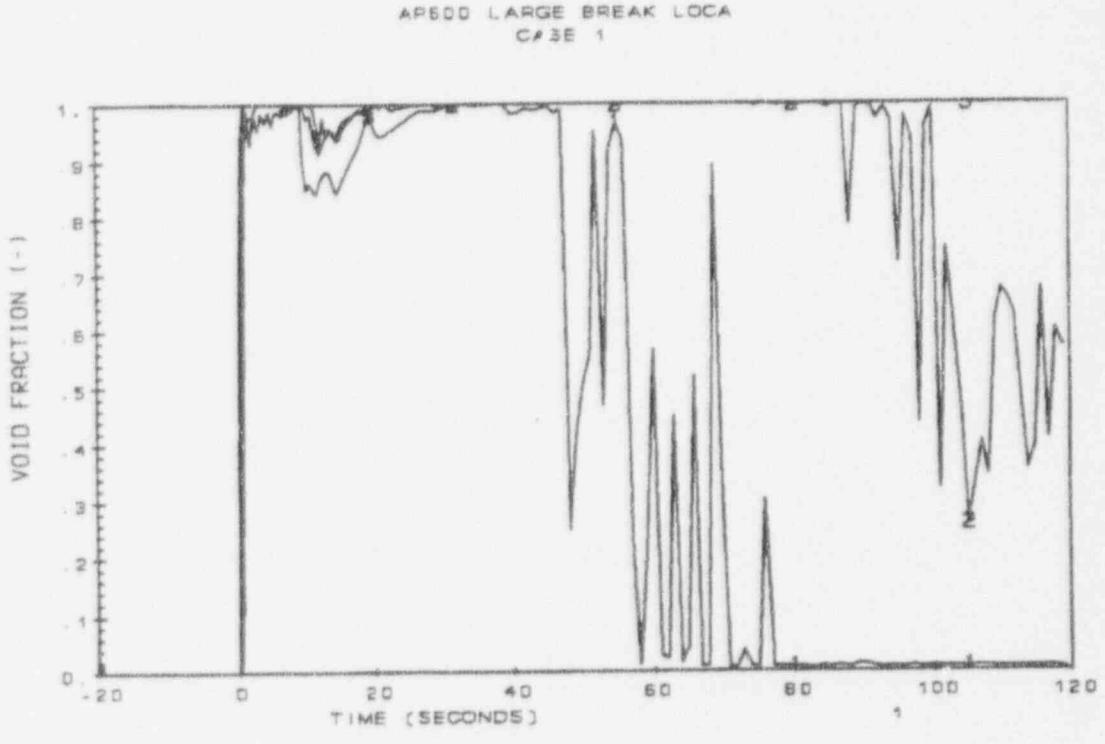

Figure 2.2-27 C_D=0.8 DECLG Transient, Core Void Fraction Hot Assembly Bottom, Midplane, Top

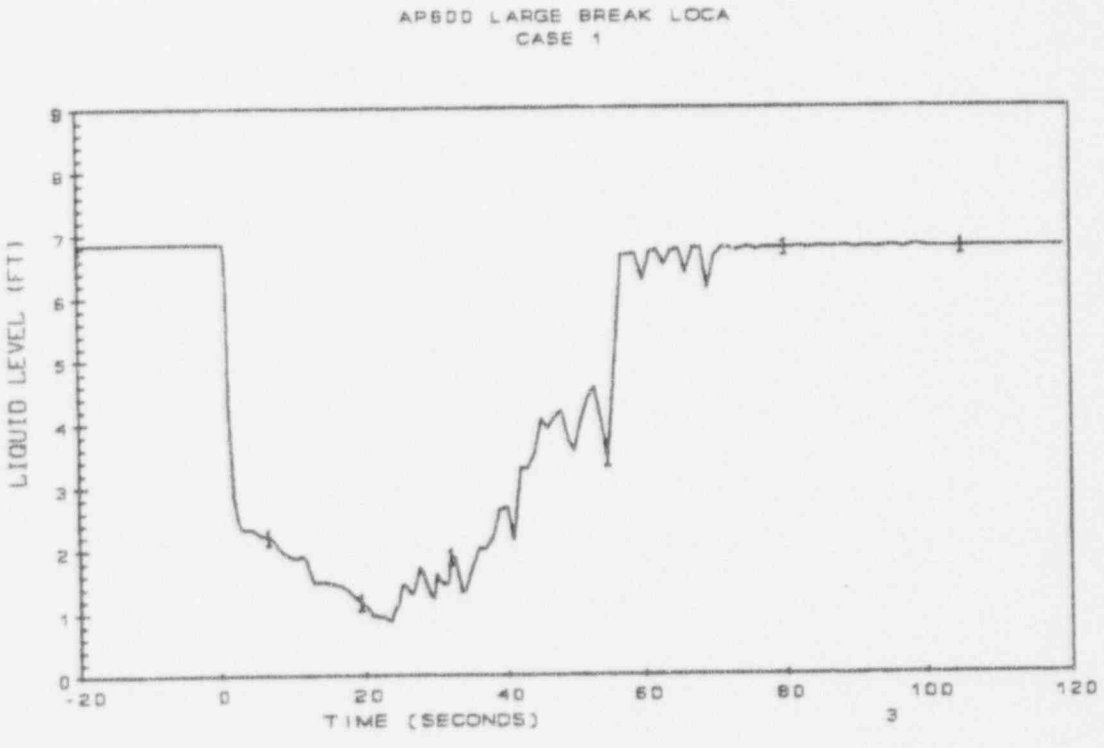

Figure 2.2-28 C_D=0.8 DECLG Transient, Lower Plenum Liquid Level From Vessel Bottom to Bottom of Active Fuel

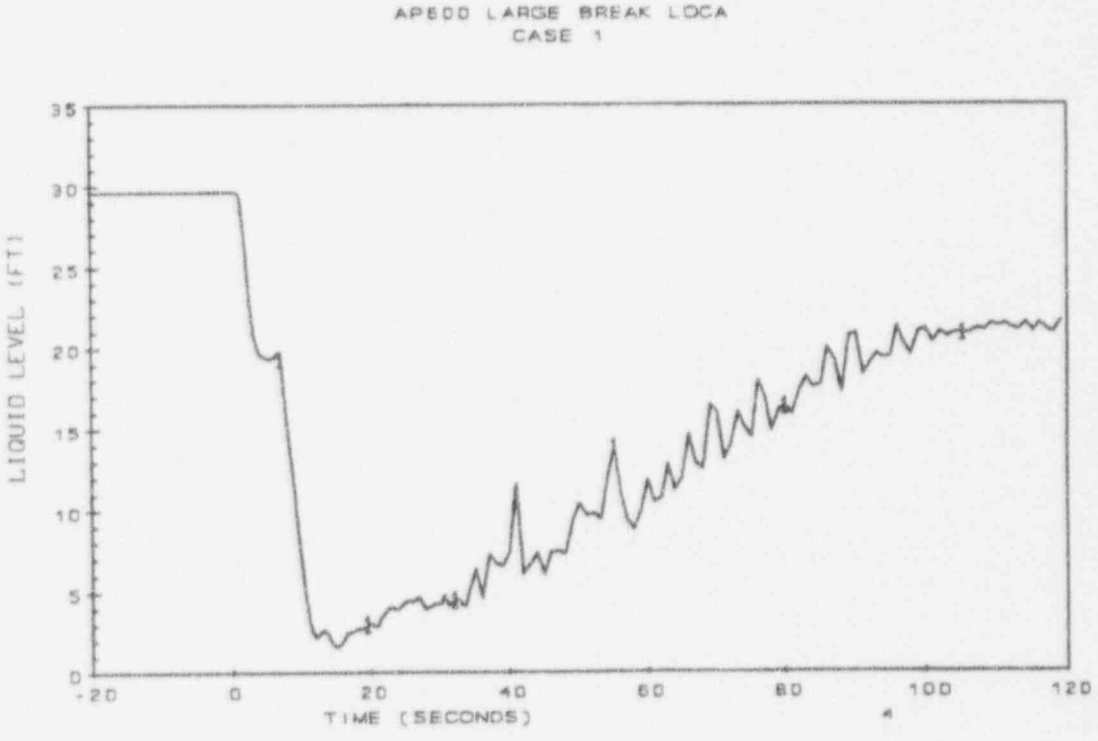

Figure 2.2-29 C_D=0.8 DECLG Transient, Downcomer Liquid Level From Bottom of Annulus

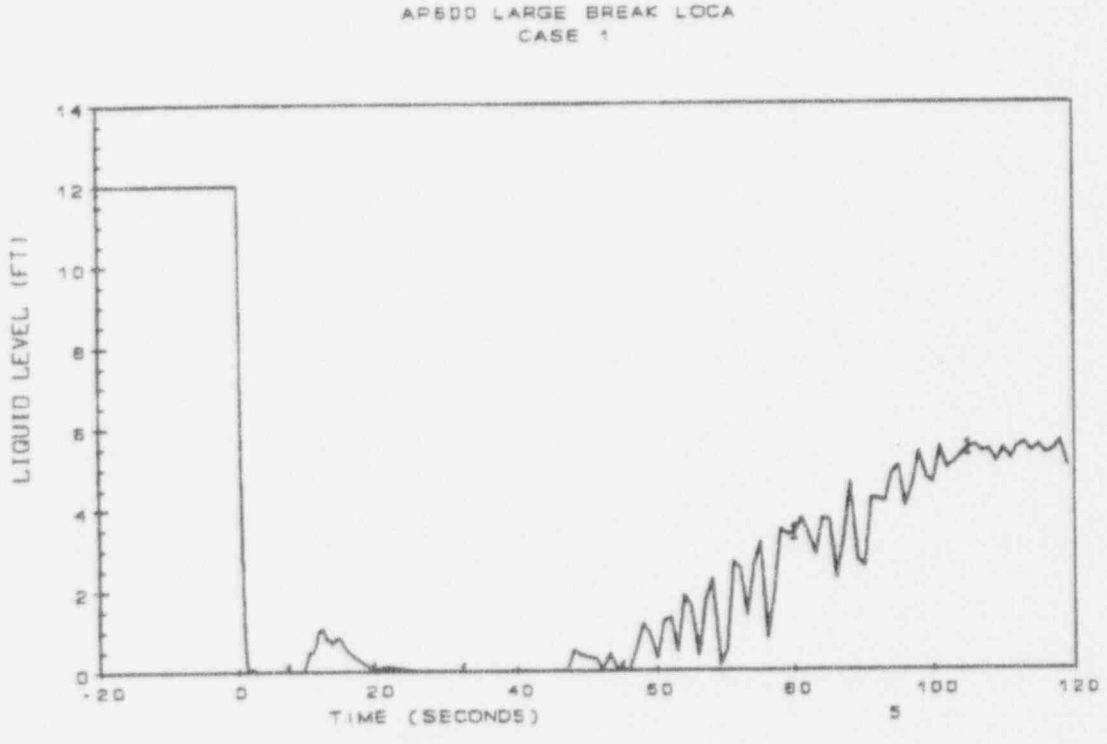

Figure 2.2-30 C_D=0.8 DECLG Transient, Core Hot Assembly Liquid Level

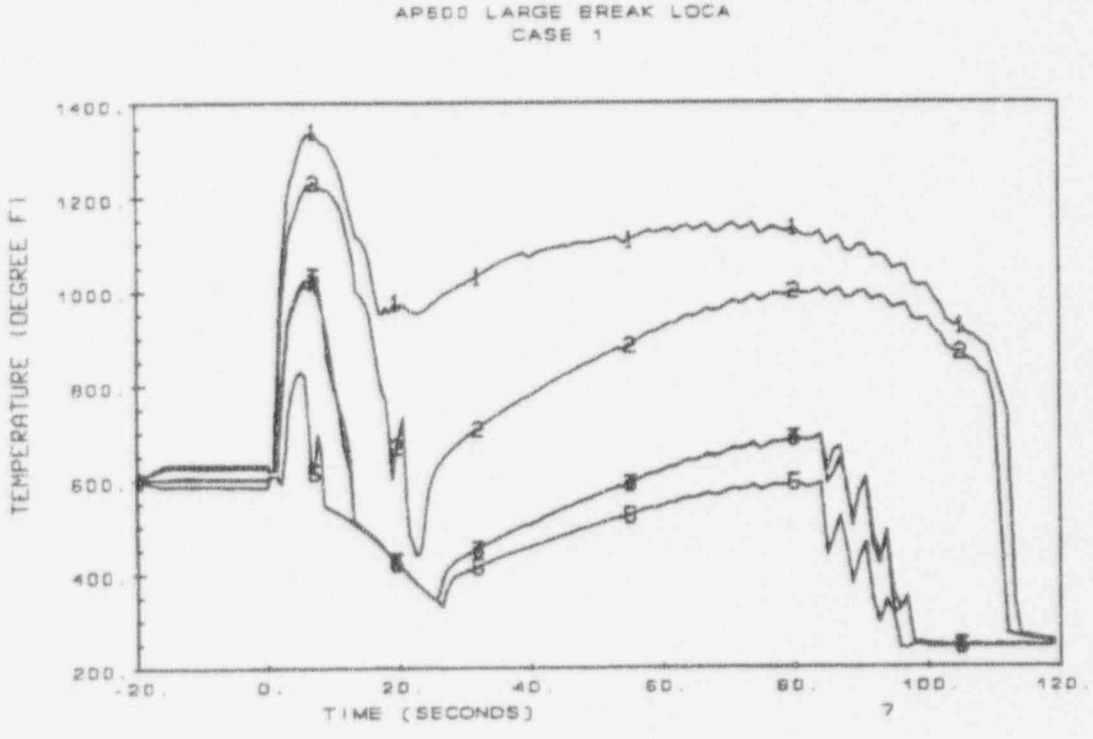

Figure 2.2-31 C_p=0.8 DECLG Transient, PCT at 6.0 Ft. Elevation, Rods 1 thru 5

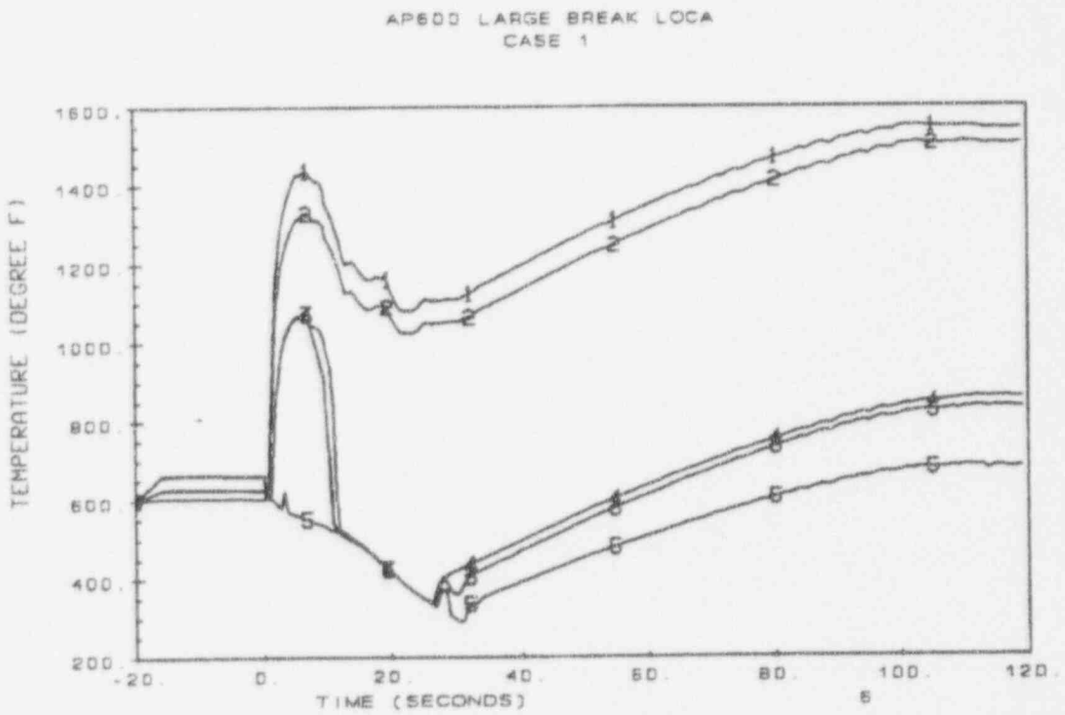

Figure 2.2-32 C_D=0.8 DECLG Transient, PCT at 8.5 Ft. Elevation, Rods 1 thru 5

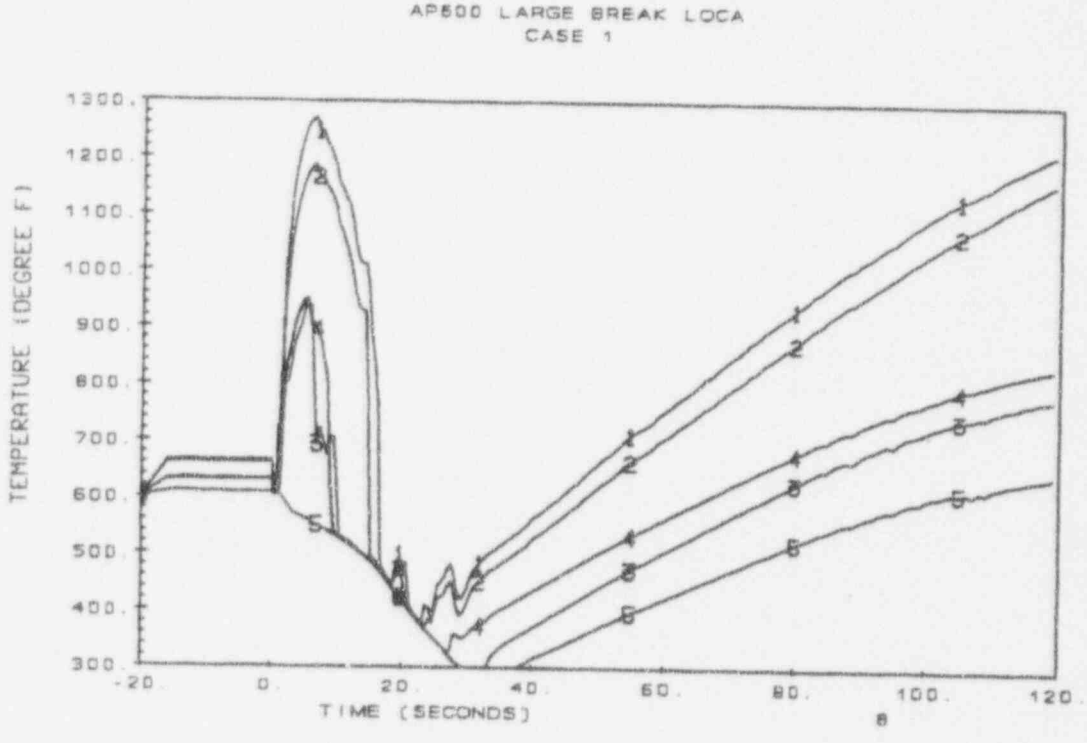

Figure 2.2-33 C_D=0.8 DECLG Transient, PCT at 10.0 Ft. Elevation, Rods 1 thru 5

2.3 Conclusions

The noding approach used on the AP600 plant is very similar to that used for the three- and four-loop current plants as shown earlier. The loop noding is also consistent between the AP600 and the three- and four-loop plants.

The large-break LOCA transient behavior of the AP600 is similar to the current three-loop performance except for improved core cooling performance during blowdown due to the flow from the upper head region, resulting in significant rewetting of the fuel rods. The lower kw/ft. of the AP600 core design also results in reduced clad heat-up and the resulting peak cladding temperatures. The accumulator delivery is also prolonged in the AP600 due to the larger accumulator volume and the fact that both accumulators are available to inject into the reactor vessel, and one is not lost on the broken loop, as in the three-loop calculation.

The passive safety systems have almost no influence on the resultant calculation behavior of the transient, with the exception of the accumulator, which exists in current plants. The flow that is injected from the CMT is only approximately 0.6 percent of the CMT inventory. This flow, which is injected early in the blowdown portion of the transient before the accumulators are on, will bypass the core through the break. Once the accumulators inject, they create significant back pressure to close the CMT injection line check-valve, terminating the CMT injection. Therefore, the larger accumulators in the AP600 design are the ECCS source responsible for terminating the clad temperature rise and the final quenching of the core. Since the new passive systems are essentially inactive (and in fact the PRHR is not even modeled in this analysis) for the large-break LOCA, the reponse of the AP600 to a large-break LOCA is very similar to that of an existing PWR, which WCOBRA/TRAC is qualified to analyze.

3.0 SPECIFIC WCOBRA/TRAC VALIDATION FOR UNIQUE AP600 FEATURES

Introduction

The phenomena identification ranking table (PIRT), given in Section 2.0, indicates that the main difference between the AP600 and existing PWRs is the direct vessel, or downcomer injection.

Additional specific validation has been prepared to examine the WCOBRA/TRAC code capability to model the AP600 direct vessel injection into the downcomer. The additional validation for the thermal-hydraulic phenomena resulting from this type of injection is provided by application of the code to tests carried out on the cylindrical core test facility (CCTF) and upper plenum test facility (UPTF). This section presents the results of WCOBRA/TRAC calculations of the CCTF and UPTF tests that simulate this emergency core cooling system (ECCS) arrangement.

3.1 CCTF Validation with Direct Vessel Injection

3.1.1 CCTF Facility Description

The CCTF core-II is a large-scale experimental facility designed to study the system response of a four-loop PWR for loss-of-coolant transients (Figure 3.1-1). The facility is used to provide data on the thermal-hydraulic behavior in the primary system during the refill and reflood phases of a hypothetical loss-of-coolant accident (LOCA). CCTF has a flow area scaling of 1/21.4 of that of the reference four-loop PWR. The dimensions of the system components are provided in Table 3.1-1, where they are compared to those of a typical four-loop PWR.

The CCTF core-II represents a full-height (12-ft. heated length) core section with three intact loops and a fourth (broken) loop having a 200 percent break. The test vessel includes a downcomer, lower plenum, core region, and upper plenum with associated internals. The arrangement and dimensions for the vessel are shown in Figure 3.1-2. The configuration of the rods in the core and the upper plenum structure is shown in Figure 3.1-3.

The core has 32 rod bundles (8 x 8), each containing 57 electrically heated rods (0.421-in. outer diameter) and seven unheated and instrumented rods (0.543-in. outer diameter). The rods have a pitch of 0.563 in. Each heated rod has a nichrome heating element packed with magnesium oxide and boron nitride. The sheath is made of Inconel-600. The rods are held together by six grids, spaced at 26.2-in. intervals up the bundle.

The core is divided into the three main power zones: low, intermediate, and high, as shown in Figure 3.1-3a. The lower power zone consists of 16 bundles on the periphery of the core. The intermediate power zone consists of 12 bundles, and the high power zone consists of the four central bundles. Figure 3.1-3b shows that under guide tubes, there are four low-power bundles and six medium-power bundles; under support columns, there are eight low-power bundles and two high-

power bundles; and under open holes, there are four low-power bundles, six medium-power bundles, and two high-power bundles.

The axial power profile is shown in Figure 3.1-4. Also shown are the locations of rod thermocouples and spacer grids.

As shown in Figure 3.1-1, each loop contains a steam generator simulator (in fact, a single steam generator shell assembly houses two steam generator simulators), a pump simulator, and connecting pipework. Flow from the broken loop is discharged to 2 interconnected containment tanks via two blowdown valves, one connected to each break. Emergency core cooling system (ECCS) water can be injected either from two accumulator tanks or from a low-pressure coolant injection (LPCI) pump and its associated water storage tank to each cold leg. A hot leg injection system, which also has two accumulator tanks, can provide injection to each hot leg. In addition, a further injection system is available that can provide ECCS water to injection ports in the downcomer.

The CCTF core-II facility is extensively instrumented. Instrumentation was supplied by Japan Atomic Energy Research Institute (JAERI) and the US Nuclear Regulatory Commission (NRC) and is briefly described below.

Rod temperatures are recorded by thermocouples located axially and radially throughout the core. Additional thermocouples are also located in the core, upper plenum, lower plenum, downcomer, and the primary loops to record the wall and fluid temperatures.

Absolute and pressure difference measurements are obtained from pressure cells in the core, downcomer, lower plenum, and primary loops.

Liquid level measurements are obtained in four different ways: differential pressure readings; servo-manometer readings in containment tank-I; conductivity type liquid level detectors; and a fluid distribution grid (optical type liquid level detector) in the downcomer and upper plenum.

Mass flowrate measurements are made by electromagnetic flow meters for ECCS mass flow; drag disks for flow between the downcomer and core; a venturi tube for the steam vented from containment tank-II; and turbine meters for the flow in the upper plenum, end-box region, and through the vent valves (not used). Velocimeters are used to give the fluid velocity (and hence core flooding rate) in the lower plenum. Spool piece instruments are used to obtain fluid densities, velocities, mass flowrates, and void fractions in the loops. Power sensors record the power level of the rods. More details of the CCTF core-II facility can be found in the *Data Report on Large Scale Reflood Test-78.*[7]

3.1.2 Test Description

Test C2-AA2 (run 58) was selected for analysis. This test models downcomer injection as part of the ECCS, similar to the AP600 design.

Figure 3.1-5 shows the sequence of events for the test, and Table 3.1-2 contains a summary of the initial and boundary conditions.

The primary system was heated with preheaters to its specified temperature of 248°F and pressurized to 29 psi with steam. The water in the low-pressure coolant injection (LPCI) tanks and accumulator tanks was heated to its specified temperature of 95°F. The LPCI water was circulated to ensure that the injection lines were at the same temperature. The accumulator tanks were pressurized with nitrogen to give sufficient head for the required injection flow. The steam generator secondary fluid was also heated and pressurized. The heaters were then turned off, and the lower plenum was filled to a level of 2.82 ft. When the initial conditions had been established, power was applied to the heater rods, and the data recording was started. The heater rods were then heated under near-adiabatic conditions until the clad temperature of four rods had reached 1331°F.

At 85.5 seconds, accumulator injection to the lower plenum and the downcomer injection ports was initiated. When the water had reached the bottom of the heated length of the core, the rod power decay sequence was initiated. The water injection to the lower plenum was redirected to the cold legs at 97 seconds. Just before the end of accumulator injection to the cold legs at 116 seconds, LPCI flow was initiated to the cold legs and maintained for the remainder of the test. Downcomer injection was also maintained for the same period.

The generated steam and the entrained water flowed via the broken loop to the containment tanks. The steam was vented to the atmosphere to maintain a constant pressure in the containment tanks. After all the thermocouples on the surface of the heater rods had indicated quenching, the power supply to the heater rods and the ECCS water injection were turned off. Then the recording system was stopped, terminating the test.

3.1.3 Test Results

The water level in the downcomer rapidly increased after 112 seconds as the main accumulator injection flow reached the vessel via the cold legs and the downcomer injection. By 150 seconds, the water level in the downcomer had stabilized and was maintained at ~21.3 ft. by the downcomer injection and LPCI flows. This level provided the hydraulic head necessary to achieve the core reflood.

Water first entered the core as a result of the rise in water level in the downcomer. The initial surge of liquid into the core was sufficient to quench the lowest elevations of the rods throughout the core. After this time, the flow into the core became oscillatory as steam production, and the resultant core

pressurization counteracted the hydraulic head of liquid in the downcomer. The rods at mid and upper elevations continued to heat up until they were cooled by the enhanced heat transfer in the proximity of the quench front. The peak clad temperature of 1582°F was recorded at 152 seconds, 6 ft. above the bottom of the heated length. The quench front progression up the core was directly related to the power level in the rod bundles. The central high-powered bundles quenched up to 100 seconds later than the low-powered periphery rod bundles. A total core quench was achieved at 772 seconds.

3.1.4 WCOBRA/TRAC CCTF Model

The WCOBRA/TRAC model of CCTF uses a one-dimensional mesh for the loops and employs a sub-channel formulated three-dimensional mesh for the pressure vessel. The axial momentum equation is retained in a standard form, and the two transverse momentum equations are combined to give a single transverse momentum equation that is applied to each transverse (gap) connection irrespective of its orientation within the transverse plane.

First, the vessel component model is described. This is followed by a description of the one-dimensional loop nodalization.

3.1.4.1 WCOBRA/TRAC Vessel Component Model

A noding diagram of the vessel model used in the analysis is shown in Figure 3.1-6. It shows the channel and interchannel connections (gaps). [

]^{a,c}

The noding used in the CCTF downcomer injection test model is consistent with that used in the AP600 plant model. [

]^{a,c}

[

]^{a,c}

The arrangement of four channels in the core regions [ ]^{a,c} was chosen to model the different power regions within the core and also to lump together regions of the core that share a similar type of geometry due to their position in relation to guide tubes, support columns, and open flow holes in the upper core support plate.

Grouped together are low-powered bundles below support columns (channel 14), low-powered and medium-powered bundles below the open hole regions of the upper core support plate (channel 15), and low- and medium-powered bundles below guide tubes (channel 16). The high-power bundles are represented by channel 17.

Six WCOBRA/TRAC rods are used to model the 1824 fuel rod simulators. Table 3.1-3 shows which rods and bundles they each represent and to which core channels they are connected. Channels 8 to 13 form the downcomer annulus at this elevation.

[

]^{a,c}

[

]^{a,c}

[

]^{a,c}

[

]^{a,c}

The fuel rod simulators and solid structures within the vessel component are modeled using the rod and unheated conductor models.

3.1.4.2 One-Dimensional Component Models

A diagram of the one-dimensional components used to model the CCTF loops is shown in Figure 3.1-15. [

]^{a,c}

Each of the cold leg and hot leg PIPEs is broken into mesh cell lengths such that no one cell produces an overly restrictive limit on the time step due to the Courant limitation. The length and elevation to and from the pipe wall is included by representing the pipe wall by two radial heat transfer nodes.

[

]^{a,c} Since the CCTF facility maintains prototypical piping lengths, the loop node sizes are similar to those for VRA and the AP600.

[

]^{a,c}

The steam generator components are modeled with the secondary side divided into [

]^{a,c} The flow area of these nodes is equal to the flow area of a single tube multiplied by the number of tubes in the tube bundle. The volume of the inlet plenum modeled corresponds to the physical volume of the plenum. The height of the plenum is set equal to the vertical distance from the top of the tube sheet to the outside bottom surface of the shell to conserve elevation. The distance between the shell bottom and the cold leg centerline is modeled as part of the cold and hot leg PIPEs. The area of the junction connecting the plenum to the piping is set equal to the area of the connecting pipes in the facility. The top area of the plenum is set equal to the tube bundle area.

[

]^{a,c}

3.1.5 WCOBRA/TRAC Calculation and Data Comparisons

The calculation simulated the experiment from 85 seconds, immediately prior to the start of accumulator injection, to the end of the test at 850 seconds. The calculation was started at this time to achieve a more accurate representation of the rod temperatures before the reflood phase of the experiment had begun. Figures 3.1-16 to 3.1-50 compare the calculated results to the experimental data. All the figures, except Figures 3.1-31 to 3.1-33, reference the start of the experiment as time zero on the 'x' axis. The calculated results are plotted from 85 seconds. Figures 3.1-31 to 3.1-33 depict the quench envelopes that reference the beginning of core recovery (BOCREC) as time zero on the 'x' axis. BOCREC occurred at 93 seconds.

The experimental data are represented by digitized plot profiles in all the figures except the heater rod temperatures due to a corruption of the datatape. The digitized plots are simple averaged representations of the data and do not depict the fluctuations that occurred in the experimental readings. To aid the reader, each plot references the figure number used in the full data report.[7]

A review of the experimental heater rod thermocouple data shows that the thermal response across the core is dominated by the power rating of the individual rod assemblies. Rod assemblies of equal power rating exhibited very similar behavior. Their position in the core relative to the geometric configurations (open hole, support column, or guide tube) in the upper support plate had no significant influence on the results. The data from three assemblies, representing the three different power levels in the core, were selected to compare against the calculated temperatures of rods 1, 3, and 6. Rods 1, 3, and 6 model low-, medium-, and high-powered regions in the core, respectively. Rod 3, however, is grouped with rod 2, a low-powered rod, in channel 15 (Table 3.1-3). Therefore, it is to be expected that the thermal response of rod 3 will be reduced due to the influence of rod 2 on the common fluid conditions.

The calculated clad temperatures for the low-, medium-, and high-powered rods are compared against the data in Figures 3.1-16 to 3.1-30. The clad temperature histories are given at five elevations, 1.25 ft., 3.33 ft., 6 ft., 8 ft., and 10 ft. The clad temperature comparisons for the low-powered rod (Figures 3.1-16 to 3.1-20) show that the lower elevations quench out earlier in the calculation, although the prediction of the maximum clad temperatures at each of the lower elevations is good. As the transient progresses, the degree of subcooling at the quench front reduces to zero. As a consequence, the calculated rate of the quench front progression reduces below that seen in the experiment (Figure 3.1-31). The reasons for the change in the calculated rate of quench front progression are as follows. At mid elevations, the power rating is large, and the liquid subcooling at the quench front is reduced to zero. This can produce high calculated steam flows as the channel cells fill with water, which are sufficient to drag liquid slugs from the quench front. The liquid slugs pass out of the core, causing a reduction in the core collapsed liquid level, which tends to reduce the quench front progression. Because the surface area of the liquid slugs is relatively small, the interfacial heat transfer is low. After 420 seconds, the calculation underpredicts the experimental quench front elevation, the cross-over point occurring at ~7.5 ft. The quench front progression is well predicted from 300 seconds to 500 seconds and this leads to a good prediction of the 8-ft. elevation

temperature. The 10-ft. elevation is calculated to be partially quenched by the liquid slugs passing out of the core, and the temperature is underpredicted from 440 seconds to 600 seconds, although the final quench is calculated to be delayed.

The rod temperature comparisons for the medium- and high-powered rods are shown in Figures 3.1-21 to 3.1-30. The influence of the predicted quench front progressions (Figures 3.1-32 and 3.1-33) again have a pronounced effect on the calculated clad temperature histories. The higher clad temperatures associated with the higher rated rods tend to cause the loss of subcooling at the quench front to occur earlier and at lower elevations. The reduction in the predicted quench front progression therefore occurs earlier compared to the low-powered rod. This allows the clad temperatures at upper elevations to increase significantly higher than the experimental temperatures, especially for the high-powered rod (Figure 3.1-30). The experimental peak clad temperature (PCT) of 1582°F was recorded by thermocouple TE31Y17 at 152 seconds (Figure 3.1-28). This thermocouple was located at the 6-ft. elevation in one of the four high-powered assemblies (assembly 31). The calculated PCT of 1684°F is predicted after 264 seconds at the 7.94 ft. elevation. The calculated PCT occurs 105 seconds later than the experiment and is located 2 ft. higher. This agrees with the underprediction of the quench front progression later in the transient, which promotes excessively high rod temperatures at upper elevations, especially for the high-powered rods.

The upper plenum pressure history is shown in Figure 3.1-34. The downcomer differential pressure is plotted in Figure 3.1-35. This figure indicates that the downcomer quickly fills with water after the initiation of accumulator injection at 85.5 seconds. The water level is maintained up to the height of the cold leg nozzles by the low-pressure coolant injection (LPCI) and the downcomer injection. The WCOBRA/TRAC calculation accurately predicts this filling sequence. The hydraulic head of water in the downcomer provides the necessary driving pressure to force the water into the core and initiate the core reflood. Figure 3.1-36 shows the core differential pressure. The agreement between the calculated results and the data is very good up to 300 seconds. After this time, the calculation is slightly below the data. This indicates that the core water level is slightly underpredicted after this time. This may be related to the flow behavior at the quench front, which is discussed later in connection with the thermal response of the core. After the initial pressure fluctuations that correspond to the start of the core reflood (~90 seconds), the calculation continuously underpredicts the pressure data for the duration of the test. This discrepancy becomes smaller as the transient progresses. The reason for the difference is the underprediction of the pressure loss from the upper plenum to the containment tank (Figure 3.1-37). One of the main contributors to this pressure loss is the pump simulator in the broken loop (loop 4 in the calculation). The pressure loss across the pump simulator is shown in Figure 3.1-39. The experimental and calculated water and steam mass flows passing through the pump simulator are shown in Figures 3.1-42 and 3.1-43, respectively. The calculated steam and water flows are less than the corresponding experimental flows. It is these reduced flows that cause the underprediction of the pressure loss along the pump side broken loop (i.e., hot leg pipe, steam generator simulator, loop seal pipe, pump simulator and cold leg pipe to the containment tank).

The steam and water mass flows in the hot leg of the broken loop are shown in Figures 3.1-46 and 3.1-47, respectively. The calculation underpredicts the degree of liquid entrainment passing from the

upper plenum into the hot leg for the majority of the test. The lower calculated water mass flow has an effect on condensation of steam and results in higher calculated steam mass flows compared to the data. As the water flows in to the steam generator simulator, the water evaporates, creating more steam. This results in the experimental steam flow increasing above the calculated flow downstream of the steam generator simulator, as shown in Figure 3.1-43. Evidence of lower calculated water flow in the pump side broken loop is also obtained from the fluid temperature comparisons in the hot leg and loop seal pipe (Figures 3.1-49 and 3.1-50). In Figure 3.1-49, the calculated temperatures are above saturation, whereas the experimental fluid temperatures remain at saturation indicating the presence of more liquid. The higher saturation temperature in the experiment correspond to the higher pressure in the broken loop compared to that of the calculation. The temperature difference is more pronounced in the loop seal pipe (Figure 3.1-50).

The experimental data show that the intact loop flows exhibit similar behavior. The flows in loop 1 were selected for comparison and are shown in Figures 3.1-40, 3.1-41, 3.1-44 and 3.1-45. The calculated hot leg steam flows are in close agreement with the data up to 300 seconds. After this time, the calculated steam flow remains at a fairly constant level, whereas the experimental steam flow reduces as a result of increased condensation corresponding to the higher water mass flow (Figure 3.1-44). The steam flows are in closer agreement towards the end of the test when the calculated water mass flow accurately represents the data. The calculated cold leg mass flows are compared to the data in Figures 3.1-40 and 3.1-41. The calculated accumulator injection into the cold leg is in close agreement with the data. This flow dominates the plot and no useful information can be extracted from the comparison for the remainder of the test. The calculation overpredicts the cold leg steam flow, as shown in Figure 3.1-41. The differential pressure across the pump simulator in loop 1 (Figure 3.1-38) is, however, in closer agreement, indicating that the experimental water mass flow may be greater than the calculated flow.

The experimental and calculated broken cold leg vessel side fluid temperatures are compared in Figure 3.1-48. The calculation and the data show the fluid to be at saturation temperature, indicating that water is spilling from the downcomer into the broken leg and subsequently, flowing to the break. The saturation temperature in the data is higher than the calculated saturation temperature, indicating that the system pressure is higher in the experiment.

3.1.6 Summary

The calculation provides a reasonable prediction of the thermal-hydraulic behavior in CCTF run 58. Nothing unusual or different from other CCTF with accumulator injection in only the cold legs was observed. Downcomer filling and core flows are in close agreement with the data. The calculated entrained flows in the broken loops are lower than the data. This results in an underprediction of the system pressure as a consequence of smaller calculated pressure losses in the broken loops. The maximum clad temperatures in the lower half of the core are well predicted. The modeling of the fluid hydraulics at the quench front produce a conservative prediction of the clad temperatures at upper elevations. The WCOBRA/TRAC calculation predicted this particular test with the same precision as the cold leg injection CCTF tests, as shown in the CQD.[3]

TABLE 3.1-1
COMPONENT DIMENSIONS OF CCTF COMPARED TO PWR

Component		PWR	CCTF	Ratio
PRESSURE VESSEL				
Vessel Inside Diameter	(in.)	173.0	42.7	
Vessel Thickness	(in.)	8.5	3.54	
Core Barrel Outside Diameter	(in.)	152.5	37.8	
Core Barrel Inside Diameter	(in.)	148.0	36.6	
Thermal Shield Outside Diameter	(in.)	164.2		
Thermal Shield Inside Diameter	(in.)	158.7		
Downcomer Length	(in.)	190.9	190.9	1/1
Downcomer Gap	(in.)	4.5	2.4	
Downcomer (+ Baffle) Flow Area	($ft.^2$)	45.5	2.12	1/21.44
Lower Plenum Volume	($ft.^3$)	1045.3	48.73	1/21.44
Upper Plenum Volume	($ft.^3$)	1539.7	72.0	1/21.44
FUEL (HEATED ROD				
Number of Bundles	(-)	193	32	
Rod Array	(-)	15 x 15	8 x 8	
Rod Heated Length	(in.)	144.0	144.0	1/1
Rod Pitch	(in.)	0.563	0.563	1/1
Fuel Rod Outside Diameter	(in.)	0.422	0.421	1/1
Thimble Tube Diameter	(in.)	0.546	0.543	1/1
Instrument Tube Diameter	(in.)	0.546	0.543	1/1
Number of Heater Rods	(-)	39372	1824	1/21.58
Number of Non-Heated Rods	(-)	4053	224	1/18.09
Core Flow Area	($ft.^2$)	56.9	2.7	1/21.2
Core Fluid Volume	($ft.^3$)	633.9	32.2	1/19.6
PRIMARY LOOP				
Hot Leg Inside Diameter	(in.)	29.0	6.11	1/4.75
Hot Leg Flow Area	($ft.^2$)	4.59	0.205	1/22.54
Hot Leg Length	(in.)	155.1	155.1	1/1
Pump Suction Inside Diameter	(in.)	31.0	6.1	1/5.07
Pump Suction Flow Area	($ft.^2$)	5.24	0.205	1/25.77
Pump Suction Length	(in.)	313.0	313	1/1

TABLE 3.1-2 CCTF TEST CONDITIONS						
Test No.	**Total Power (MW)**	**Power Decay**	**Radial Power A:B:C**	**PCT at start of reflood (°F)**	**System Pressure (psi)**	**ECCS Flowrate Location and Duration**
58	9.36	ANSx1.2 + 1.1xActinide	1.36:1.2:0.76	1467	1467	(1) Acc. flow to lower plenum 2.86 ft^3/sec. from 85.5 to 103 sec. (2) Acc flow to cold legs 2.86 ft^3/sec. from 87.5 to 11.3 sec. (3) LPCI flow to cold legs 0.0777 ft^3/sec. from 85.5 to 1008 sec. (4) Downcomer injection 0.3143 ft^3/sec. from 85.5 to 1008 sec.

TABLE 3.1-3 CCTF ROD-TO-CHANNEL CONNECTIONS			
WCOBRA/TRAC Rod No.	**Core Channel in which Rod is Located**	**Description of Assemblies Represented by the Rod**	**No. of Fuel Rod Simulators Represented**
1	14	8 low-power assemblies under support columns	456
2	15	4 low-power assemblies under open holes	228
3	15	6 medium-power assemblies under open holes	342
4	16	4 low-power assemblies under guide tubes	228
5	16	6 medium-power assemblies under guide tubes	342
6	17	4 high-power assemblies	228

TABLE 3.1-4 NOMINAL STEAM AND ECCS INJECTION RATES							
Run/Phase/ Subphase	**Evaluation Period**	**ECCS Injection**		**Steam Injection**		T_{ECC}	T_{SUB}
		1	**2**	**Core**	**SG**		
	(seconds)	(lb/s)		(lb/s)		(°F)	(°F)
272 A	57 - 81	2011	2006	496	196	93	211
274 BI	59 - 108	1863	1884	459	198	257	101
274 BII	280 - 324	1951	0	227	0	257	56
274 BIII	337.5 - 344.5	1951	1840	225	0	257	47

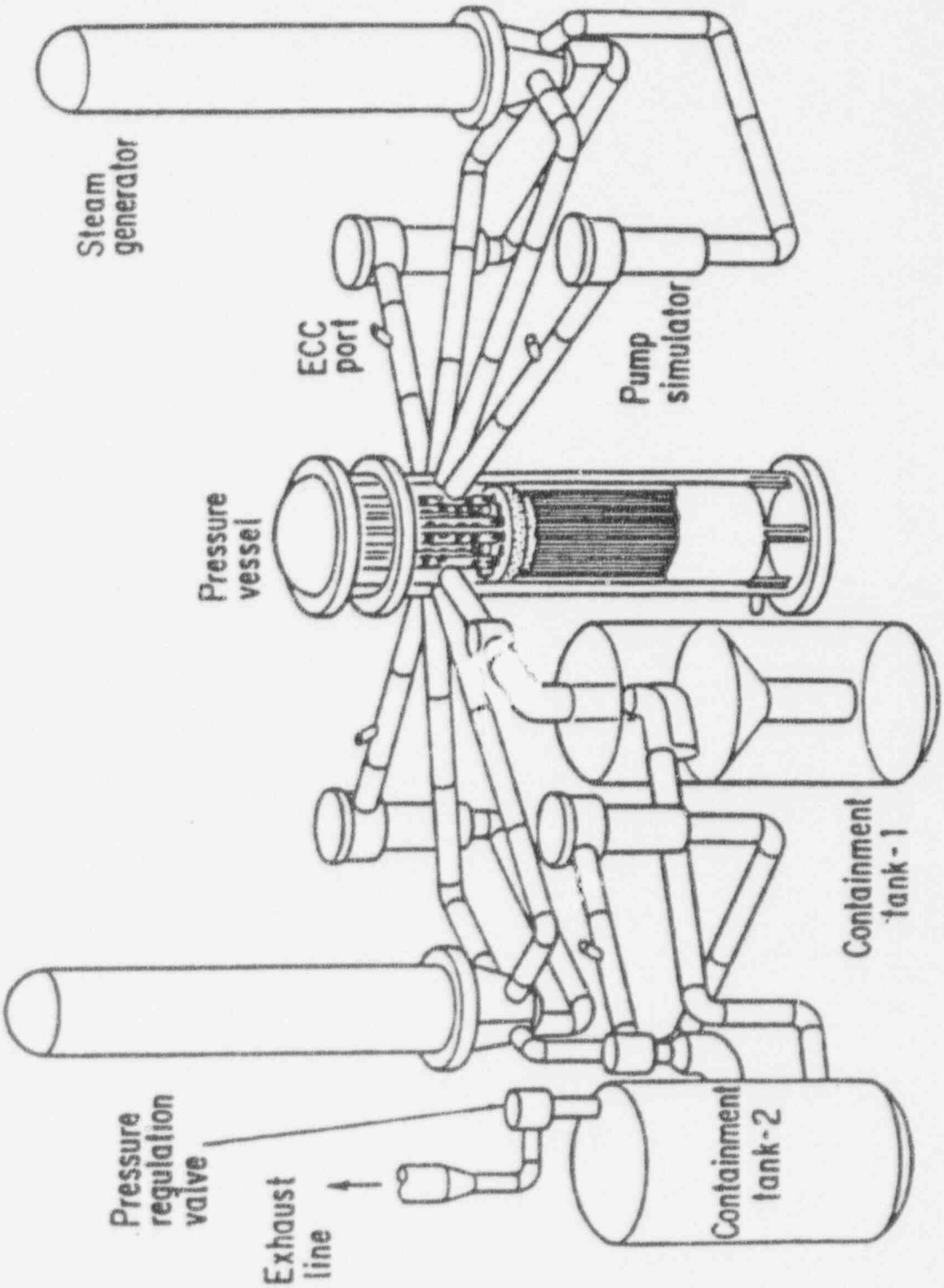

Figure 3.1-1 CCTF Core-II Test Facility

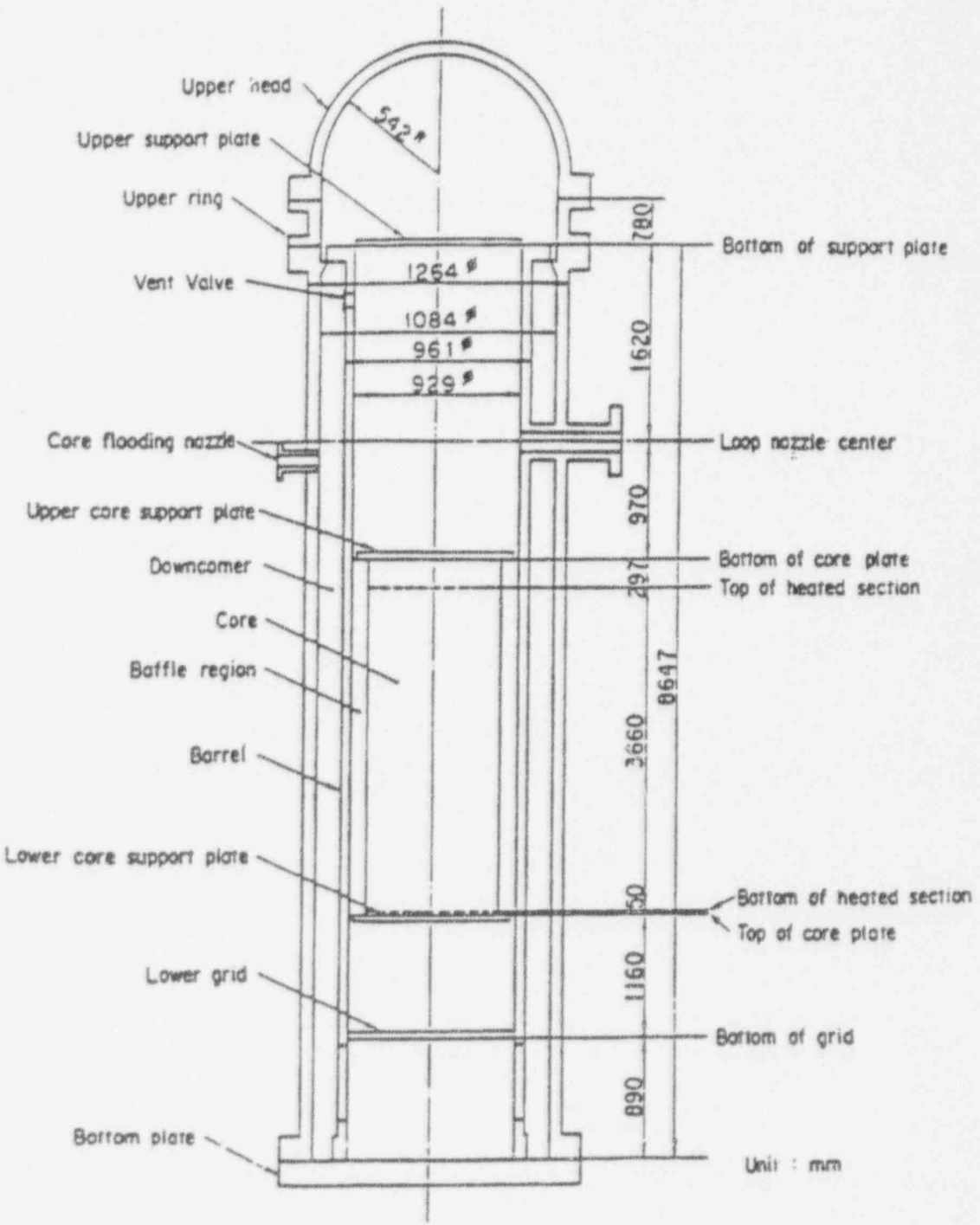

Figure 3.1-2 Diagram of CCTF Pressure Vessel

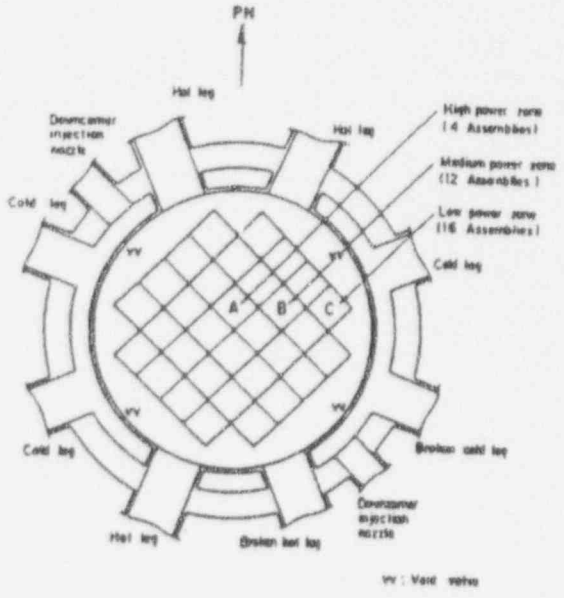

Figure 3.1-3a Cross Section of CCTF Pressure Vessel

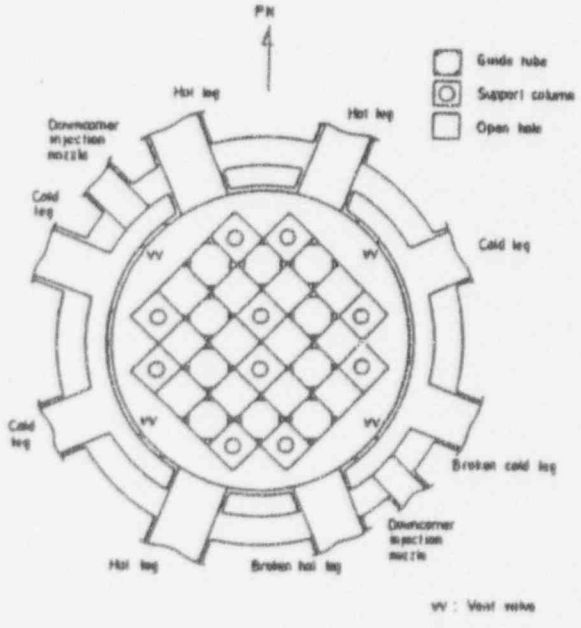

Figure 3.1-3b Cross Section of CCTF Upper Plenum

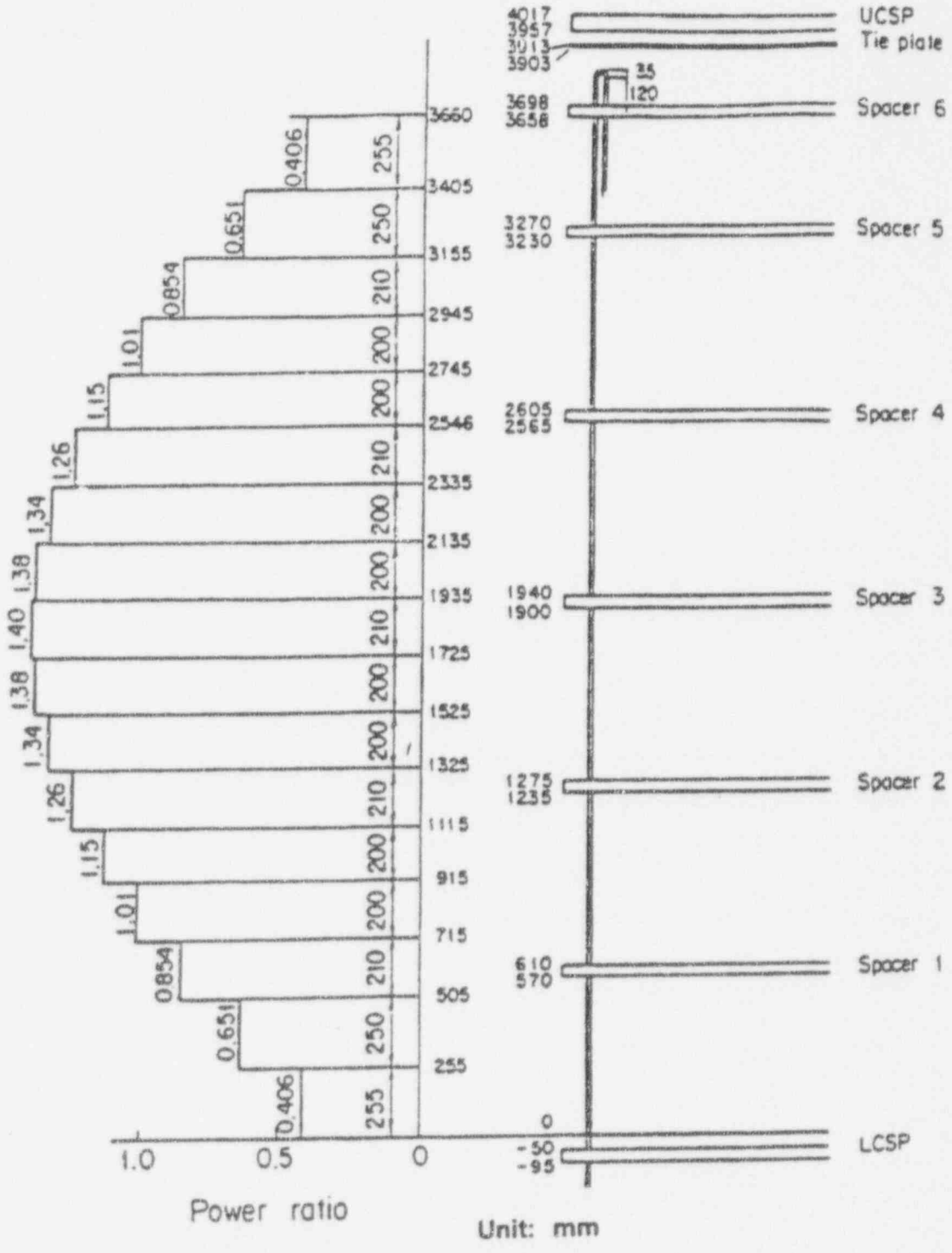

Figure 3.1-4 Axial Power Profile of Heated Rods in CCTF Core

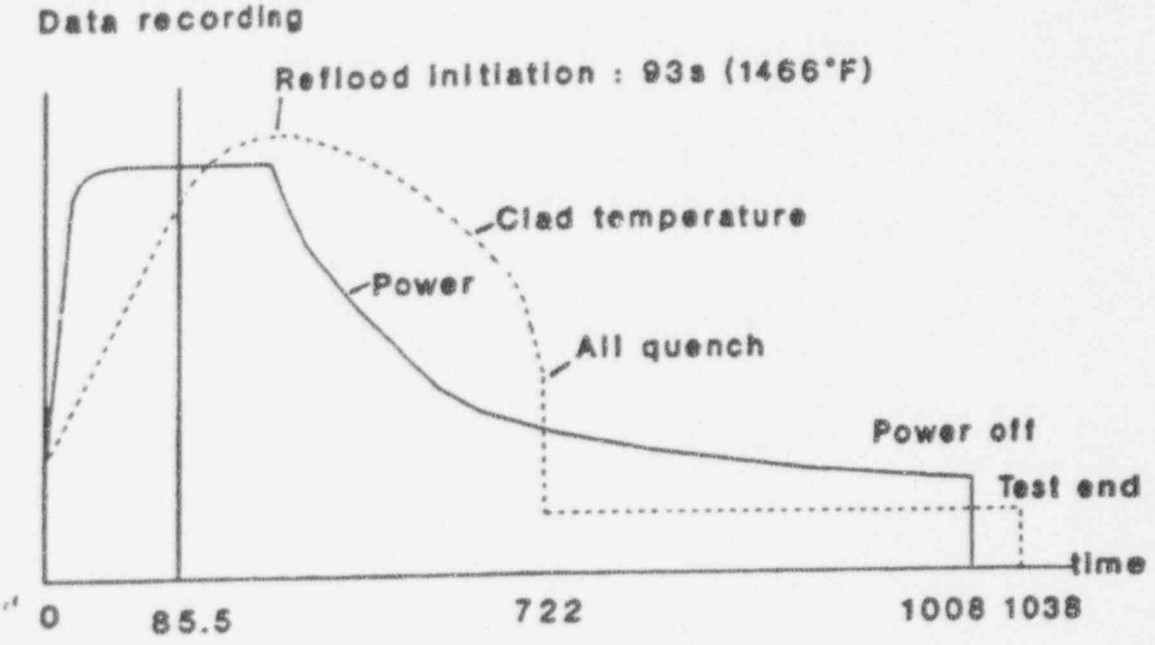

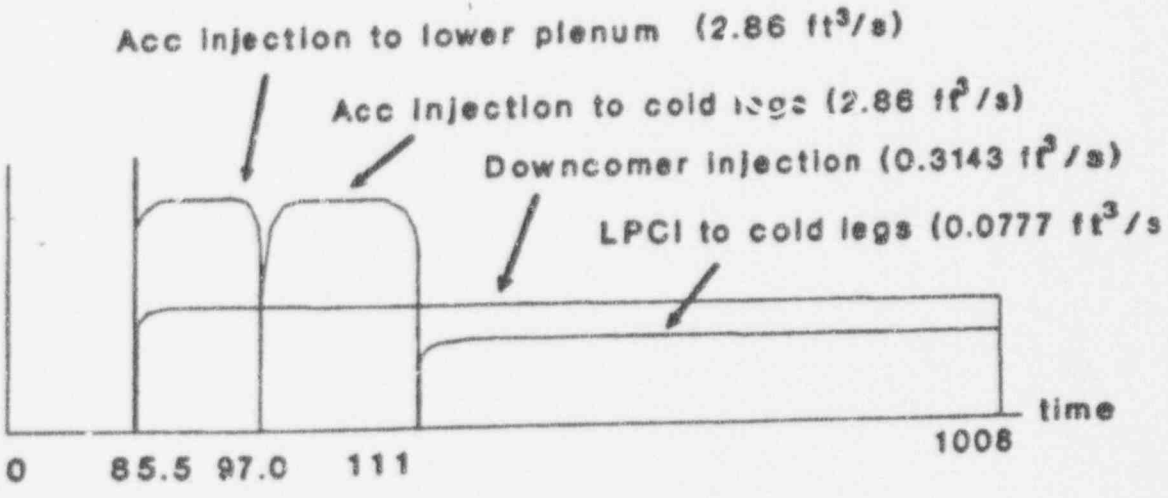

Figure 3.1-5 Test Sequence of Test C2-AA2 (Run 58)

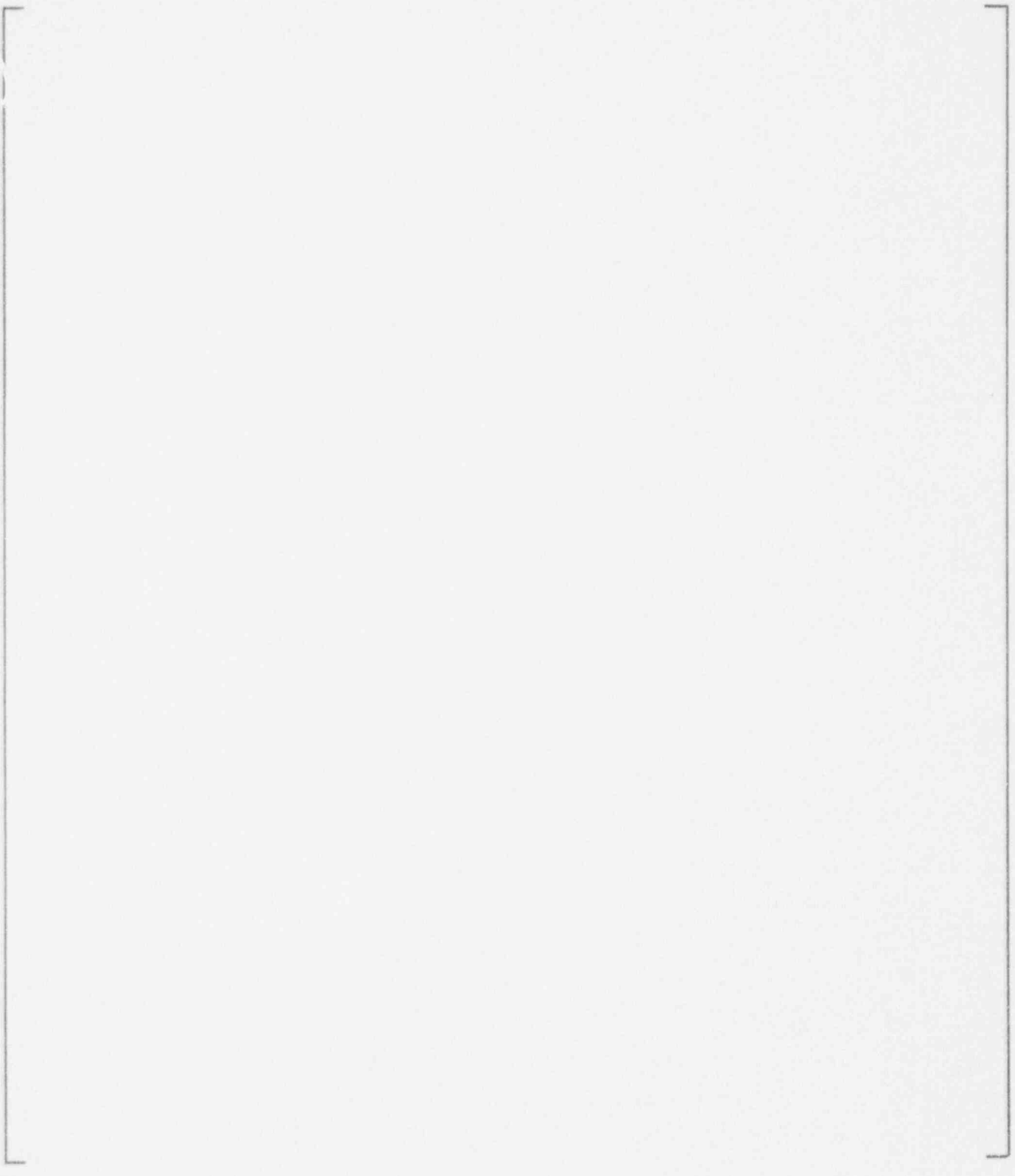

a,c

Figure 3.1-6 WCOBRA/TRAC CCTF Vessel Noding - Plan View

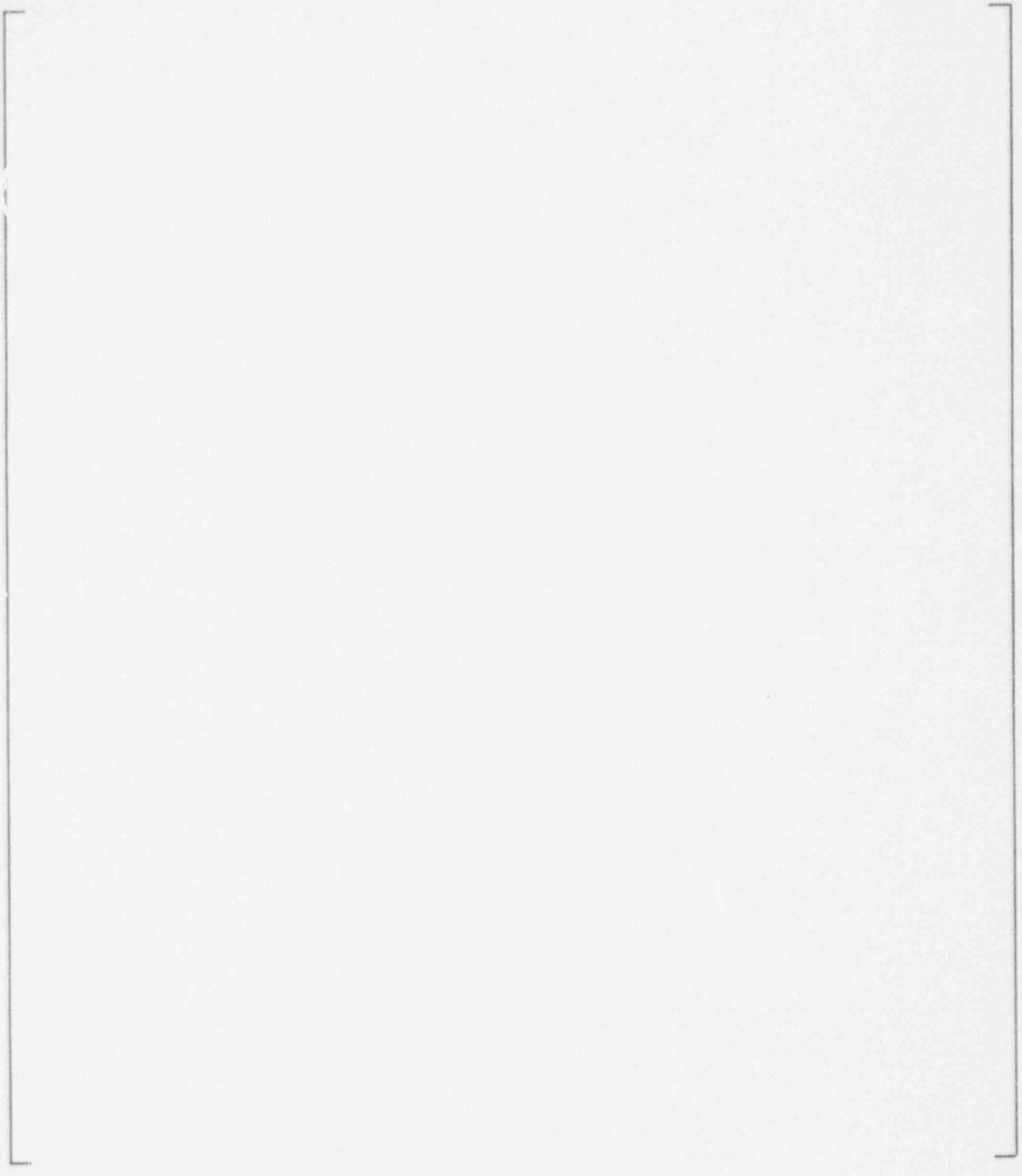

Figure 3.1-7 WCOBRA/TRAC CCTF Lower Plenum Noding (Section 1)

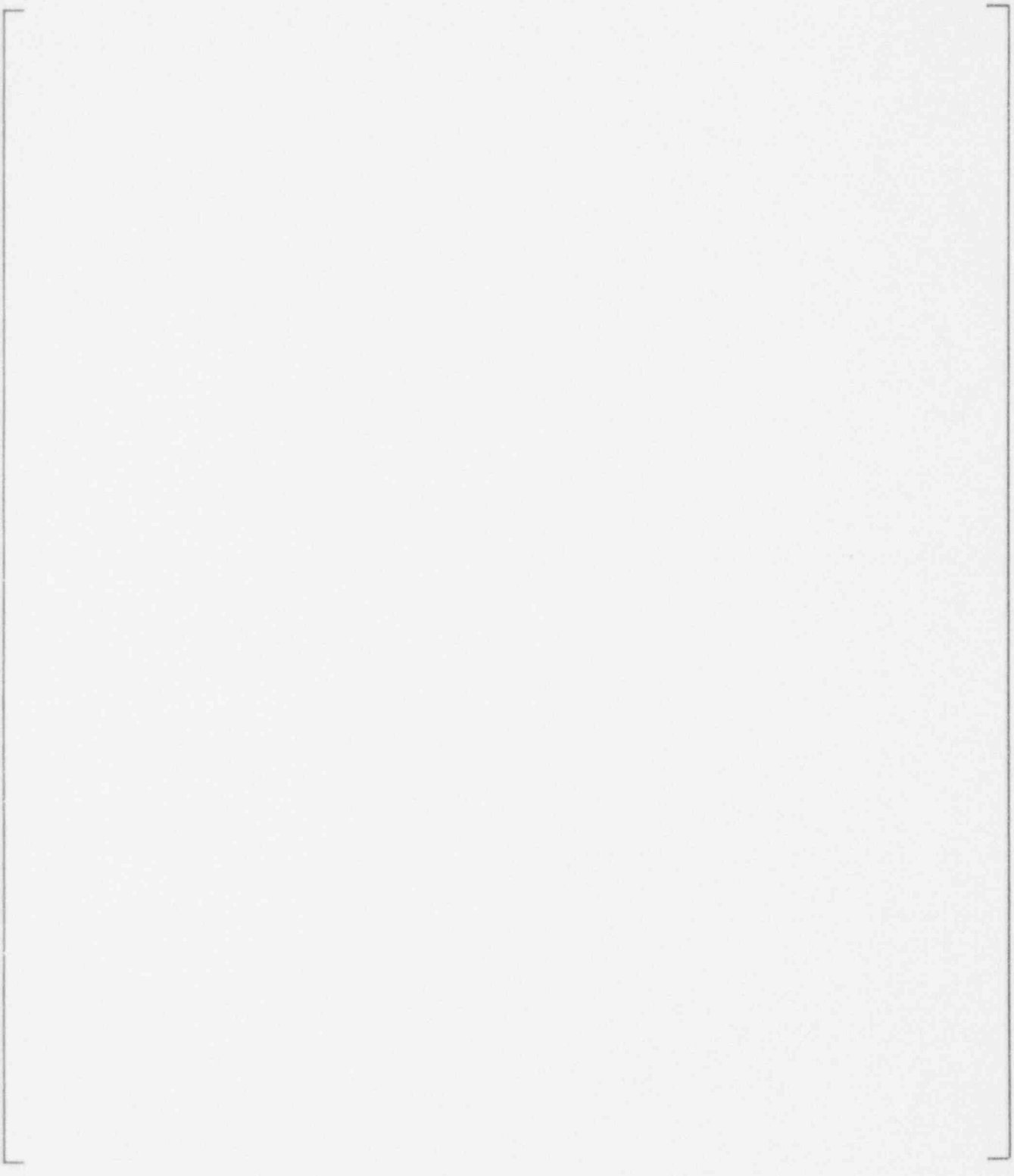

a,c

Figure 3.1-8 WCOBRA/TRAC CCTF Core Region Noding (Section 2)

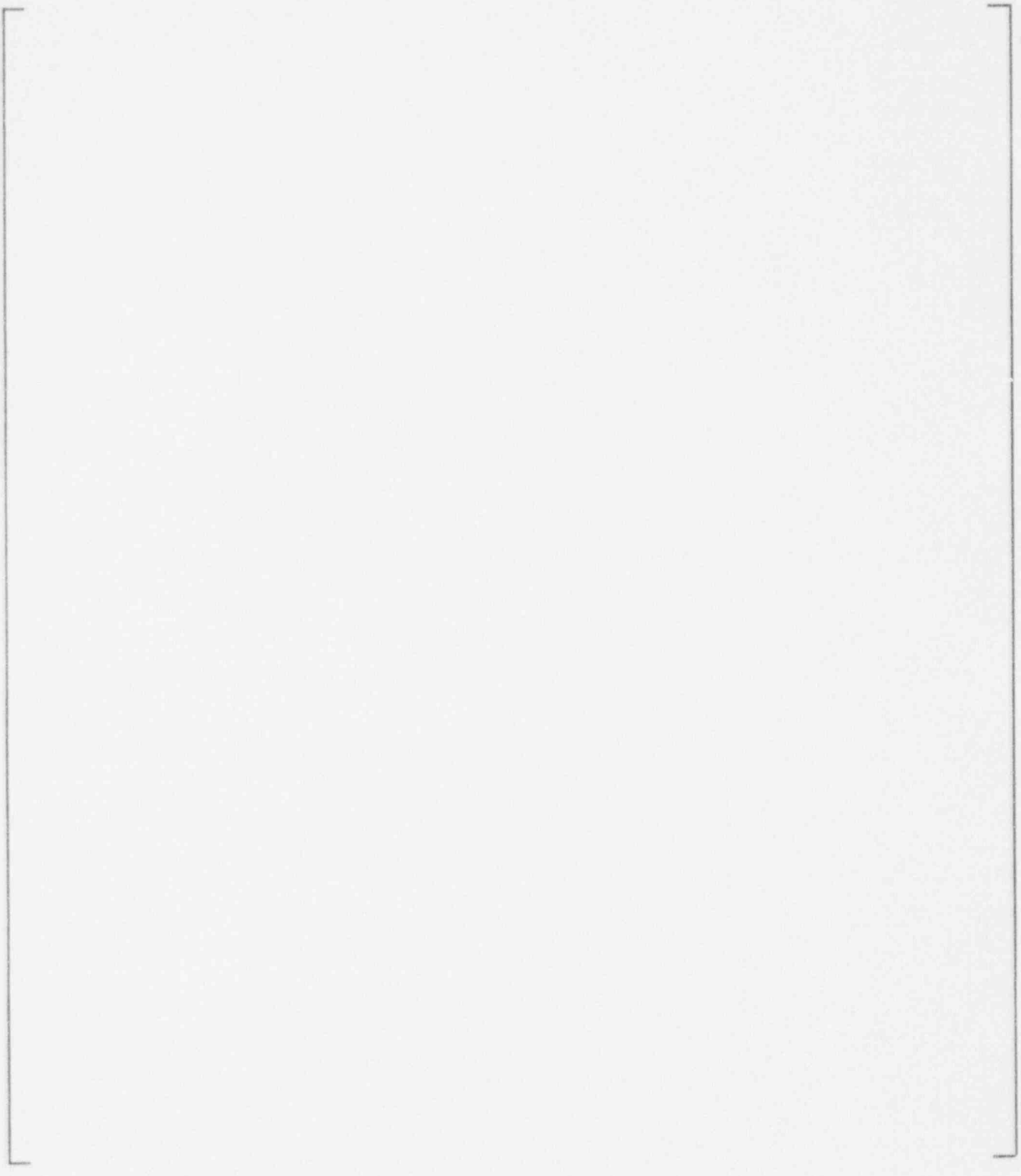

a,c

Figure 3.1-9 WCOBRA/TRAC CCTF Tie-Plate Region Noding (Section 3)

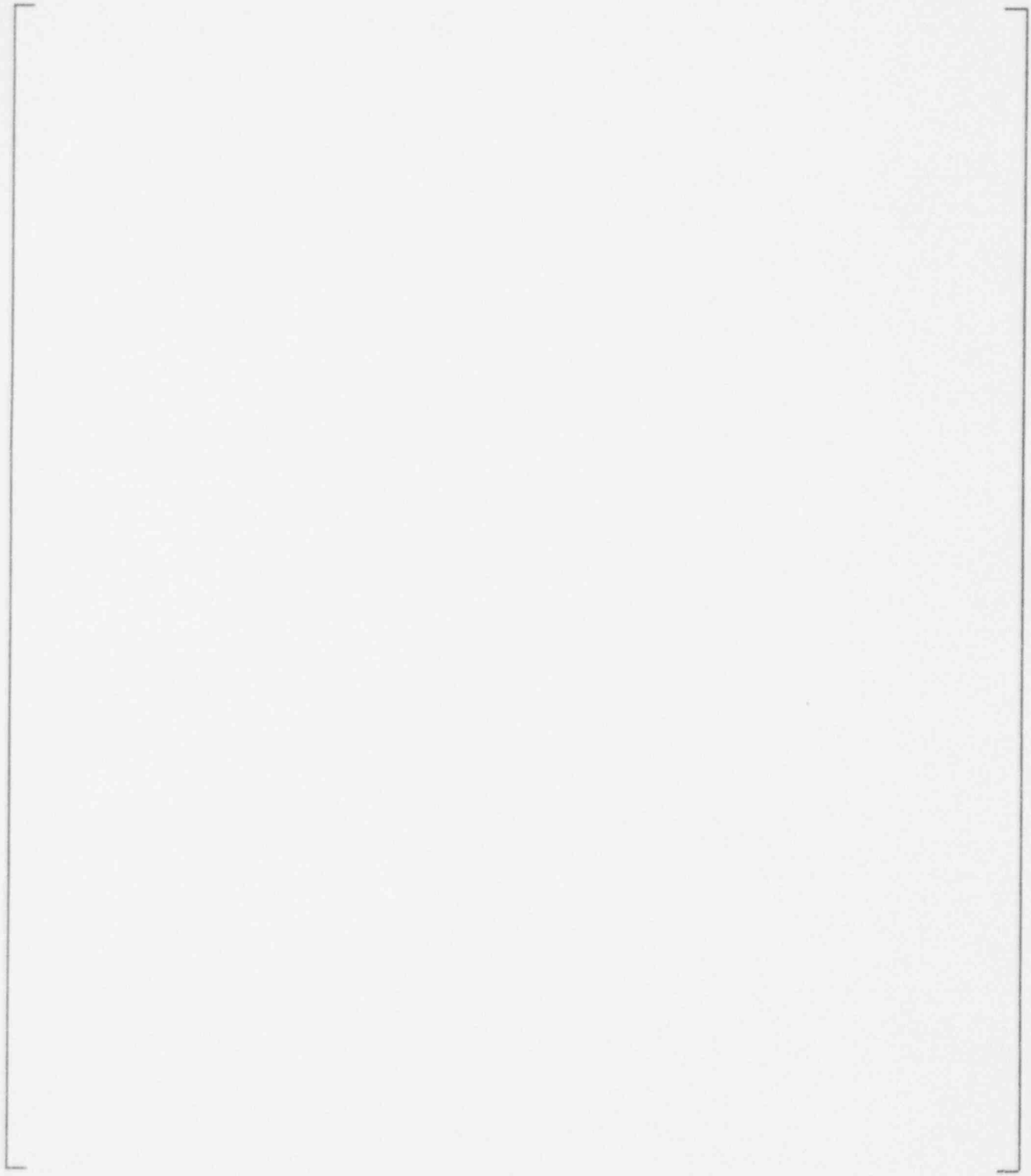

a,c

Figure 3.1-10 WCOBRA/TRAC CCTF Upper Plenum Region Noding (Section 4)

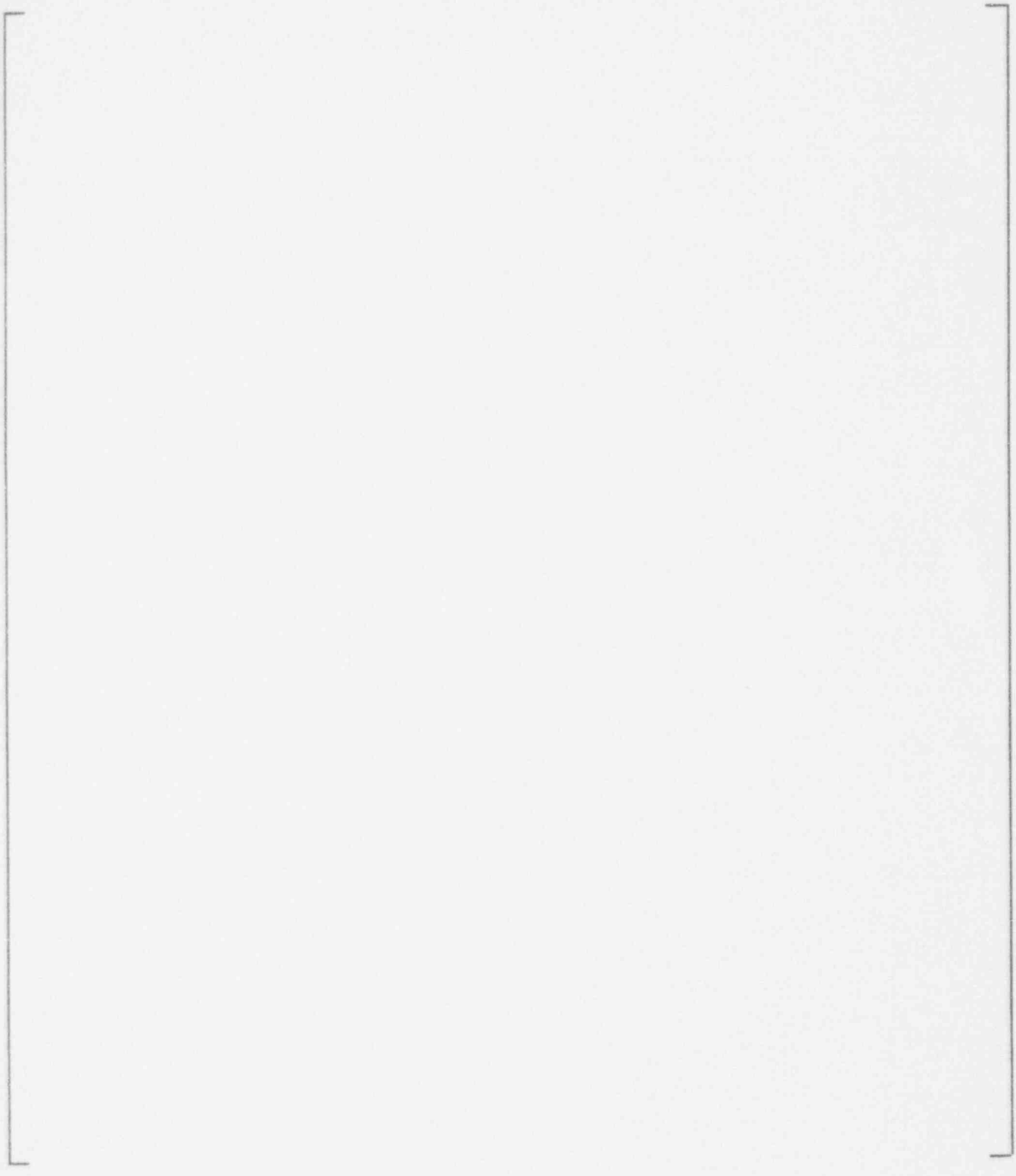

a,c

Figure 3.1-11 WCOBRA/TRAC CCTF Upper Plenum Region Noding (Section 5)

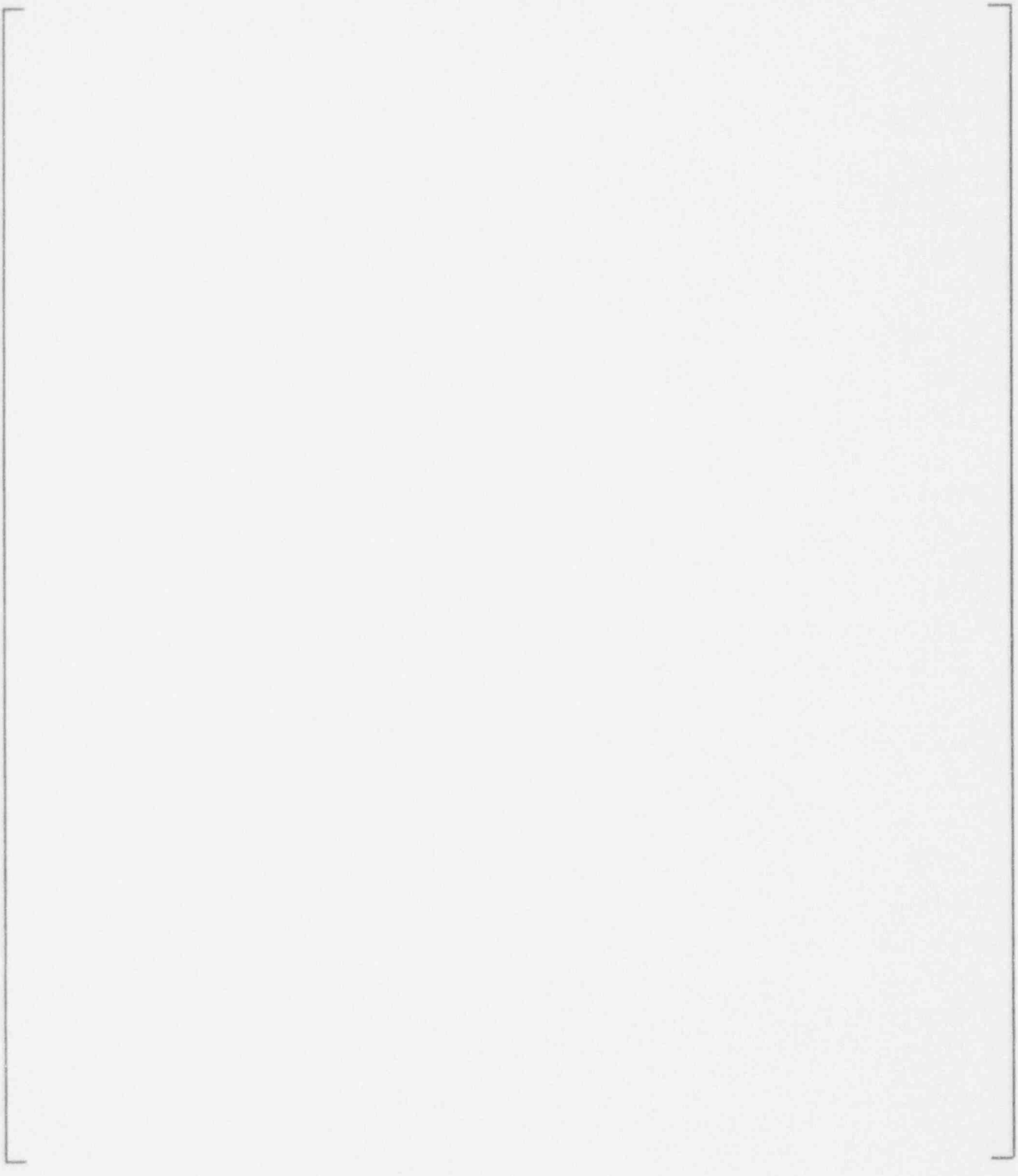

a,c

Figure 3.1-12 WCOBRA/TRAC CCTF Loop Connection Region Noding (Section 6)

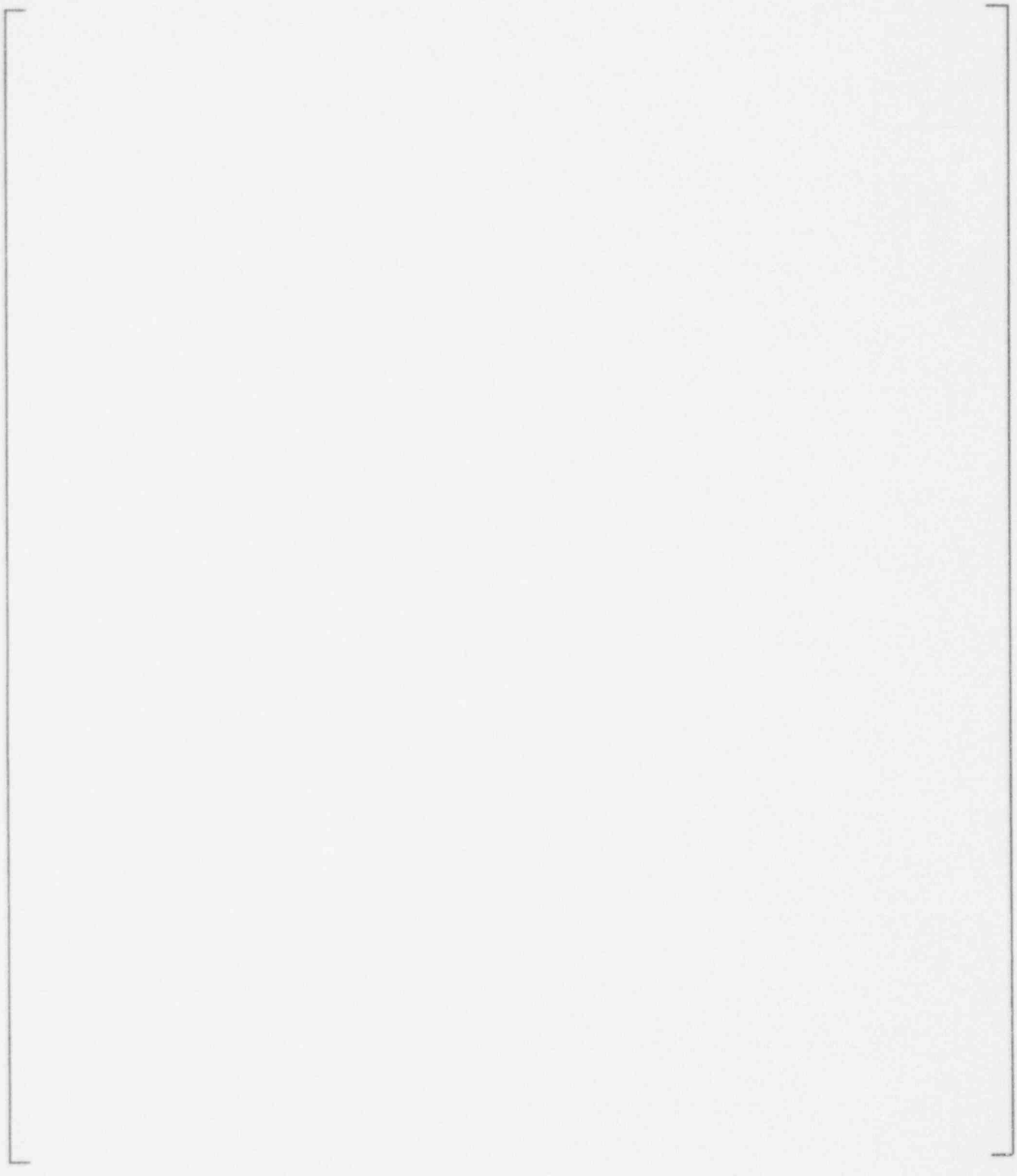

a,c

Figure 3.1-13 WCOBRA/TRAC CCTF Upper Head Region Noding (Section 7)

a,c

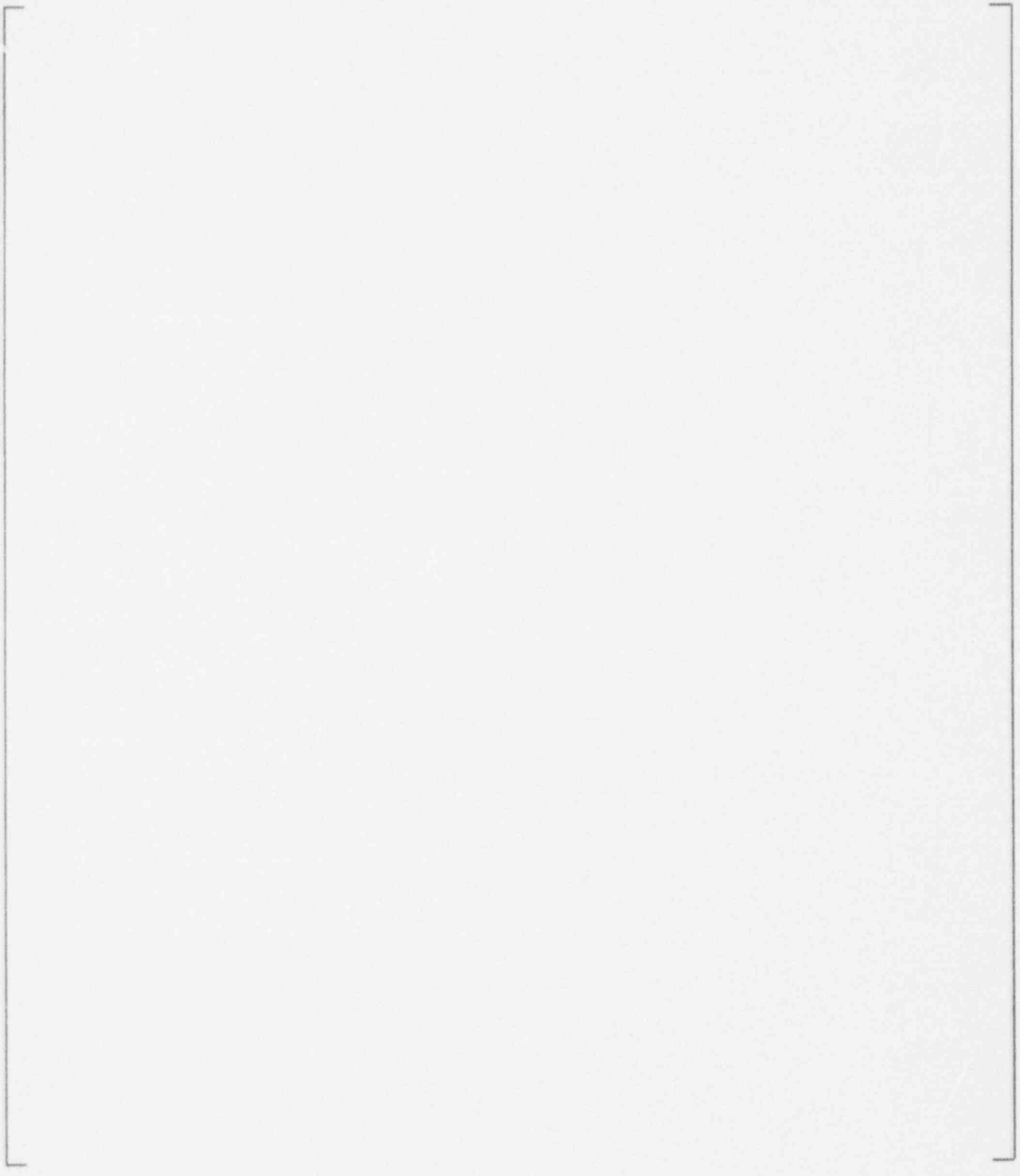

Figure 3.1-14 WCOBRA/TRAC CCTF Downcomer Channel Arrangement

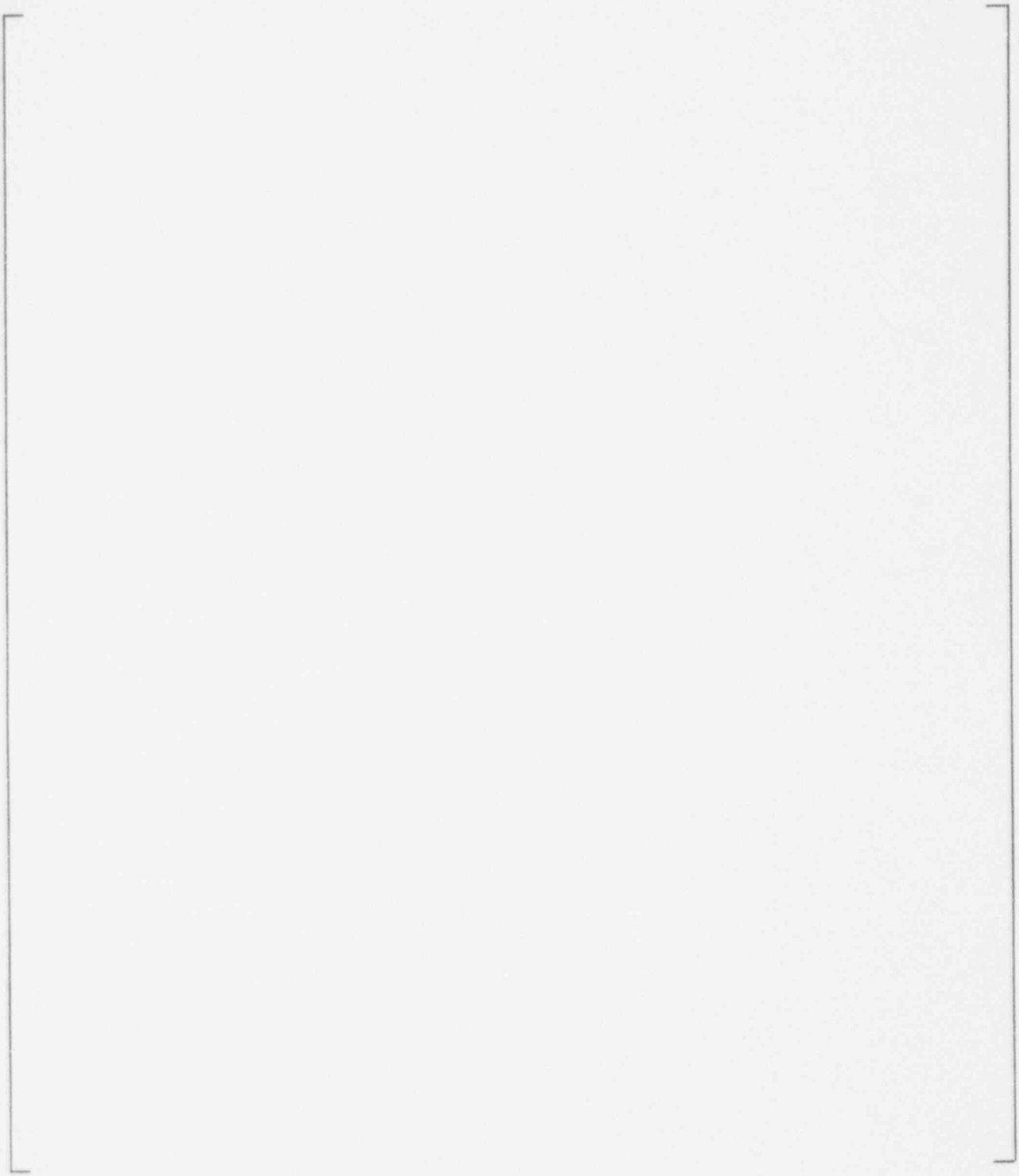

a,c

Figure 3.1-15 WCOBRA/TRAC CCTF Loop Noding Diagram

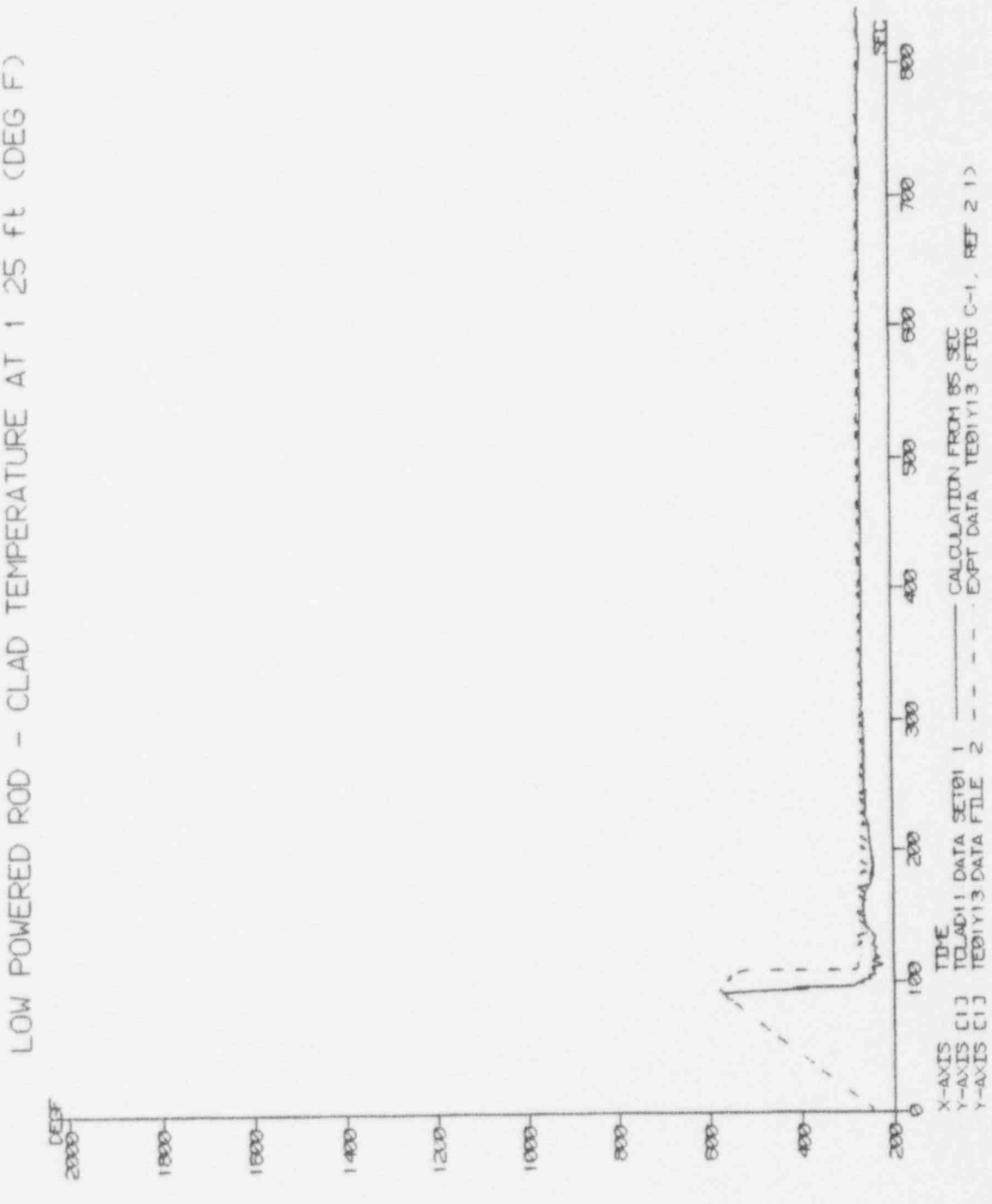

Figure 3.1-16 CCTF Run 58, Low-Powered Rod, Clad Temperature at 1.25 ft.

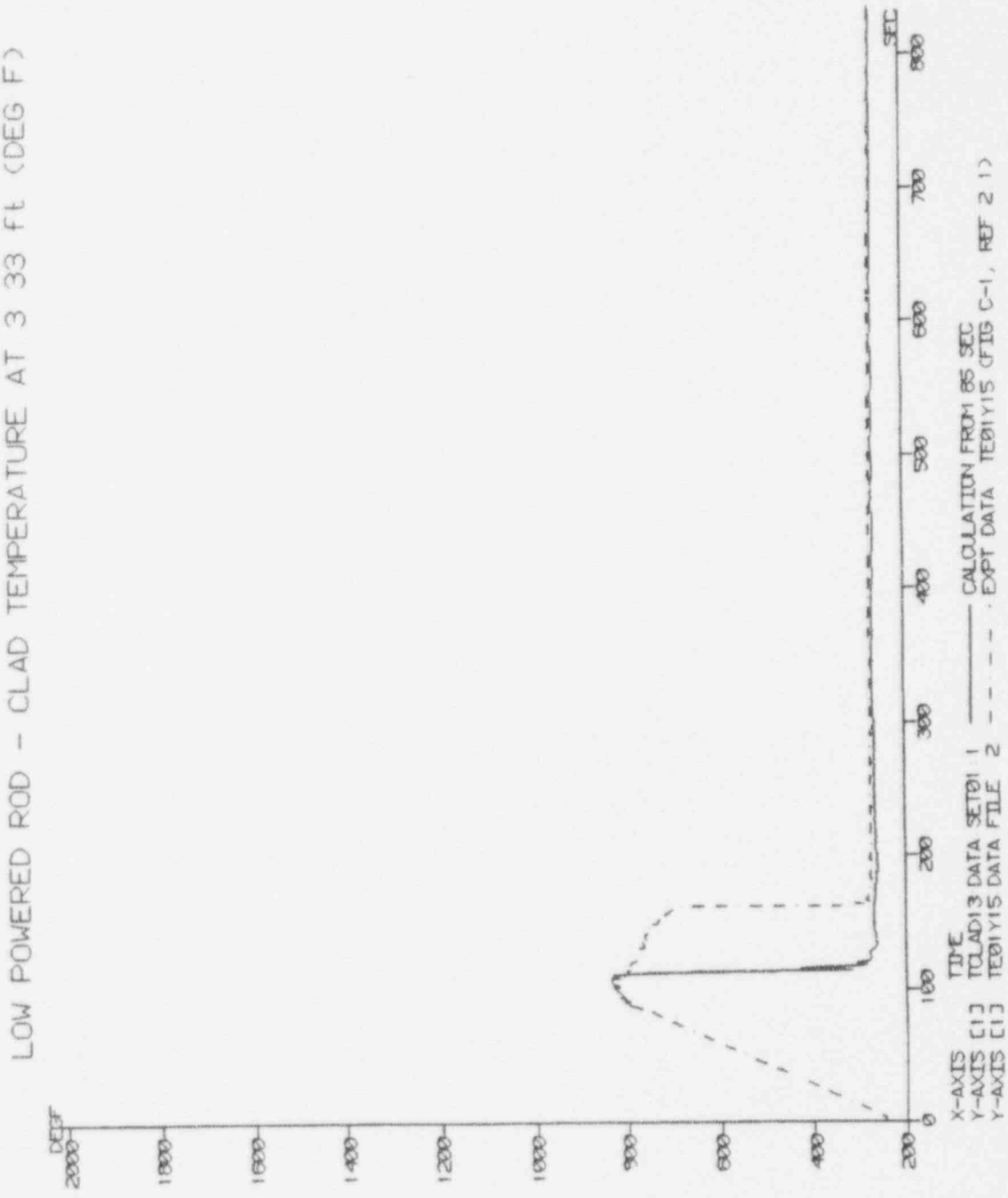

Figure 3.1-17 CCTF Run 58, Low-Powered Rod, Clad Temperature at 3.33 ft.

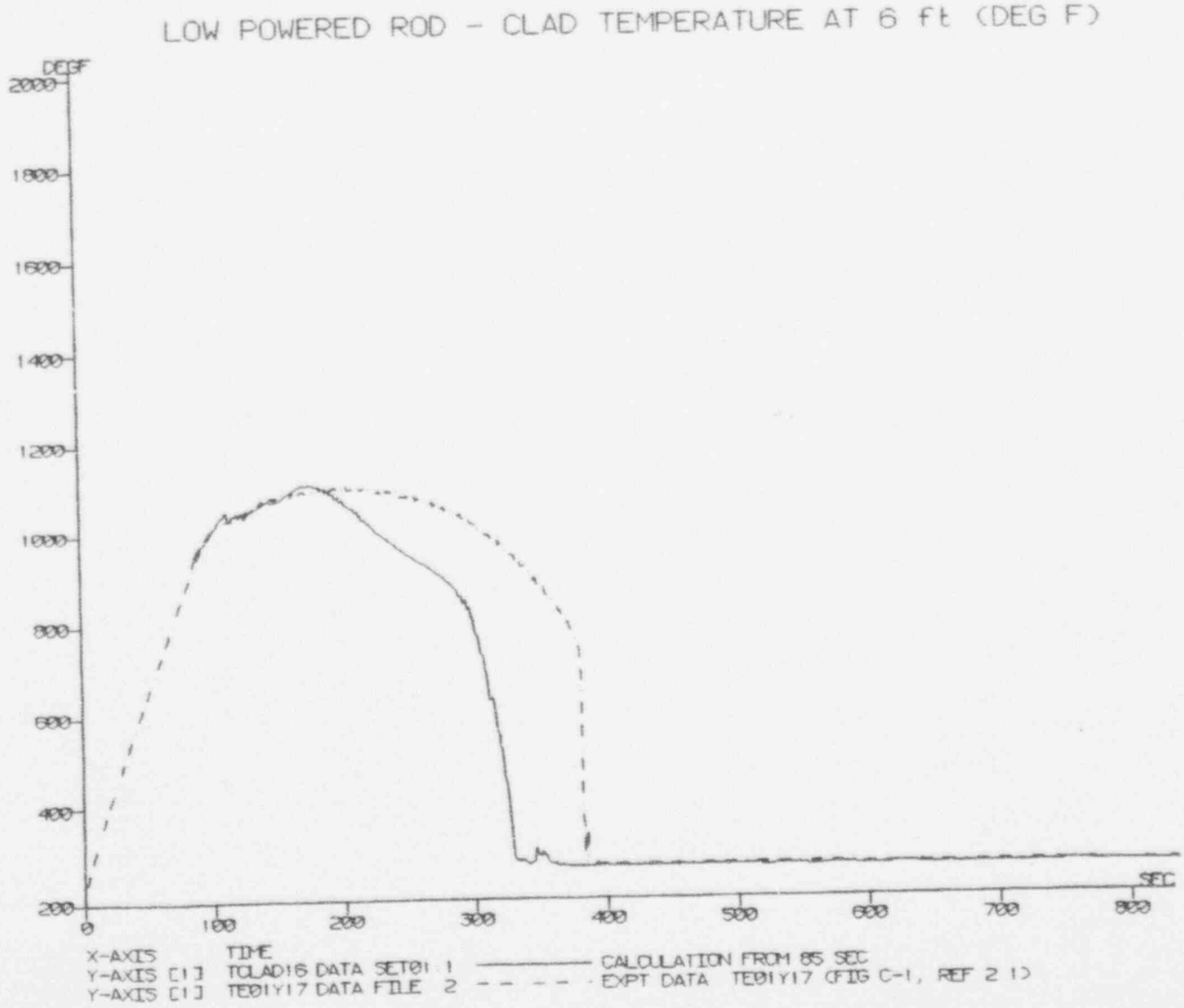

Figure 3.1-18 CCTF Run 58, Low-Powered Rod, Clad Temperature at 6 ft.

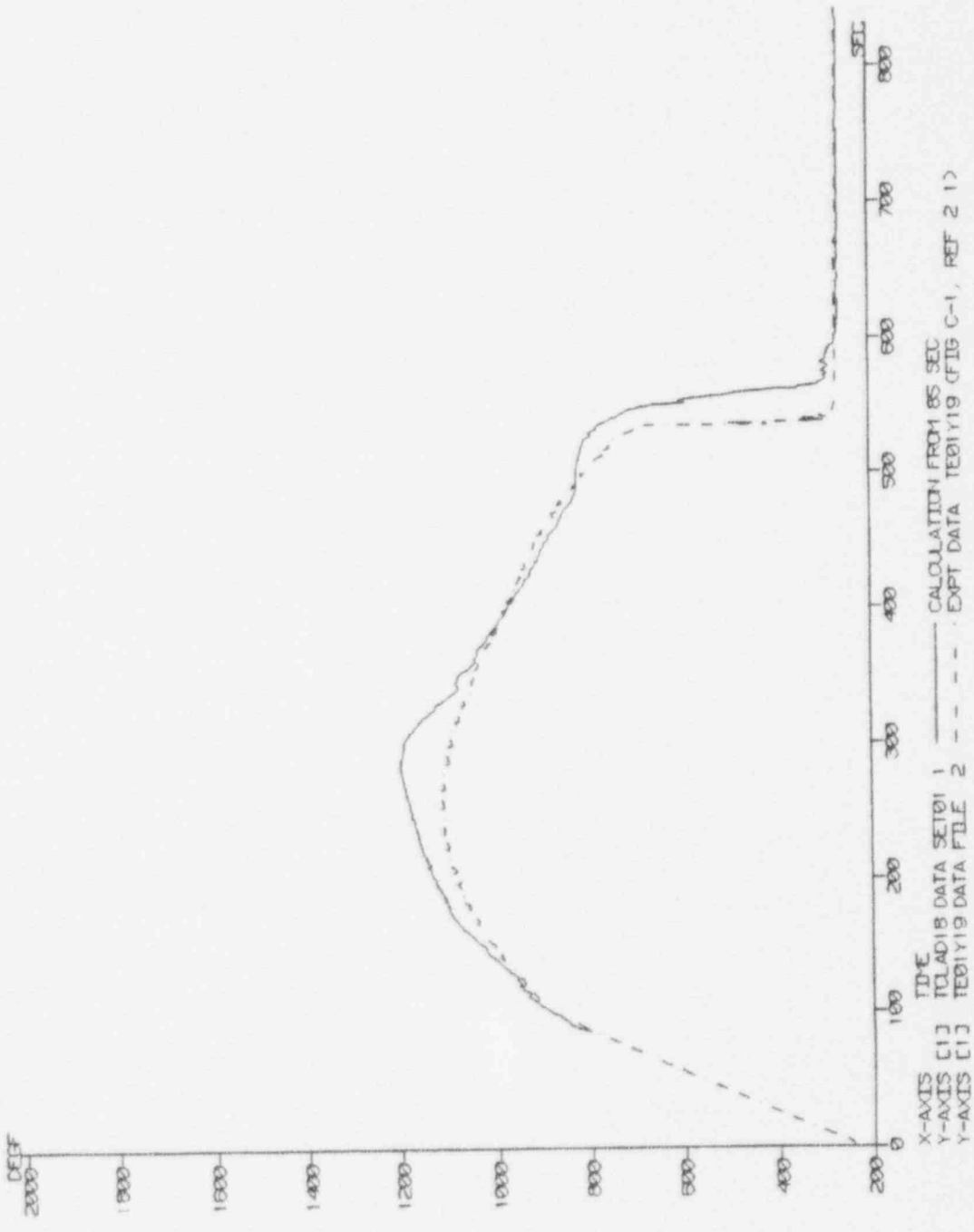

Figure 3.1-19 CCTF Run 58, Low-Powered Rod, Clad Temperature at 8 ft.

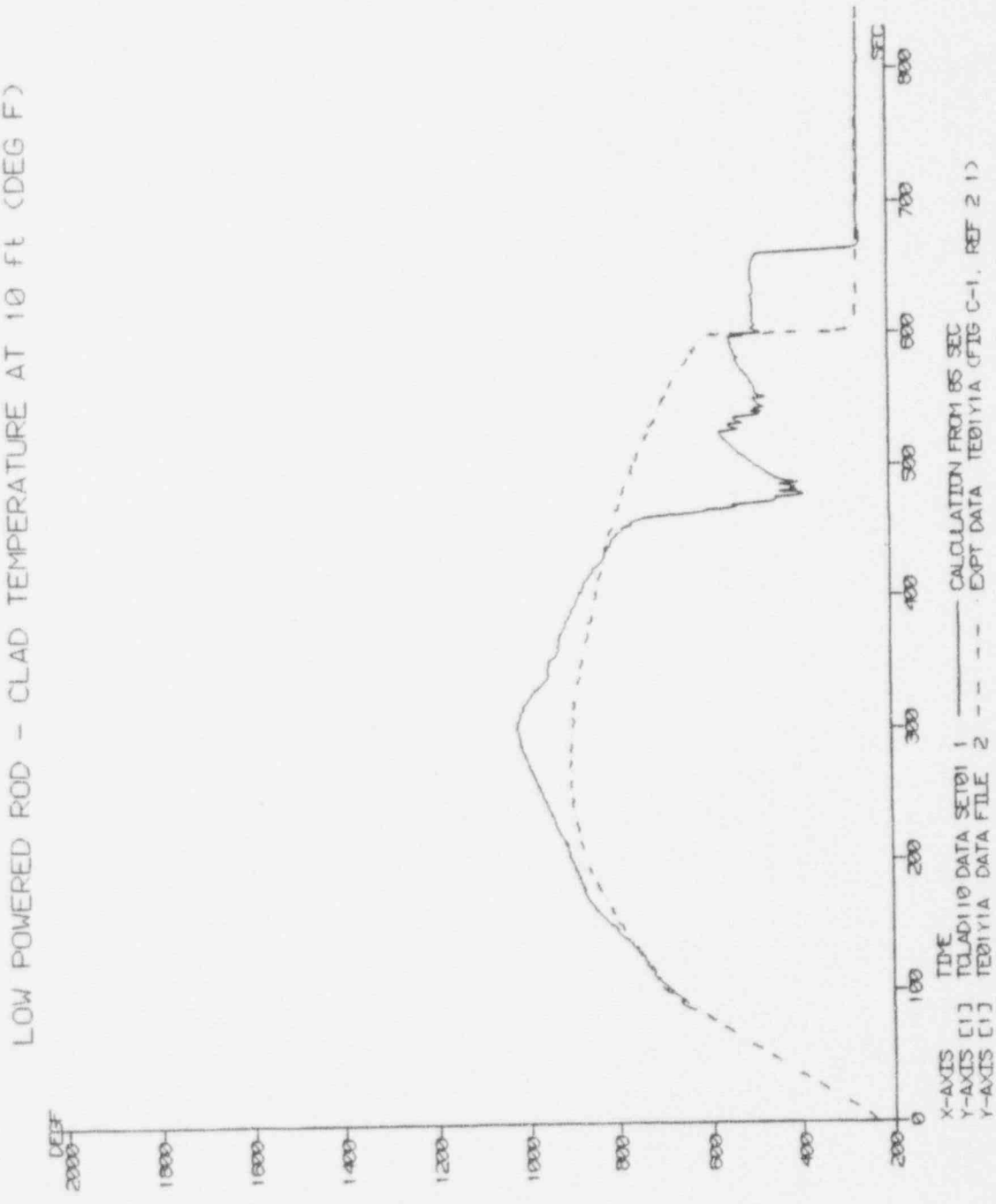

Figure 3.1-20 CCTF Run 58, Low-Powered Rod, Clad Temperature at 10 ft.

Figure 3.1-21 CCTF Run 58, Medium-Powered Rod, Clad Temperature at 1.25 ft.

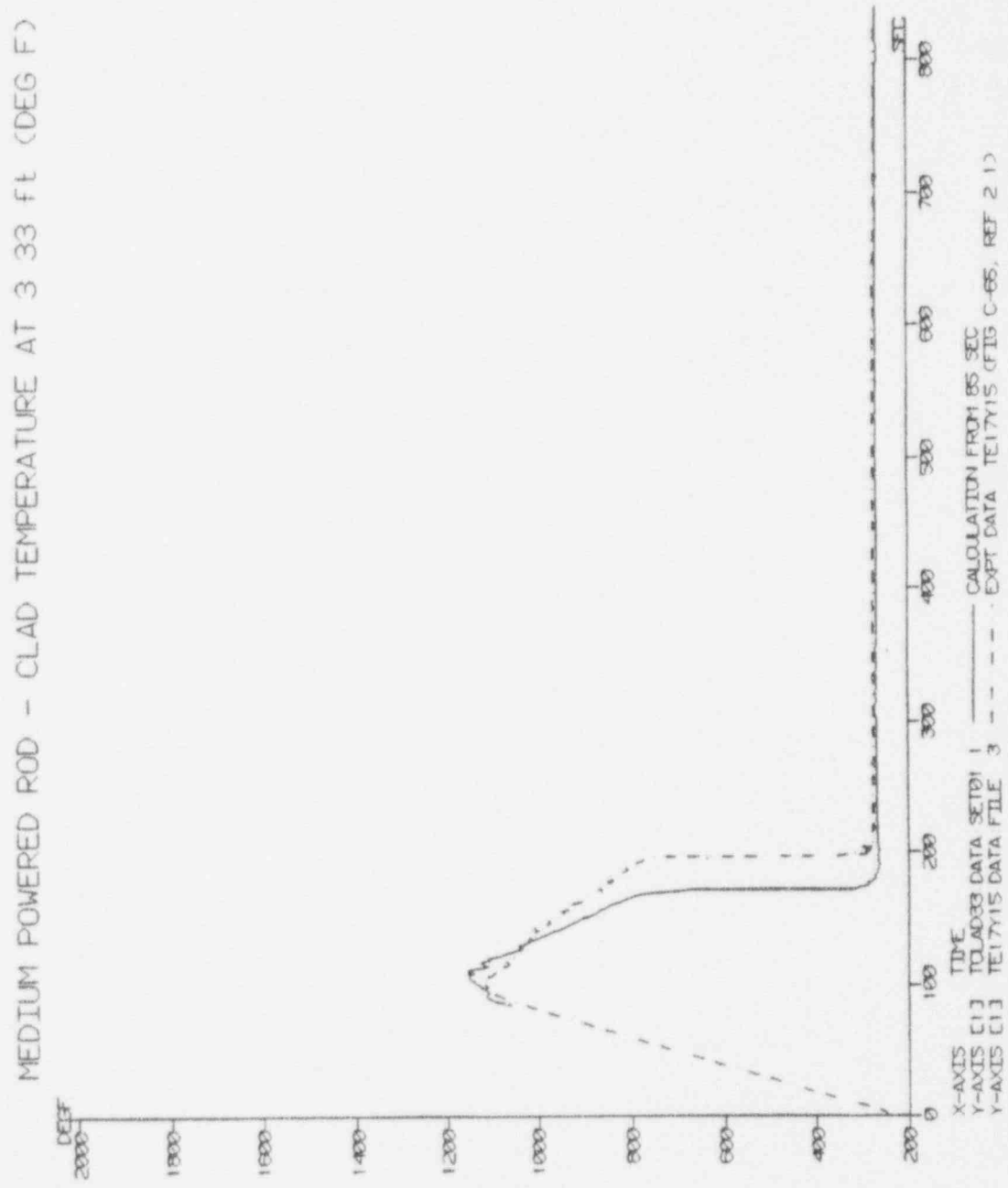

Figure 3.1-22 CCTF Run 58, Medium-Powered Rod, Clad Temperature at 3.33 ft.

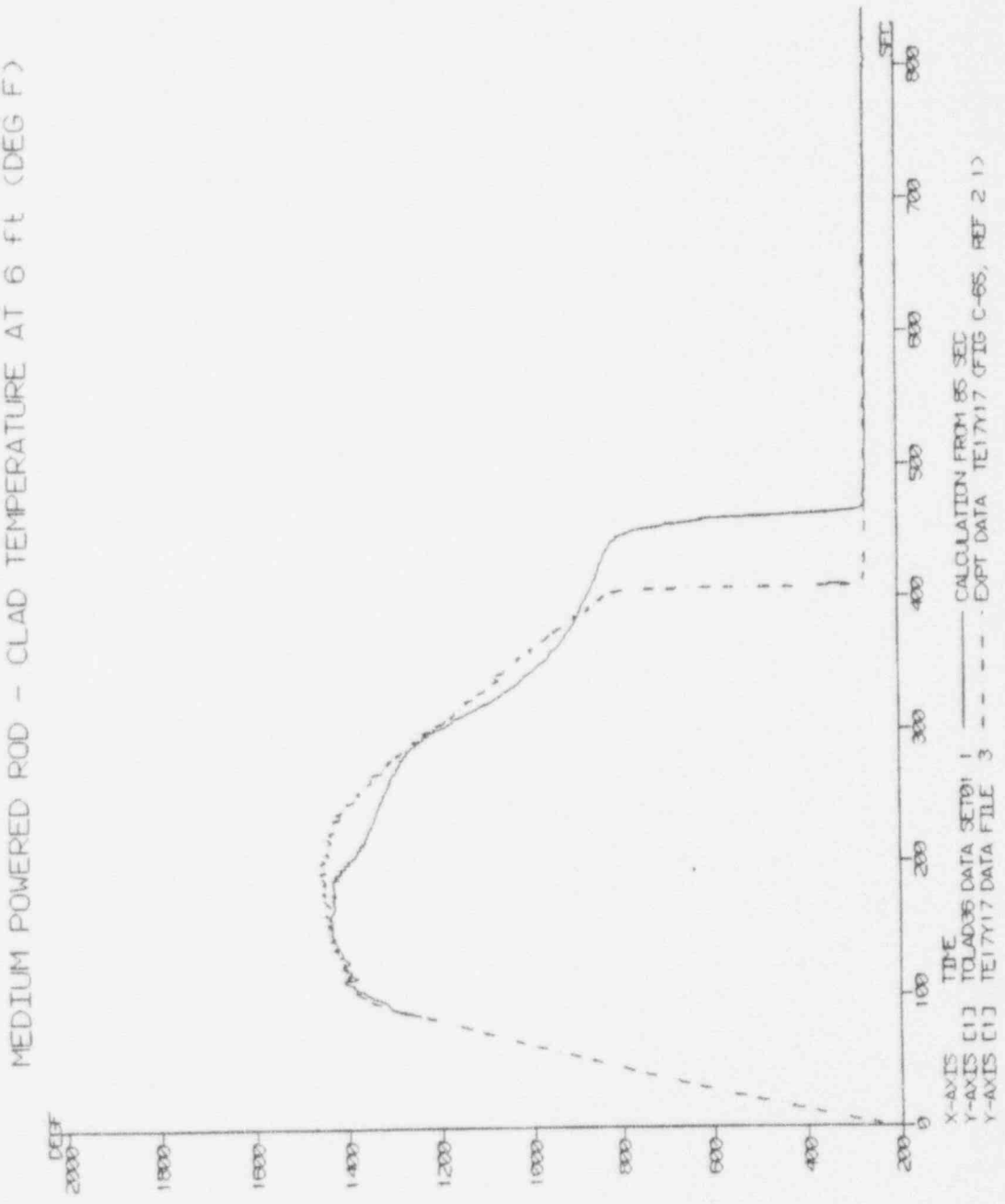

Figure 3.1-23 CCTF Run 58, Medium-Powered Rod, Clad Temperature at 6 ft.

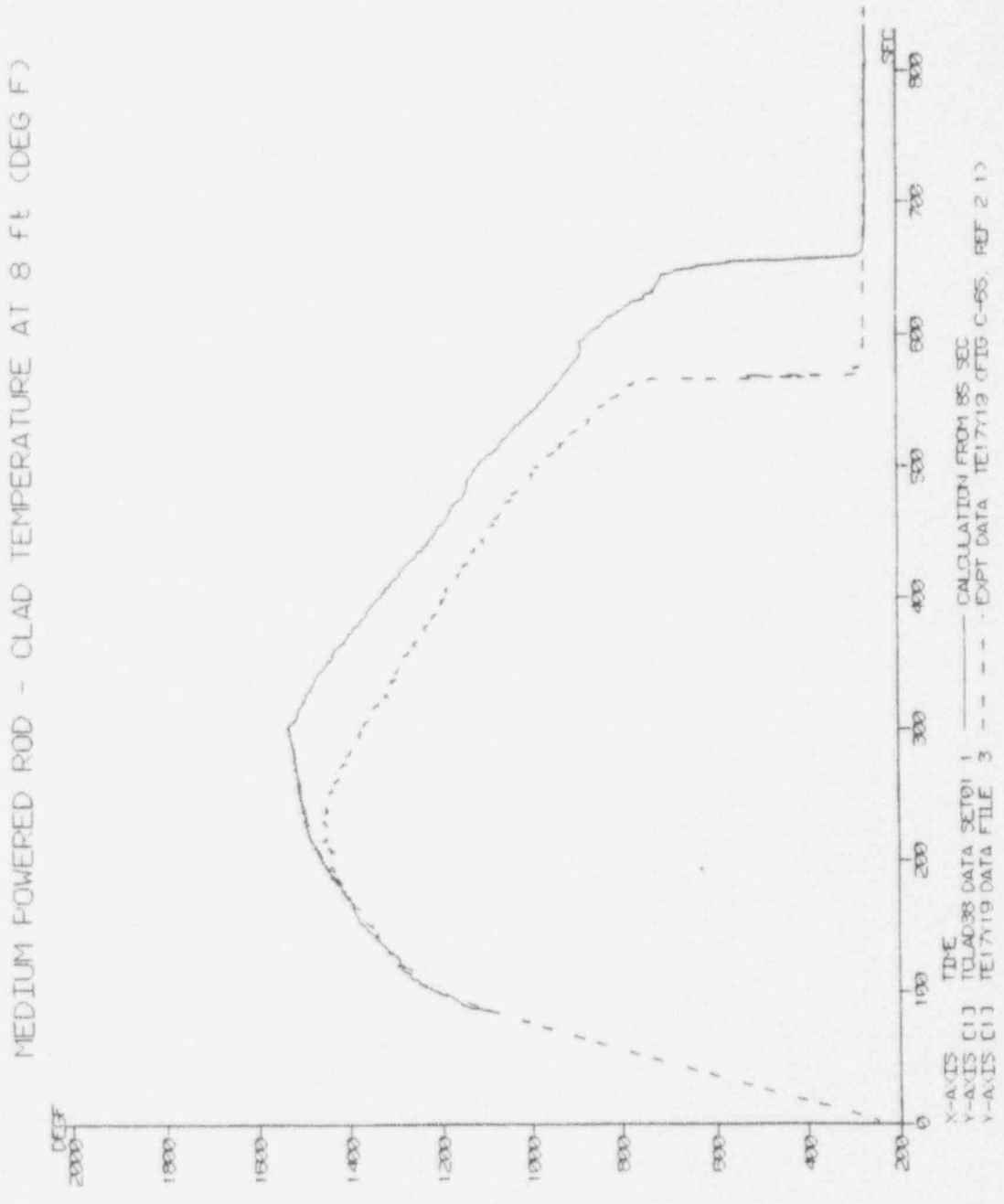

Figure 3.1-24 CCTF Run 58, Medium-Powered Rod, Clad Temperature at 8 ft.

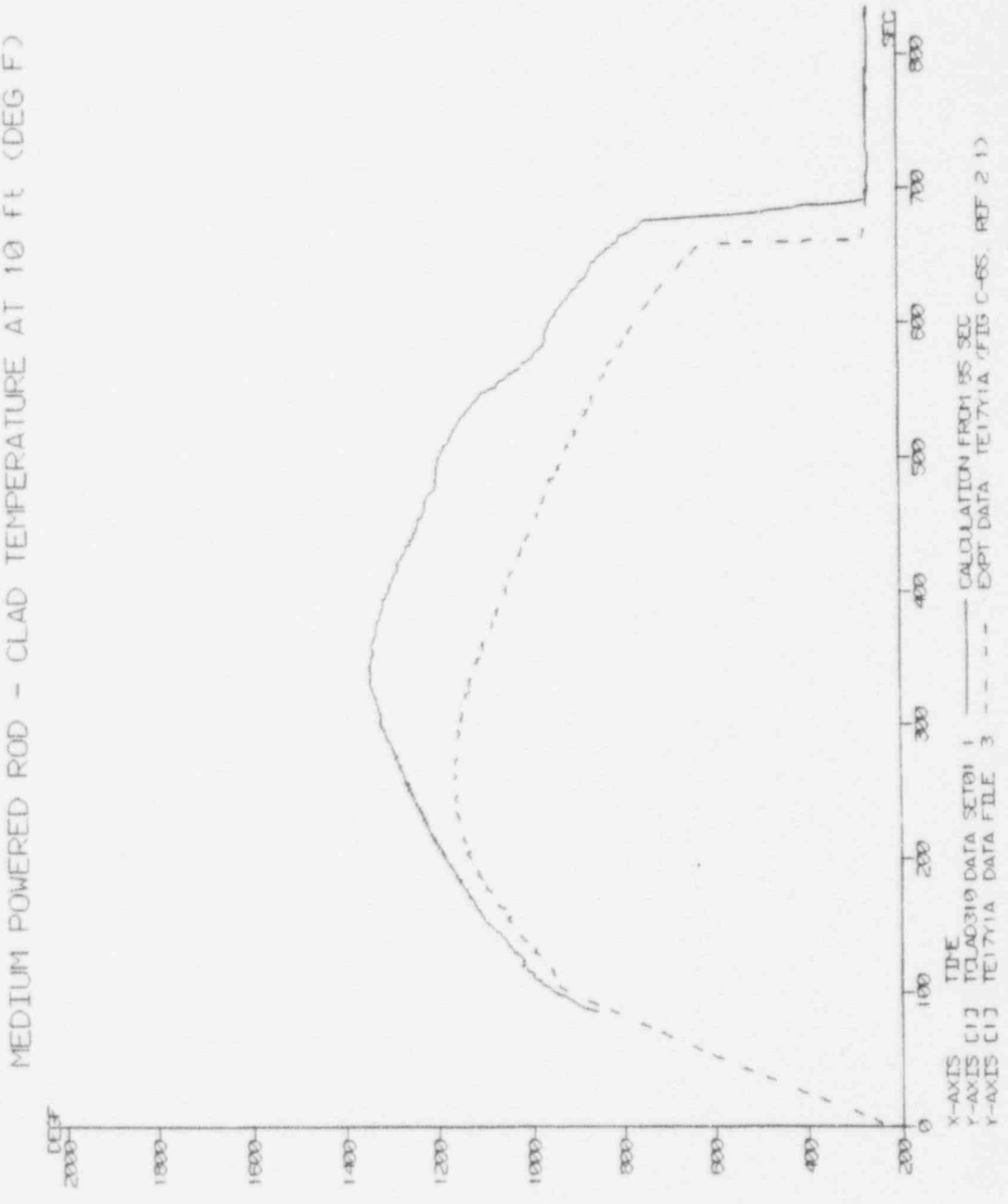

Figure 3.1-25 CCTF Run 58, Medium-Powered Rod, Clad Temperature at 10 ft.

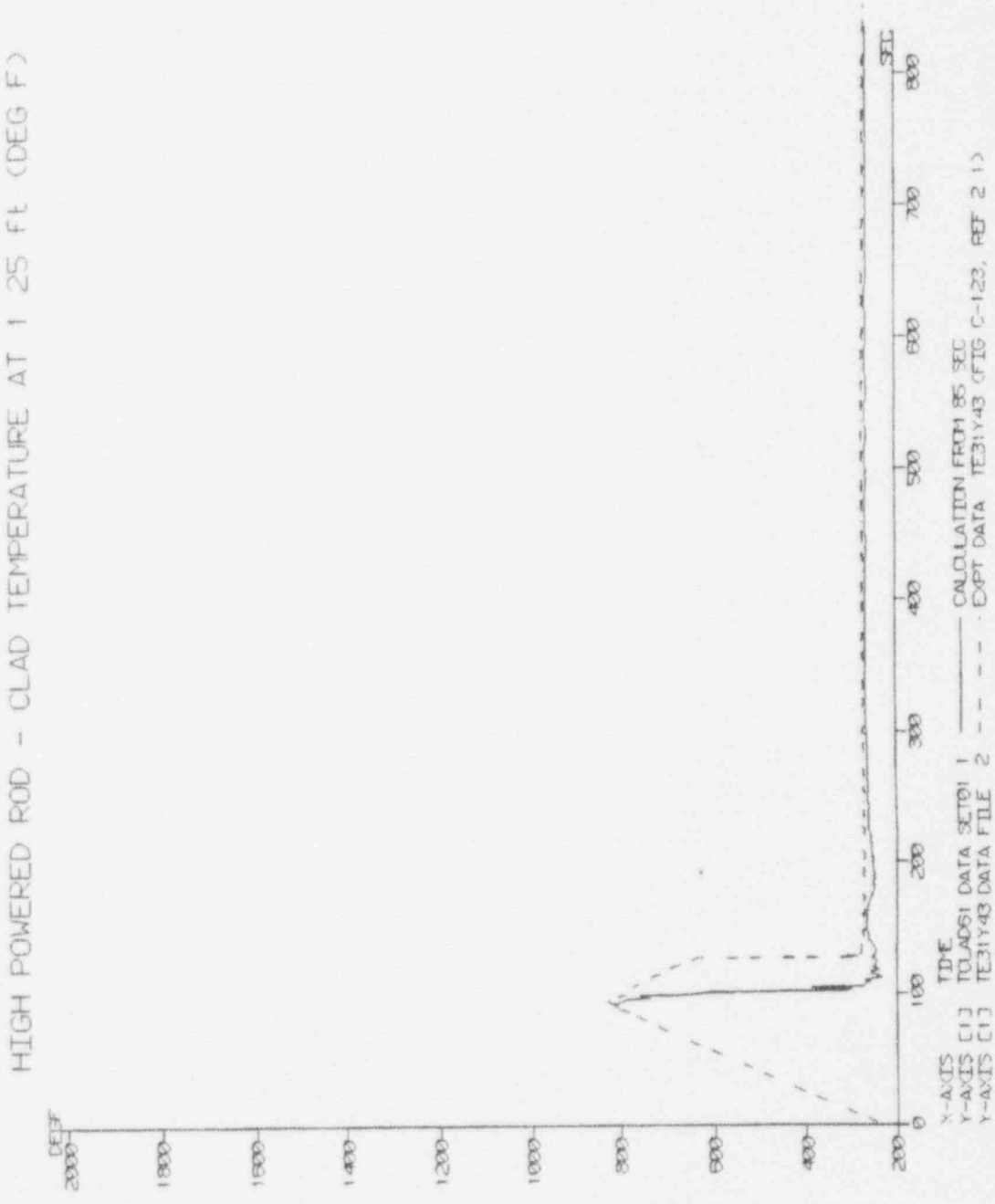

Figure 3.1-26 CCTF Run 58, High-Powered Rod, Clad Temperature at 1.25 ft.

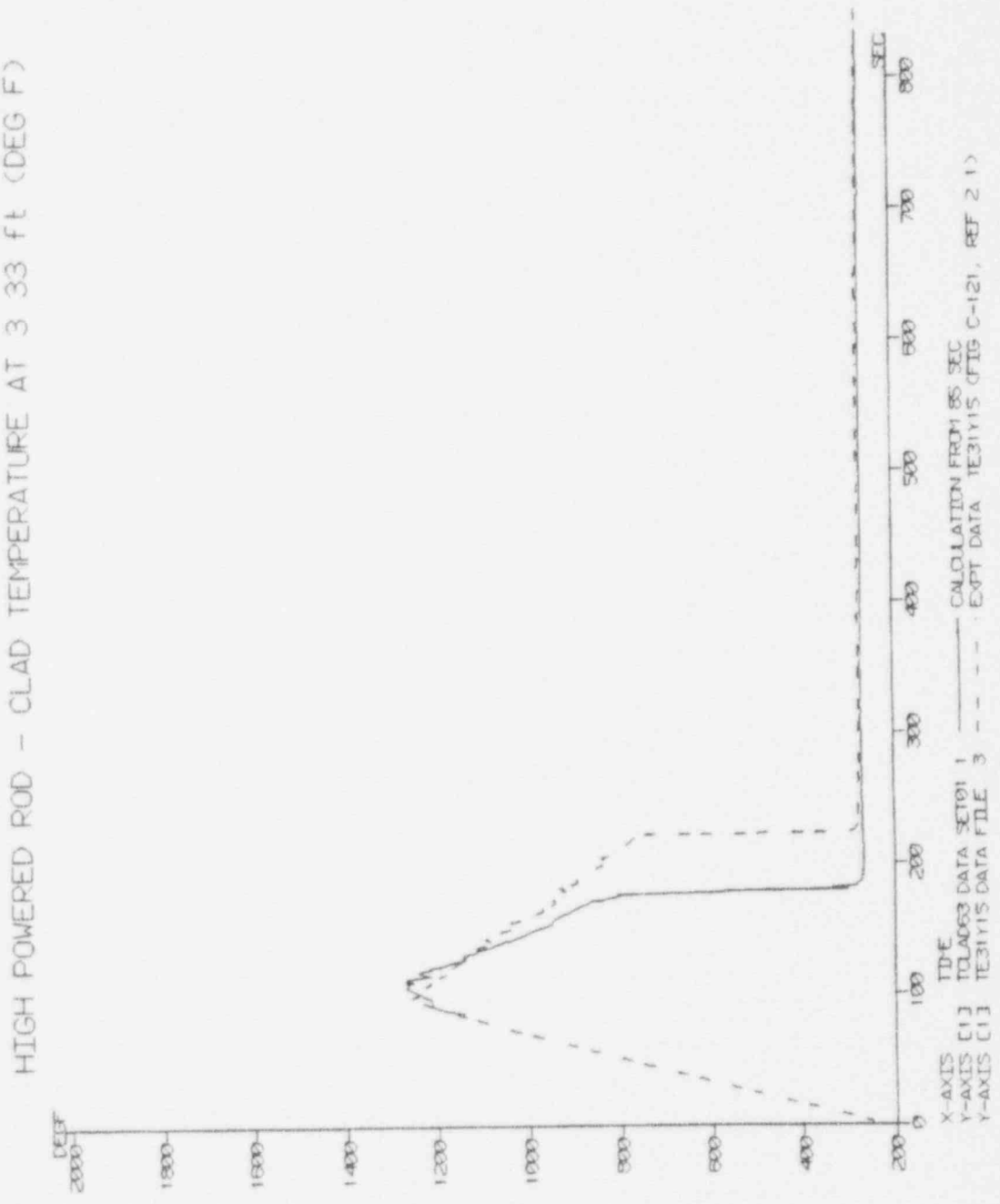

Figure 3.1-27 CCTF Run 58, High-Powered Rod, Clad Temperature at 3.33 ft.

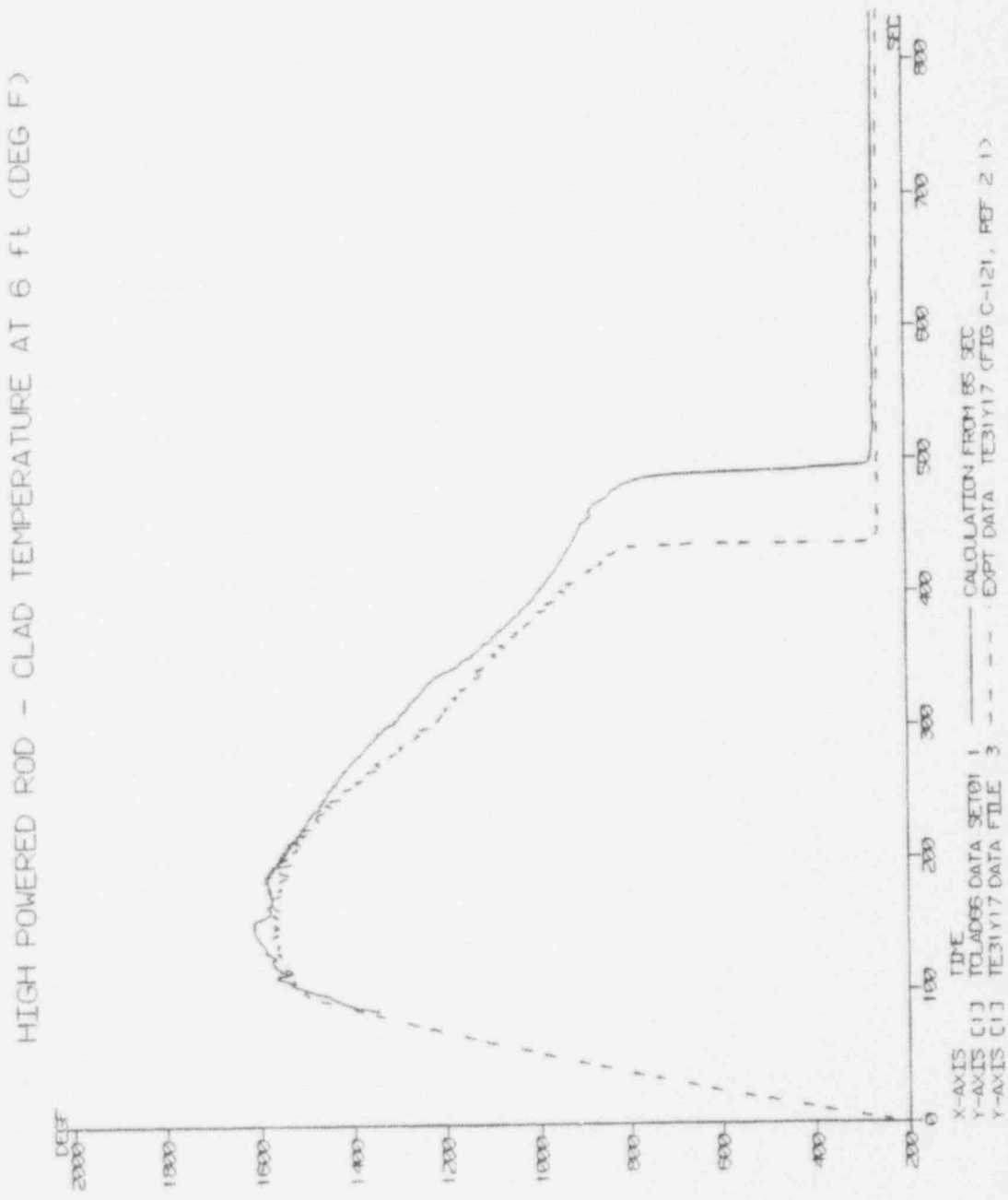

Figure 3.1-28 CCTF Run 58, High-Powered Rod, Clad Temperature at 6 ft.

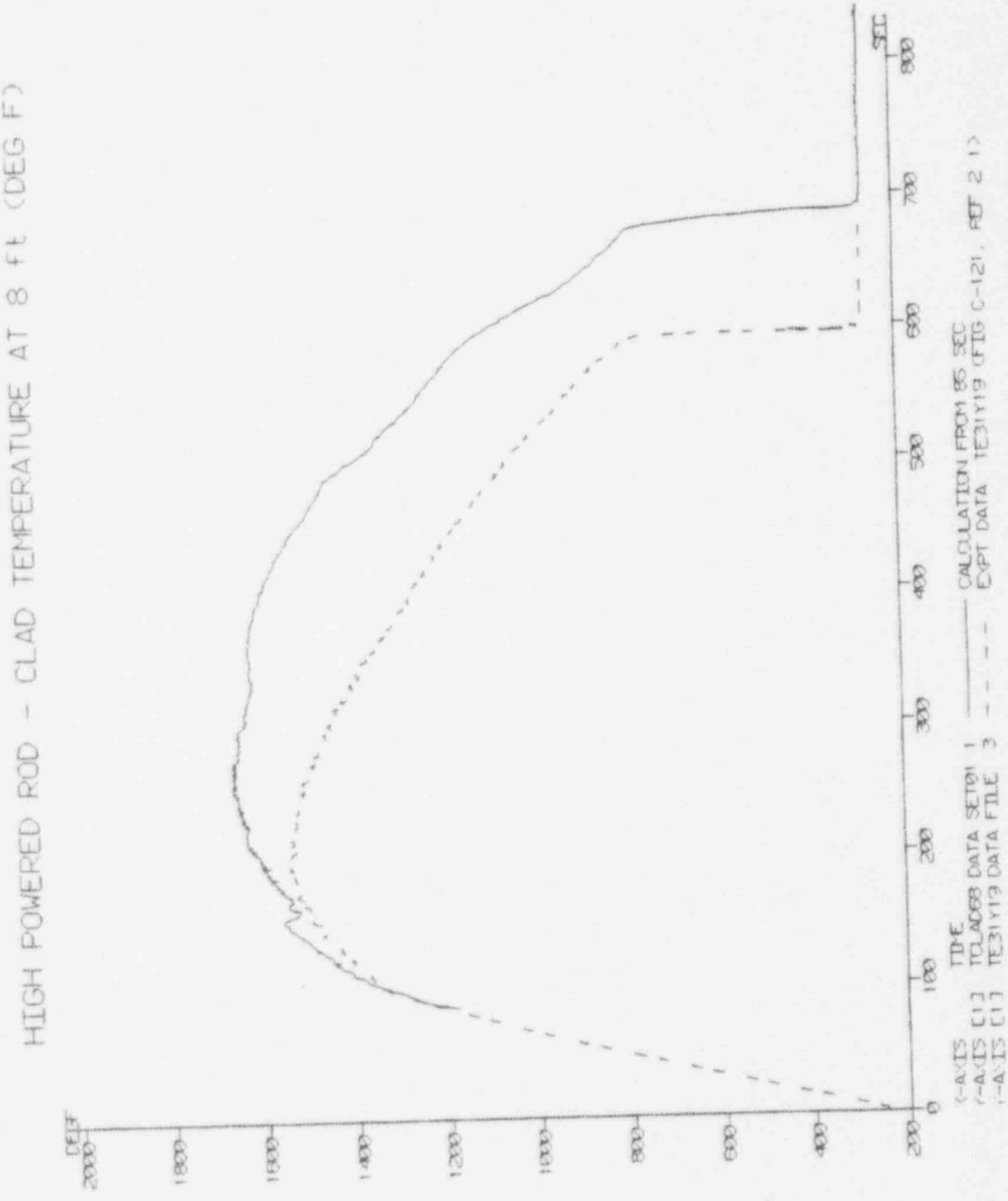

Figure 3.1-29 CCTF Run 58, High-Powered Rod, Clad Temperature at 8 ft.

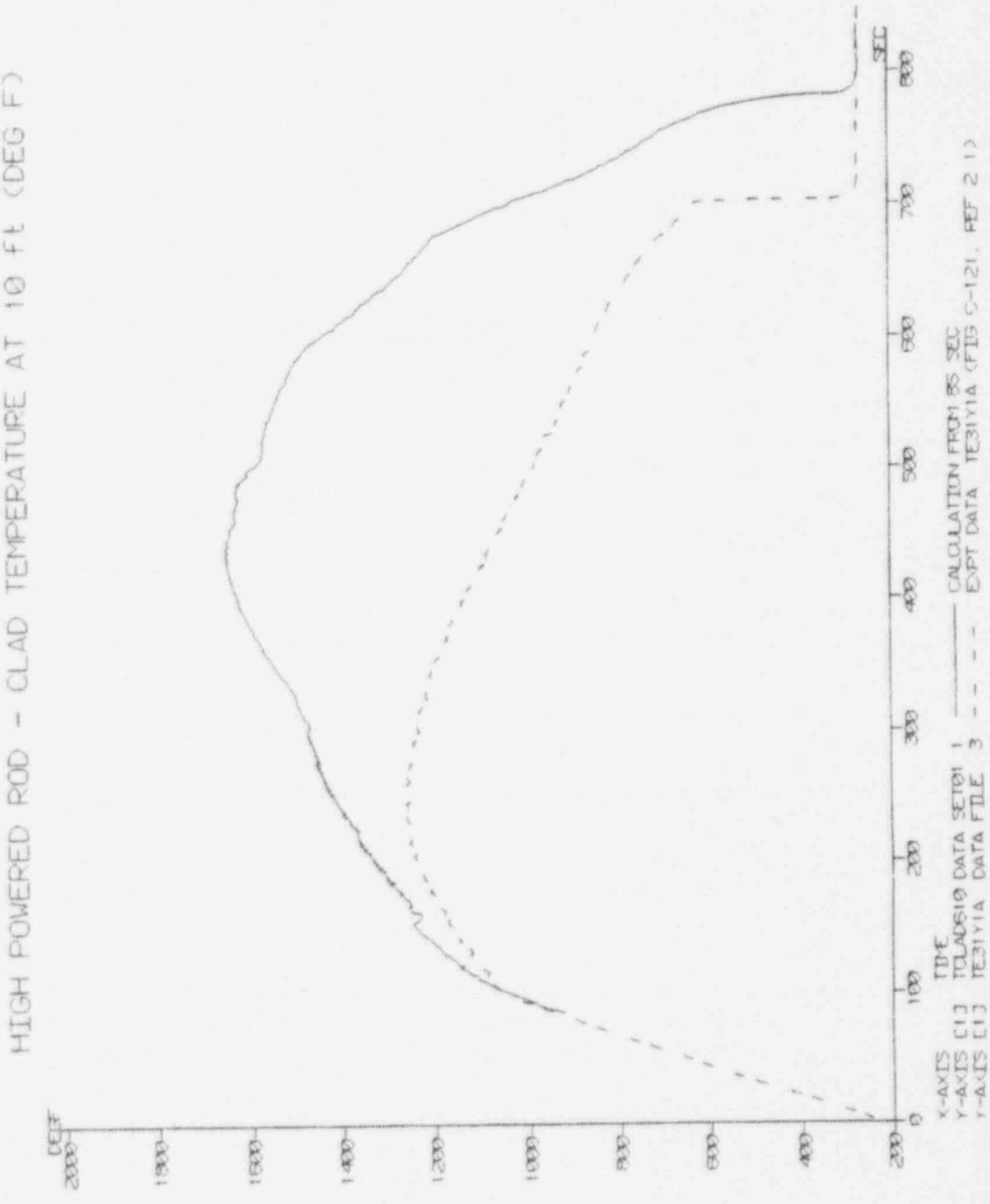

Figure 3.1-30 CCTF Run 58, High-Powered Rod, Clad Temperature at 10 ft.

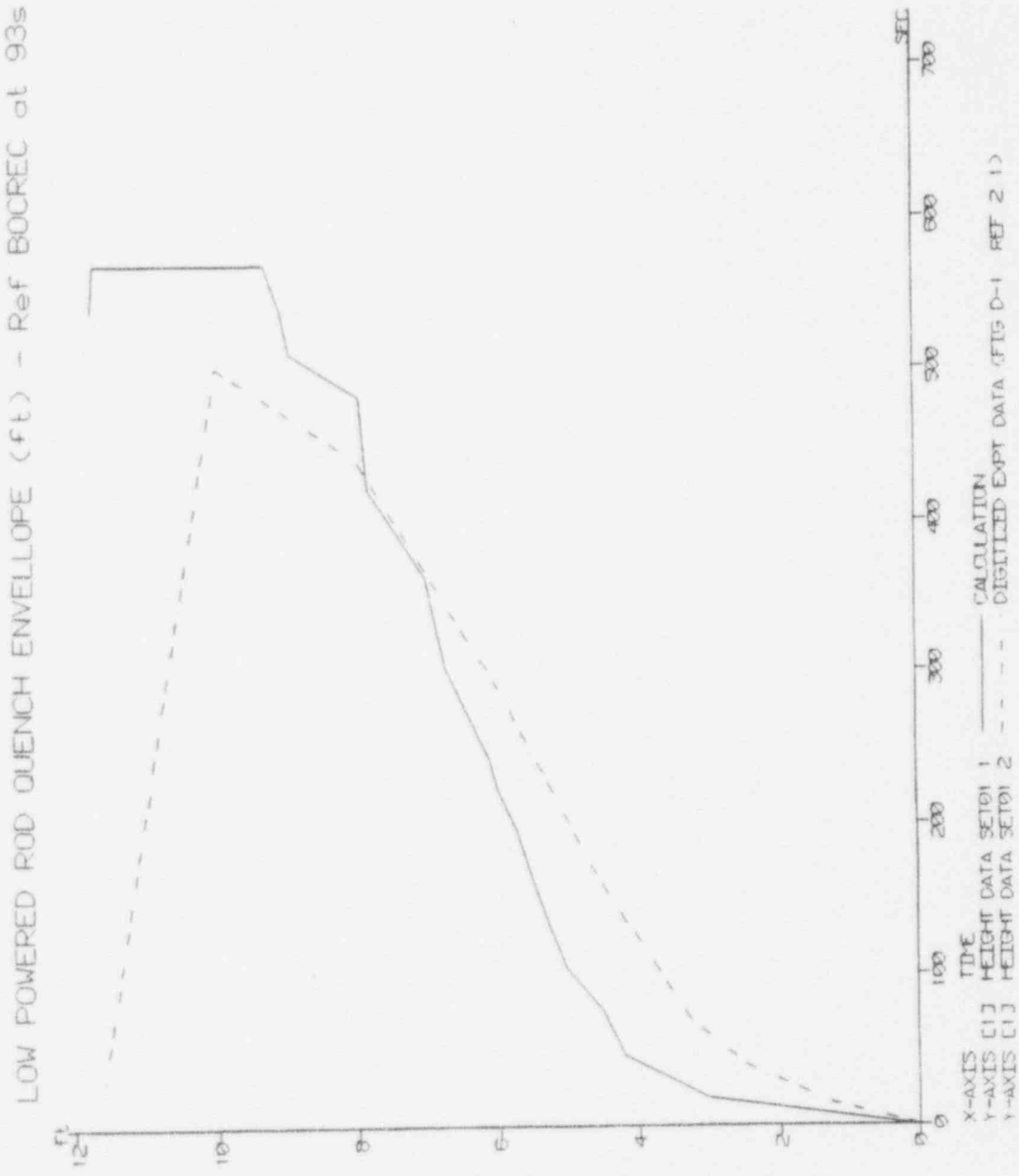

Figure 3.1-31 CCTF Run 58, Quench Envelope - Low-Powered Rod

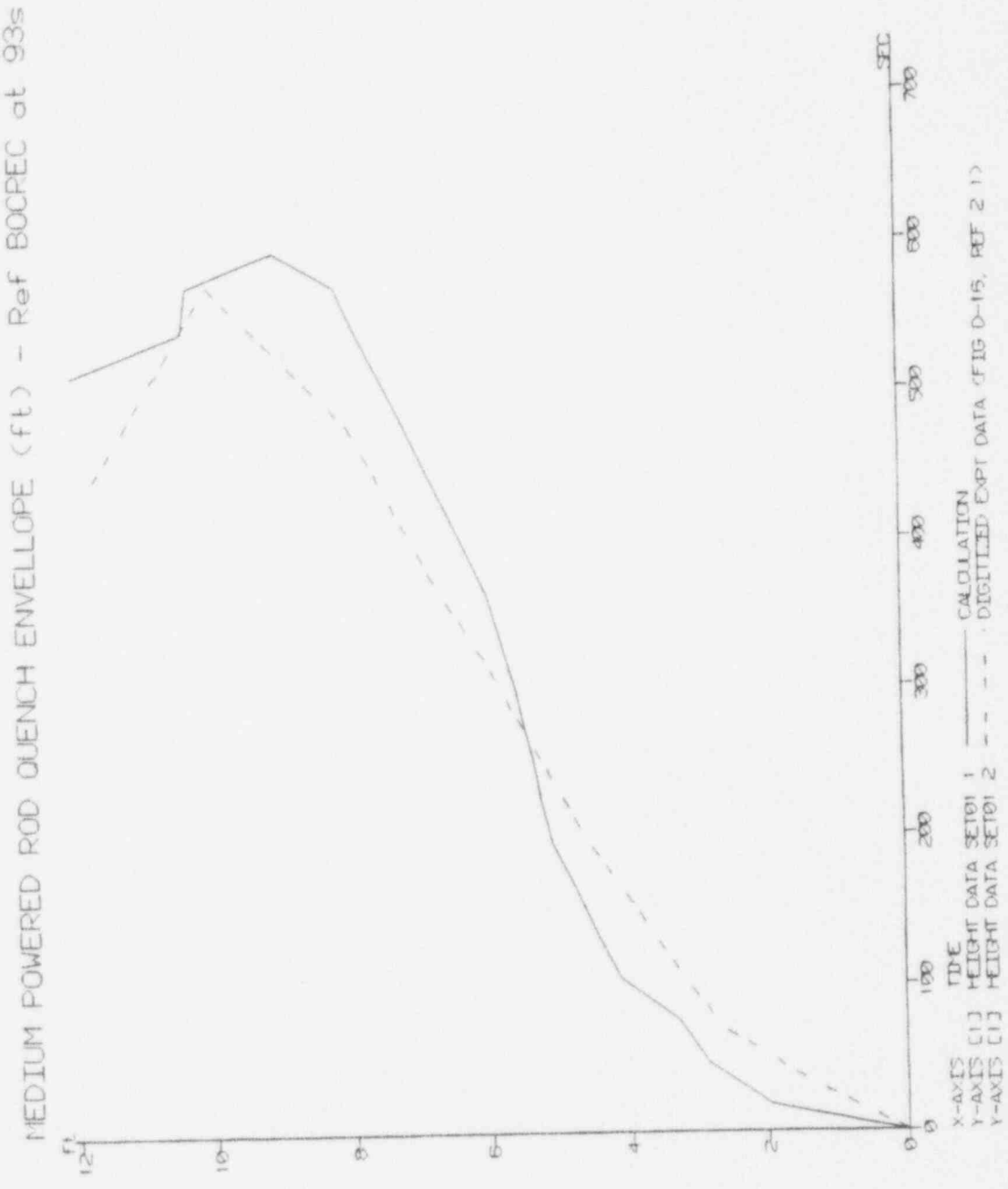

Figure 3.1-32 CCTF Run 58, Quench Envelope - Medium-Powered Rod

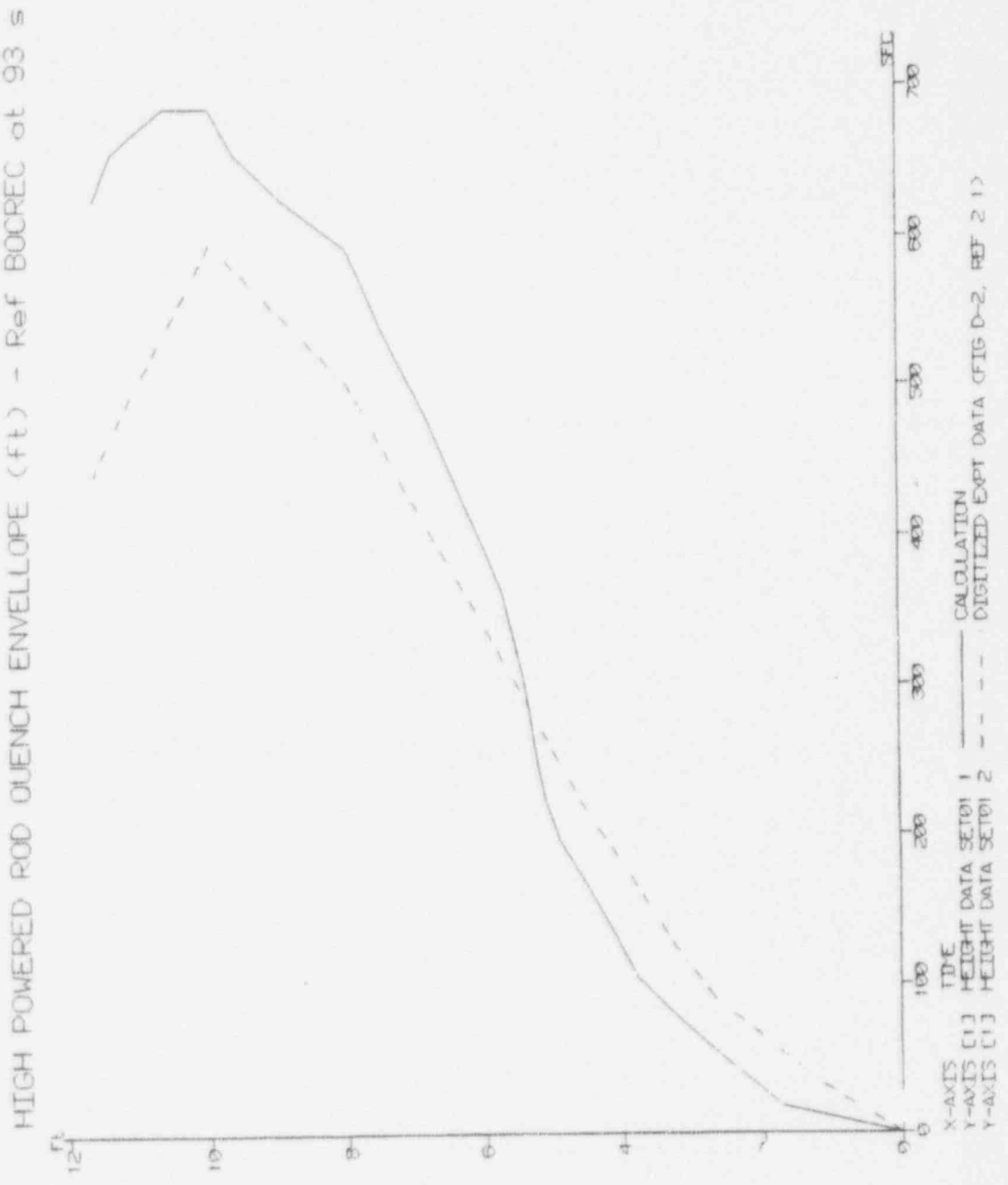

Figure 3.1-33 CCTF Run 58, Quench Envelope - High-Powered Rod

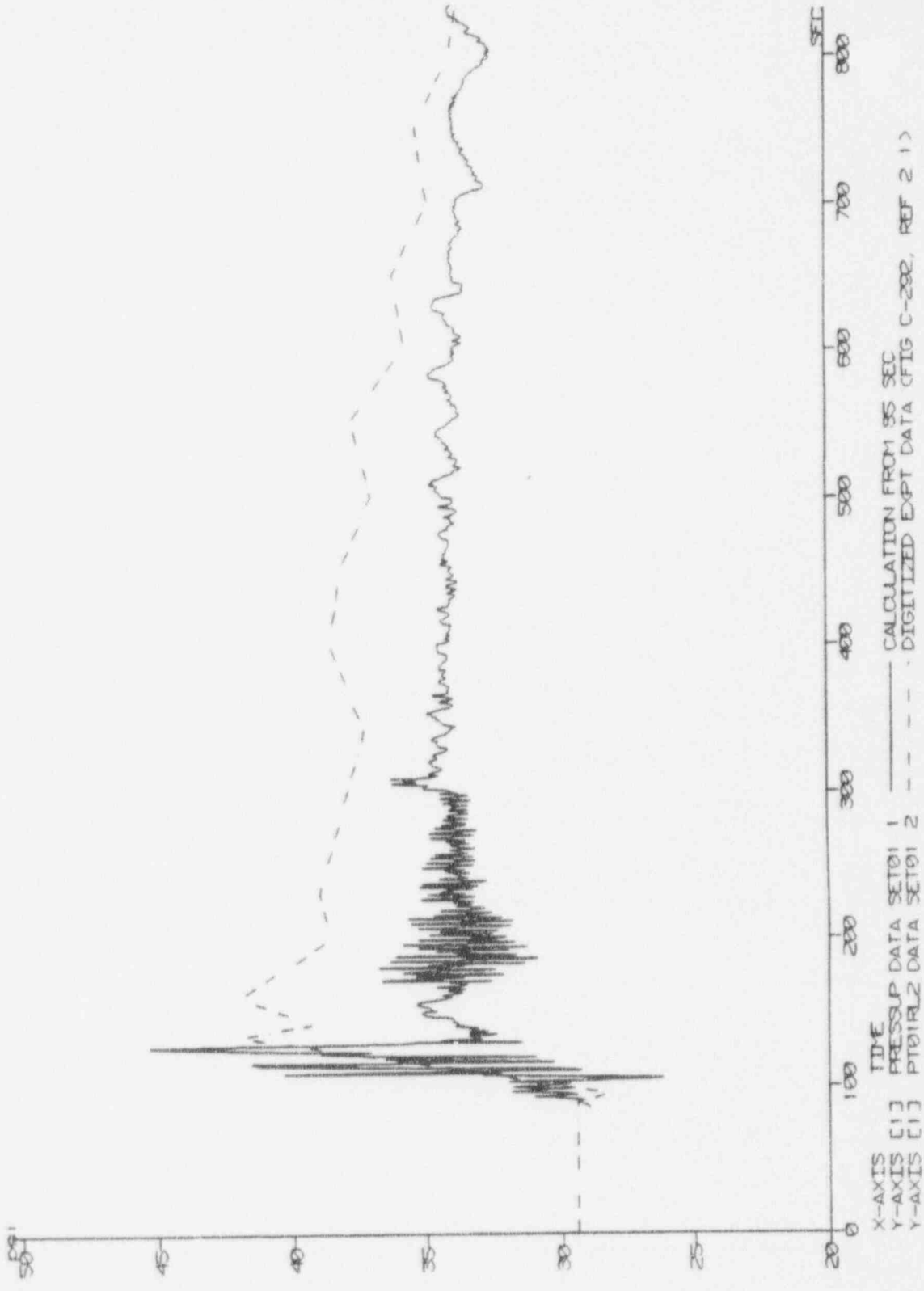

Figure 3.1-34 CCTF Run 58, Upper Plenum Pressure

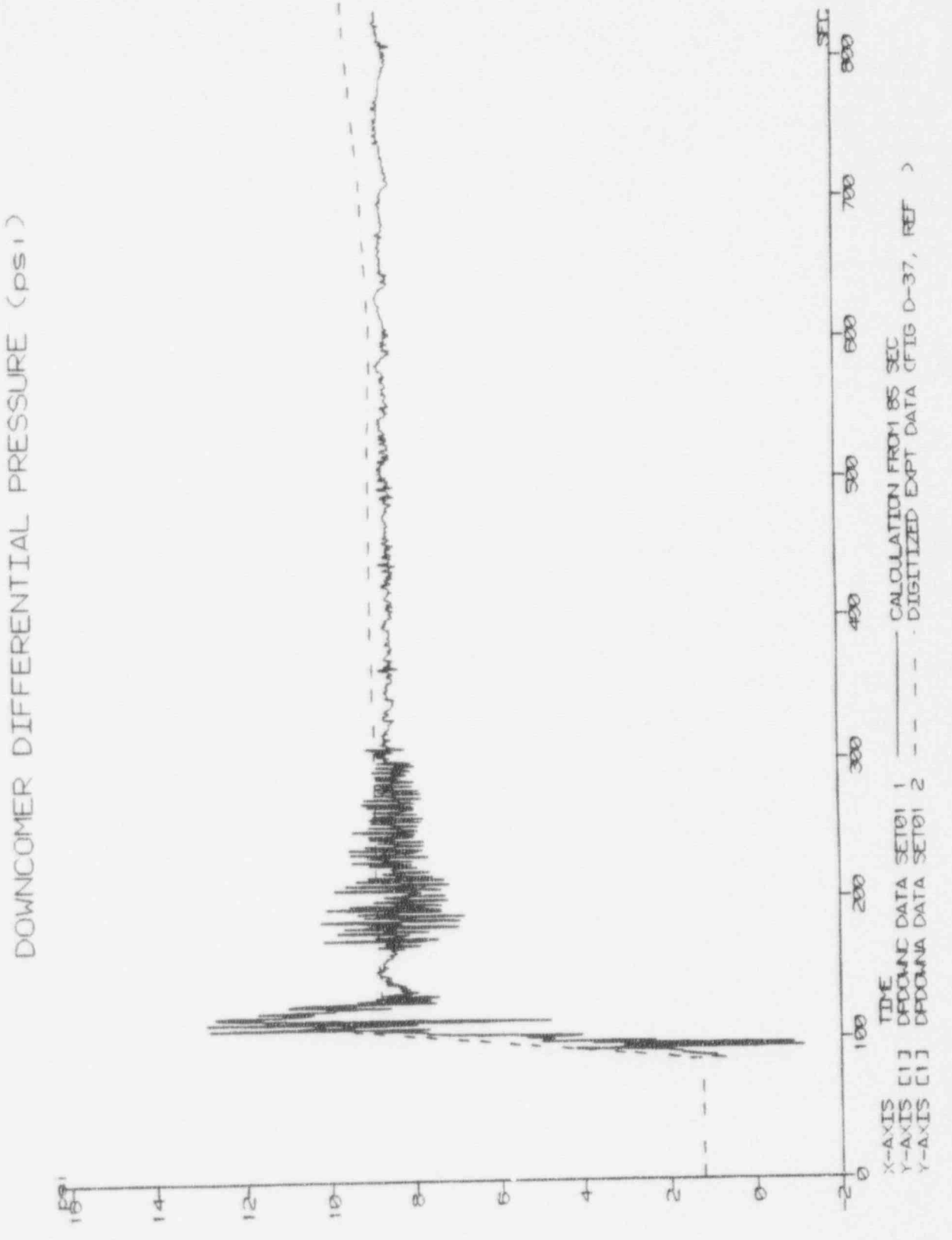

Figure 3.1-35 CCTF Run 58, Downcomer Differential Pressure

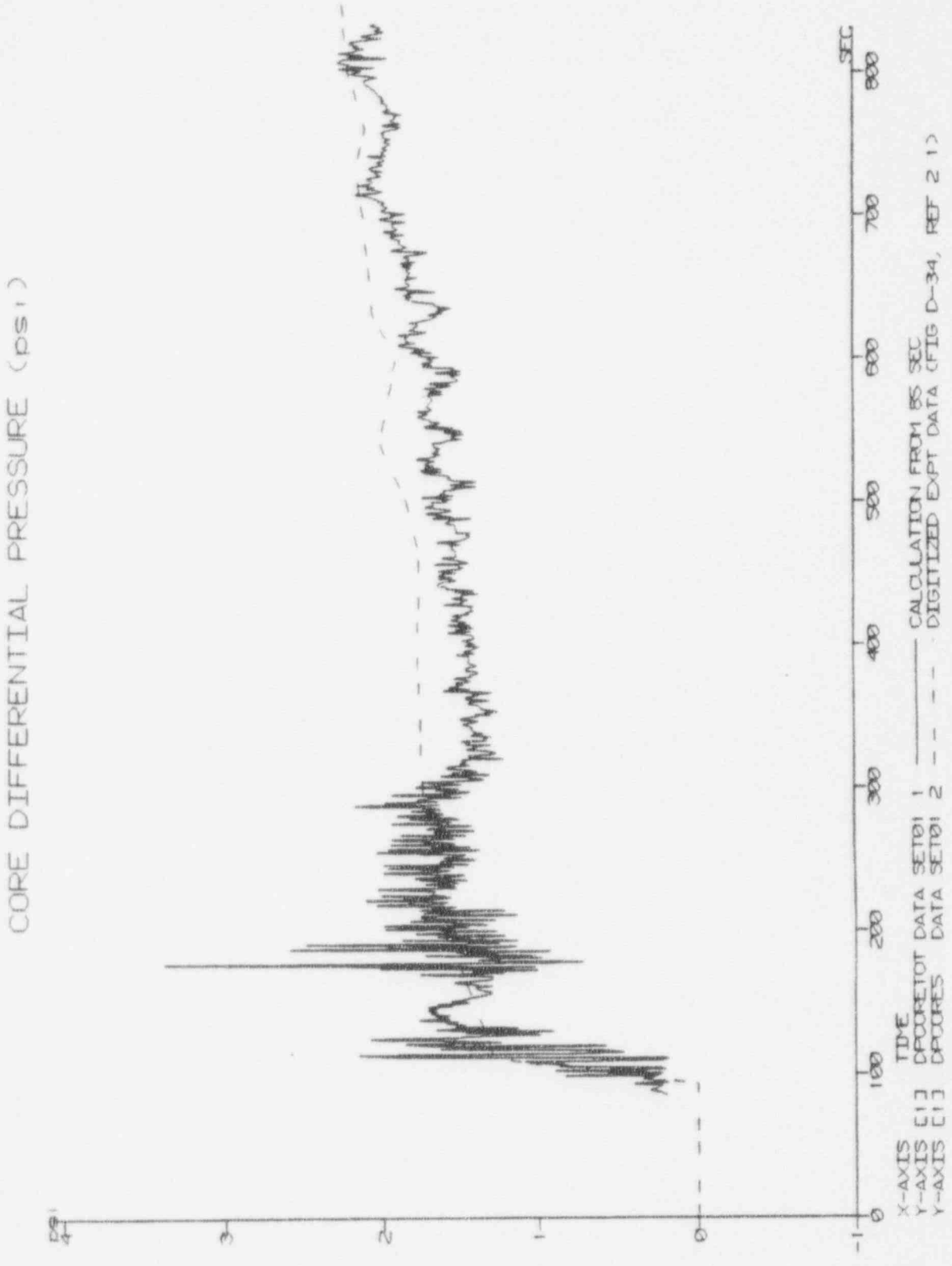

Figure 3.1-36 CCTF Run 58, Core Differential Pressure

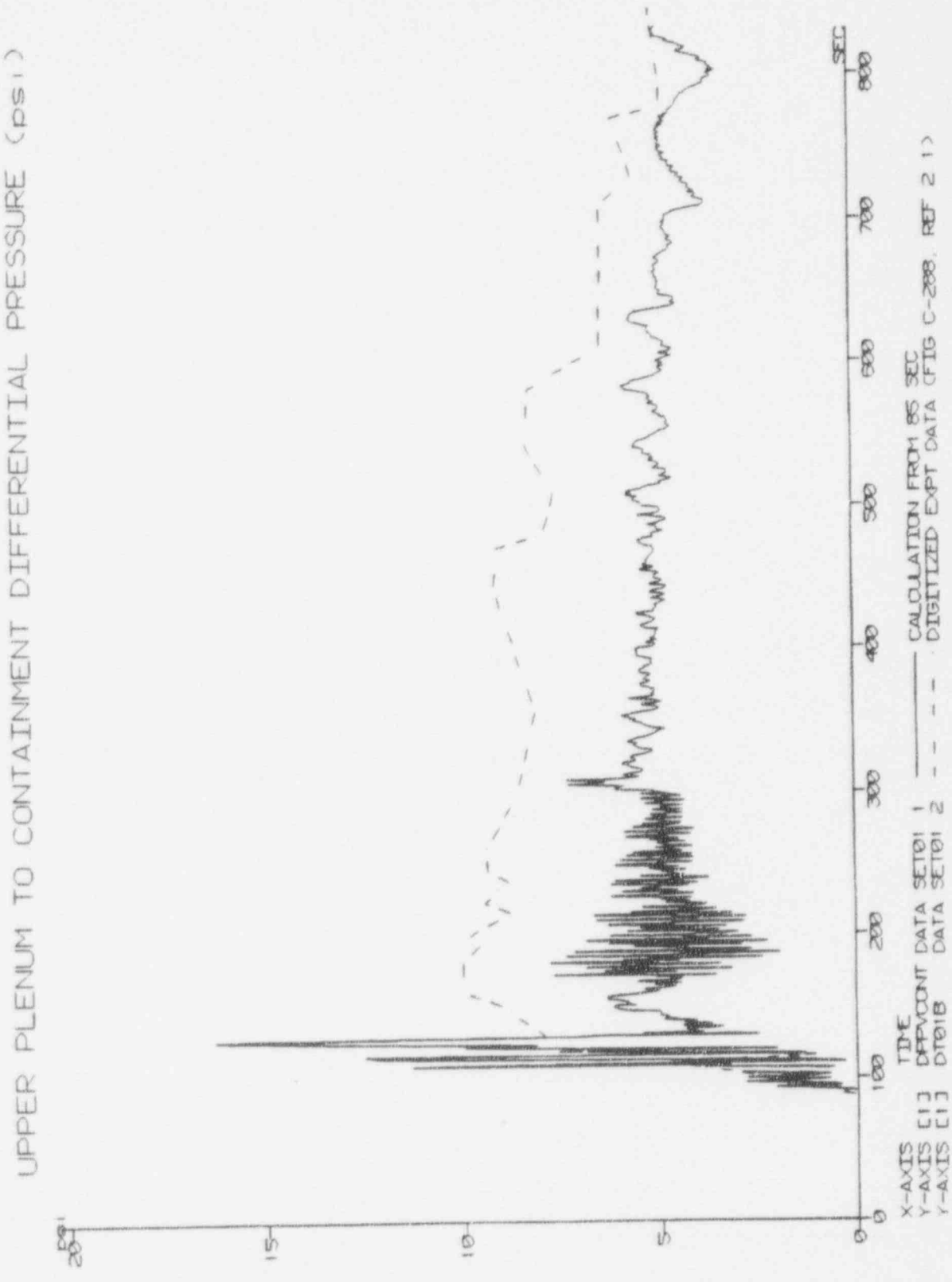

Figure 3.1-37 CCTF Run 58, Upper Plenum to Containment Differential Pressure

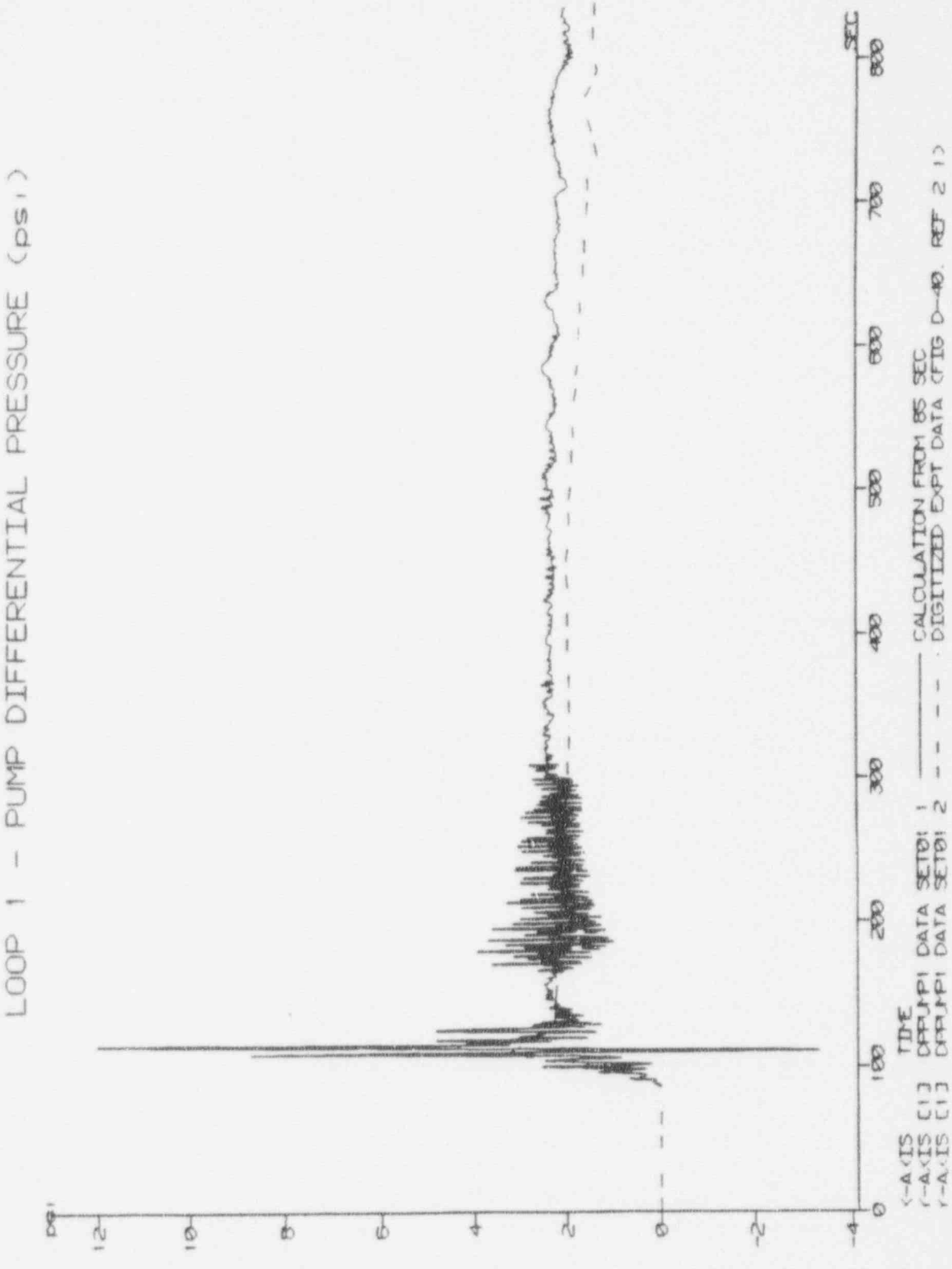

Figure 3.1-38 CCTF Run 58, Loop 1 Pump Simulator Differential Pressure

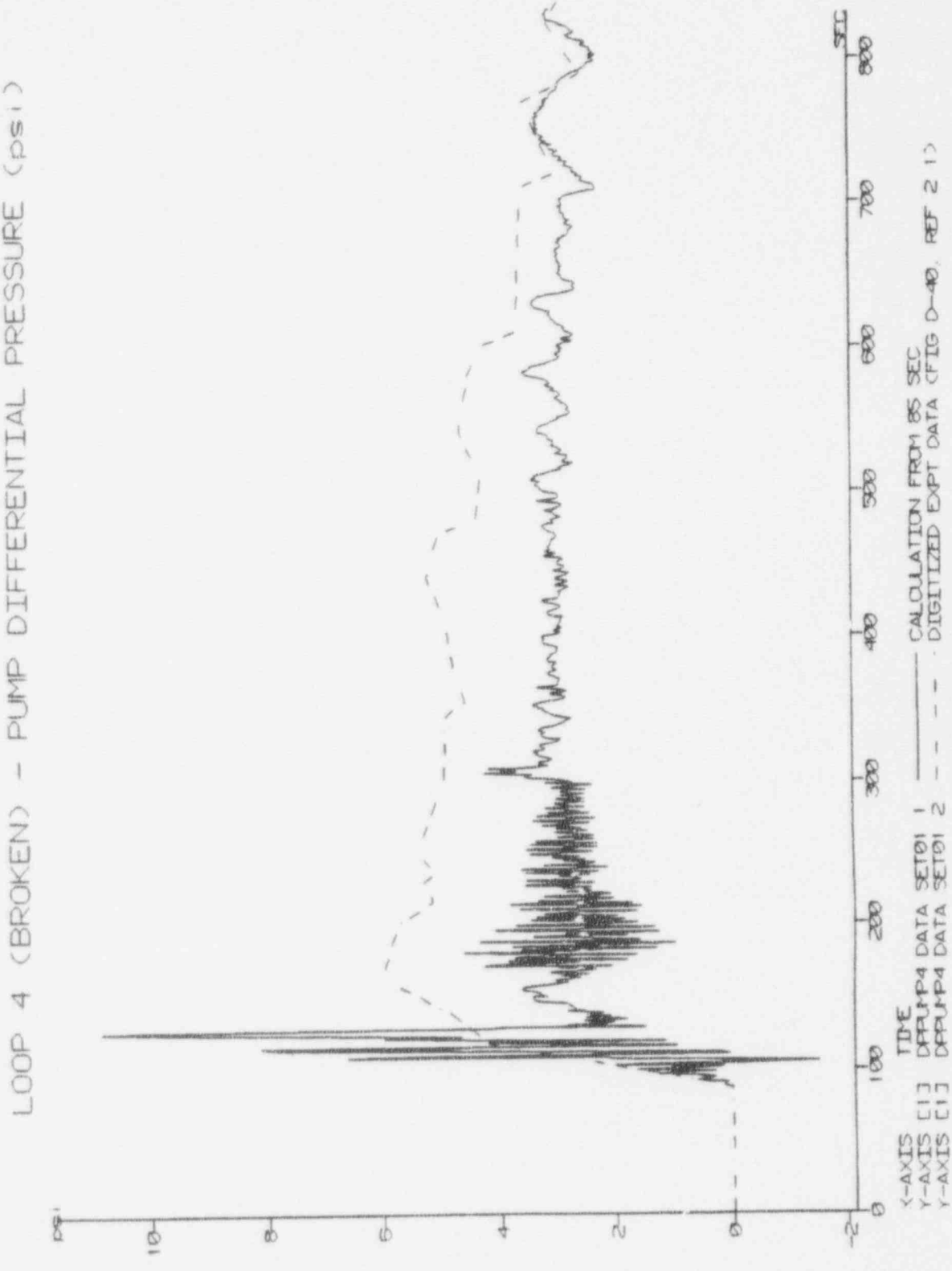

Figure 3.1-39 CCTF Run 58, Loop 4 Pump Simulator Differential Pressure

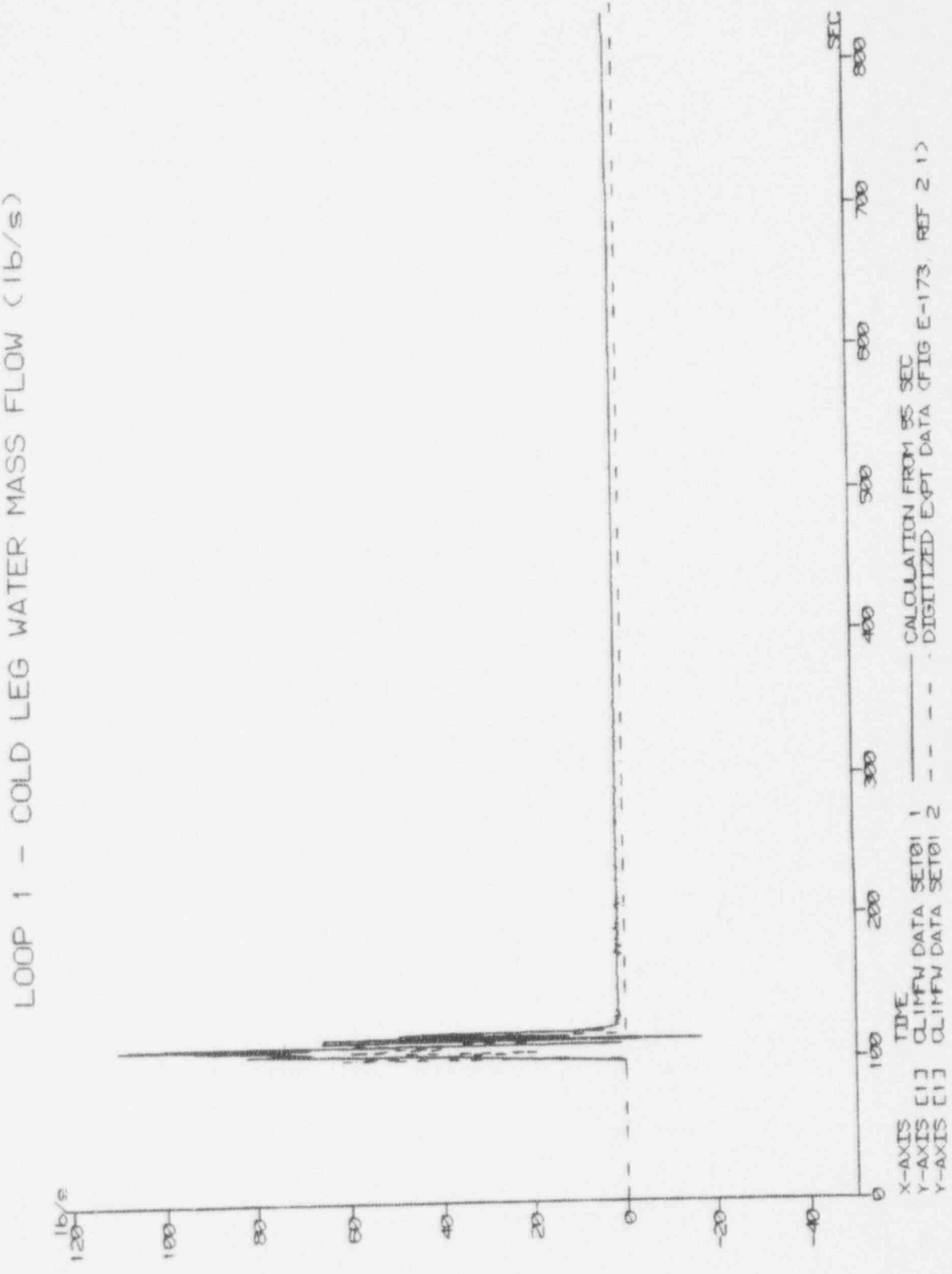

Figure 3.1-40 CCTF Run 58, Loop 1 Cold Leg Water Mass Flow

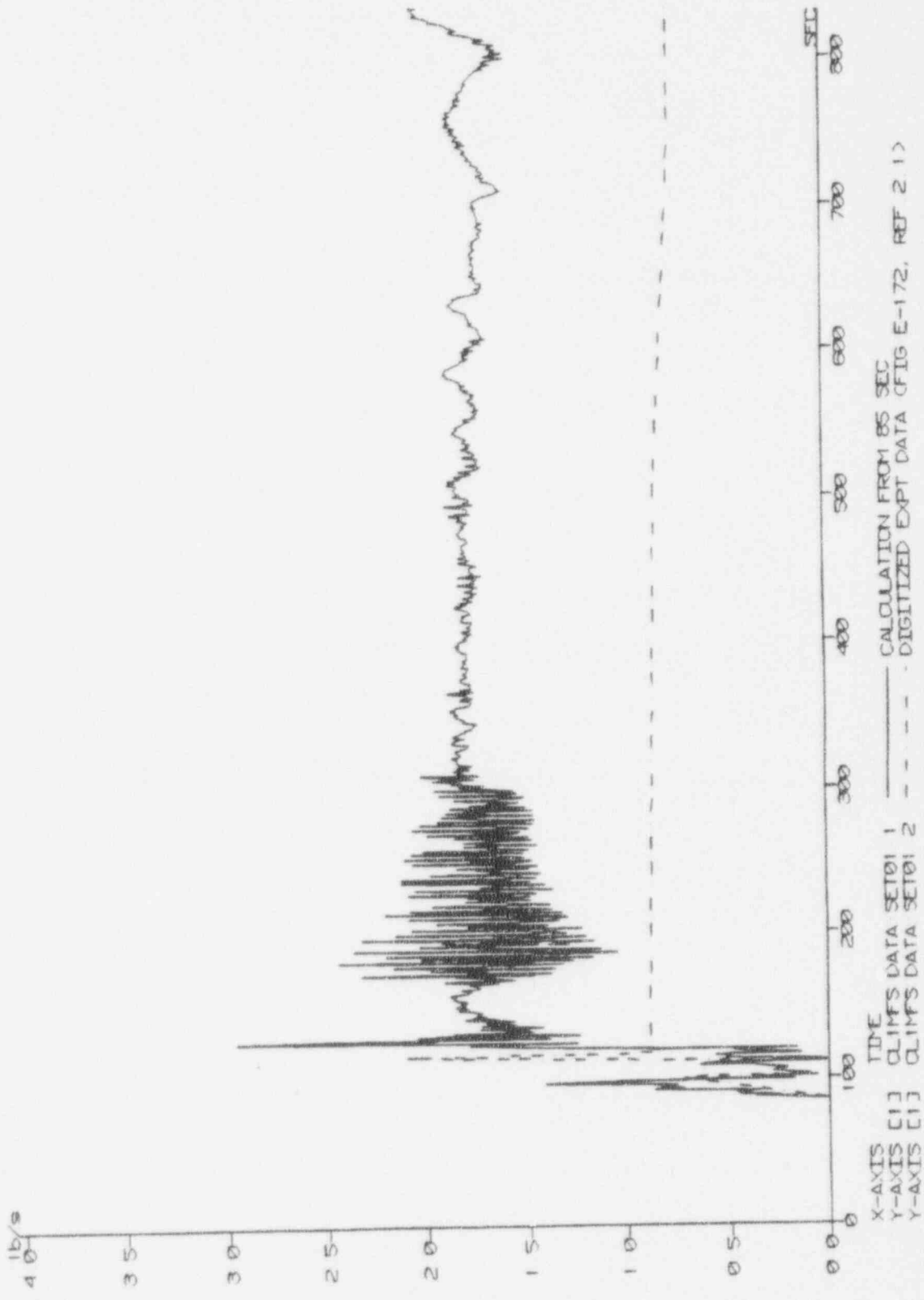

Figure 3.1-41 CCTF Run 58, Loop 1 Cold Leg Steam Mass Flow

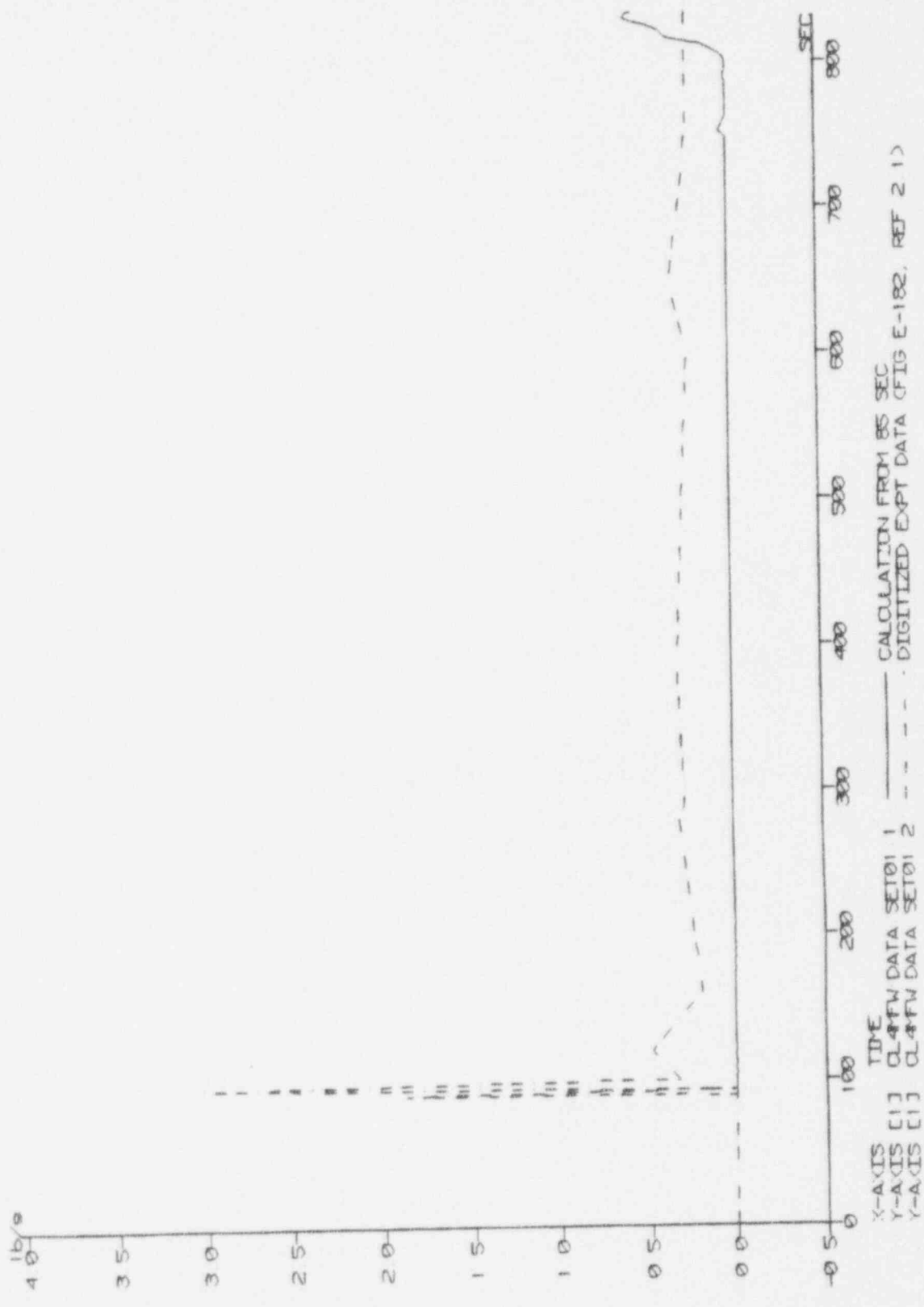

Figure 3.1-42 CCTF Run 58, Loop 4 Cold Leg Water Mass Flow

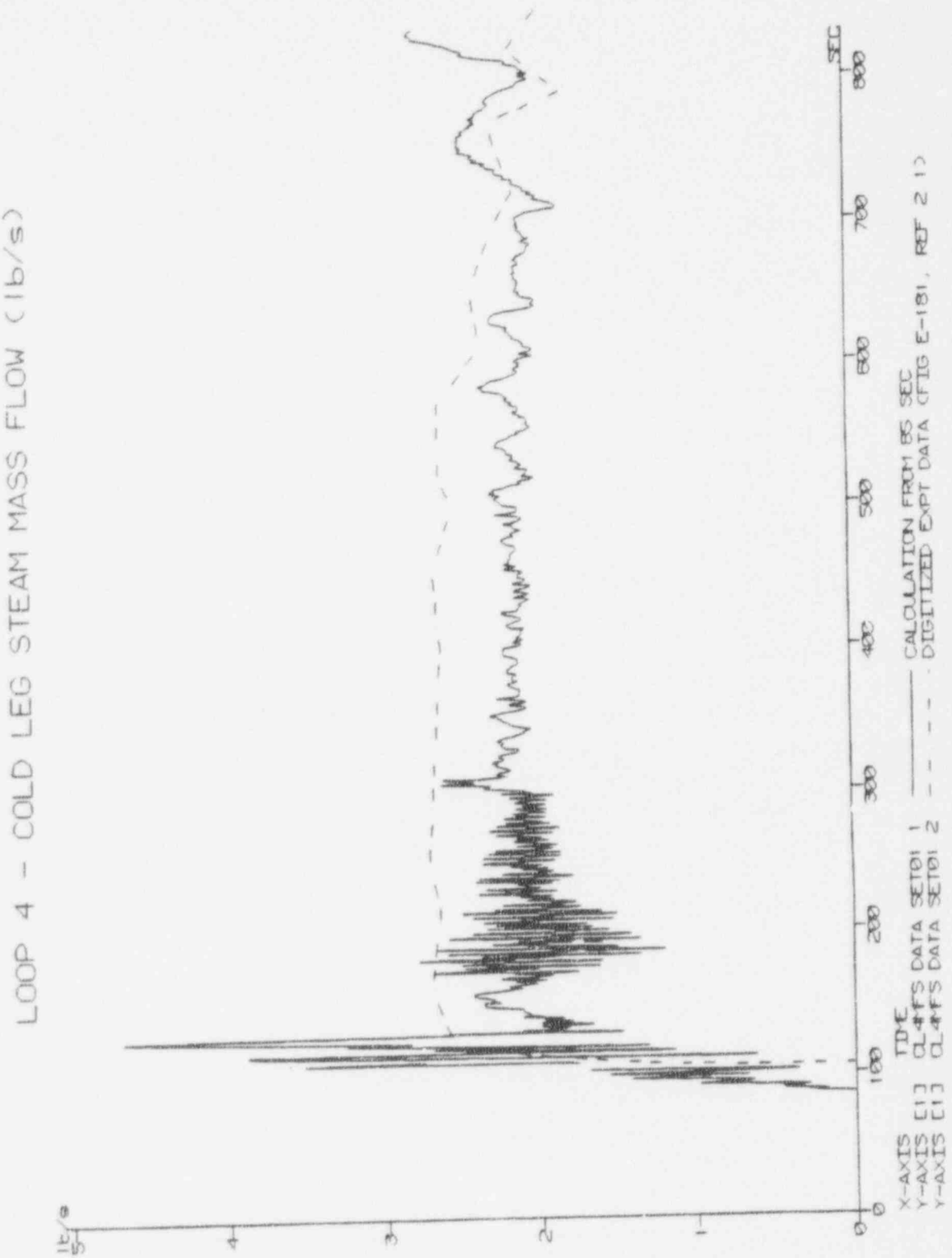

Figure 3.1-43 CCTF Run 58, Loop 4 Cold Leg Steam Mass Flow

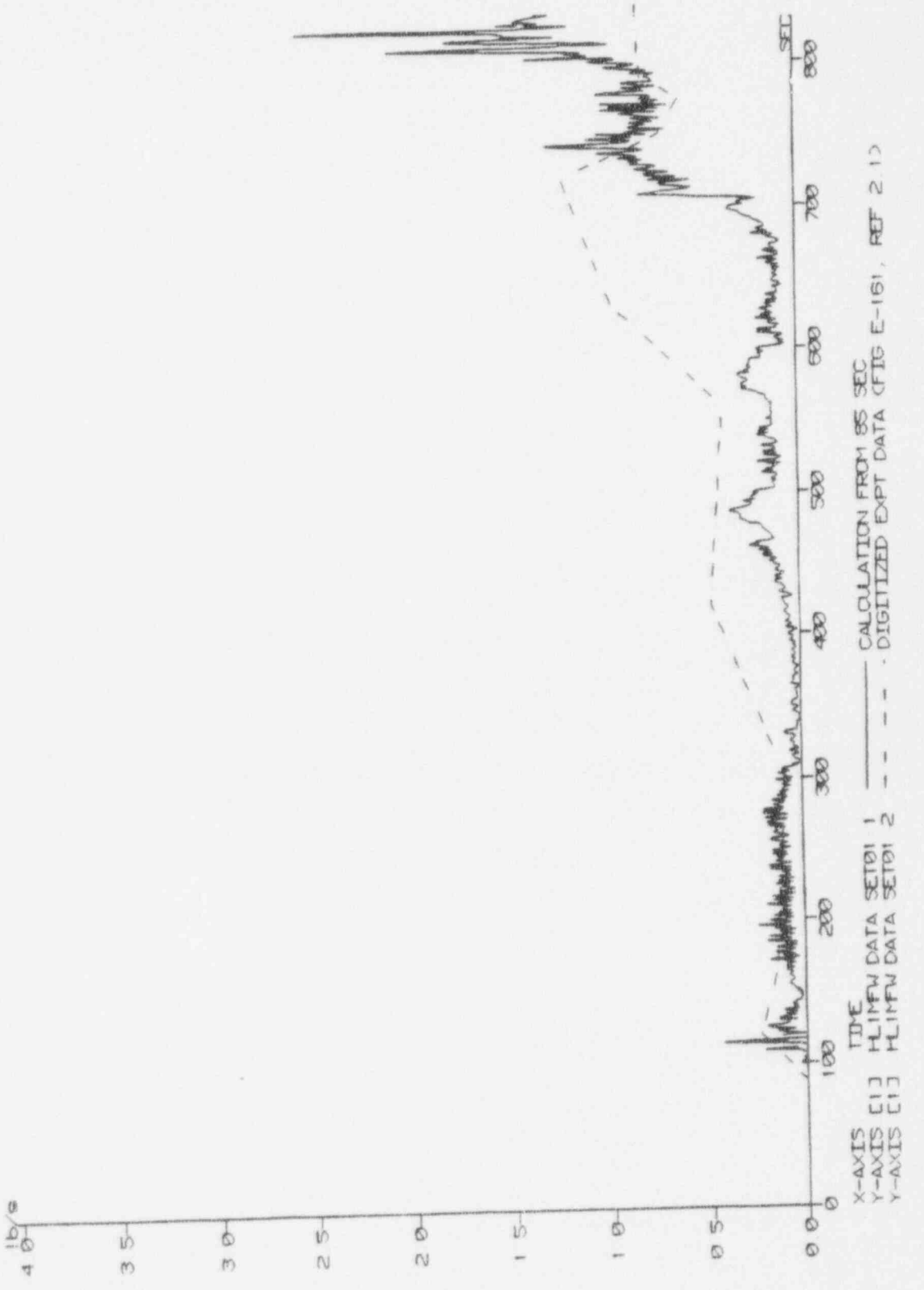

Figure 3.1-44 CCTF Run 58, Loop 1 Hot Leg Water Mass Flow

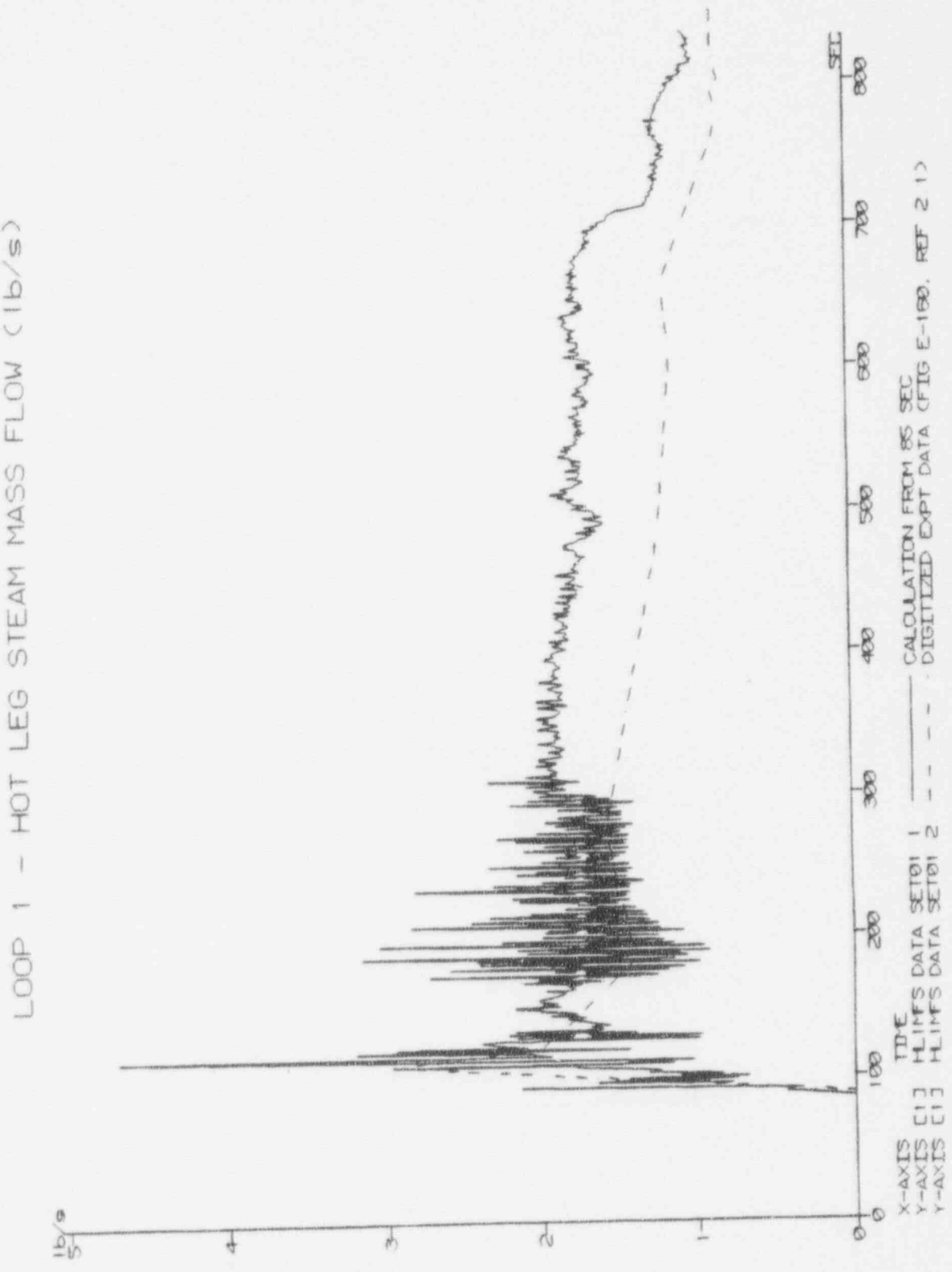

Figure 3.1-45 CCTF Run 58, Loop 1 Hot Leg Steam Mass Flow

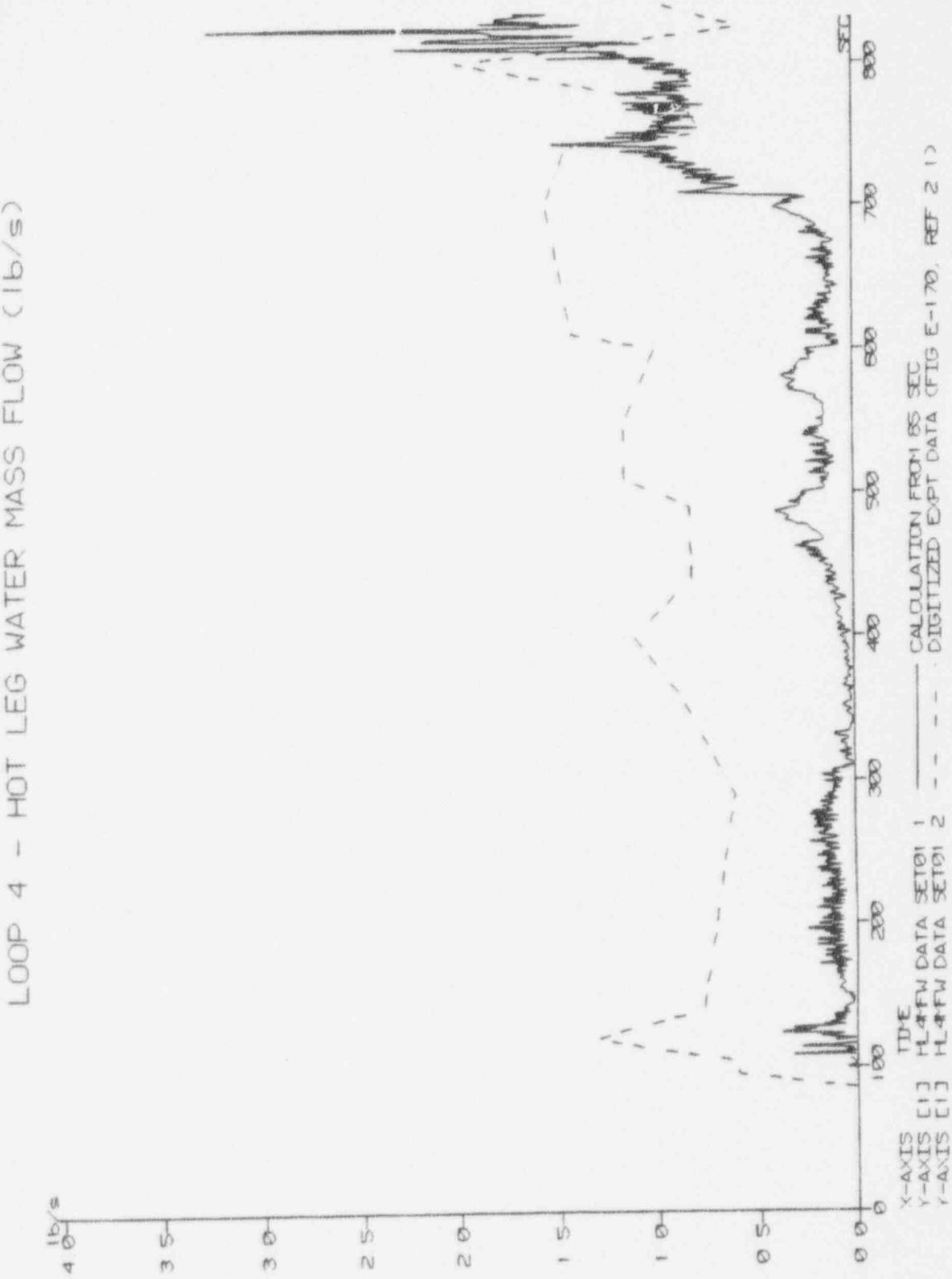

Figure 3.1-46 CCTF Run 58, Loop 4 Hot Leg Water Mass Flow

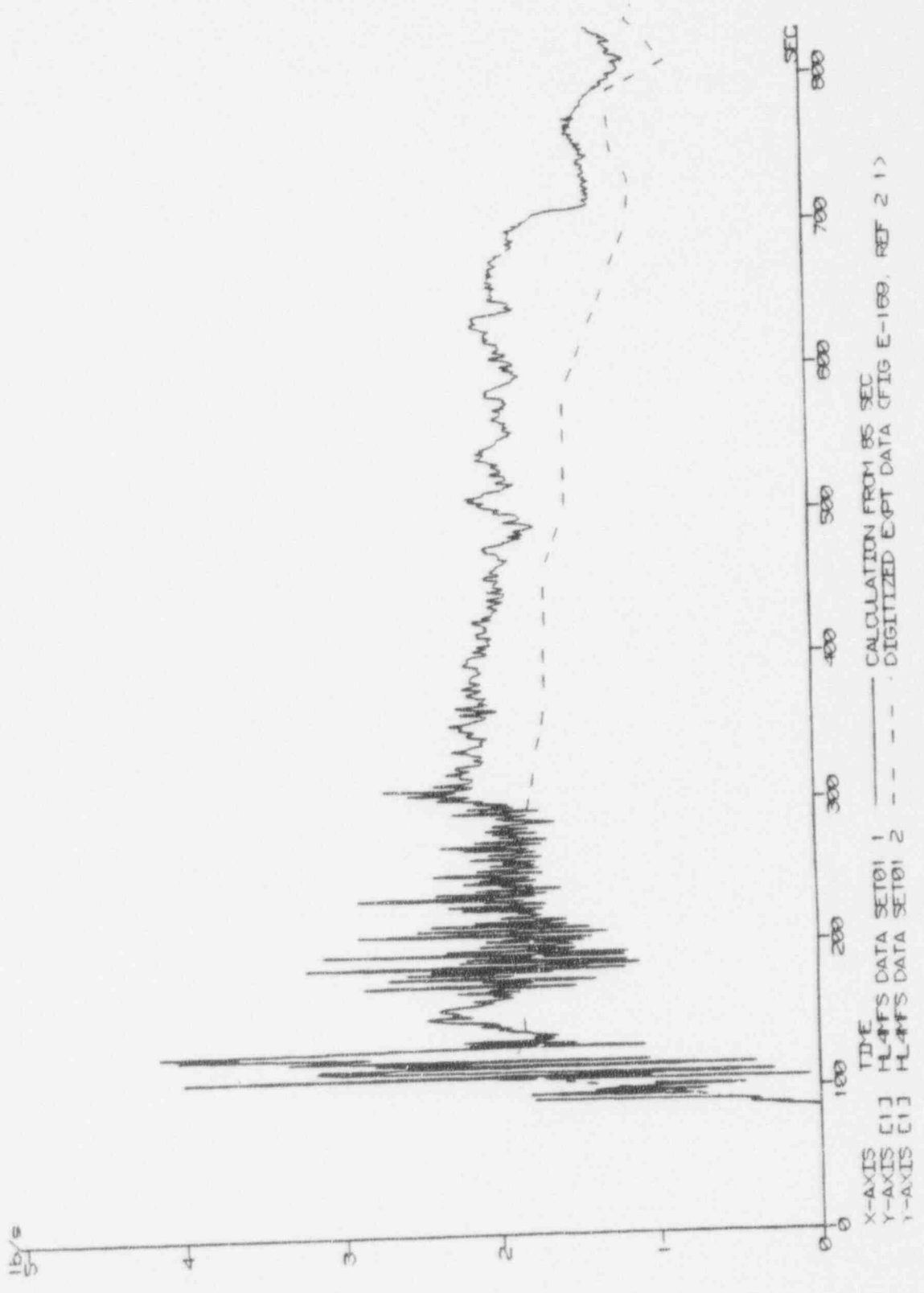

Figure 3.1-47 CCTF Run 58, Loop 4 Hot Leg Steam Mass Flow

Figure 3.1-48 CCTF Run 58, Pressure Vessel Side, Loop 4 Cold Leg Fluid Temperature

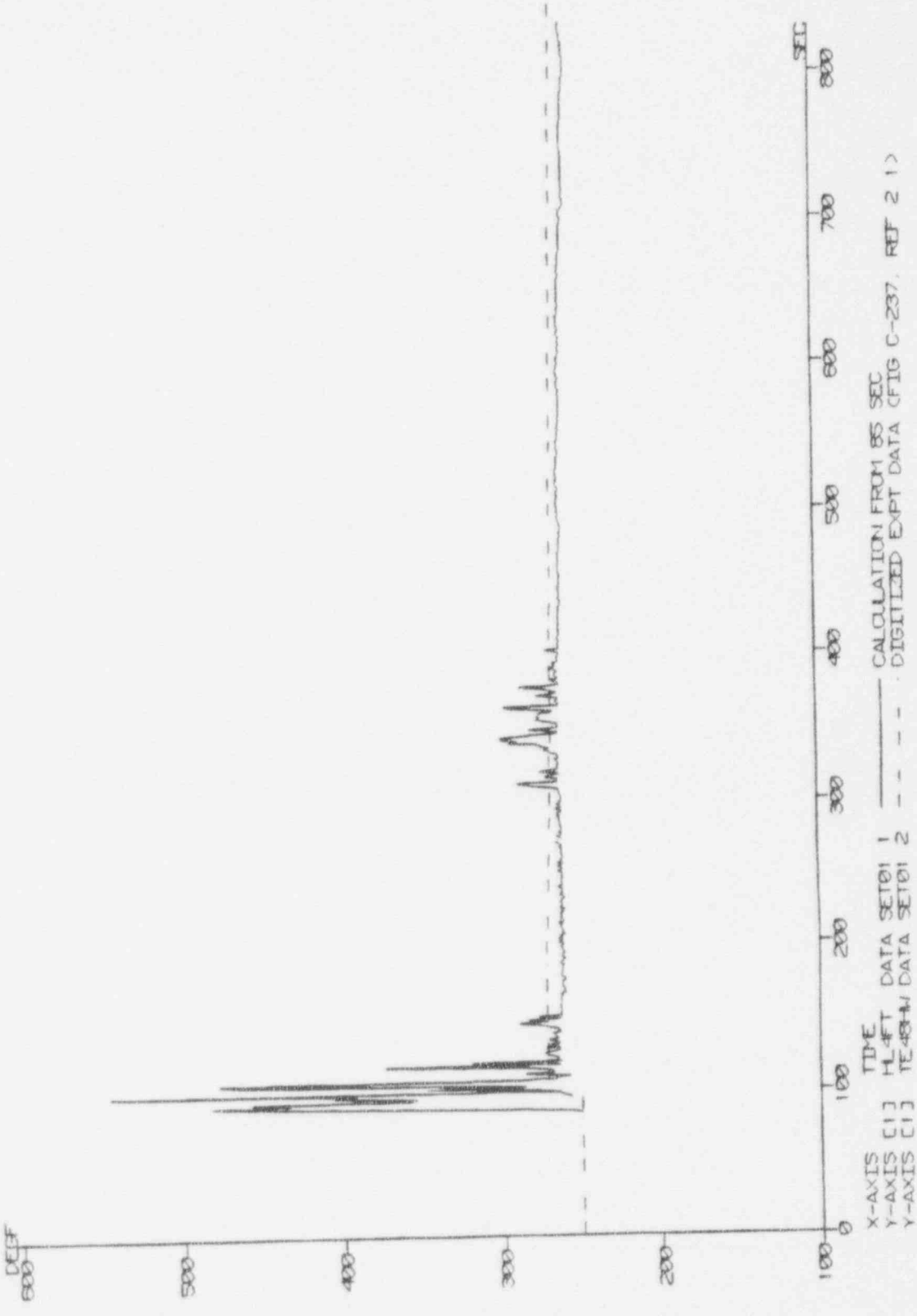

Figure 3.1-49 CCTF Run 58, Loop 4 Hot Leg Fluid Temperature

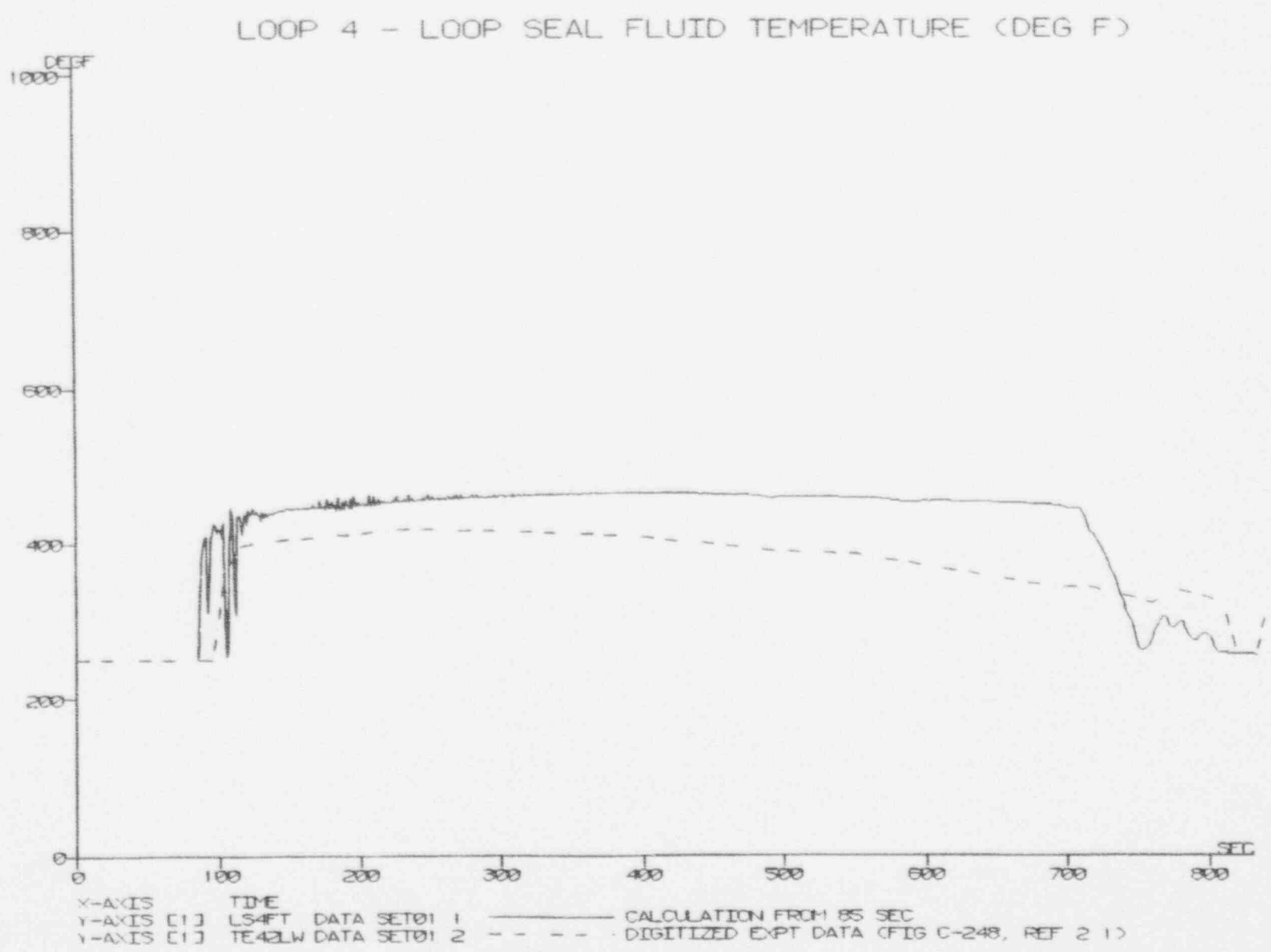

Figure 3.1-50 CCTF Run 58, Loop 4 Seal Fluid Temperature

3.2 UPTF WCOBRA/TRAC Validation

3.2.1 Facility Description

The UPTF is a full-scale model of a PWR primary circuit built and operated by the Federal Republic of Germany Ministry for Research and Technology as part of the trilateral two-dimensional/three-dimensional research program with the United States Nuclear Regulatory Commission and the Japan Atomic Energy Research Institute. UPTF provides experimental data on multi-dimensional two-phase and single-phase flow in a PWR primary circuit.

UPTF has been designed to investigate:

- Water entrainment and separation processes in the upper plenum
- Co-current and counter-current steam water flow phenomena in the upper core tie-plate region including water break-through into the core
- Co-current and counter-current steam/water flow in the downcomer and possible bypass of the ECCS water to the broken cold leg
- Condensation and mixing processes in the hot and cold legs of the loops, in the upper plenum, and in the downcomer as a result of the injection of cold ECCS water
- Loop behavior with regard to possible water plug formation and oscillations in the hot and cold legs of the loops with ECCS injection

The range of investigation is achieved by varying the configuration of the facility. Full details of the facility and its instrumentation are given in documents by R. Emmerling[8] and Sarkar and Liebert.[9]

The design of the facility is based on a 3900 MWt German PWR. There are three intact loops and a loop with a break in the cold leg. The break is represented by gate valves and orifice plates to control the flow, and a containment simulator gives the desired back pressure. The broken loop cold leg contains a water separator whose purpose is to prevent water from entering the containment simulator. The steam generators are simulated by four steam/water separators. On the intact loops, a feedback system is used to simulate reverse heat transfer in the steam generators by injecting steam at a rate equal to the water penetration rate into the steam generator simulators. Adjustable passive resistances are used to simulate the four reactor coolant pumps. The facility does not contain a heated core, but the internals of the top quarter of the core and the upper plenum are full-scale replicas. The core itself is simulated by a steam/water injection system to set up the appropriate flow conditions in the vessel. A feedback system is used to inject steam into the core to simulate steam generation as ECCS water enters the core. The steam for this purpose is supplied from the GKN power station at which UPTF is situated and is stored under saturated conditions in a storage tank at 290 psi prior to injection into the vessel. The water injection is used to simulate water entrainment from the core due to steam upflow. The tubes that deliver the fluid to the core come up through the lower plenum.

The reactor vessel is shown in Figure 3.2-1. The upper plenum contains 61 guide tubes, eight support columns above fuel assemblies and eight support columns outside the periphery of the core (Figure 3.2-1). The downcomer width is 9.84 in., and the vessel internal diameter is 191.7 in.

Upflow of steam and droplets through the core during reflood is simulated by injection of steam and water into dummy fuel rod assemblies. The dummy fuel rod assemblies represent the upper quarter of a core with 193 assemblies of 16 x 16 arrays of fuel rods (Figure 3.2-2). Sixty-one of the assemblies are below guide tubes and have control rod spider simulators (Figure 3.2-3). The remaining assemblies are below flow restrictors in the upper core plate. The water and steam injection nozzles are shown in Figure 3.2-4. There are 17 independently controlled injectors that provide a separate nozzle for each dummy fuel rod assembly.

The dummy control rods terminate at the s[illegible]t of the guide tubes (Figure 3.2-3), and the guide tubes are sealed to prevent flow from the upper plenum to the upper head. Thus, the upper head is isolated from the rest of the vessel and has no effect on the tests.

The steam generator simulators for the intact and broken loops and the broken cold leg water separator are shown in Figure 3.2-5. Flow enters an inlet plenum, which has the same volume as a PWR steam generator, and rises through cyclone tubes. The cyclones separate the water and the steam so the water can be removed from the loop. The steam flows through the steam generator upper plenum and returns to the cold leg. The steam generator simulators can inject steam to replace the liquid that is separated, but which would be boiled by reverse heat transfer in a real steam generator.

The primary coolant loops are shown in Figure 3.2-6. The cold legs have an inner diameter of 29.5 in. The ECCS injection ports are at an angle of 60 degrees to the cold leg centerline and are 19.1 ft. from the inside wall of the vessel. The hot legs have an inner diameter of 29.5 in. The ECCS injection ports are located within the hot legs and inject parallel with it towards the vessel. The nozzles are 47.2 in. from the inside wall of the vessel. There are two downcomer injection nozzles that deliver ECCS water directly to the downcomer. They are located 13.8 in. above the middle of the cold leg centerline, each midway between a pair of adjacent cold legs, and have an inner diameter of 11.8 in.

A steam injection port on intact loop 2 simulates a pressurizer.

A tripped pump is simulated by an adjustable flow resistance. In the refill-reflood period of a LOCA, there is no significant positive head produced by the tripped pump, so this simple pump simulator is adequate.

The water drainage system removes the large quantities of water that accumulate during a test. In this test, water is drained from the broken cold leg water separator and the lower plenum.

UPTF is extensively instrumented, a full description of which can be found in *2-D/3-D Program UPTF Test Instrumentation*.[9] The data produced from the instrumentation is continuously recorded throughout a test. This data may then be post-processed to give computed parameters. An example of a computed parameter derived from raw data is liquid level, which can be derived from the measurement of differential pressure.

The instrumentation in specific locations of the test facility is detailed below.

The downcomer is instrumented with fluid distribution grids, turbine meters, differential and absolute pressure transducers, and fluid and wall thermocouples.

The lower plenum and core regions are instrumented with optical liquid level detectors, differential pressure transducers, and fluid and wall thermocouples.

The instrumentation in the upper plenum is summarized as follows:

- Wall and fluid thermocouples
- Fluid thermocouples in end boxes and below the tie-plate
- Differential pressure transducers across the tie-plate
- Differential pressure transducers and capacity liquid level detectors in the upper plenum
- Optical liquid level detectors and fluid distribution grids
- Video probes in the upper plenum
- Break-through detectors below the tie-plate
- Tie-plate drag bodies in end boxes
- Turbine meters in end boxes and in the upper plenum

The remainder of the facility (intact and broken loop hot and cold legs, containment simulator and drainage vessels) is instrumented with fluid thermocouples and absolute and differential pressure transducers.

3.2.2 UPTF Test 21 Description

The UPTF test 21 consisted of five runs. Two of the runs simulated ECCS delivery to the vessel via downcomer injection ports, and these have been selected for analysis. The runs are identified as phase A run 272 and phase B run 274.[10]

The test facility was configured for test 21 as shown in Figure 3.2-6. The steam supply used in the test was supplied from the storage tank and was injected into the system via the core simulator and steam generator simulators 1, 2, and 3. The ECCS water supply was provided from the two storage tanks and was injected into the downcomer via the two injection nozzles. ECCS injection into the cold legs was not used and the intact cold legs were blocked off at the pump simulators.

The general flow of steam and ECCS water for test 21 is shown in Figures 3.2-6 and 3.2-7. The hot and cold leg break valves in loop 4 were maintained in the closed and open positions, respectively, for the duration of the test. Consequently, the flow path for the injected steam was from the steam generator simulators, along the hot legs of the intact loops to the core, where it mixed with the steam injected through the core simulator nozzles, up the downcomer, and out of the broken cold leg.

The test procedure for each run was as follows. The pressure in the containment simulator was kept constant at 42.8 psi, and the lower plenum was filled with liquid at 266°F (~5°F subcooled) to a level of 2.0 ft. Steam injection to the core and to the steam generator simulators was initiated, and approximately 15 sec later, ECCS injection to the downcomer injection nozzles commenced. Table 3.2-1 shows the steam and ECCS injection rates and the ECCS subcooling for the two runs. In run 272 A, 2000 lb/sec of ECCS at 93.2°F was injected through each of the downcomer injection nozzles, and a total of 700 lb/sec of steam was injected via the core and steam generator simulators. Run 274 B was divided into three subphases. Subphase I was essentially a repeat of run 272 A, but with an ECCS temperature of 257°F. Subphase II only had one downcomer injection nozzle operating (again at ~2000 lb/sec) and was 45°F less subcooled (compared to the system pressure obtained in the test) than subphase I. The core steam injection was reduced to 227 lb/sec and there was no steam generator injection. Subphase III was similar to subphase II, but with ECCS injection of ~2000 lb/sec into both downcomer nozzles.

3.2.3 Test Results

Run 272A

After the start of steam injection, the pressure in the vessel rapidly increased over the initial 17 seconds of the test from 42.8 psi to 89 psi. This pressure was subsequently reduced to ~70 psi as the ECCS flow entered the downcomer, causing significant steam condensation. The effects of condensation were reflected in the reduced steam flow entering the containment tank. The steam flow up the downcomer, 2 seconds after the start of ECCS injection was, however, sufficient to cause partial ECCS water bypass to the broken cold leg and to push ECCS water into the cold legs opposite

the broken loop. At the same time, water penetration to the lower plenum occurred. Throughout the test, the flow characteristics in the vessel was erratic with periods of high ECCS bypass alternating with periods of increased water penetration to the lower plenum. The results indicate that increased water penetration to the lower plenum is directly related to the greater momentum of the liquid slug discharges from the intact cold legs. After 85 seconds, the water level in the lower plenum remained constant at 1.83 m. Additional water reaching the lower plenum after this time was swept up the downcomer by the counter-current steam flow.

Run 274 B

The subphases of run 274 B differ from run 272 A in terms of the degree of subcooling and the rates of injection flows. The degree of subcooling, which was less in all the subphases of run 274 B compared to run 272 A, had a significant effect on the flow behavior. Although the overall characteristics of the two tests (run 272 A and 274 B) were similar, the degree of subcooling in run 274 B reduced the rate of condensation and subsequently, the slug-type flow behavior in the downcomer and the plug-type flow discharge from the broken cold leg. This produced a smoother delivery of water to the lower plenum and a less erratic ECCS bypass flow. Increased water delivery to the lower plenum again corresponded to slug flow entering the downcomer from the intact cold legs.

3.2.4 WCOBRA/TRAC UPTF Model

3.2.4.1 Vessel Component Model

Figure 3.2-8 and Figures 3.2-9 to 3.2-12 illustrate the channel arrangement in the VESSEL and show the interchannel transverse connections (gaps). The downcomer noding used for UPTF is similar to that used for the AP600. [

]^{a,c} The thermal capacity of the vessel and core barrel are represented by heat slabs so that the wall to fluid heat transfer can be calculated.

3.2.4.2 One Dimensional Component Models

The intact cold legs and downcomer injection are modeled as shown in Figure 3.2-13 and Figure 3.2-14, respectively. [

]^{a,c}

The reverse core steam flow is modeled by a mass source boundary condition in channel 9 of section 3 at the 16th axial level. This includes both the steam injected within the core and the steam injected at the three intact-loop steam generator simulators, which are not explicitly modeled.

3.2.5 Modeling of UPTF Test 21 with WCOBRA/TRAC

Run 272 A was run for 90 seconds of simulation time to completely cover the period of ECCS injection. The calculation begins 31 seconds into the test which corresponds to the start of steam injection.

Run 274 B consists of three distinct subphases, which are modeled as two separate transients in the calculations. The first transient starts at 31 seconds (the time of steam injection initiation) and lasts for 90 seconds. There then follows a long period with no injection, which is not modeled. At 231 seconds, the steam flow resumes and marks the start of the second transient. There then follow two distinct periods of downcomer injection; in subphase II both downcomer injection nozzles are used to deliver the ECCS water, whereas in subphase III only one nozzle is used. The calculation models both subphases in one transient, which lasts for 175 seconds.

The boundary conditions are taken from a Quick Look Report on Test No. 21,[10] and the calculations are set up in the following way. For approximately the first 15 seconds, only steam was injected via the mass source boundary condition in channel 7, the steam flow being ramped in from zero to its full value over the first few seconds. Steady steam flow conditions were obtained before the ECCS flows were started; these were ramped up to their full values over 1 to 3.5 seconds, depending on the subphase of the test. The calculation was then run out for the duration of the test transient.

3.2.6 Calculation and Data Comparison

The results of the calculations and comparisons with the experimental data are presented in Figures 3.2-16 to 3.2-39. For each run, plots are given of pressure and mass accumulation and mass flowrates within various parts of the system and where possible, compared with the experimental data. The digitized plots are simple averaged representations of the data and do not depict the fluctuations that occurred in the experimental readings. To aid the reader, each experimental plot references the

figure number used in the Quick Look Report[10]. This Quick Look Report presents mass balances for Phases A and B. For Phase A, there is a discrepancy with up to at least 20 percent less mass measured in the system than was known to have been injected. For Phase B I, the discrepancy is up to at least 25 percent more measured mass from 70 seconds to 90 seconds and up to 25 percent less measured mass after this time. The discrepancy for Phases B II and III is up to 8 percent less measured mass in the system than that known to have been injected. These discrepancies need to be considered in the comparison of calculations and test results given below. In the figures and the following discussion, all times refer to those of the experiment.

Phase A (Run 272)

The results for Phase A are shown in Figures 3.2-16 to 3.2-23.

The lower plenum liquid inventory is shown in Figure 3.2-16. The measured inventory shows a rise during the first 15 seconds of steam injection. The Quick Look Report [10] attributes the inventory rise to the effect of dynamic pressure from the injected steam on the differential pressure instrumentation from which the liquid inventory is derived. This is not shown in the calculation. At 46 seconds, ECCS injection through the downcomer nozzles begins and by 50 seconds in the calculation, the lower plenum inventory rises as two separate slugs of liquid penetrate the downcomer. At 64 seconds, a third slug of liquid reaches the lower plenum, and the level temporarily rises again. Throughout the rest of the calculation, however, the injected steam flow from the core prevents downflow of liquid to the lower plenum and gradually sweeps out liquid by entrainment. In the experiment, the penetration of liquid to the lower plenum was unsteady but much greater and continued until approximately 80 seconds, giving a much higher lower plenum liquid inventory.

The break steam flowrates are compared in Figure 3.2-17. The calculation agrees well with the experiment. Following the initiation of ECCS injection at 46 seconds, the steam flowrate reduces rapidly as a consequence of condensation of steam on the much cooler ECCS liquid. The experimental steam flowrate remains oscillatory for the remainder of the test (although this much detail is not reflected in the digitized plots), while in the calculation, the steam flowrate remains approximately constant for the remainder of the transient, again suggesting that the calculation is underpredicting the condensation rate.

The break mixture flowrate is shown in Figure 3.2-18, while integrated flowrates are compared in Figure 3.2-19. This shows the calculation overpredicting the bypassed flow from approximately 50 to 100 seconds.

The downcomer pressure is shown in Figure 3.2-20. After the start of steam injection to the core, the pressure increases rapidly in both experiment and calculation. This is followed by a rapid depressurization as injected steam is condensed on the subcooled ECCS water. Throughout the transient the calculation overpredicts the downcomer pressure, although the general trend is well predicted. This suggests that WCOBRA/TRAC is underpredicting the steam condensation rate.

The downcomer collapsed liquid levels are compared in Figure 3.2-21. This shows the calculation underpredicting the amount of liquid in the downcomer. In the calculation, ECCS liquid only penetrates the downcomer channels below cold leg 3 and the adjacent downcomer injection channel to any significant extent. Liquid from the other downcomer injection nozzle (adjacent to the break) is mainly discharged directly out of the break. This behavior is similar to that which occurred in the experiment, except that in the experiment there was more liquid penetration to the lower plenum. In the calculation, the upflow of steam in the downcomer stops the ECCS liquid from penetrating a level half way down the core. Figure 3.2-22 shows the calculated average downcomer flowrate just above the bottom of the core barrel. This indicates that only three slugs of ECCS liquid enter the lower plenum.

Figure 3.2-23 shows the liquid inventories of the cold legs. The calculation predicts the cold leg 3 inventory reasonably well, although there are no significant liquid slug discharges. Virtually no filling of cold legs 1 and 2 is calculated, whereas in the experiment, filling these legs is similar to that of cold leg 3.

In summary, the calculation gives a higher break flow than that which occurred in the experiment and corresponding smaller liquid inventories in the lower plenum, downcomer, and intact cold legs. Thus, WCOBRA/TRAC overpredicts the ECCS bypass for this test.

Phase B I (Run 274)

The results for Phase B I are shown in Figures 3.2-24 to 3.2-31.

The lower plenum liquid inventory is shown in Figure 3.2-24. As for Phase A, the experiment shows a rise in inventory before ECCS injection due to dynamic pressure of the steam. This is not shown in the calculation. At approximately 50 seconds, the inventories start to rise in both experiment and calculation as ECCS liquid reaches the lower plenum. The inventory in the calculation initially rises more rapidly than that in the experiment. The filling of the lower plenum in the experiment occurs over the whole of the transient, whereas the calculation shows no filling from 70 to 110 seconds (a small amount of liquid is entrained and removed from the lower plenum during this period). Overall, the predicted liquid inventory in the lower plenum is reasonable.

Figure 3.2-25 shows the steam break flowrate. The flow is well predicted before the initiation of ECCS at 46 seconds. After ECCS injection commences, the steam flowrate is underpredicted, indicating more condensation of steam in the calculation than occurred in the test.

The break mixture flowrate and integrated flowrate are shown in Figures 3.2-26 and 3.2-27. The calculation overpredicts the amount of liquid bypassing to the break, largely from 70 to 110 seconds.

The downcomer pressure is shown in Figure 3.2-28. The pressurization is again overpredicted, but following the ECCS injection, the calculation shows good agreement with the experiment. Neither

calculation nor experiment shows the depressurization that was observed in Phase A. This is due to the much smaller subcooling in Phase B I.

The calculated downcomer collapsed liquid level is shown in Figure 3.2-29 (no equivalent data was available for the experiment). This rises rapidly until 70 seconds, and thereafter remains roughly constant, reflecting the high bypass rate of ECCS liquid to the break during this period. The liquid mainly penetrates the downcomer by the channels below cold leg 3. The calculated downcomer flowrates (Figure 3.2-30) show constant steam upflow over the whole of the transient, and two periods of liquid downflow from 50 to 70 seconds and from 110 seconds onwards. From 70 to 110 seconds, there is a slight amount of liquid entrainment up the downcomer from the lower plenum.

Figure 3.2-31 shows the liquid inventories of the cold legs. Cold leg 3 is calculated to steadily fill with liquid throughout the transient, whereas in the experiment, the filling was more rapid. Cold legs 1 and 2 were predicted to have virtually no liquid filling, whereas in the experiment, there was some filling (and subsequent discharging) but to a lesser extent than in Phase A.

In summary, the calculation gives a reasonable prediction of ECCS penetration to the lower plenum and an overprediction of break flow. The overprediction of ECCS bypass for this test is not as severe as for Phase A.

Phases B II and III (Run 274)

The results for Phases B II and III are shown in Figures 3.2-32 to 3.2-39.

The lower plenum liquid inventory is shown in Figure 3.2-32. The gradual buildup of mass during Phase B II (while injection is from one downcomer injection nozzle only) is not predicted. The ECCS injection is only into the downcomer nozzle adjacent to the break, and all the ECCS is calculated to bypass directly out of the break. The rapid increase in mass when the other downcomer injection begins at 325 seconds (Phase B III) is more accurately predicted, but is about 50 percent too low.

The break steam flowrates are compared in Figure 3.2-33. Prior to ECCS injection at 246 seconds, the flowrate is well predicted. The rapid fall in flowrate at 246 seconds due to condensation of steam on the ECCS liquid is also well predicted, although the rate for the remainder of Phase B II is generally underpredicted. The further decrease at 325 seconds (the start of Phase B III) is also predicted, although the flowrate remains too low throughout the whole of this phase.

The break mixture flowrates and integrated flowrates are shown in Figures 3.2-34 and 3.2-35. During Phase B II, the bypass flow to the break is very well predicted, but there is a small overprediction during Phase B III.

The downcomer pressure in Figure 3.2-36 shows a generally good agreement, with a rise in pressure prior to ECCS injection, followed by a constant pressure during Phase B II in both calculation and

experiment. A small fall in pressure when the additional downcomer injection flow of Phase B III is begun is followed by a pressure rise, which is also well predicted.

The calculated downcomer collapsed liquid level is shown in Figure 3.2-37 (no equivalent data was available for the experiment). This rises rapidly due to condensation of steam on liquid already in the downcomer. When the ECCS injection commences at 246 seconds, it is all initially bypassed out of the break, as indicated by the constant level. At 330 seconds, the level rises as the additional downcomer injection flow of Phase B III penetrates the downcomer. This is also shown in the downcomer flow rates in Figure 3.2-38, which indicate a large liquid downflow from 330 to 340 seconds, followed by an oscillatory period of liquid upflow and downflow. Most of the ECCS downflow occurs in the channels below cold leg 3 and the adjacent downcomer injection nozzle.

The cold leg liquid inventories in Figure 3.2-39 show no calculation of liquid filling during Phase B II, whereas the experiment showed gradual filling of cold leg 2 and smaller filling of cold legs 1 and 3. During Phase B III, filling is predicted in all three cold legs. This reflects the filling in the experiment, although to a lesser extent.

In summary, the calculation gives a higher break flow than in the experiment and corresponding smaller inventories in the lower plenum, downcomer, and intact cold legs. ECCS bypass is overpredicted, particularly of the downcomer injection adjacent to the break.

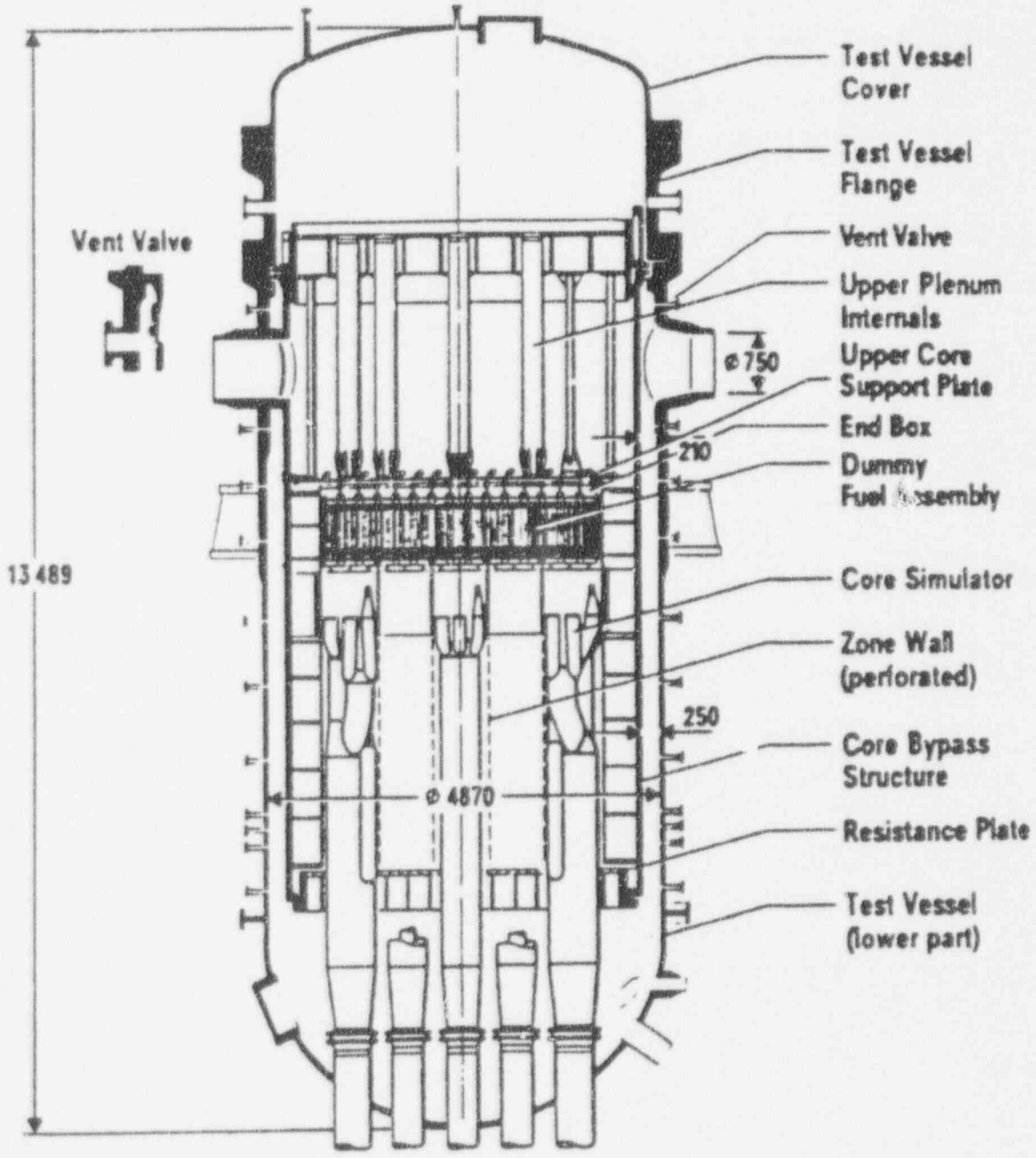

Figure 3.2-1 UPTF Test Vessel and Internals

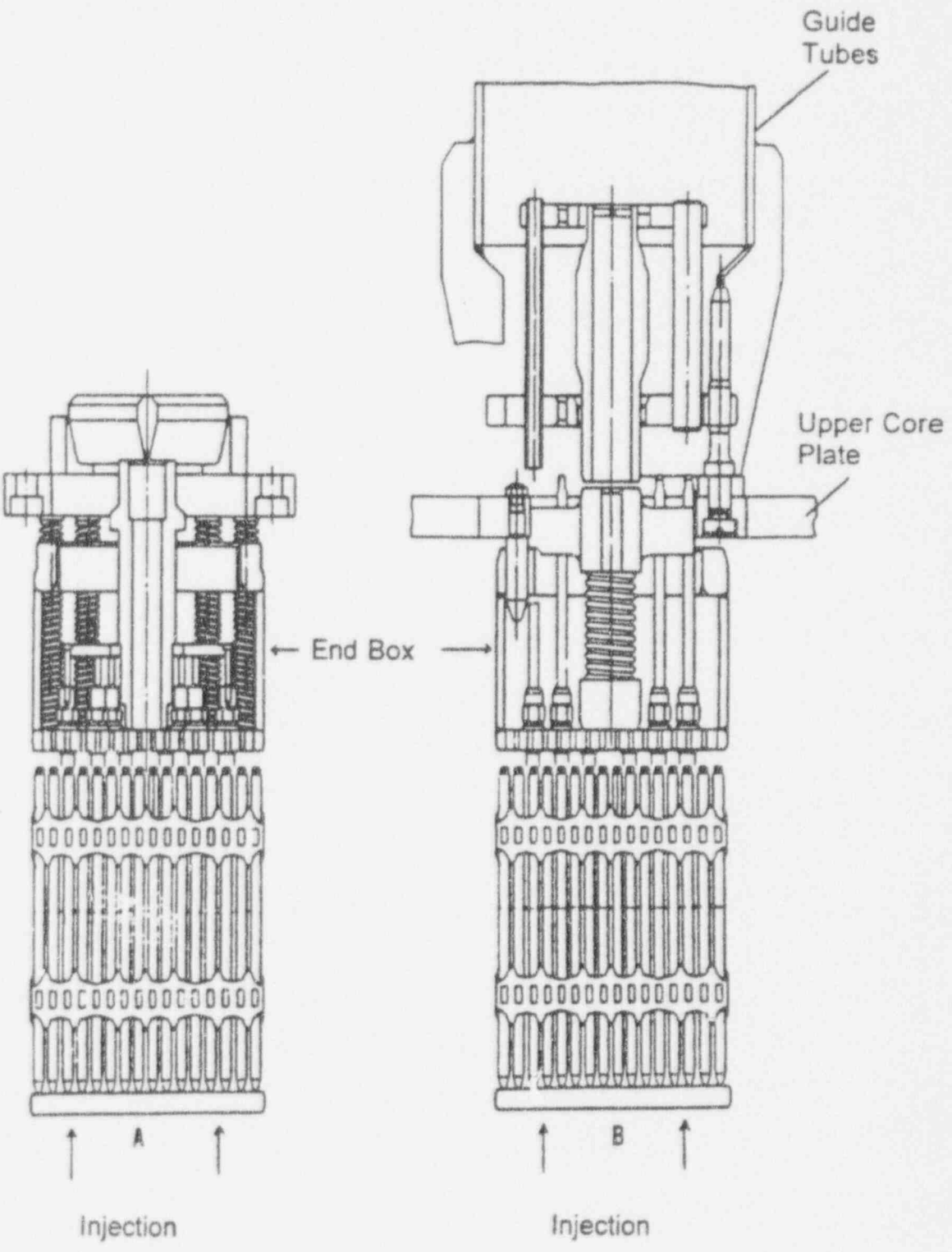

Figure 3.2-2 UPTF Dummy Fuel Assembly and End Box with Flow Restrictor (A) or Spider (B)

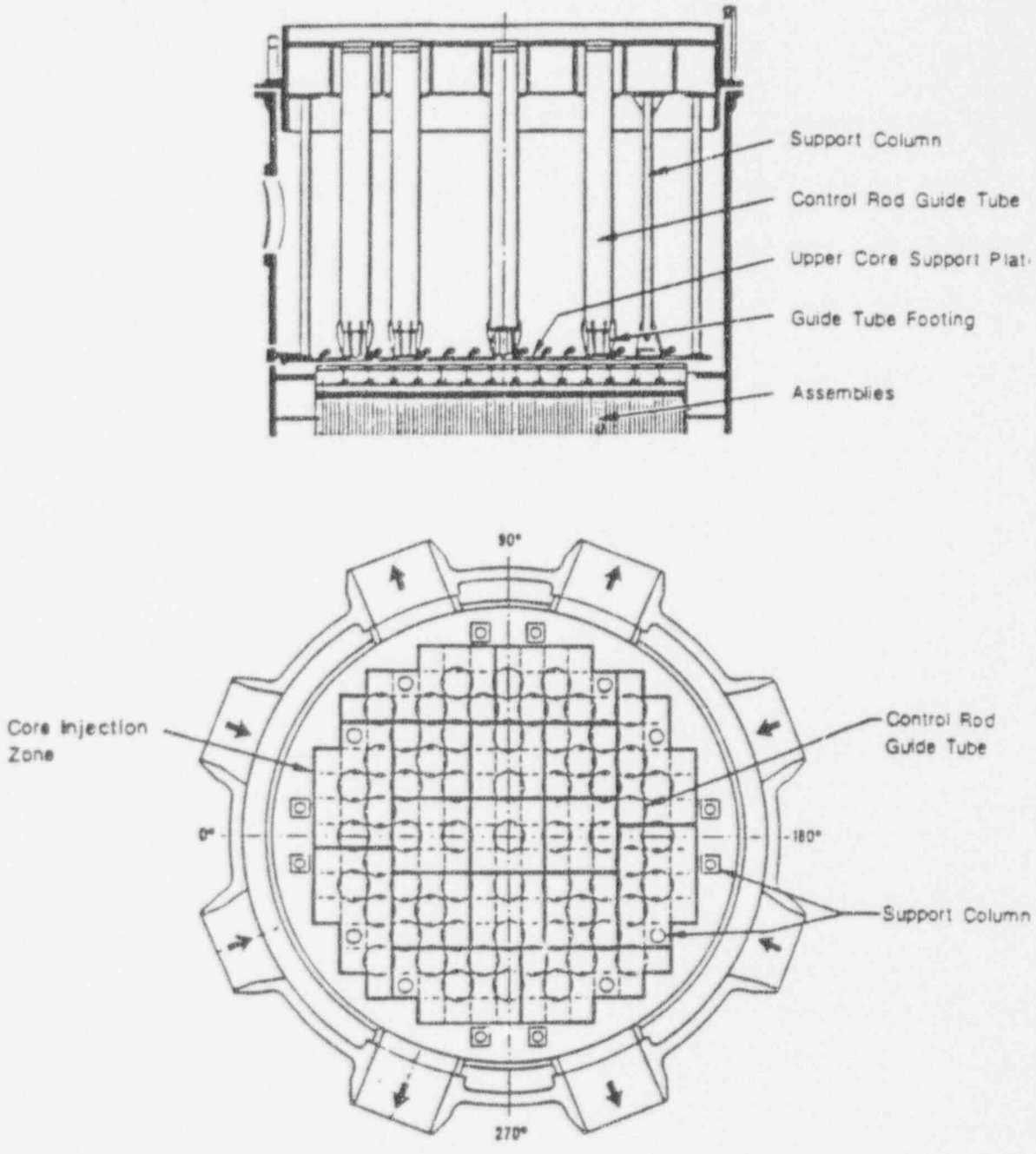

Figure 3.2-3 UPTF Upper Plenum Structure

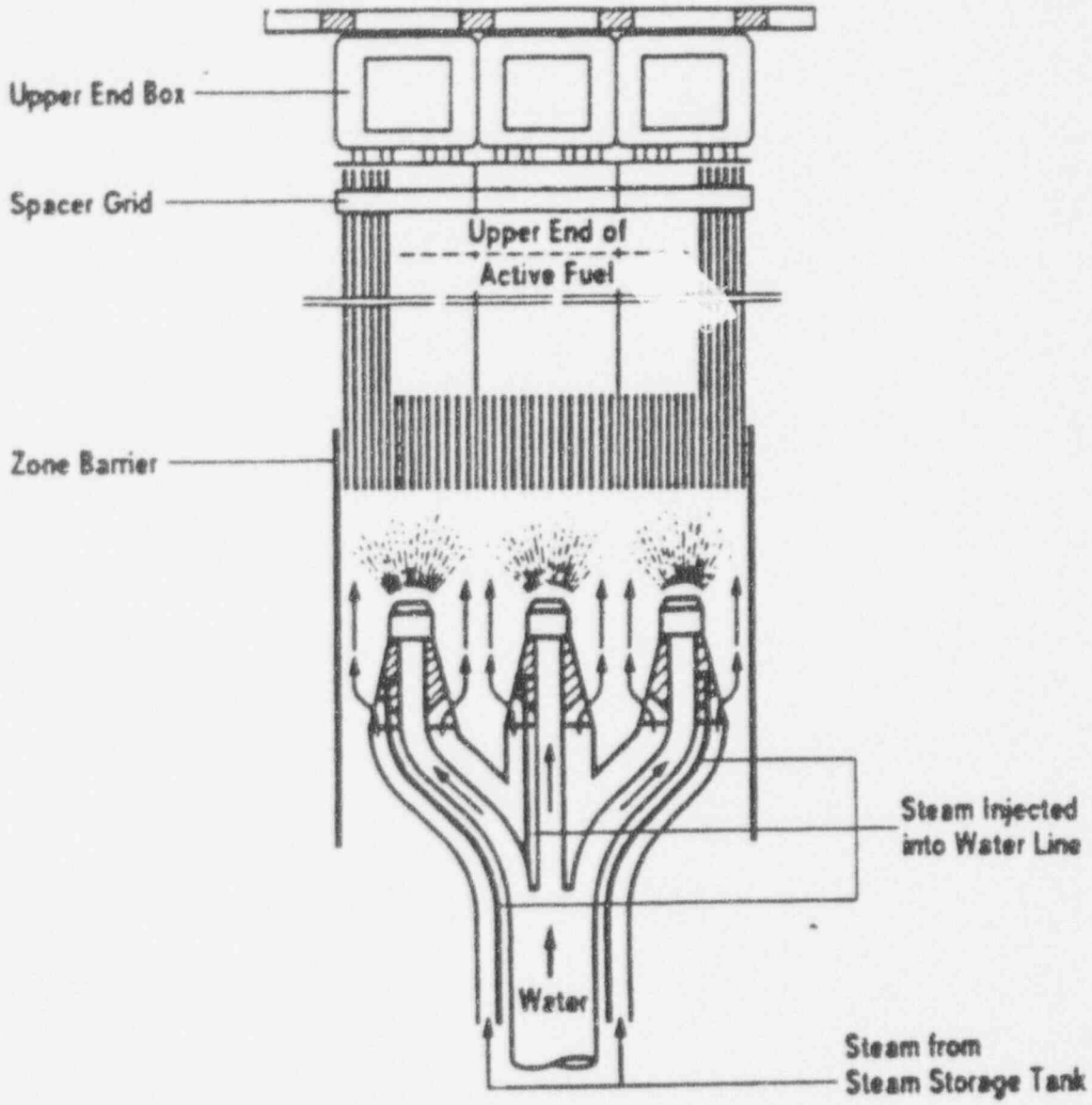

Figure 3.2-4 UPTF Core Simulator Injection Assembly

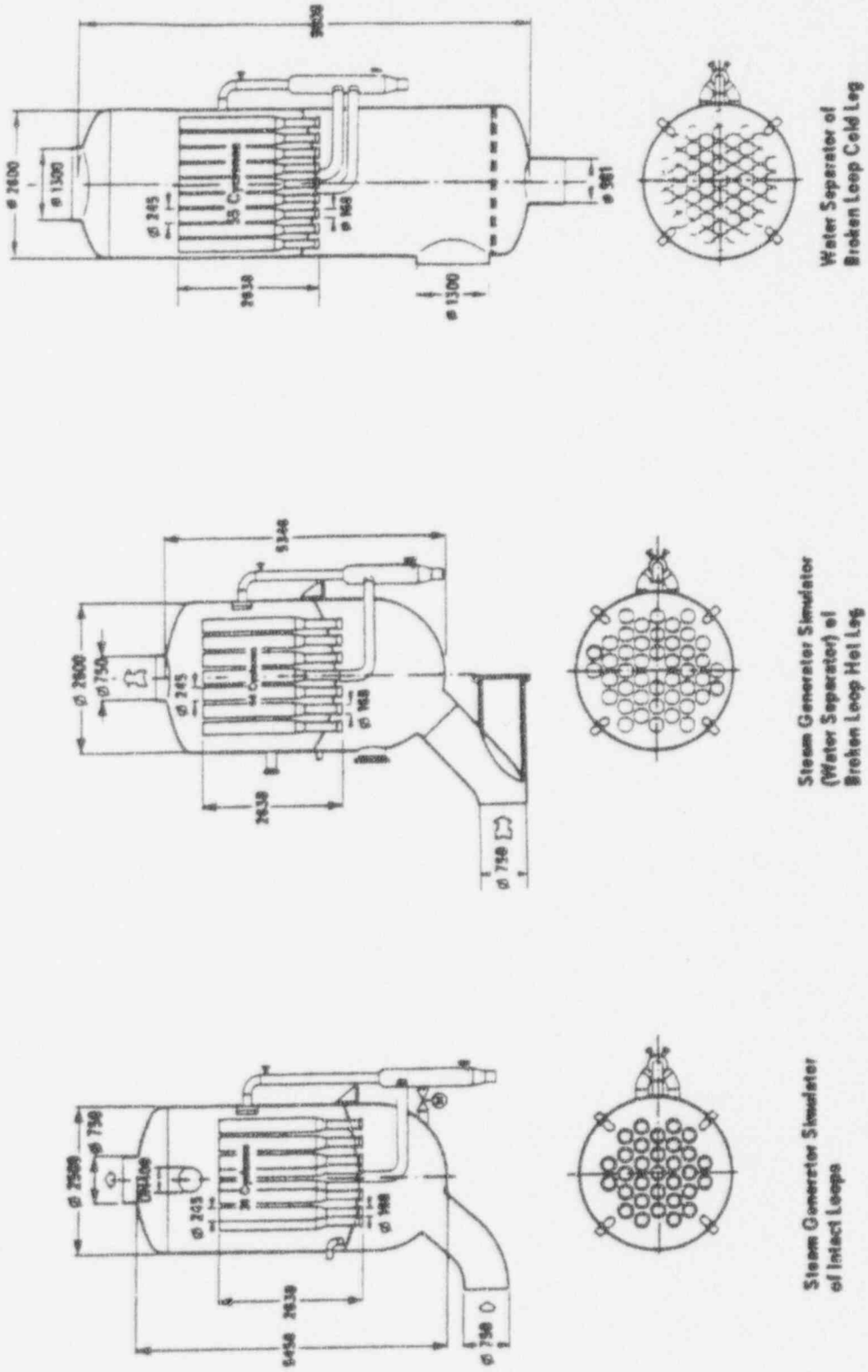

Figure 3.2-5 UPTF Steam Generator Simulators and Water Separators

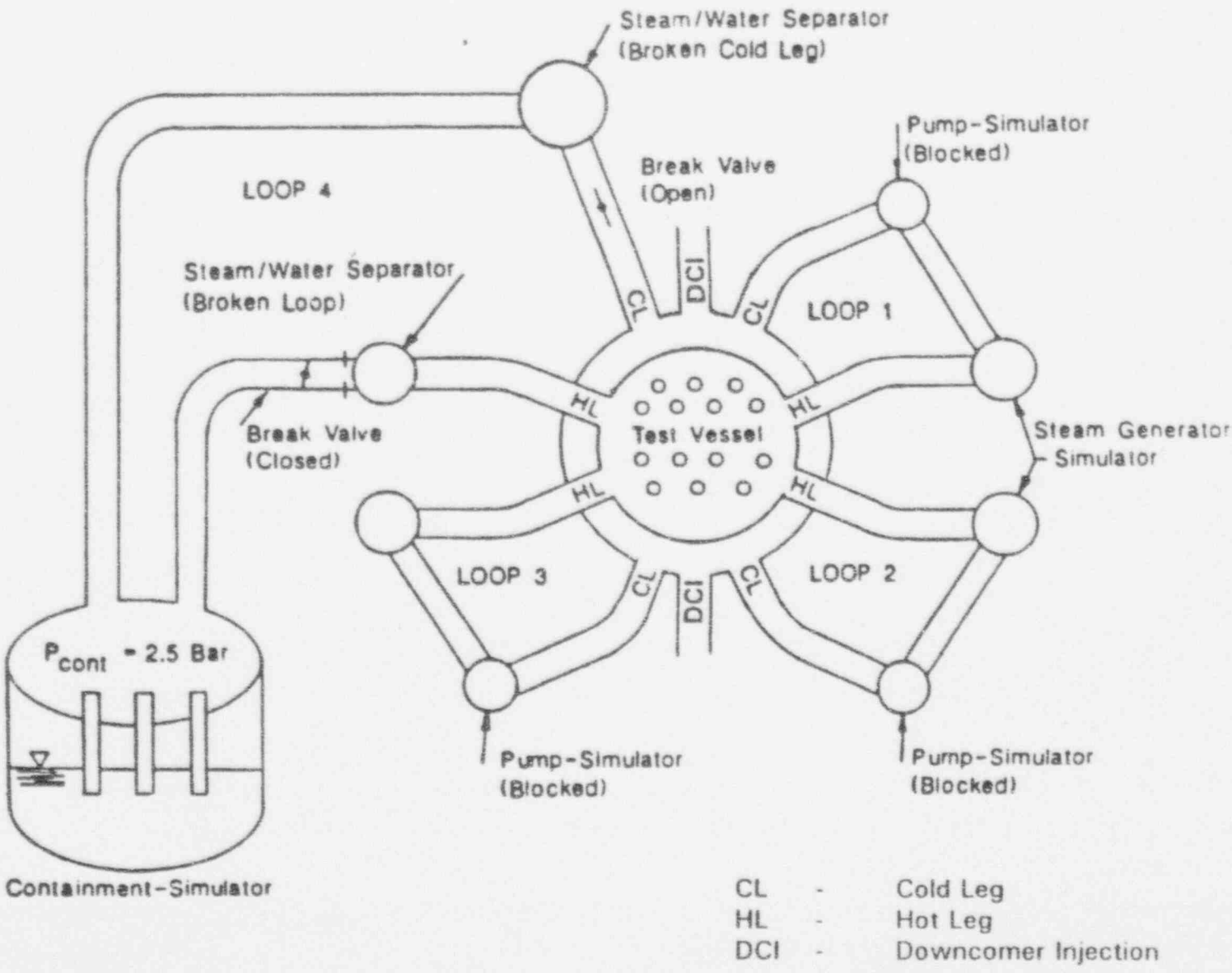

Figure 3.2-6 UPTF Configuration for Test 21

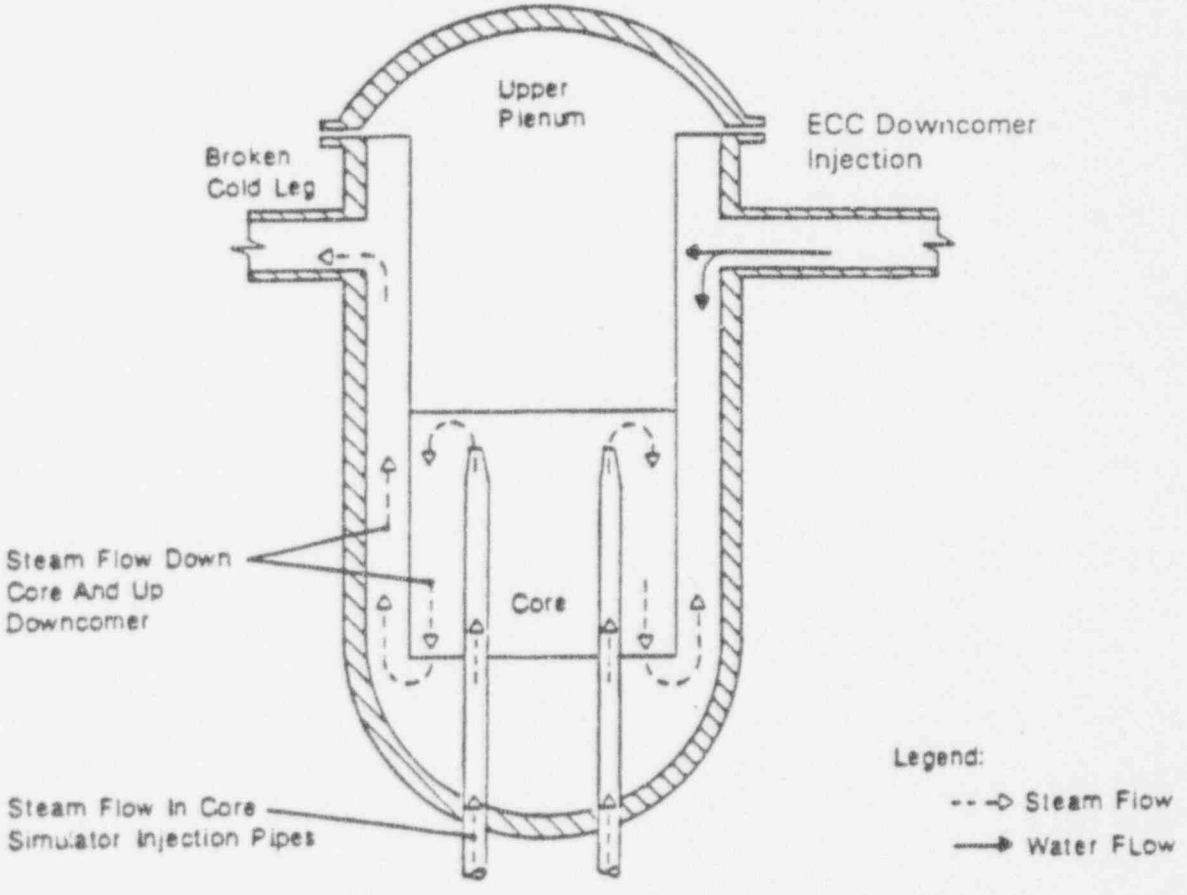

Figure 3.2-7 Steam and Water Injection in UPTF Test 21

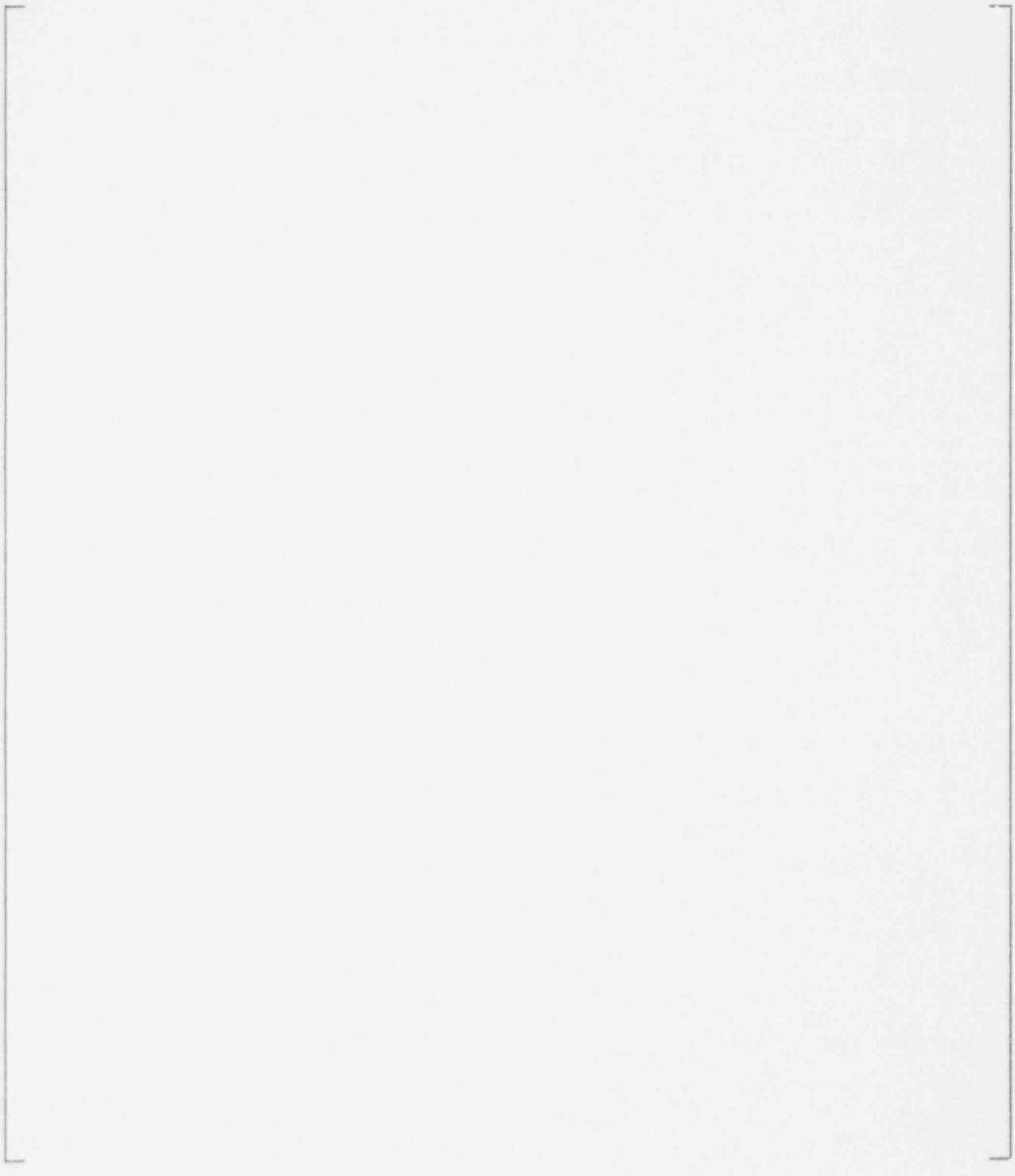

a,c

Figure 3.2-8 WCOBRA/TRAC UPTF Vessel Noding - Plan View

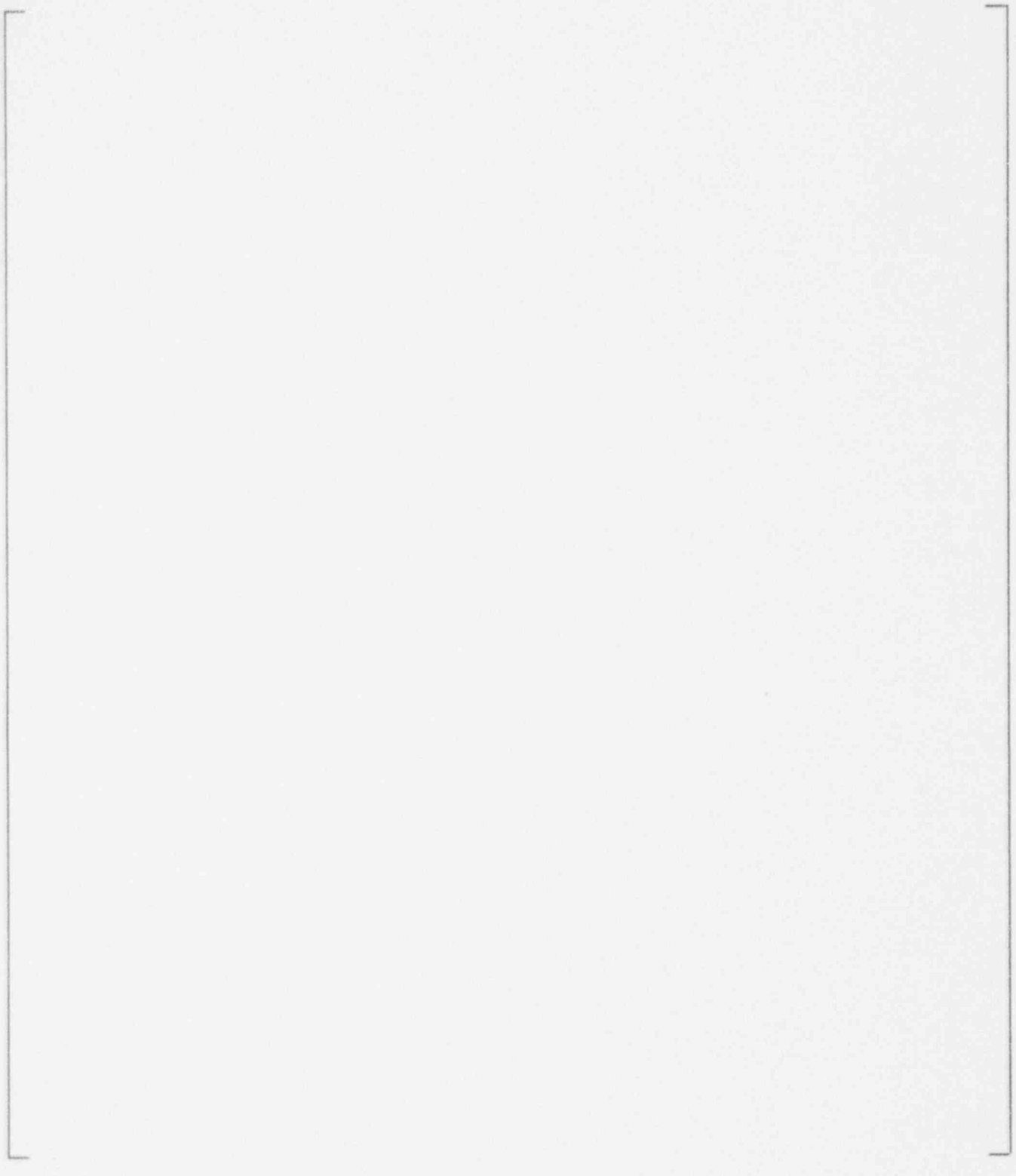

a,c

Figure 3.2-9 WCOBRA/TRAC UPTF Vessel Sections 1 and 2

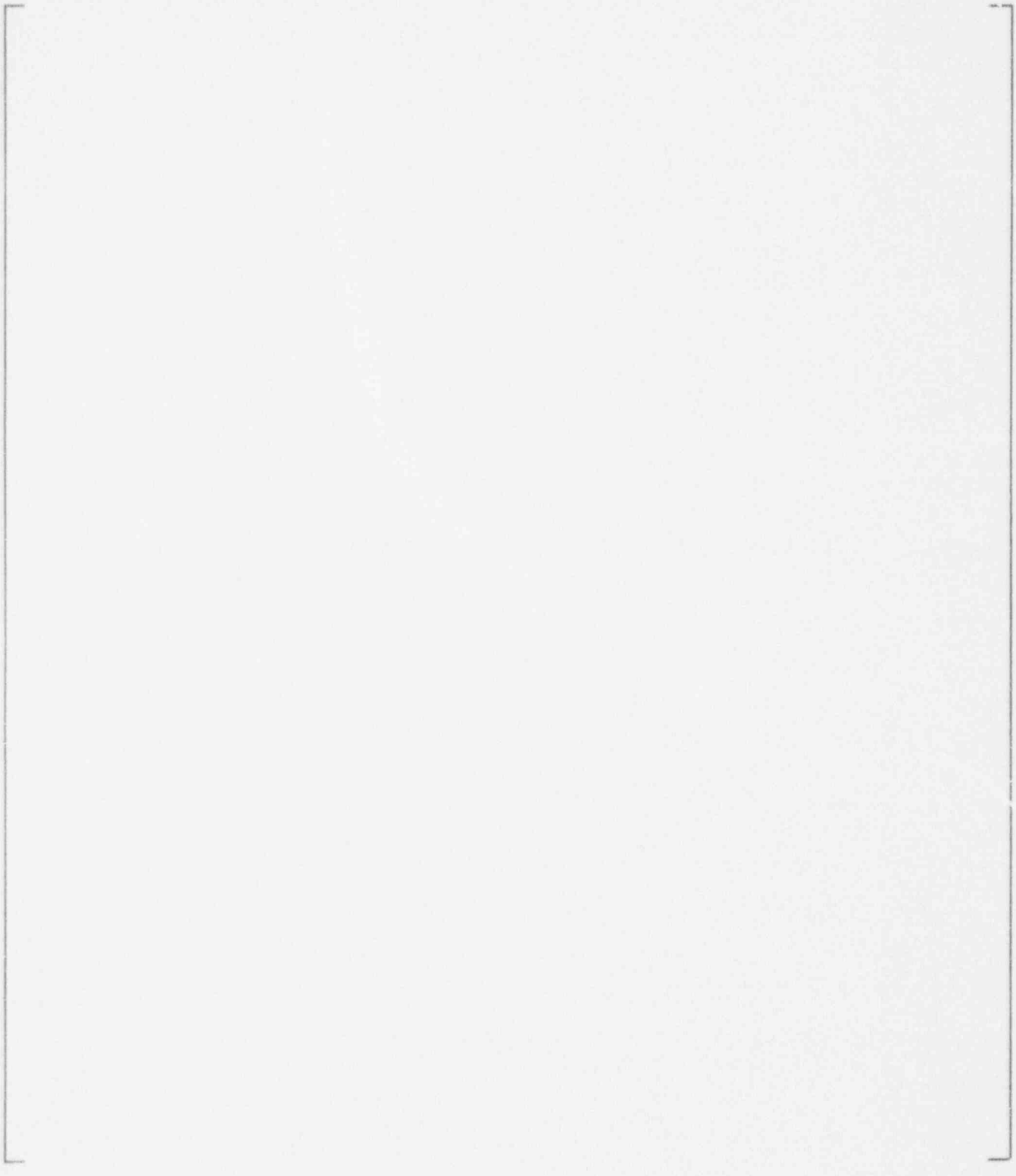

a,c

Figure 3.2-10 WCOBRA/TRAC UPTF Vessel Sections 3 and 4

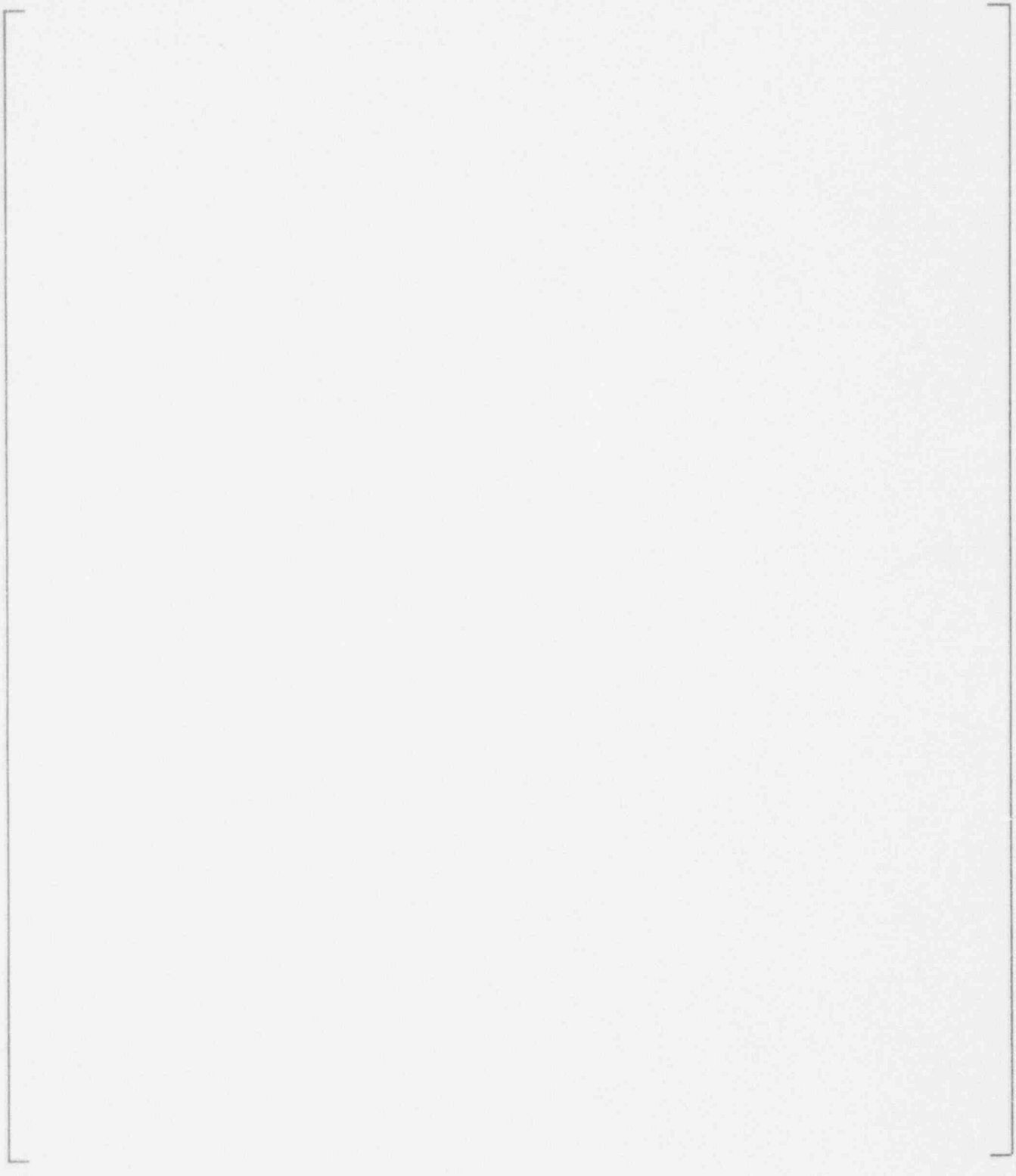

a,c

Figure 3.2-11 WCOBRA/TRAC UPTF Vessel Sections 5 and 6

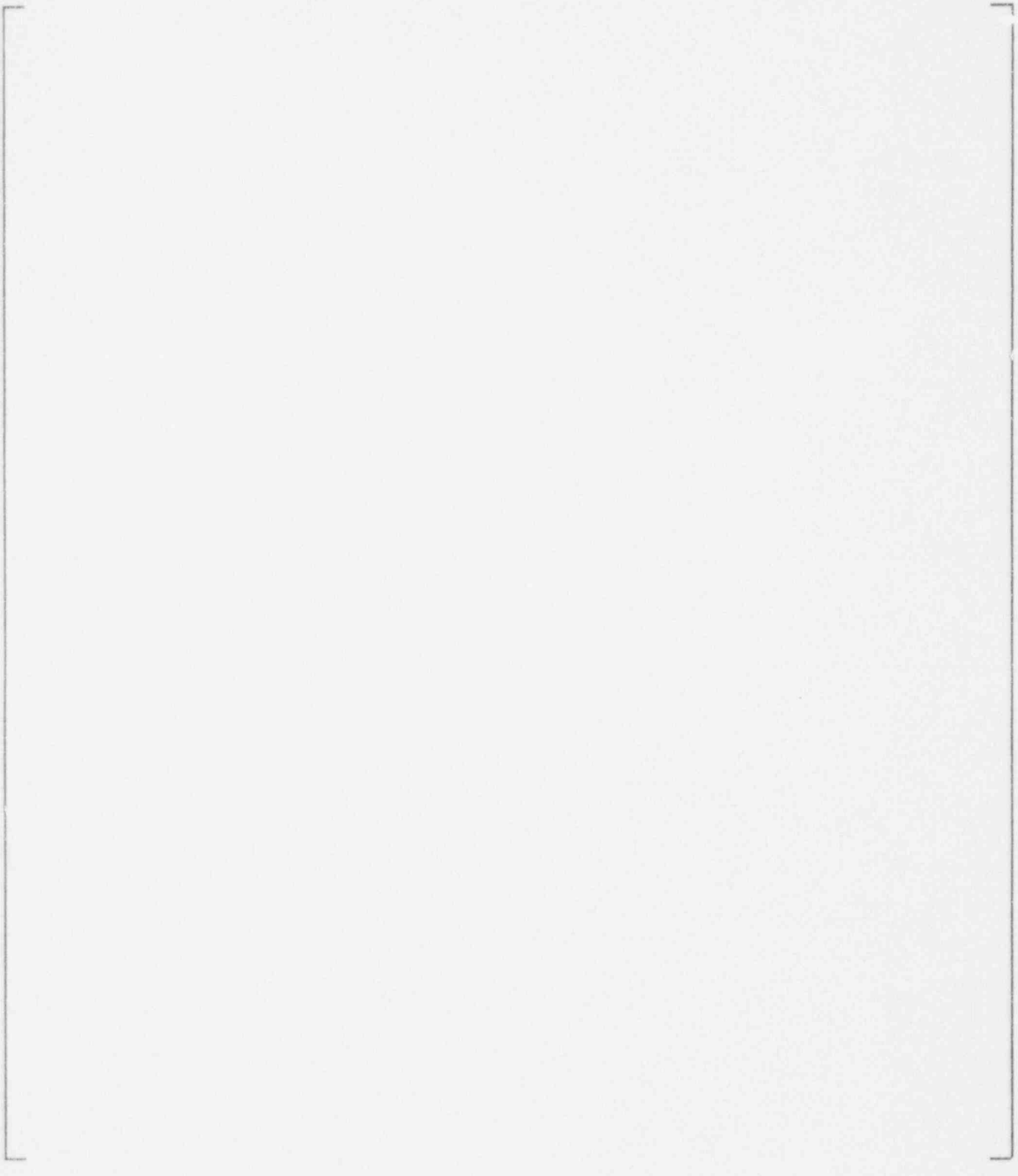

a,c

Figure 3.2-12 WCOBRA/TRAC UPTF Vessel Sections 7 and 8

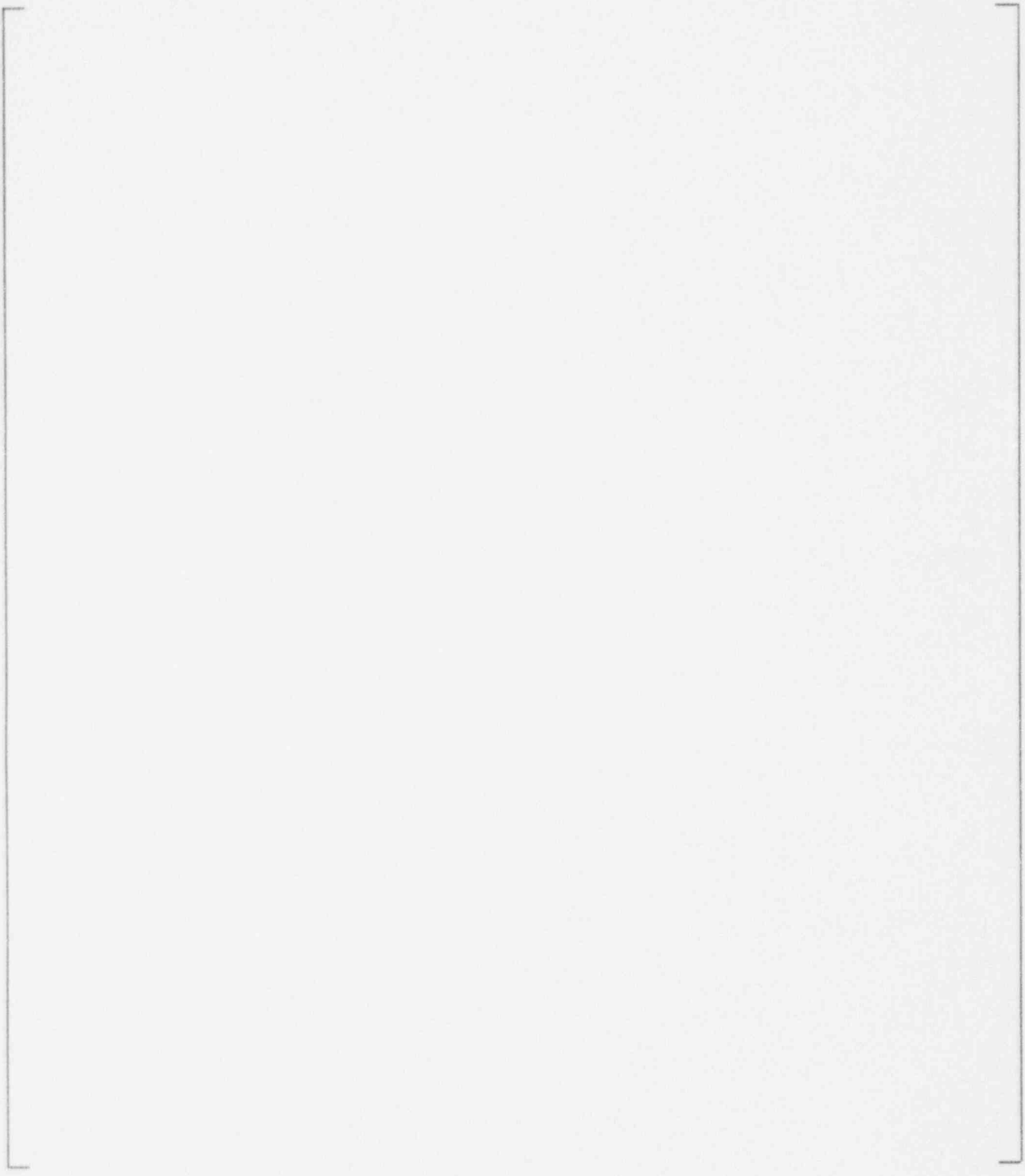

a,c

Figure 3.2-13 WCOBRA/TRAC UPTF Intact Loop Noding

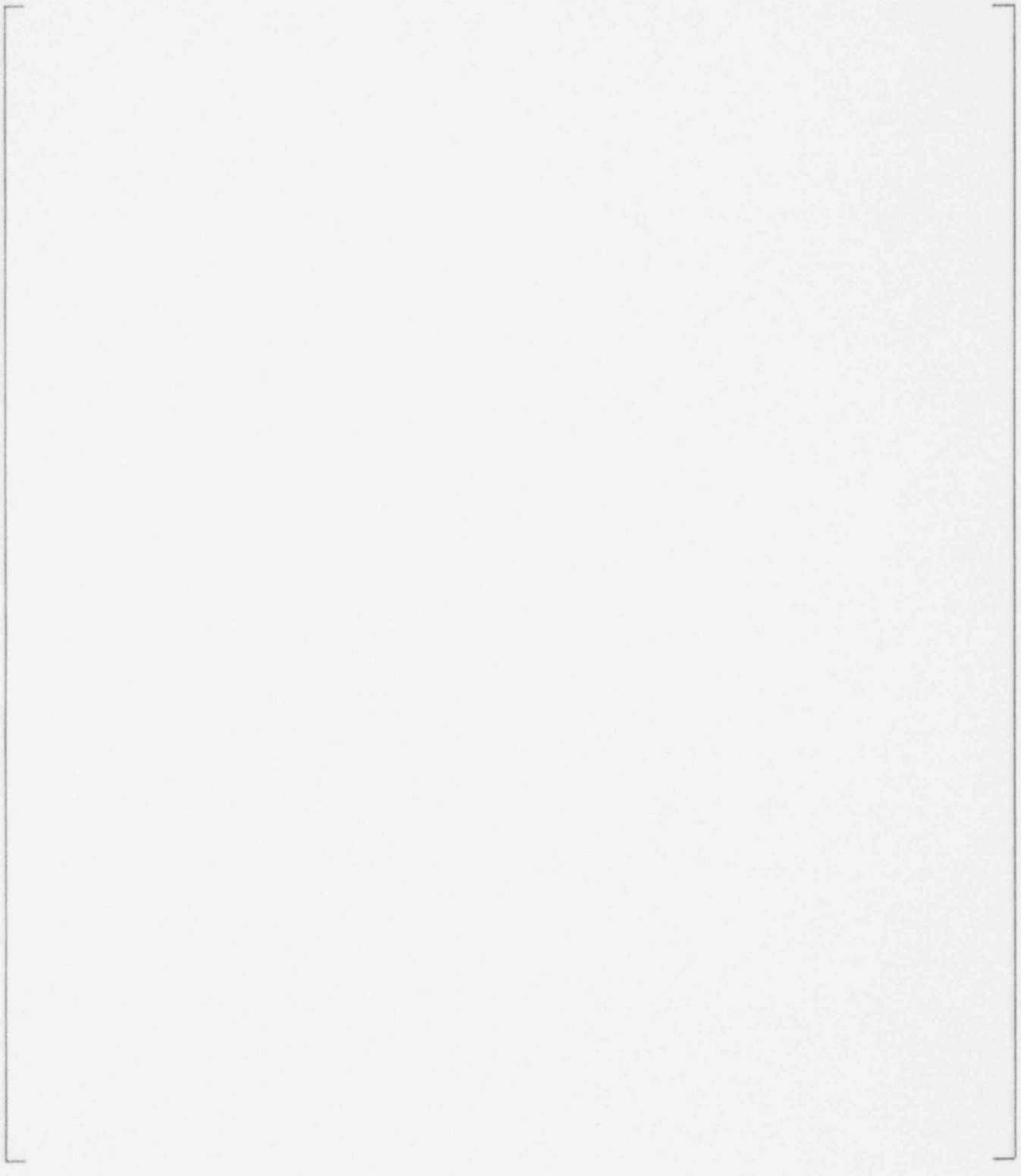

a,c

Figure 3.2-14 WCOBRA/TRAC UPTF Broken Loop Noding

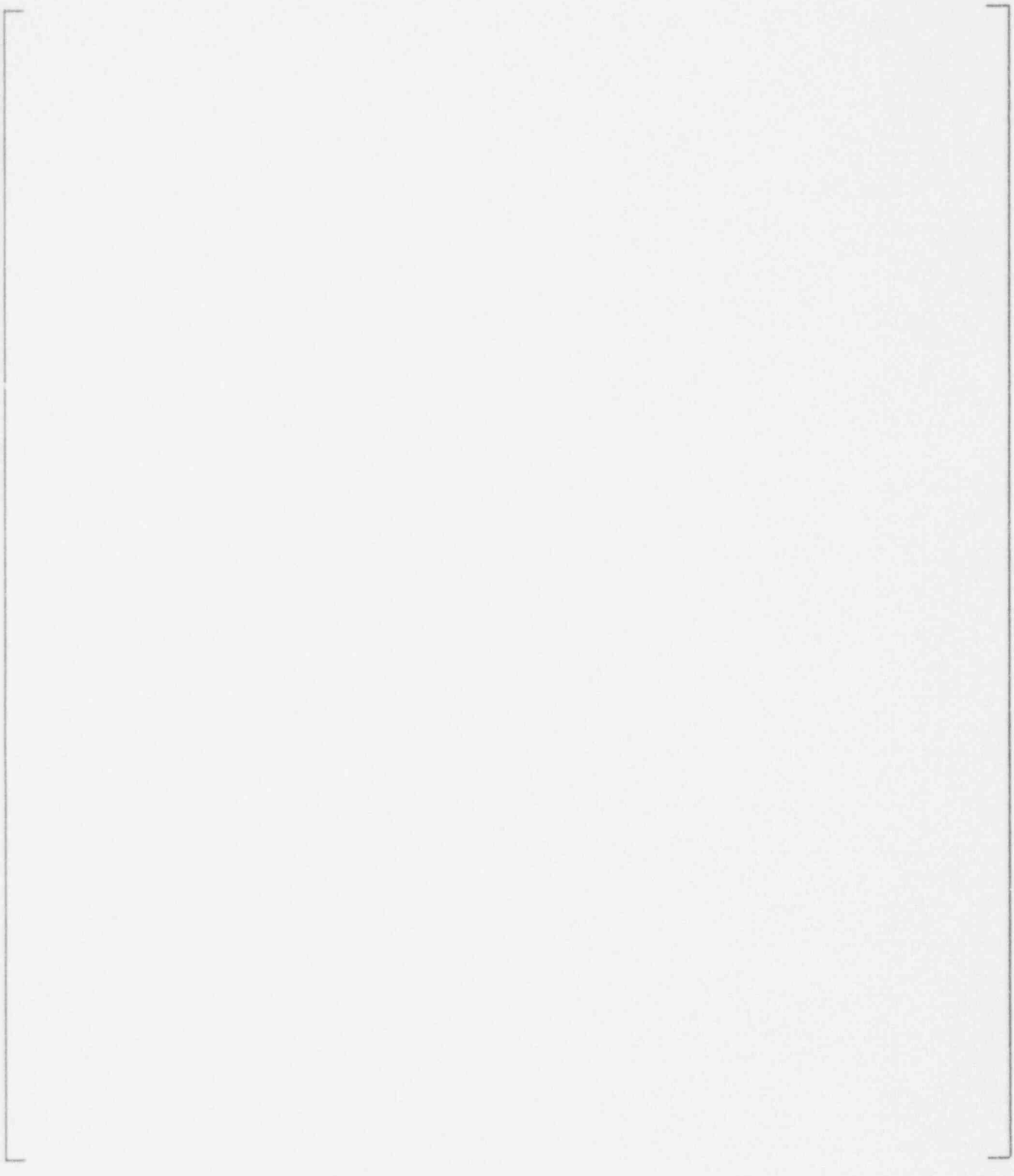

a,c

Figure 3.2-15 WCOBRA/TRAC UPTF Downcomer Injection Noding

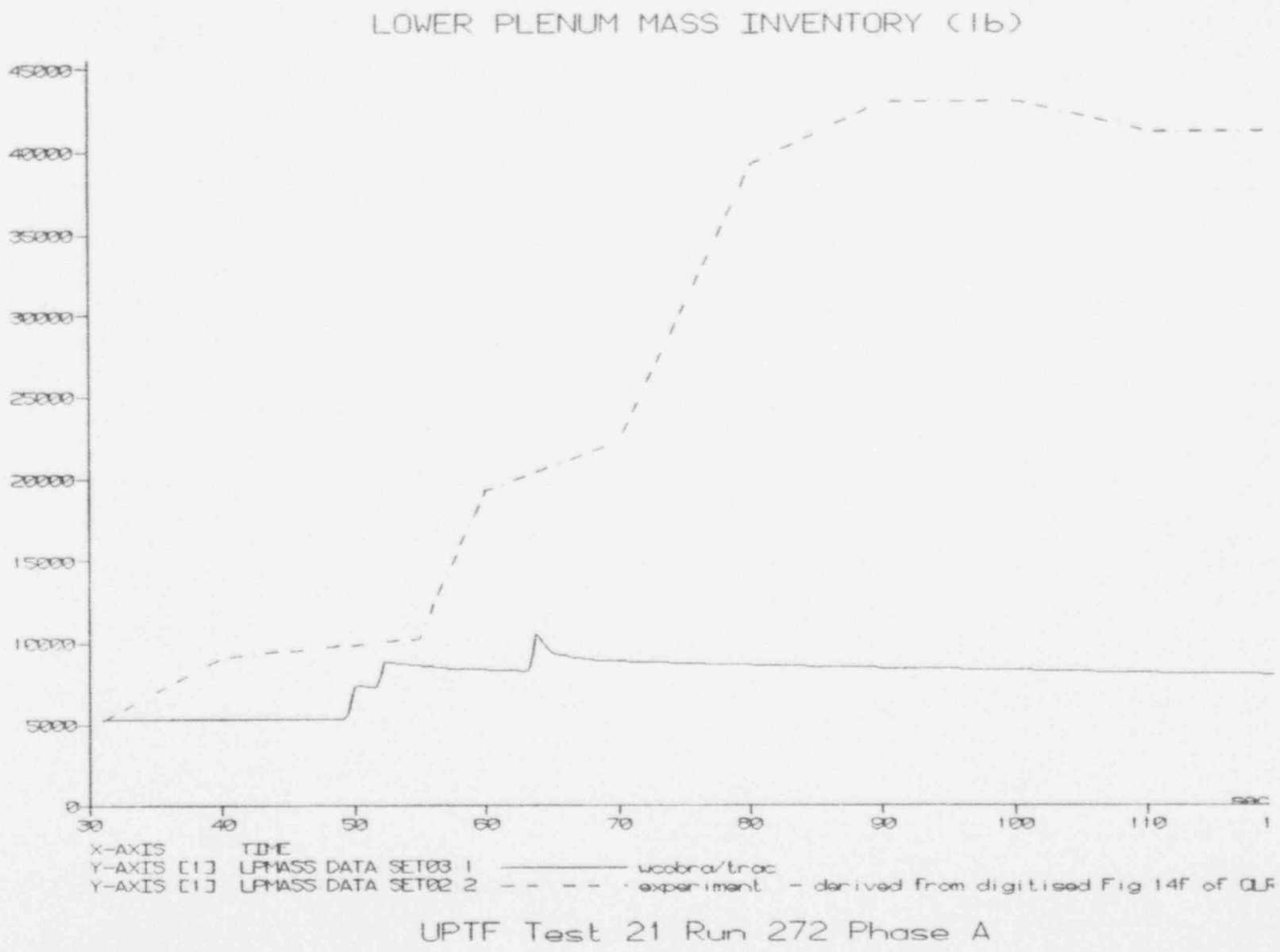

Figure 3.2-16 UPTF Test 21 Phase A, Lower Plenum Mass Inventory

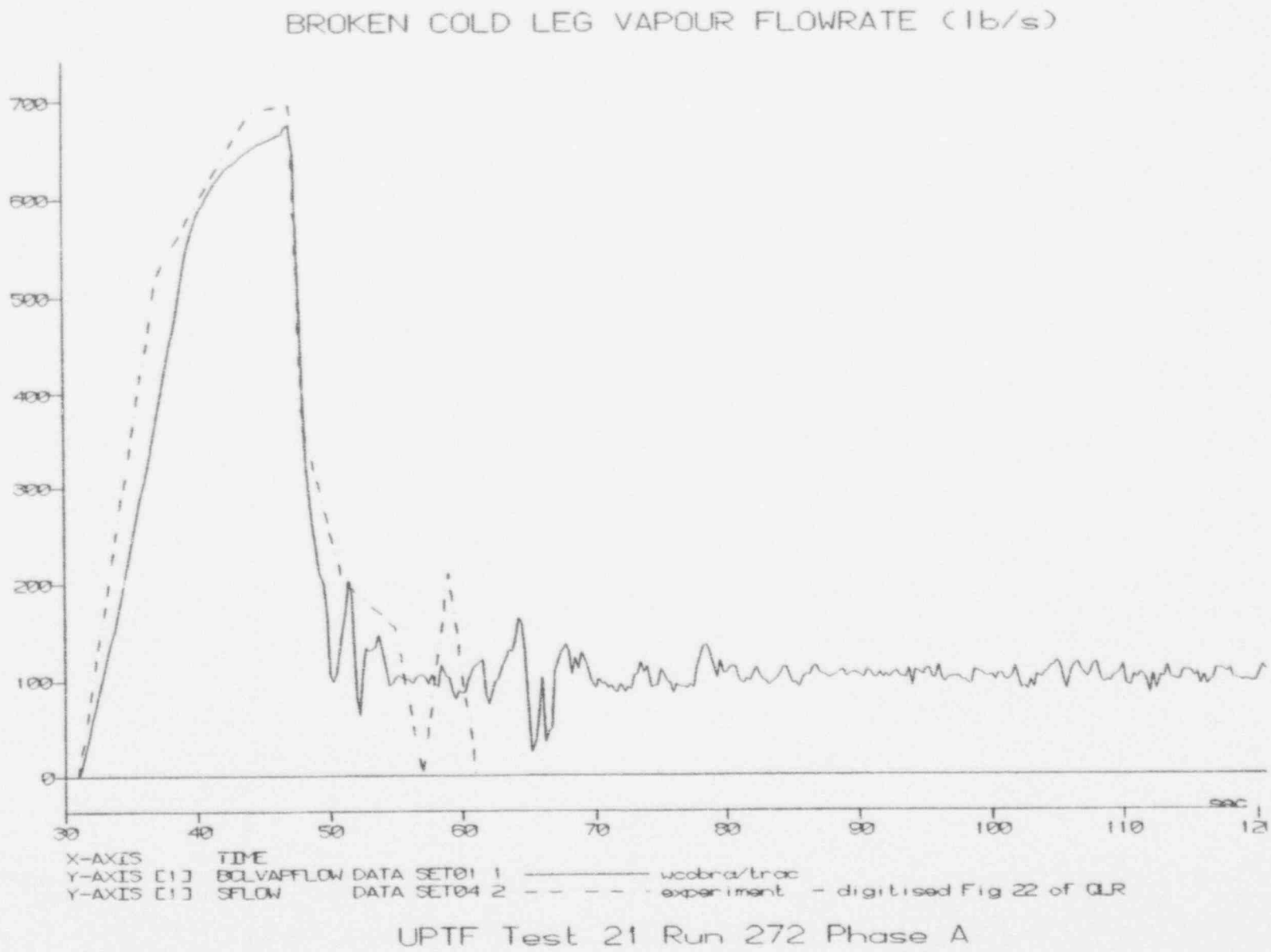

Figure 3.2-17 UPTF Test 21 Phase A, Broken Cold Leg Steam Mass Flow

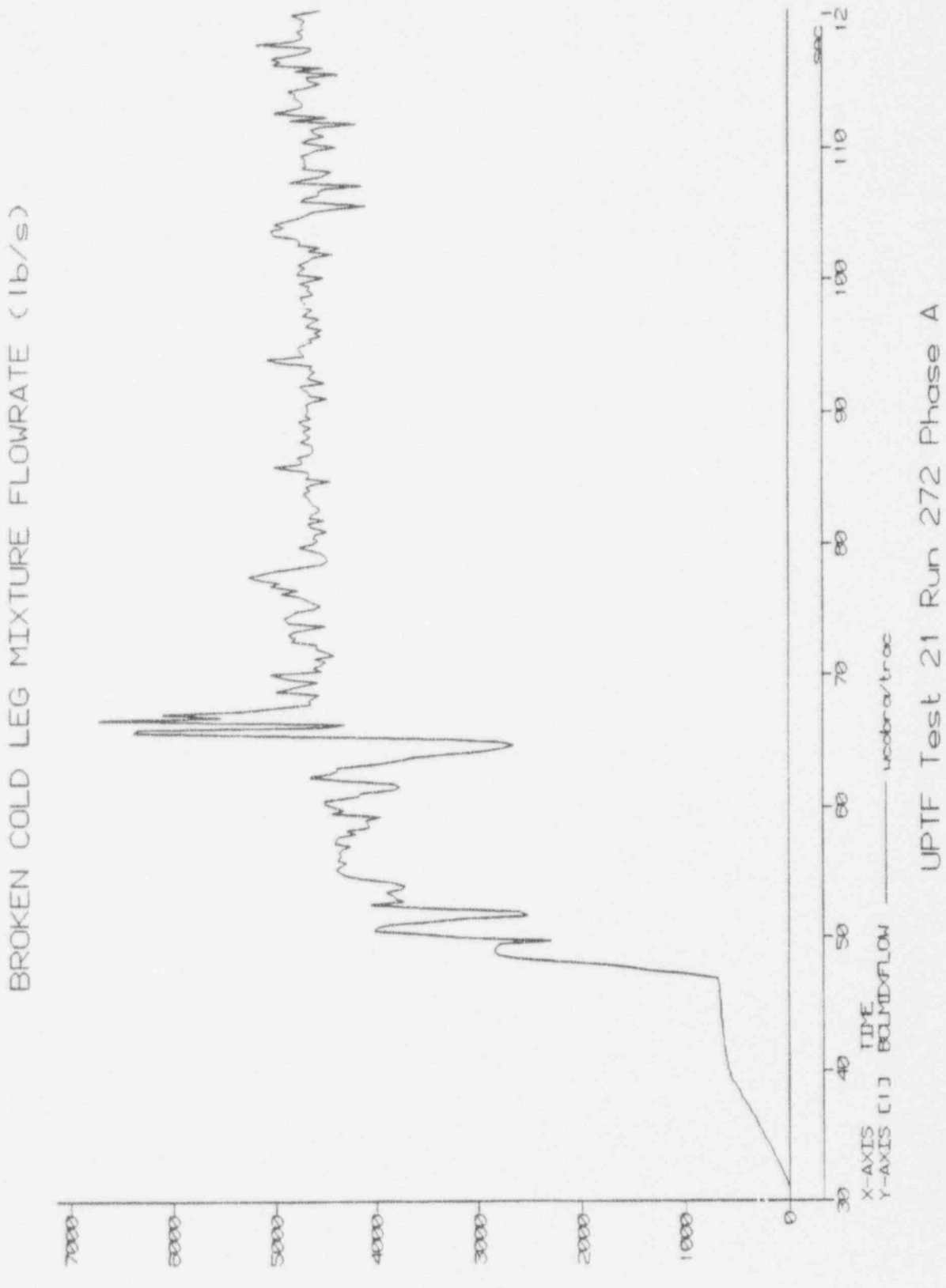

Figure 3.2-18 UPTF Test 21 Phase A, Broken Cold Leg Mixture Mass Flow

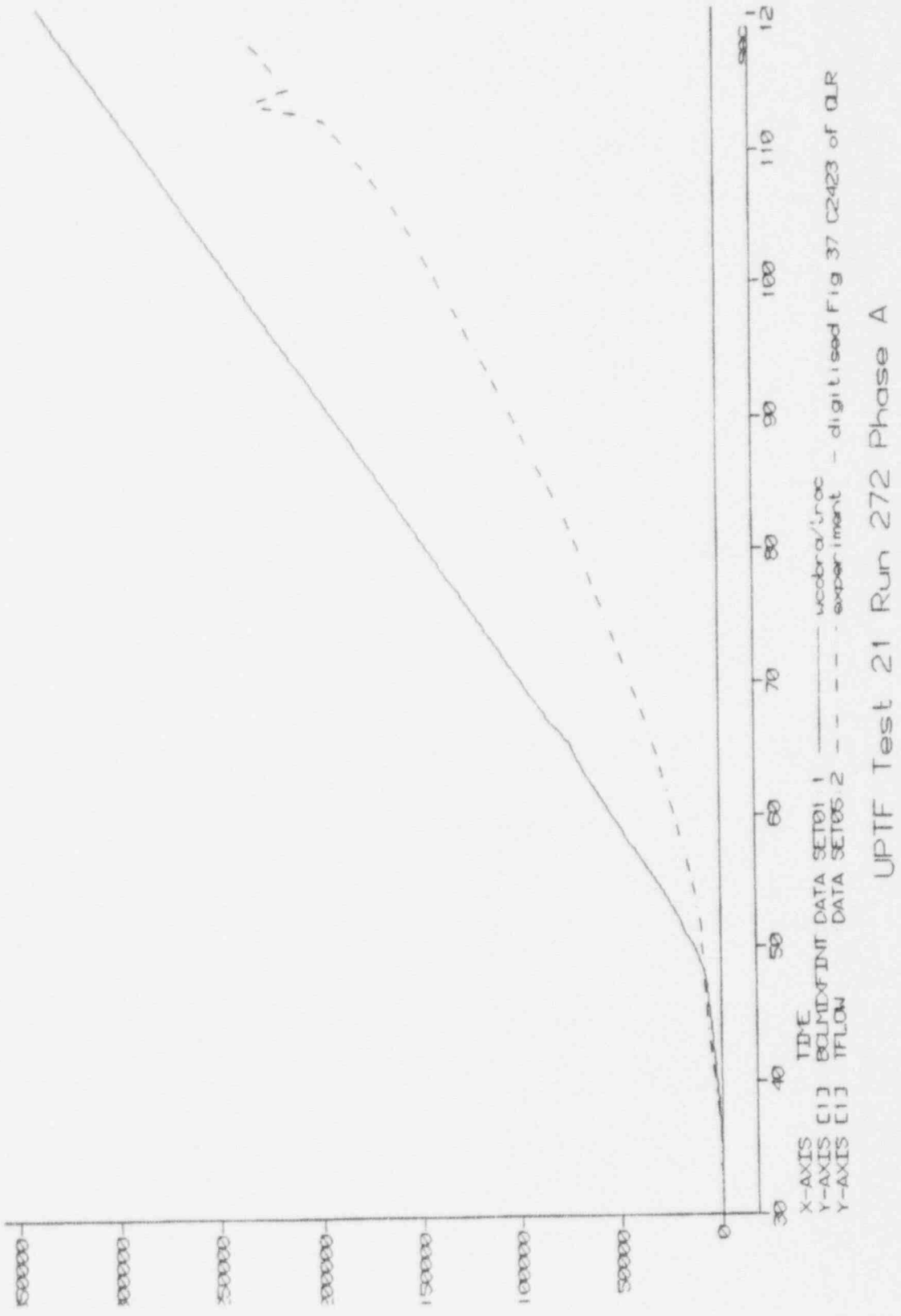

Figure 3.2-19 UPTF Test 21 Phase A, Broken Cold Leg Integrated Mixture Mass Flow

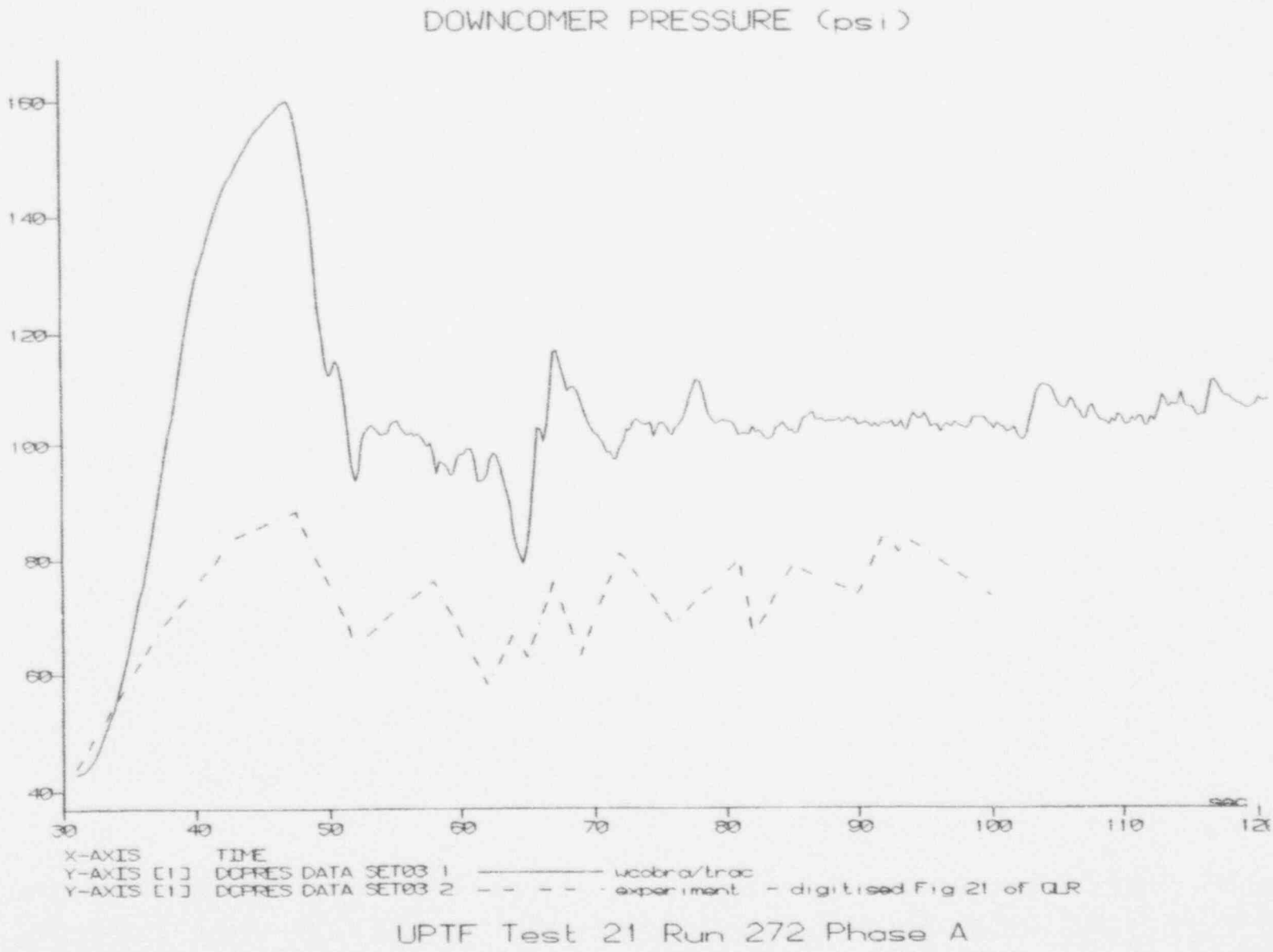

Figure 3.2-20 UPTF Test 21 Phase A, Downcomer Pressure

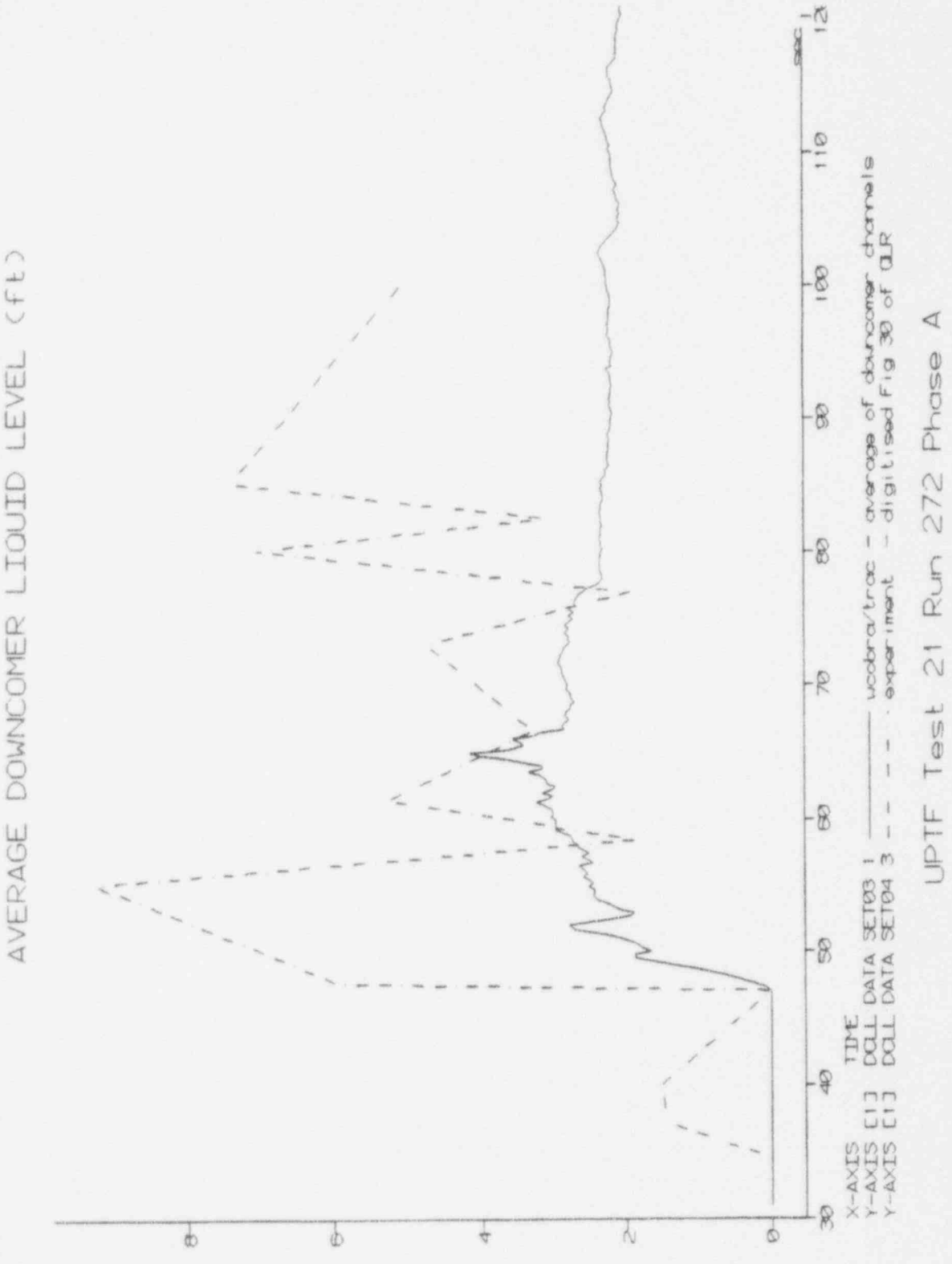

Figure 3.2-21 UPTF Test 21 Phase A, Downcomer Collapsed Liquid Level

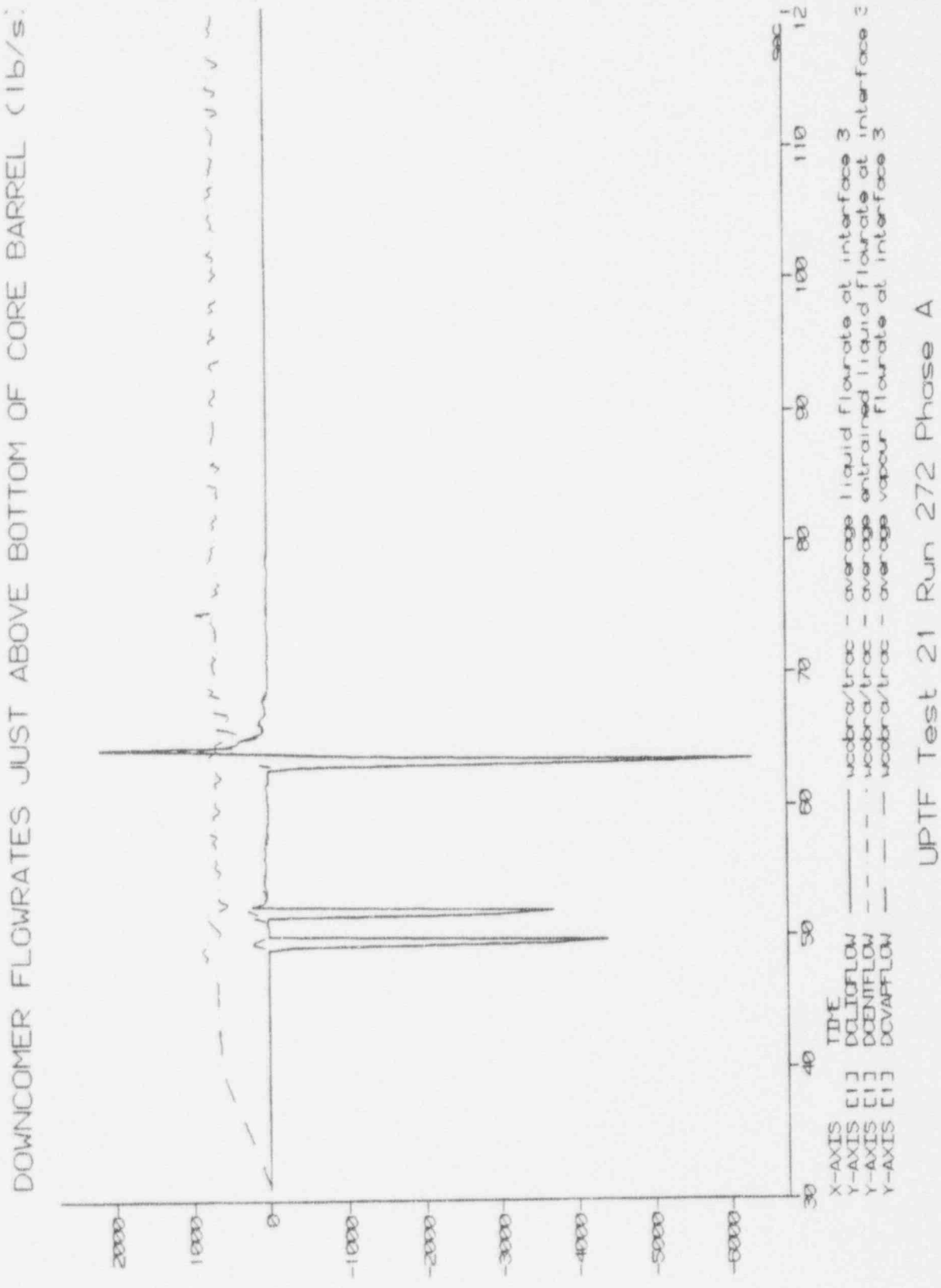

Figure 3.2-22 UPTF Test 21 Phase A, Downcomer Mass Flow Above Bottom of Core Barrel

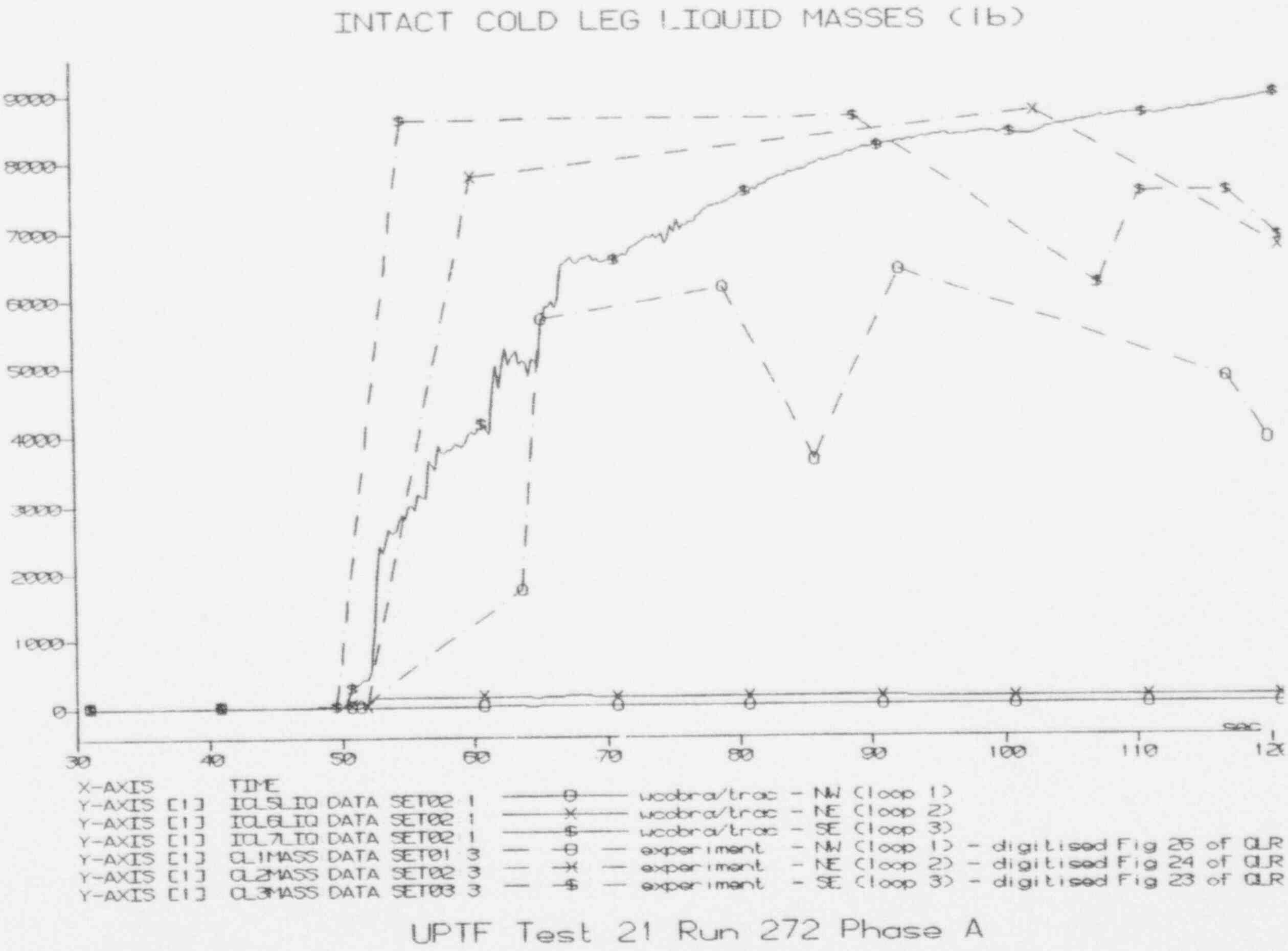

Figure 3.2-23 UPTF Test 21 Phase A, Intact Cold Leg Mass Inventories

Figure 3.2-24 UPTF Test 21 Phase B I, Lower Plenum Mass Inventory

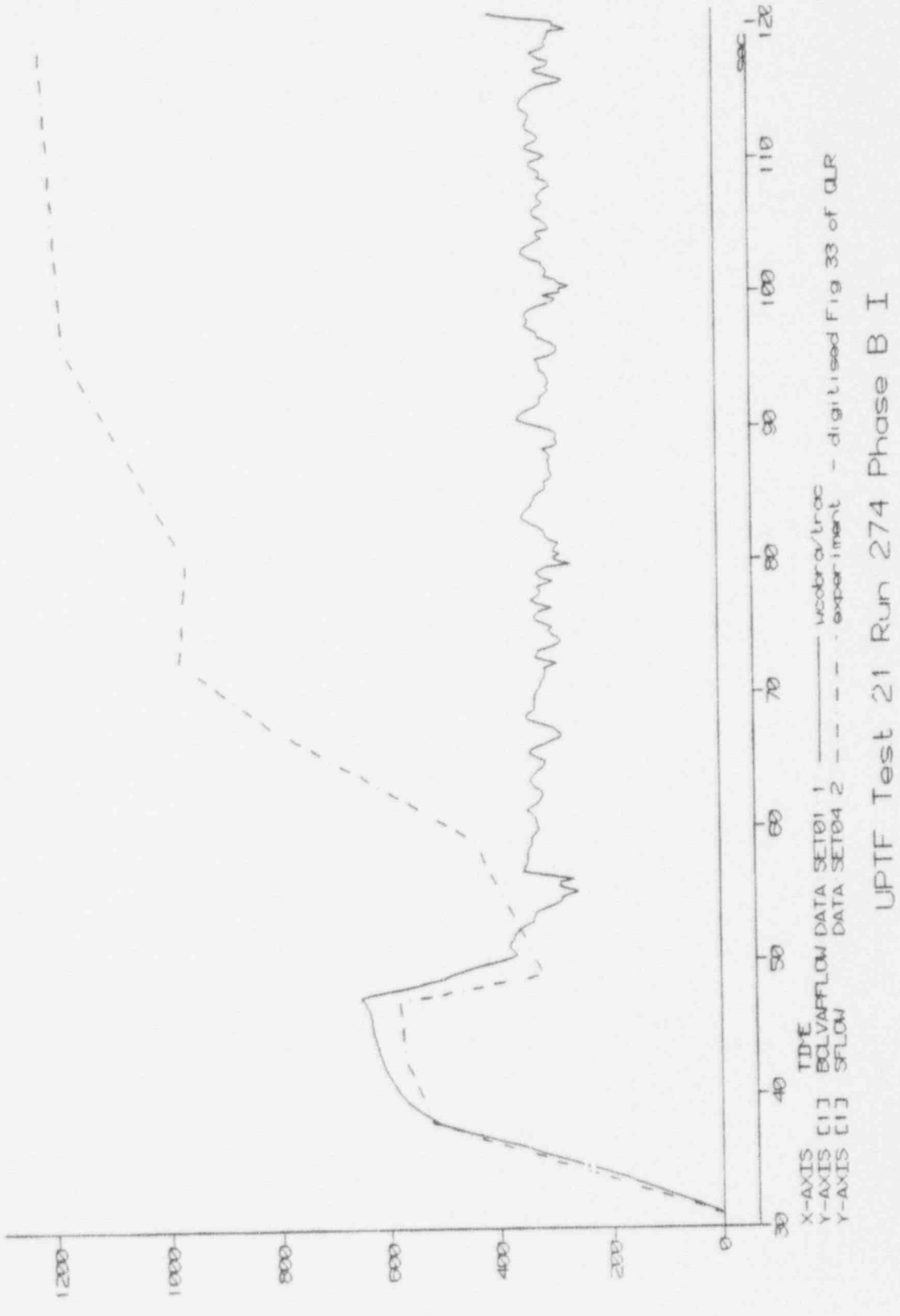

Figure 3.2-25 UPTF Test 21 Phase B I, Broken Cold Leg Steam Mass Flow

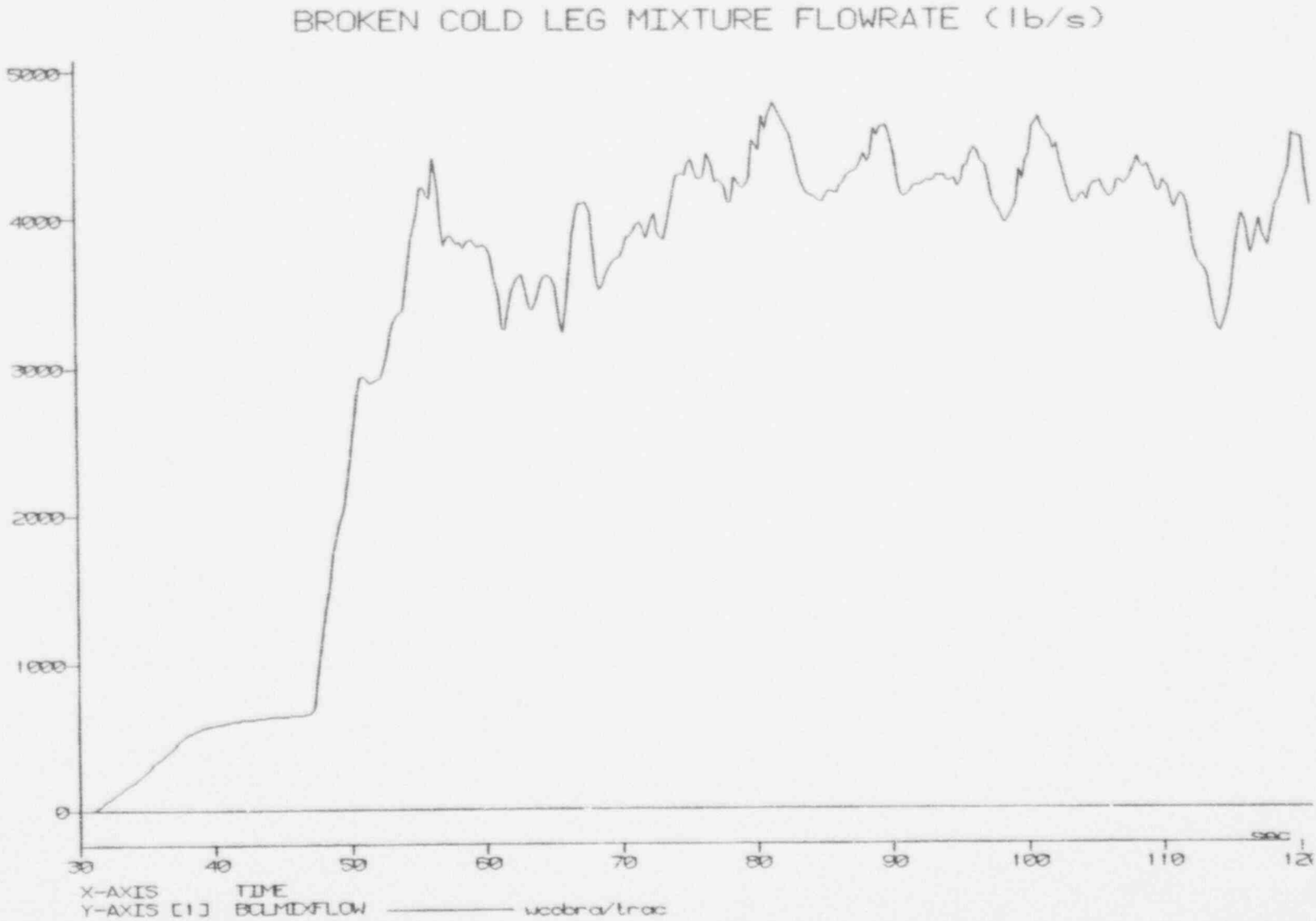

Figure 3.2-26 UPTF Test 21 Phase B I, Broken Cold Leg Mixture Mass Flow

Figure 3.2-27 UPTF Test 21 Phase B I, Broken Cold Leg Integrated Mixture Mass Flow

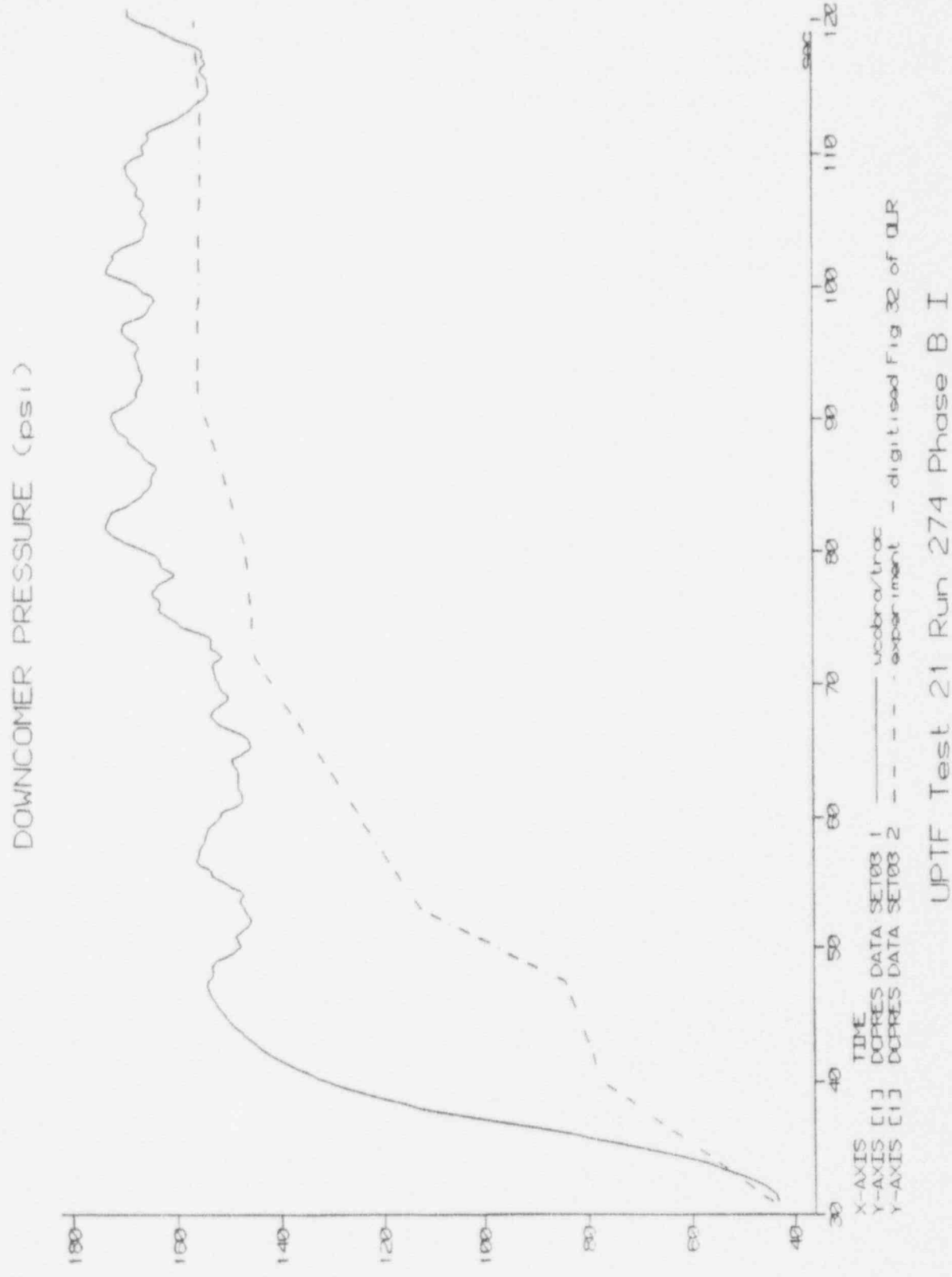

Figure 3.2-28 UPTF Test 21 Phase B I, Downcomer Pressure

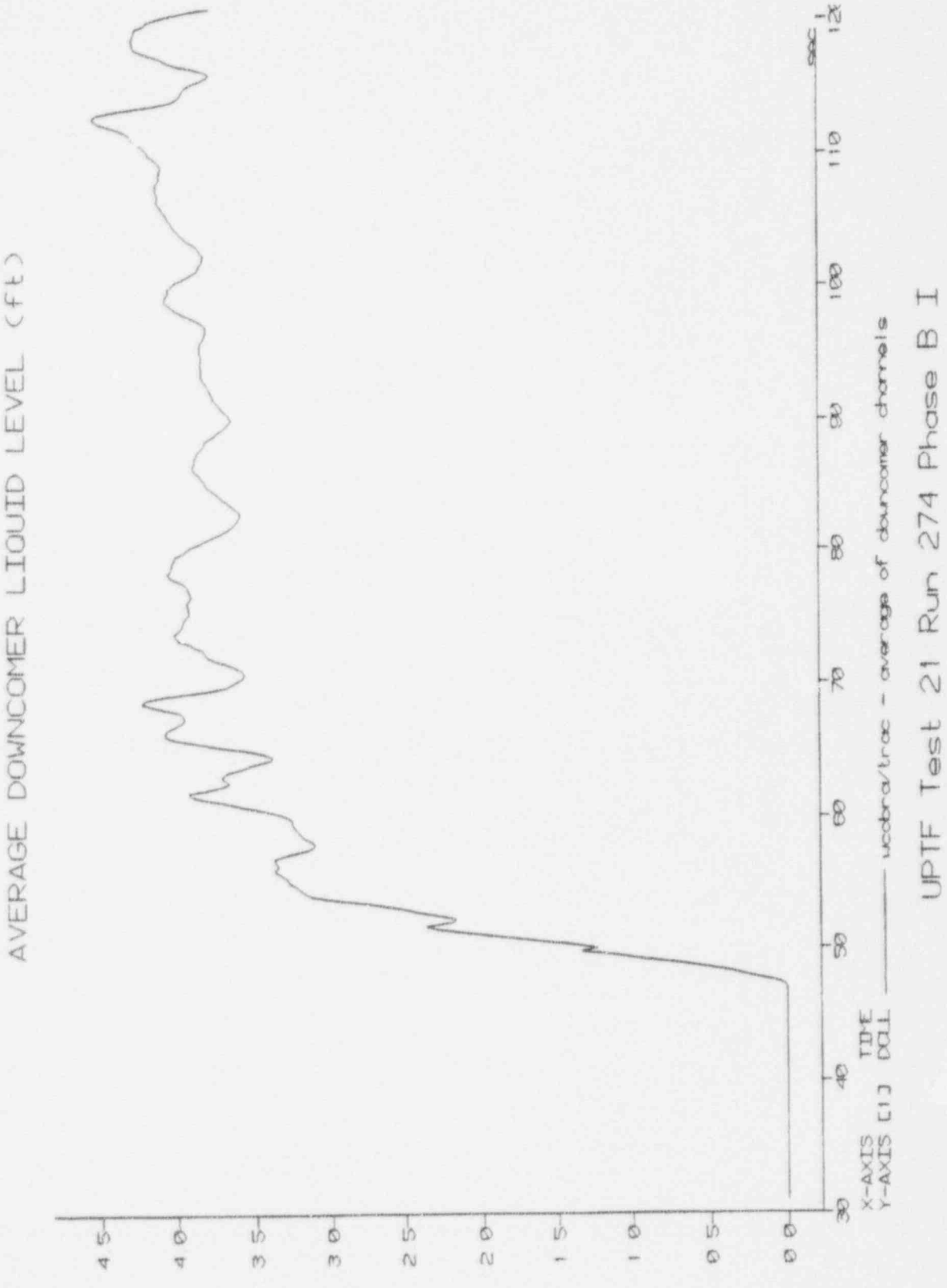

Figure 3.2-29 UPTF Test 21 Phase B I, Downcomer Collapsed Liquid Level

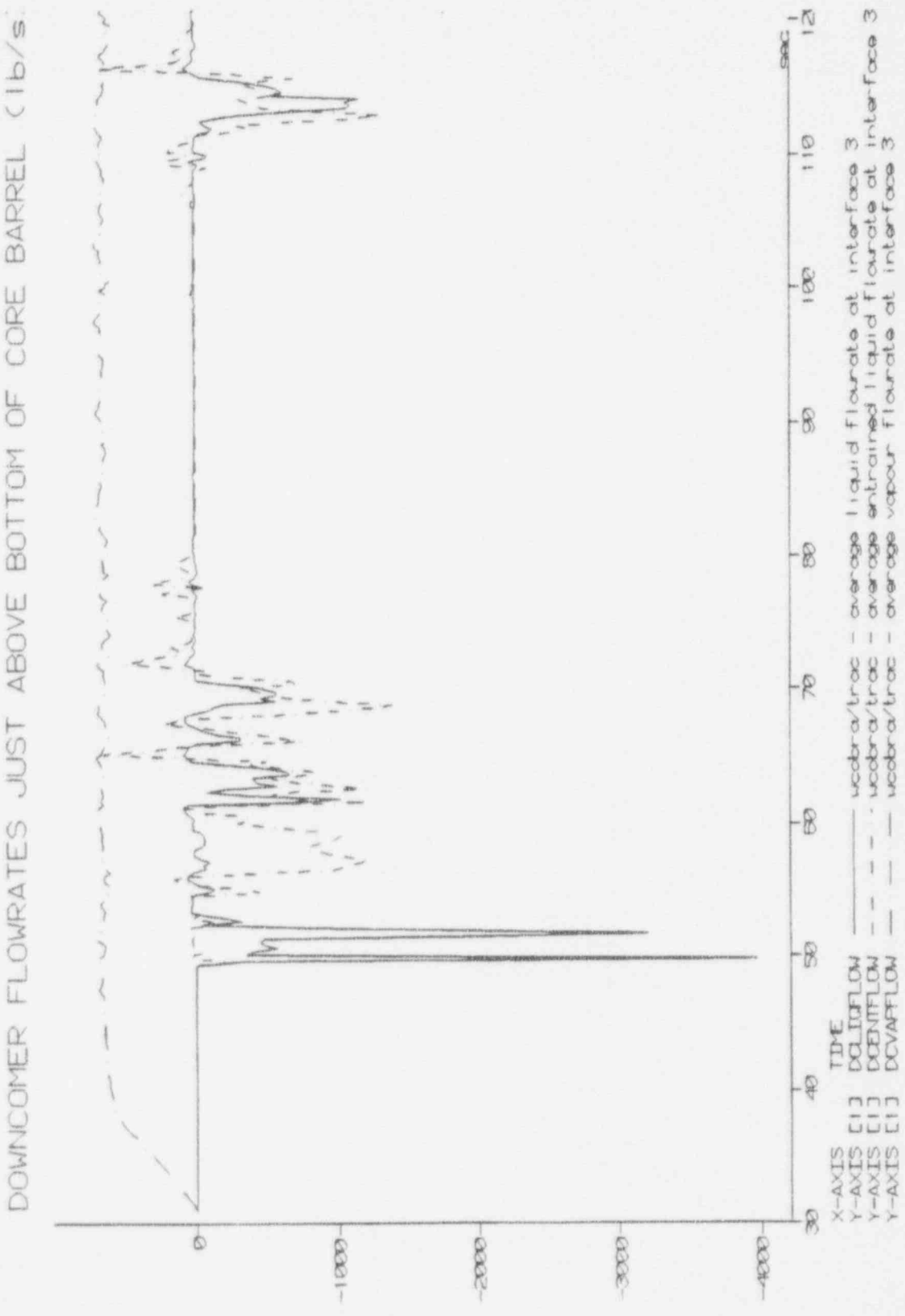

Figure 3.2-30 UPTF Test 21 Phase B I, Downcomer Mass Flow Just Above Bottom of Core Barrel

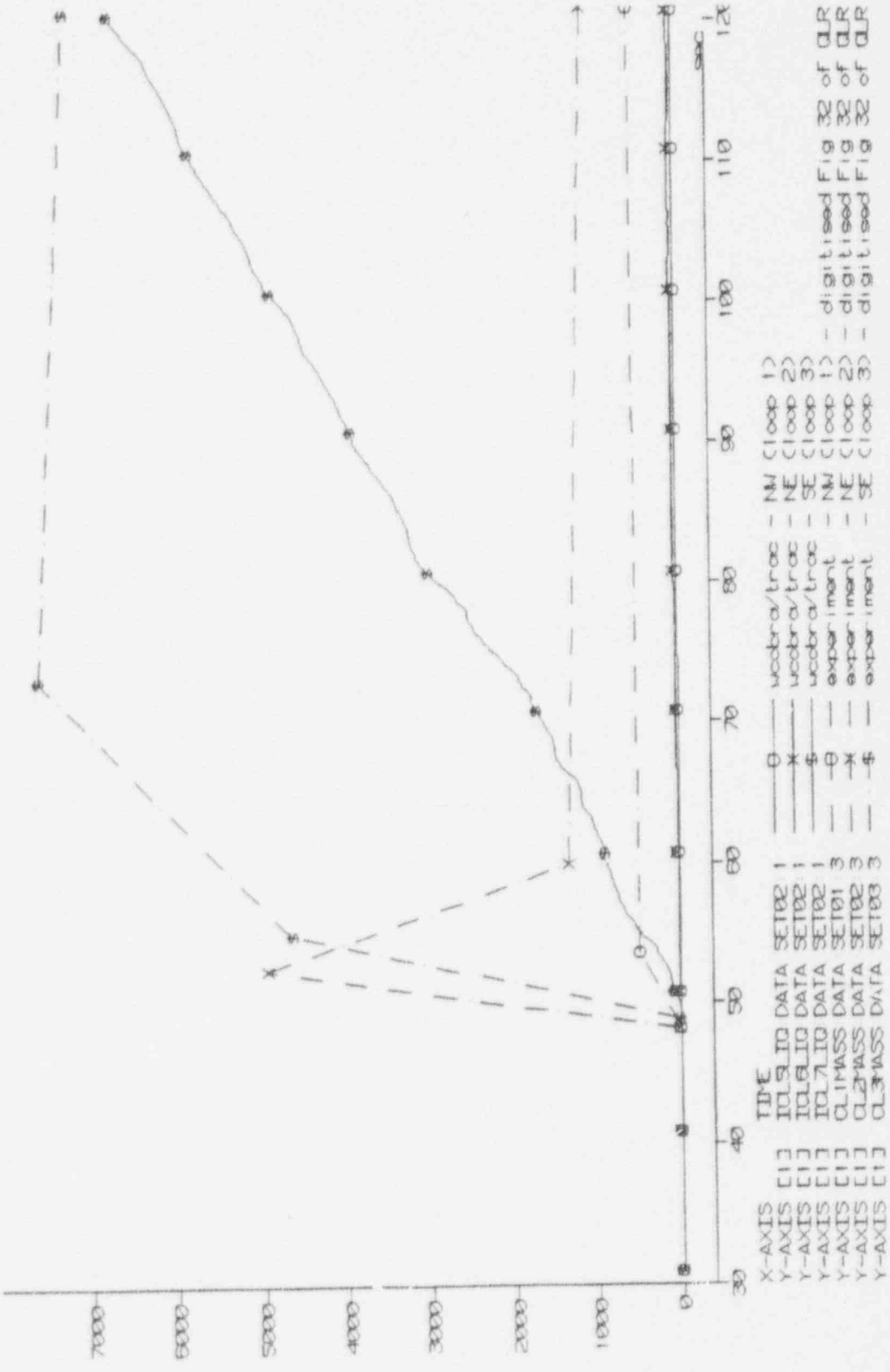

Figure 3.2-31 UPTF Test 21 Phase B I, Intact Cold Leg Mass Inventories

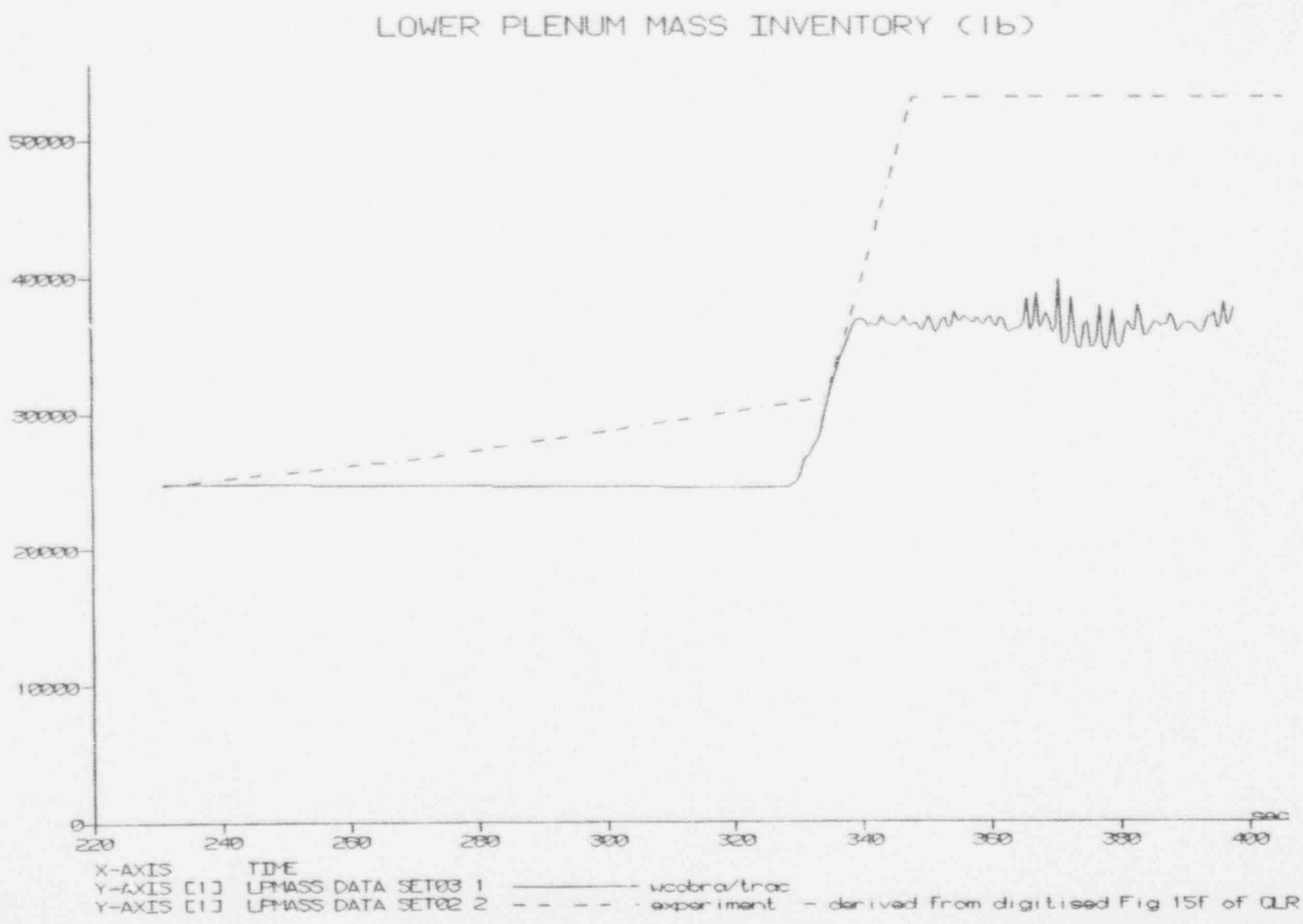

Figure 3.2-32 UPTF Test 21 Phases B II & III, Lower Plenum Mass Inventory

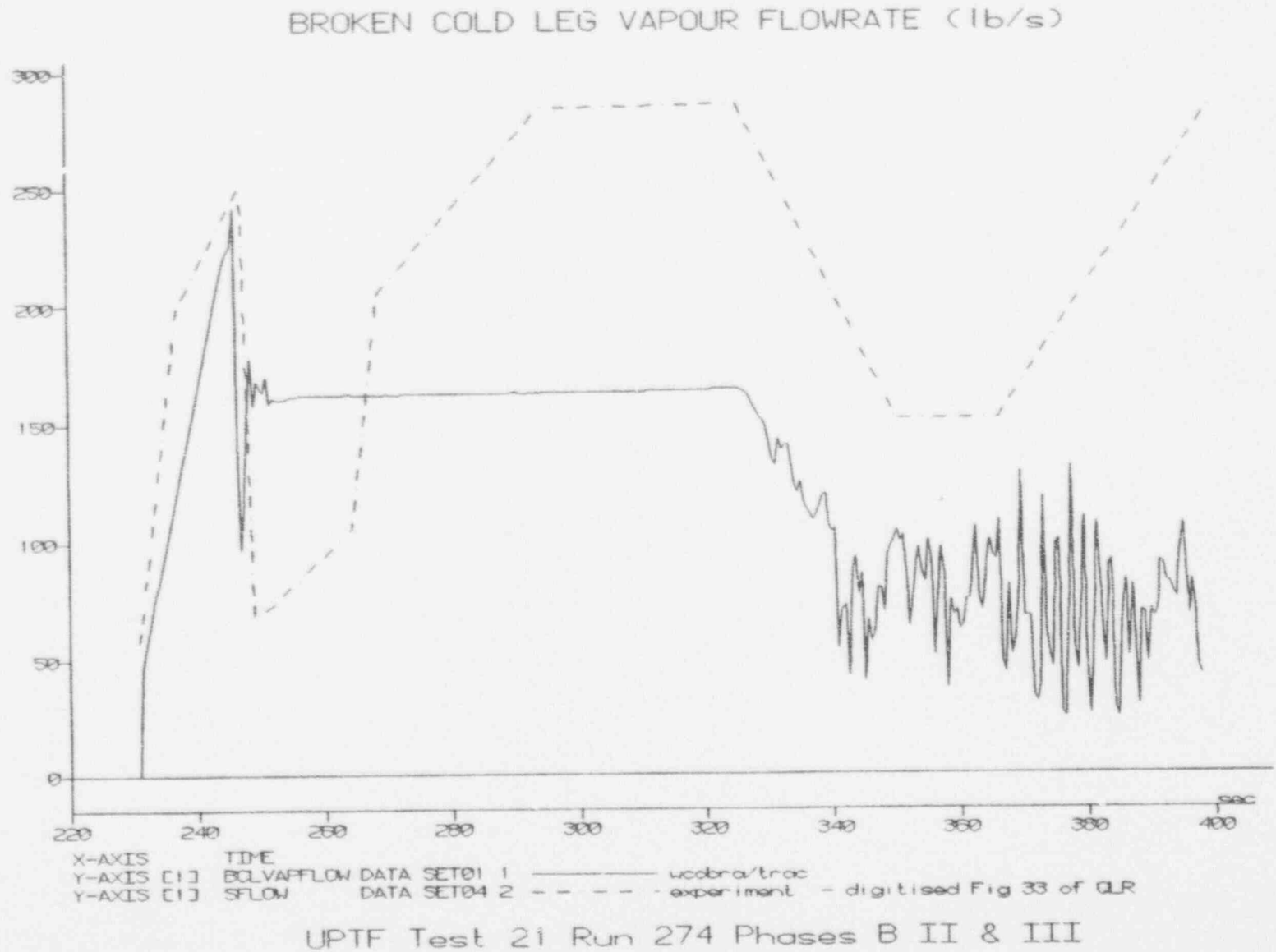

Figure 3.2-33 UPTF Test 21 Phases B II & III, Broken Cold Leg Steam Mass Flow

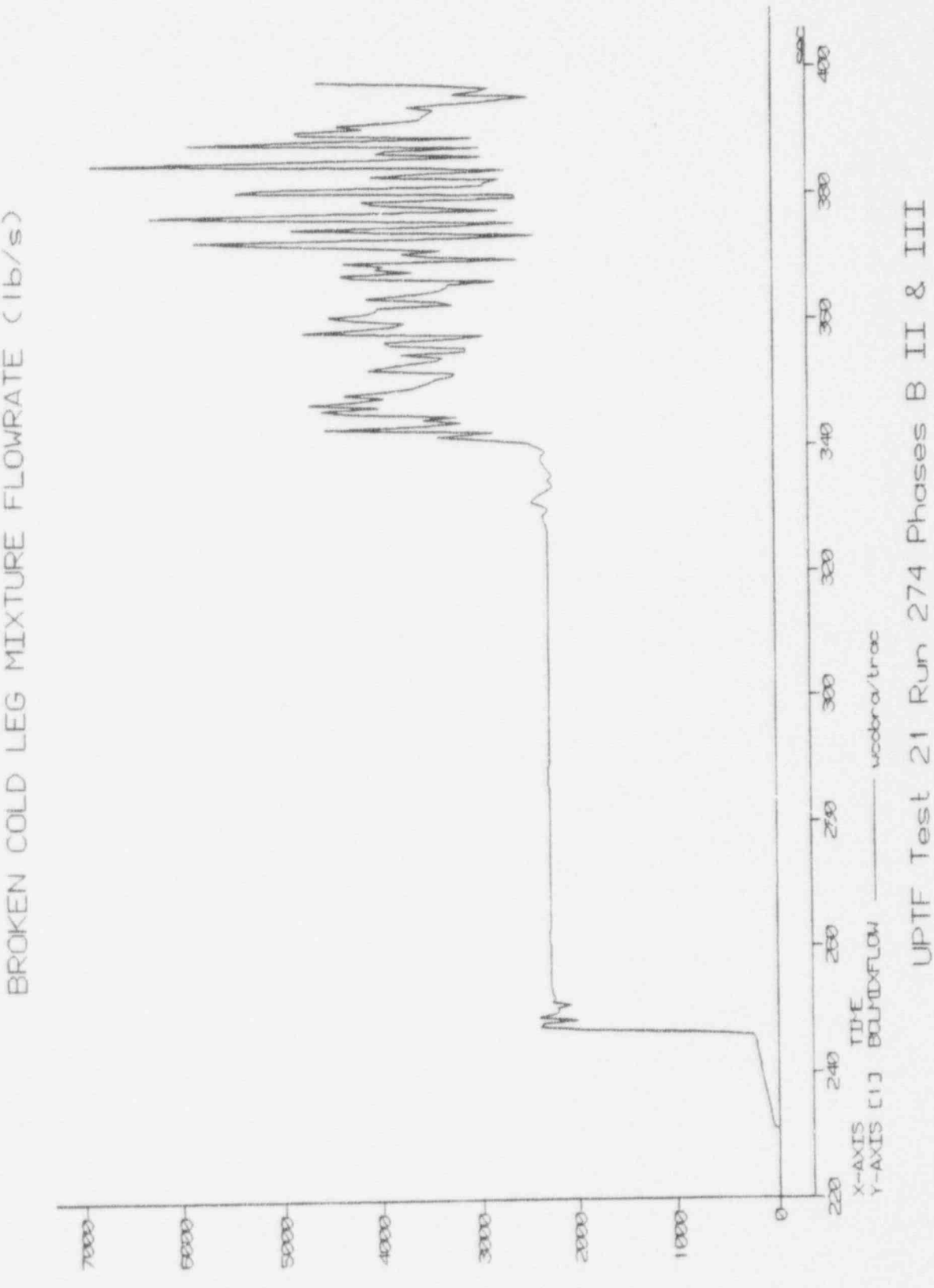

Figure 3.2-34 UPTF Test 21 Phases B II & III, Broken Cold Leg Mixture Mass Flow

Figure 3.2-35 UPTF Test 21 Phases B II & III, Broken Cold Leg Integrated Mixture Mass Flow

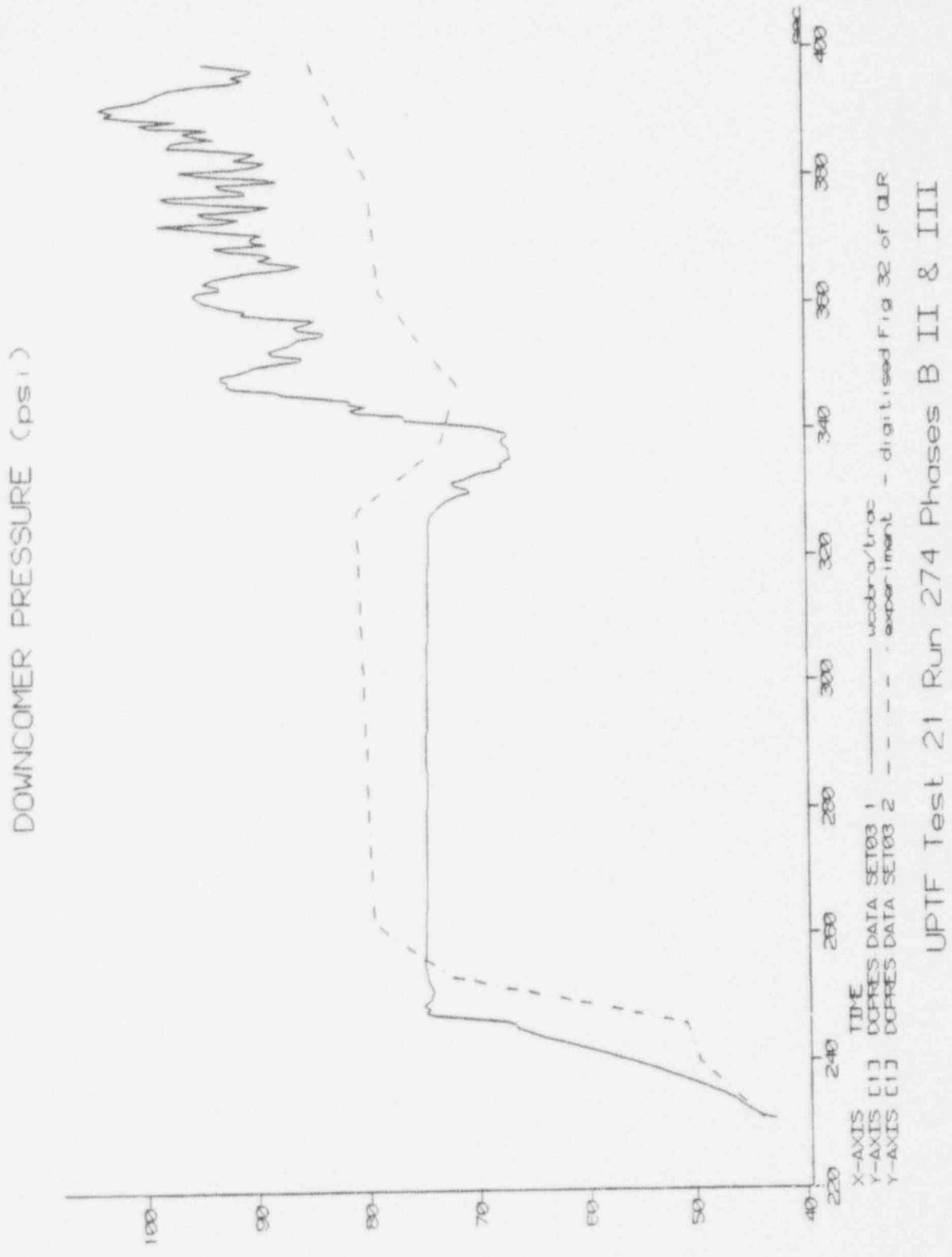

Figure 3.2-36 UPTF Test 21 Phases B II & III, Downcomer Pressure

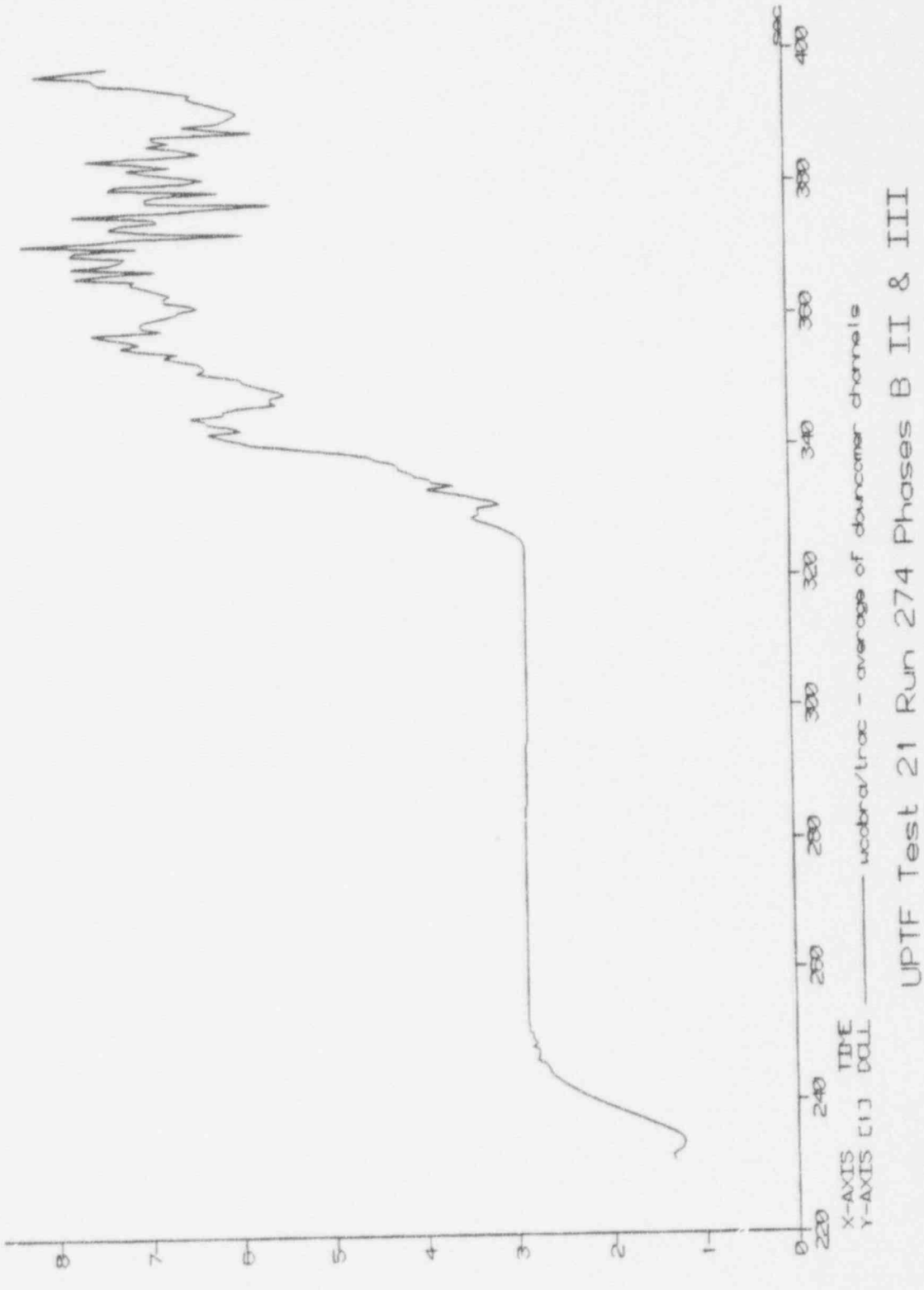

Figure 3.2-37 UPTF Test 21 Phases B II & III, Downcomer Collapsed Liquid Level

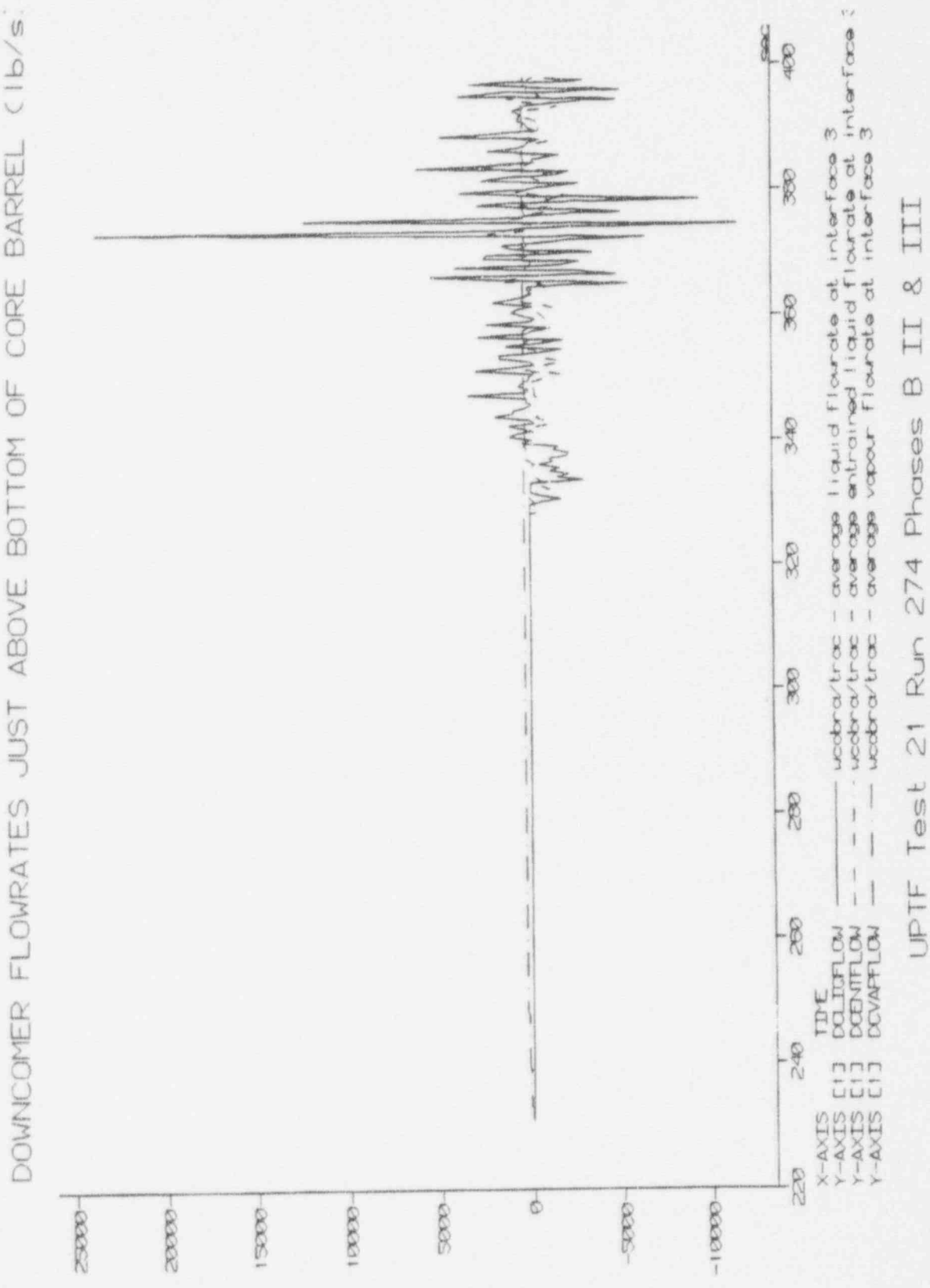

Figure 3.2-38 UPTF Test 21 Phases B II & III, Downcomer Mass Flow Just Above Bottom of Core Barrel

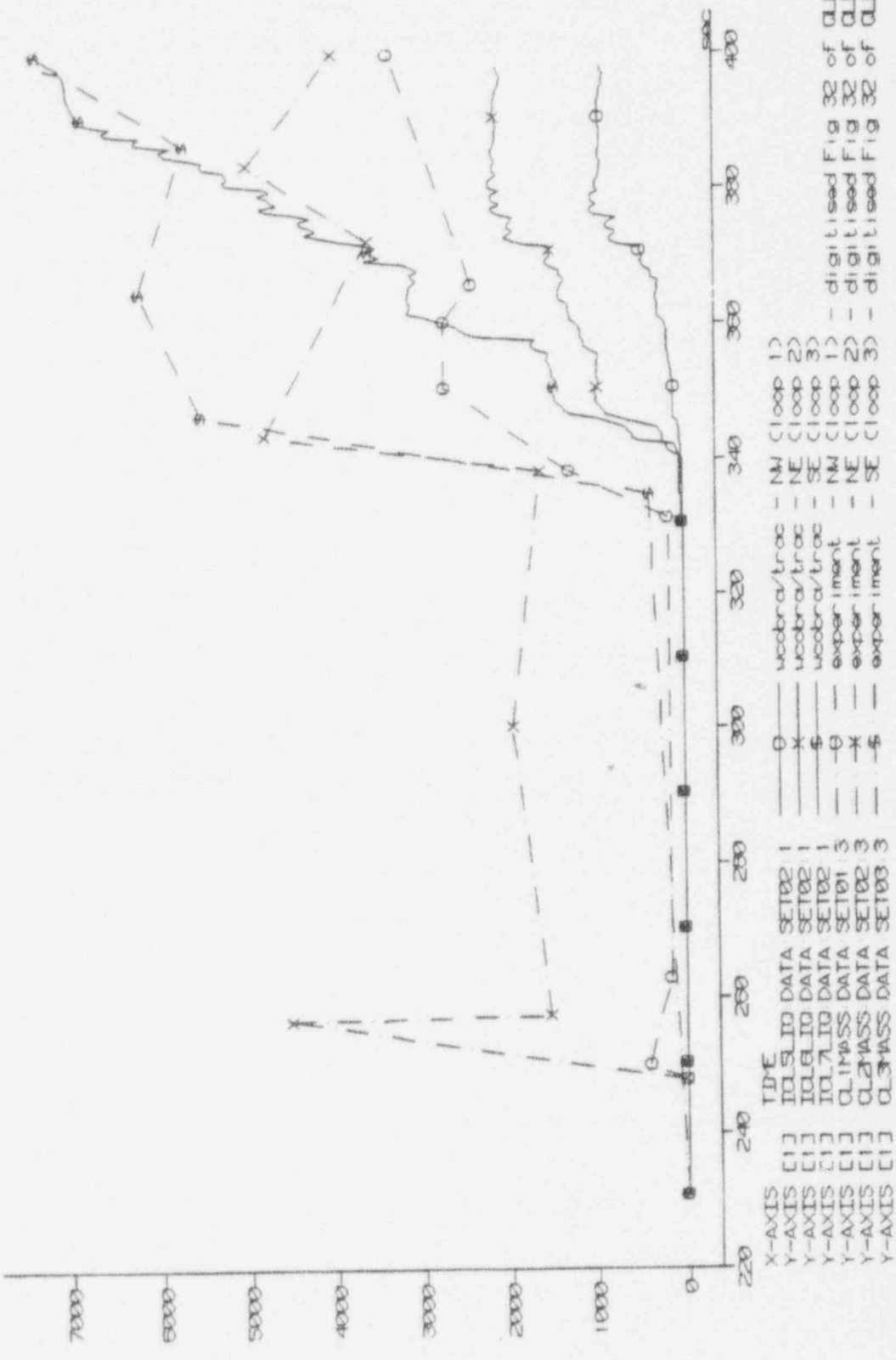

Figure 3.2-39 UPTF Test 21 Phases B II & III, Intact Cold Leg Mass Inventories

3.3 Conclusions

WCOBRA/TRAC calculations of CCTF run 58 and UPTF test 21 runs 272 phase A and 274 phase B have been performed to provide code validation for large-break LOCA applications for the AP600 plant. The CCTF and UPTF tests have downcomer ECCS injection representative of that of the AP600.

The calculation results of CCTF run 58 showed reasonable agreement with the thermal-hydraulic behavior of the test. Peak clad temperatures were generally overcalculated compared to those of the test, particularly for the hot rod and at upper locations.

The calculation results of the UPTF tests showed an overprediction of the liquid discharged from the break (bypass) and an underprediction of the injected liquid entering the lower plenum.

The overall conclusion is that WCOBRA/TRAC has been shown to be valid for calculating the thermal-hydraulic behavior associated with downcomer injection during a large-break LOCA. WCOBRA/TRAC overpredicts the liquid discharge from a cold leg break, (bypass), and thereby underpredicts the rate of filling of the lower plenum by the downcomer injection water, resulting in an overprediction of the peak clad temperature.

4.0 APPLICATION OF THE WCOBRA/TRAC CODE UNCERTAINTY TO THE AP600

Introduction

The best-estimate methodology used for the large-break calculations was to use a "superbounded" plant calculation as the basis to determine the peak cladding temperature (PCT). Plant conditions were chosen in a conservative manner to bound the uncertainties in these parameters. The remaining uncertainty that must be accounted for is the uncertainty in the calculational method or code. In the original SSAR calculation,[5] the WCOBRA/TRAC-Mod4 code uncertainty developed for the two-loop plants was used as the basis for the code uncertainty to be applied to the AP600. At that time, the most recent WCOBRA/TRAC uncertainty from Addendum 3 to WCAP-10924 was applied to the AP600 large-break analysis.[11] Also, an additional uncertainty of 50°F was added to the calculated code uncertainty for the AP600 to retain additional conservatism in the reported AP600 large-break LOCA PCT results.

With the issuance of the WCOBRA/TRAC Code Qualifying Document (CQD),[3] the code uncertainty has been recalculated for the WCOBRA/TRAC code with an extended data base that is applicable to the AP600 large-break LOCA. Therefore, the code uncertainty derived in the WCOBRA/TRAC CQD will be used as the basis for the code uncertainty that will be applied to the AP600 large-break LOCA calculation.

4.1 Application of the CQD Uncertainty to the AP600 Large-Break LOCA Calculation

The details of the calculational method to derive the WCOBRA/TRAC code uncertainty are given in Section 19 of the CQD for WCOBRA/TRAC, and only the results and the application of the results for the AP600 large-break LOCA analysis will be given in this report.

The calculated code uncertainty consists [

]^{a,c}

[

]^{a,c} The experiments that were used to derive the code uncertainty for each PCT are shown in [ ]^{a,c}, which was taken from the WCOBRA/TRAC CQD. Since the large-break LOCA transient for the AP600 is essentially the same as that for a three- or four-loop PWR, the same data can be used to develop the code uncertainty for the AP600.

[

σ_3]^{a,c} Figure 4.1-1 shows graphically, how the uncertainties can affect the code comparisons to the data for the reflood peak.

The spread of the different test data for each test or data set can be seen in Figure 4.1-1, [

]^{a,c}

The final numerical values for the WCOBRA/TRAC code uncertainty for each PCT at different elevations are summarized in Tables 4.1-2 and 4.1-3.

[

$\Delta PCT_{1,j}$]^{a,c}

Figures 4.1-2 and 4.1-3 show the calculated values of the code bias and total uncertainty plotted as a function of elevation. [

]^{a,c}

The PWR PCT can occur at any elevation, but particularly between the core mid-plane, 6-ft., and 10-ft. elevations depending on the axial power shape, design of the reactor vessel internals, and the

emergency core cooling system (ECCS). [

]^{a,c}

The above average values for the code uncertainty are shown on Figures 4.1-2 and 4.1-3.

a,c

TABLE 4.1-1
TEST GROUPING FOR DIFFERENT PEAK CLADDING TEMPERATURES

TABLE 4.1-2
CALCULATION OF WCOBRA/TRAC CODE UNCERTAINTY - BLOWDOWN PCT

a,c

TABLE 4.1-3
CALCULATION OF WCOBRA/TRAC CODE UNCERTAINTY - REFLOOD PCT

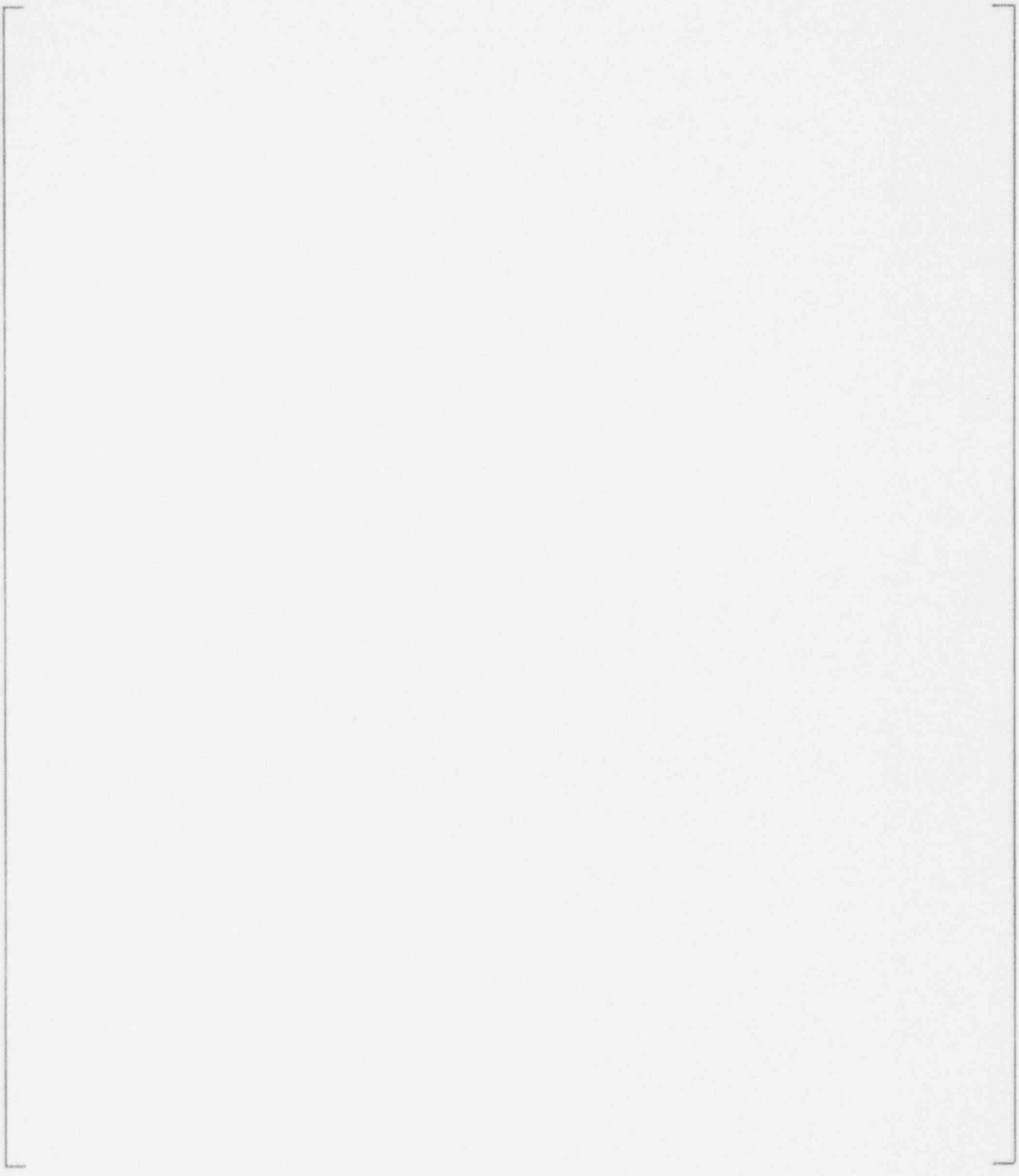

a,c

Figure 4.1-1 Components of WCOBRA/TRAC Code Uncertainty for Reflood PCT at 6-ft. Elevation

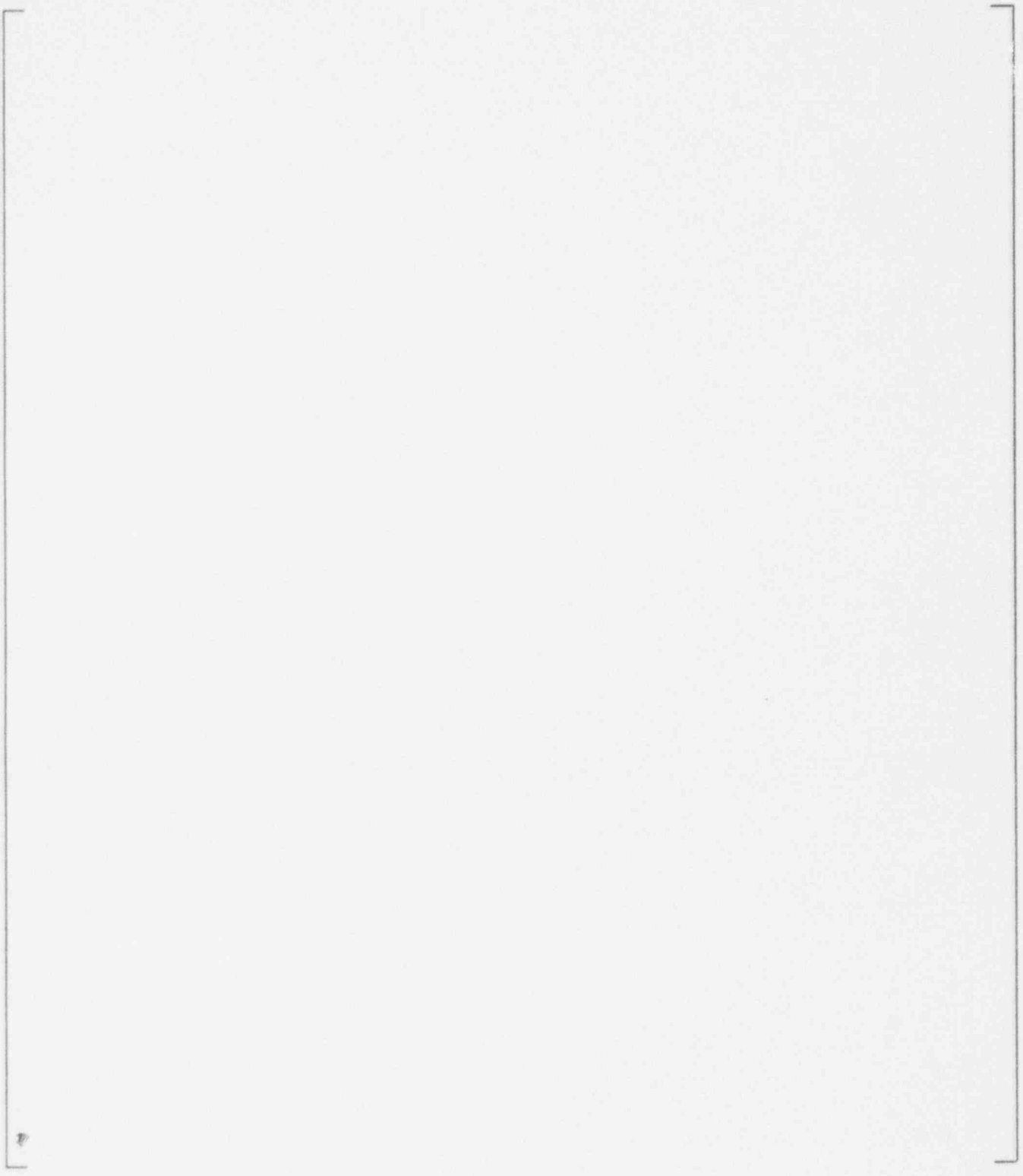

a,c

Figure 4.1-2 Average Code Bias and Uncertainty for Blowdown

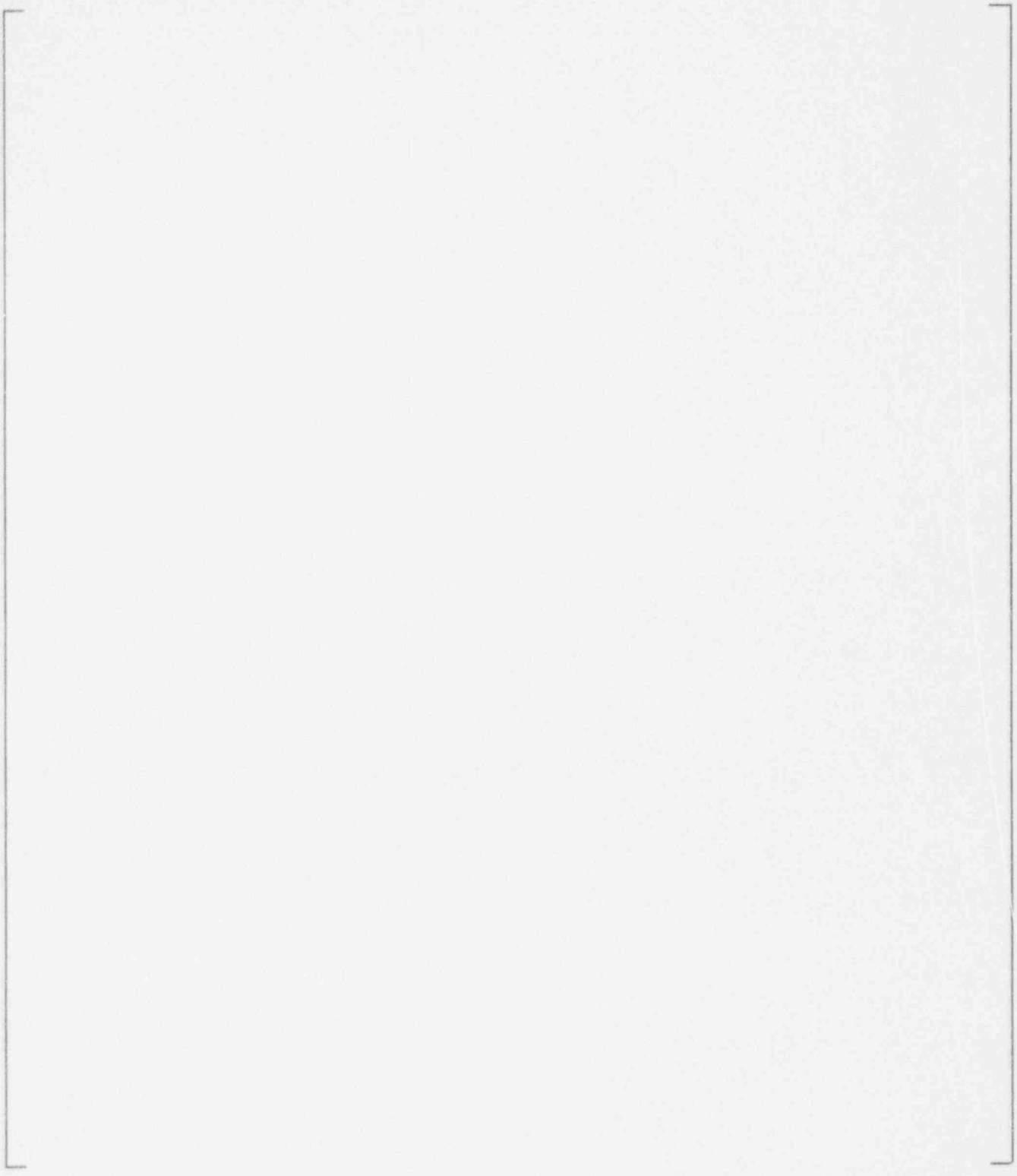

a,c

Figure 4.1-3 Average Code Bias and Uncertainty for Reflood

4.2 AP600 Large-Break LOCA 95th Percentile PCT

The results of the large-break spectrum are given in Table 4.2-1, which is the same as Table 15.6.5-7 in the AP600 SSAR. The blowdown and reflood peak cladding temperatures (PCTs), as given in the table, indicate that the $C_D = 0.8$ case is the most limiting since the other cases quench during the blowdown phase of the transient. Note, as mentioned earlier in Section 2.0 of this report, that large-break LOCA calculations that have been performed since the SSAR calculations are also indicating that the hot rod will quench during blowdown even for the $C_D = 0.8$ case, such that the SSAR case is most limiting.

[

]^{a,c} To calculate the 95th percentile PCT, the code uncertainty values from Equations 4-2 and 4-3 will be used with the $C_D = 0.8$ case from the SSAR.

[

]^{a,c} (4-8)

This value included an additional 50°F, which was added specificaliy to be conservative for the AP600. [

]^{a,c}

TABLE 4.2-1
AP600 SSAR LARGE-BREAK LOCA
BREAK SPECTRUM PEAK CLADDING TEMPERATURE (PCT) RESULTS

Case	Blowdown Phase PCT	Reflood Phase PCT	Time of Reflood PCT, Elevation
C_D = 0.8 DECLG	1472°F	1565°F	102 sec. at 8.0 ft.
C_D = 1.0 DECLG	1399°F	non-limiting due to rod quench	
C_D = 1.0 CLS	1226°F	non-limiting due to rod quench	
C_D = 1.2 CLS	1428°F	non-limiting due to rod quench	
C_D = 1.0 DEHLG	711°F	at the initiation of blowdown	

The DECLG is the double-ended cold leg guillotine break
The CLS is the cold leg split break
The DEHLG is the double-ended hot leg guillotine break

5.0 CONCLUSIONS

The processes and thermal-hydraulic phenomena for AP600 large-break LOCA have been compared to existing three- and four-loop PWR large-break LOCAs and have been found to be very similar, if not identical, in most cases. The PIRT charts for the AP600 and an existing PWR were almost identical. The new passive safety features of the AP600 design, such as the core makeup tanks and ADS, play almost no role in the large-break LOCA transient, and the peak cladding temperature is terminated by the flow from the accumulators. The injection location for the passive emergency core cooling systems is different from the current Westinghouse plants. The injection location for the AP600 is into the reactor vessel downcomer, rather than the reactor cold legs. Since the injection is into the reactor vessel, both accumulators, which are larger than existing PWRs, are available to provide core cooling, which results in terminating the calculated peak cladding temperatures at low values.

The ability of the WCOBRA/TRAC code to predict the thermal-hydraulic behavior for direct vessel injection was examined by comparing the WCOBRA/TRAC code predictions to the Japanese cylindrical test facility results (CCTF) for an experiment with direct vessel injection and comparing WCOBRA/TRAC calculations to the full-scale upper plenum test facility (UPTF) experiments with direct vessel injection. The comparison of the calculations to the test data indicate that the WCOBRA/TRAC code can predict the thermal-hydraulic behavior for the direct vessel injection design, lending credibility to the resulting AP600 plant calculations.

The final calculated peak cladding temperature was calculated using the more recent WCOBRA/TRAC code uncertainty developed in the Code Qualifying Document for WCOBRA/TRAC. The revised uncertainty calculation resulted in a reduced 95th percentile peak cladding temperature as compared to the original calculation provided in the SSAR. The resulting 95th percentile calculation was significantly below the licensing limit of 2200°F, so that ample large-break LOCA margin exists for the AP600 plant.

6.0 REFERENCES

1. Kemper, R. M., J. S. Petzold, and L. E. Hochreiter, *Application of the WCOBRA/TRAC Best Estimate UPI Model to the Haddam Neck PWR with Zircaloy Fuel*, WCAP-12766, November 1990.

2. Guidotti, T. E., and M. J. Thurgood, *A COBRA/TRAC, Best Estimate Analysis of a Large Break Accident in a PWR Equipped with Upper Head Injection*, NUREG-CR-3642, March 1984.

3. Bajorek, S. M., S. K. Chow, L. E. Hochreiter, S. B. Ngayen, M. E. Nissely, K. Ohkawa, and M. Y. Young, *Code Qualification Document for Best Estimate LOCA Analysis Volume IV and V*, WCAP-12945-P, June 1993.

4. Wilson, G., et al., *Quantifying Reactor Safety Margins*, NUREG-CR-5249, December 1989.

5. Westinghouse Electric Corporation, *Simplified Passive Advanced Light Water Reactor Plant Program, AP600 Standard Safety Analysis Report*, DE-AC03-90SF18495, June 26, 1992.

6. Dederer, S. I., L. E. Hochreiter, W. R. Schwartz, D. L. Stucker, C. K. Tsai, and M. Y. Young, *Westinghouse Large-Break Best Estimate Methodology Volume 1 and Volume 2, Application to Two-Loop PWRs equipped with Upper Head Injection*, WCAP-10924-P-A, December 1988.

7. Sugimotgo, J., et al., *Data Report on Large Scale Reflood Test -78, CCTF Core-II Test C2-AA2 (Run 058)*, JAERI-memo 59-446, February 1985.

8. Emmerling, R., et al., *UPTF: Program and System Description*, Siemens U9 414/88/023, November 1988.

9. Sarkar and Liebert, *2-D/3-D Program UPTF Test Instrumentation*, KWU R515/85/23, September 1985.

10. *Quick Look Report Test No. 21 Downcomer Injection Test*, E314/90/16, September 1990.

11. Hochreiter, L. E., C. K. Tsai, S. M. Bajorek, H. C. Yeh, K. Takeuchi, T. S. Andreycheck, and R. D. Ankney, *Westinghouse Large Break LOCA Best Estimate Methodology*, Volume 2, Addendum 3, *Upper Plenum Injection Model Improvement*, WCAP-10924, Revision 2, Addendum 3, April 1991.